CASE FILE
COPY

BATTERIES FOR SPACE
POWER SYSTEMS
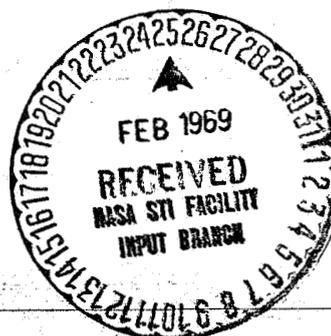
NATIONAL AERONAUTICS AND SPACE ADMINISTRATION

BATTERIES FOR SPACE
POWER SYSTEMS

PAUL BAUER

Acknowledgment

Preface

This book was written under contract to the National Aeronautics and Space Administration (NASA) by members of the staff of TRW Systems Group, 1 Space Park, Redondo Beach, Calif.   Its objectives are to—

(1) Collect and summarize all significant NASA-sponsored work published on batteries and related electrochemistry from 1959 through 1966.

(2) Review and analyze the material, its applicability, quality, and usefulness to the aerospace battery user.

(3) Define the information and data requirements of the aerospace battery user by comparing data requirements with available data and pointing out any deficiencies in available data.

(4) Establish improved methods of data presentation and show how these improvements will be advantageous to the aerospace battery user.

(5) Define three dissimilar space applications of batteries, demonstrate methods of selecting these batteries to suit the application, and integrate each battery into an electric-power subsystem.

(6) Recommend methods of providing more useful data to the aerospace-battery user participating in the NASA-sponsored battery development and testing programs.

SCOPE

Four sources of data were used.   NASA-sponsored reports, both in-house and contractual, were the primary source, representing more than 80 percent of the total document list.   Other data consisted of the Annual Power Sources Conference Reports from 1957 through 1967, the Journal of the Electrochemical Society from 1962 to the present, and Electrochemical Technology from 1965 to the present.   Because of schedule restrictions, no effort was made to report on the voluminous work done under Army, Air Force, or Navy sponsorship, and few such documents will be found in the bibliography.   This book, therefore, must be viewed as an entry only to the NASA literature, since additional background material is incomplete.

In general, this book approaches batteries from the user's viewpoint. Major emphasis is placed upon developmental work and upon general, rather than specialized, data.   Electrochemical theory is discussed only to convey a rudimentary understanding of the battery operation to potential users, who are probably electrical engineers rather than

chemists.   Greater emphasis is placed on thermodynamics than on other theoretical aspects because of its importance in solving the thermal problems associated with battery operation.

The volume is divided into 13 chapters.   Chapter 1 introduces and summarizes the state of the art of each battery system and represents the somewhat subjective opinions of the author.

Chapter 2 contains introductory material applicable to all battery systems, and gives sufficient background for a rudimentary understanding of the processes in a galvanic cell and of the operational and test problems of all types of batteries.   Chapter 3 analyzes the data requirements for the design of sophisticated, high-efficiency space electric-power systems, develops improved methods of presenting data for use by the system designer, and explains how these methods are used.   The deficiencies in the available data are analyzed and recommendations are made for data acquisition.   Where possible, all data shown in this book are presented in the format shown in this chapter.   Chapters 4 through 11 deal with individual battery systems.   Each chapter is divided into sections containing a small amount of introductory material, followed by a summary of the work done under NASA sponsorship.   Where possible, data are examined and decisions are made representing the author's opinion of the validity and usefulness of the material.   Chapter 12 deals with the basic principles of dc electric-power-system design for spacecraft, emphasizing problems encountered in selecting batteries and integrating them into a high-efficiency electric-power system.   These principles are applied in the final chapter, which analyzes three typical aerospace battery applications, and generates conceptual electric-power-system designs.

Foreword

The electrochemical cell is the oldest source of sustained electric power. By the time the first airborne electric system had risen (a battery-powered safety lamp on a manned balloon that flew from besieged Paris on November 24, 1870, landing in Norway some 800 miles away and 15 hours later), its Poggendorff battery concept was well over 25 years old. The same galvanic cells were used in bigger batteries to electrically propel the first dirigible, built in the 1880's by the Tissandier brothers of Paris. And a battery also powered the transmitter of the first Russian Sputnik.

Nevertheless, the increasingly exacting demands of space on the reliability, life, and size of on-board electrochemical energy storers have required continuing research on, and development of, space cells and batteries. Hermetically sealed cells, nonmagnetic batteries, and charge control devices are some of the new products that have resulted from this effort. Sterilizable cells, high-impact-resistant batteries, long shelf life and 5-year working life power packs are being readied for use. At the same time, research is continuing on improved and novel components, such as seals and separators, on new electrodes and electrolytes, and on associated problems in thermodynamics, quantum mechanics, and kinetics.

The purpose of this volume is to summarize the completed portions of NASA's work on batteries and related subjects in order to make the results more easily available, to point out how they can be applied in system design, while also indicating remaining difficulties and problems, thus showing where emphasis on further effort is required. Much of the knowledge that is derived from this program is directly applicable to commercial and industrial electrochemical devices, so that the author has made a useful contribution to terrestrial technology as well.

ERNST M. COHN
Head, Electrochemical Systems
Office of Advanced Research and Technology

May 28, 1968

Contents

Page

CHAPTER 1

Introduction, Summary, and Recommendations

In this chapter, the status of NASA-sponsored battery studies is viewed in relation to the requirements of present and future space missions, and recommendations are made which the author hopes will be a guide for those working in the field of space-battery development. These are based upon NASA-sponsored work. The work done by the Army, Air Force, Navy, and other governmental and private institutions and investigators is largely unrepresented in their formation.

SPACE-ORIENTED BATTERY APPLICATIONS

Primary batteries, which deliver all their energy in one short period of time (often in 10 minutes or so), are used for powering launch vehicles. These short-lived batteries must have high-energy density, high-current capabilities, and good reliability.

Secondary batteries, those which are used and then recharged, often several times (cyclically), for further use, have more numerous space applications. Batteries with a long-wet-stand time are required for interplanetary vehicles and space probes. They are discharged at launching and for course corrections a few times during flight and then deep discharged in obtaining photos and measurements at flight destination with further cycling. Batteries with limited cycle life may be used in this application, although the primary sources of power for manned vehicles are fuel cells, solar-energy conversion, and nuclear reactors; batteries are needed for emergency power supply for reentry and for eclipse periods if solar energy is used. Here, as in interplanetary probes, reliability, longevity, and rechargeability are more important than high-current performance.

The periods of charge and discharge in secondary batteries are determined by their uses. The cycles of batteries used to power planetary orbiting satellites during eclipse periods (with solar-energy converters for power during illuminated periods) are determined by the duration of the occultation period (eclipse) and thus depend upon the orbital parameters. For orbits around the Earth, the eclipse period is rarely longer than 1.2 hours (maximum for synchronous equatorial orbit, although other kinds of orbits can give longer eclipses). In other applications, timing of the cycles can be determined by the duty cycle. In these cases,

1

secondary batteries are used periodically to operate equipment for which the power output of the primary power supply is insufficient.

The choice of battery system depends on the intended use. For example, in practical aspects of the space program, such as Earth-orbiting satellites used for communication, navigation, weather observation, geological, mineralogical or agricultural surveys, mapping and aerial photography, economic considerations make long cycle life more important than light weight.

Although it is not possible to predict the nature and scope of all future space missions, it is possible to predict that power requirements will increase, creating a greater need for lightweight, highly efficient power systems. This, and the increasing use of high-voltage semiconductor devices, will make it necessary to overcome the present lack of reliability in high-voltage secondary batteries, perhaps by improved charge control. The need to store more energy may necessitate development of higher capacity cells, although this need may be met by use of smaller parallel batteries. Use of a number of parallel batteries, rather than a single one, would result in increased weight, but this is offset by the increase in reliability, since failure of one battery would not cause total mission failure.

BATTERY SYSTEMS OF INTEREST FOR THE SPACE PROGRAM

Four types of battery systems have received much support from NASA. These are the nickel-cadmium, silver-zinc, and silver-cadmium batteries and the class of batteries which use organic solvents. NASA has also supported some studies of other types of batteries, such as lead-acid and ammonia, of fundamental electrochemistry and of facets of battery technology such as charge control.

Space-battery development suffers from a lack of performance characteristics data usable by power-system-design engineers. This is further complicated by a lack of standardization of cells, of testing conditions, and of data reporting. A detailed discussion of data requirements and of deficiencies in existing design data and recommendations for a format for expressing data are contained in chapter 3. In general, design data are required on the electrical characteristics, heat dissipation, failure modes, and on charge-control requirements of secondary batteries. Of these, broad programs have been implemented only for the investigation of failure modes, and these, in spite of extensive testing, have not provided quantitative information about the rates of the individual failure processes. Definitions of failure are critical in determining the impact of service conditions on life, since a combination of unfavorable service conditions and failure criteria leads to rapid performance failure, although no physical failure has occurred.

Considerable progress in data acquisition methods and in data analysis may be expected with the help of computer control systems for battery testing, and initial steps have been taken to develop data analysis programs for the detection of impending cell failure.

Nickel-Cadmium

The nickel-cadmium battery has the highest survivability and longest cycle life and is therefore often used as a secondary (cycling) battery, especially in long-life applications even though it is heavier than the silver-cadmium battery. Improvements in this cell have been the development of inert separators and more reliable seals.

The hermetically sealed cells are designed to operate in the electrolyte-starved condition, leaving considerable surface for oxygen evolution recombination at the negative electrode. Oxygen recombination rates are dependent upon temperature. In these cells, oxygen evolution occurs near the charge voltage of the nickel electrode; consequently, the voltage rise at the end of charge is not sharp and does not clearly indicate completion of charging, particularly at high temperatures. This complicates charge control systems based upon voltage; however, the cells are able to tolerate useful continuous overcharge levels.

Because ferromagnetic metals are used, there is a strong residual magnetic field (no current flowing) whose intensity is determined by the direction and amplitude of the last current to flow. The magnetic fields during current flow are comparable to other batteries having similar structural and wiring geometry.

Currently, several companies manufacture standard lines of nickel-cadmium cells specifically designed for space applications and which are satisfactory for most uses. However, the manufacturer's quality control remains poor. Capacities of cells in a lot may vary 5 to 10 percent and lot-to-lot variations are often larger. The two greatest unsolved problems are seal integrity and divergence in performance characteristics of apparently identical cells after prolonged operation. Other significant problems are those associated with constructional errors.

Nickel-cadmium batteries have been subjected to extensive testing, primarily to expose the principal failure modes, but due to poor control of experimental variables the data are inadequate for design needs.

Summary of Recommendations.—Cell-quality improvements may be reasonably expected as a result of work along the following lines:

Redesign of cell-electrode assemblies with concern for process as well as mechanical factors should eliminate most of the mechanical problems, such as separator perforation, plate-to-plate short circuits, and burned welds. The improvement in reliability appears to be worth the probable increase in cost and weight. Continued design effort is essential until a reliable seal has been achieved to prevent loss of oxygen and water vapor.

Greater uniformity of operating characteristics among cells must be achieved by a closer control of plaque porosity, electrode loading, electrolyte content, and other manufacturing variables. The nature of these processes make both development and implementation of such controls expensive, and it is unlikely that the cell manufacturers will pursue this course without external support. Only through this close control of manufacturing variables can expensive cell-matching procedures be eliminated and the problems of cell divergence reduced.

As with other battery systems, it is necessary to develop a consistent program for performance data that will be useful in design of improved power systems. Standardization of information is easier for the nickel-cadmium system due to the use of a standard line of cells. In brief, it is necessary to determine which variables affect the voltage-current characteristics of nickel-cadmium cells and to carefully control these variables while accurate measurements of cell properties are made.

Failure modes for this system have been labeled, but much study is needed of individual failure processes, such as determination of rate constants for chemical reactions involved. Details of requirements and approaches are in chapter 3.

SILVER-ZINC AND SILVER-CADMIUM BATTERIES

Much of the NASA-sponsored work in these systems has been in the development and testing of cells for specific applications.

The silver-zinc system has been developed into a highly reliable primary battery of the reserve type (i.e., activated immediately prior to use) with energy densities up to 80 W-h/lb and is often used in launch vehicles. Performance in this application is generally excellent except for the relatively high internal heat dissipation caused by discharge of divalent silver oxide at the voltages of the lower plateau.

For use as secondary batteries, special separators are added to the silver-zinc system to delay the internal deterioration processes so that the battery has a long life (wet stand) of approximately 1 year. The rechargeability is also improved, with approximately 10 deep discharges, or 500 shallow discharges, permitted due to the addition of multiple layers of separators. These batteries have relatively high-energy density. High-current performance is poorer than that of the primary silver-zinc battery, but this is seldom important for this type of battery.

Silver-cadmium cells are rarely used in primary applications. As a secondary battery, the advantages of energy density twice that of the nickel-cadmium cell and of cycle life 1 to 2 orders of magnitude greater than the silver-zinc cell may be outweighed, for many applications, by the low cell voltage and the resultant poor system voltage regulation. Because they may be charged more rapidly than silver-zinc cells, silver-cadmium cells are useful when rapid repetition of cycles is required. Wet-stand life is approximately 1 to 2 years. Tests on their cycle life have been inconclusive; some suggest a potentiality for 10 000 shallow cycles, others show poor cyclic performance. One extended test program has been completed but with inadequate subsequent failure analysis. Cyclic life is sensitive to the method of charge control used.

In both primary and secondary space applications, silver-zinc and silver-cadmium cells are usually tailormade and no single standard line of cells has evolved.

NASA has supported studies of the reaction mechanisms of both silver and zinc electrodes. The mechanism of the silver electrode and its effect upon other components in the cell is fairly well understood. The main

problem with this electrode is the relatively high impedance of the cell during the period of the transition of the voltage between the upper and lower plateaus.

The zinc electrode represents the major limiting factor in extending the cycle life of the silver-zinc battery. It undergoes changes in physical characteristics during cycling which lead to losses in capacity. Under some conditions it grows dendrites which perforate the separators and result in short circuits. This effect may be lessened by including additives such as Teflon and by cell and power system designs in which conditions suitable for dendritic growth are avoided.

Separators are a limiting factor in the cycle life of both silver-zinc and silver-cadmium cells. New separator materials for decreasing the rate of silver migration within the cell and for stabilizing the zinc electrode have been developed. Cellulosic materials have the advantage of removing soluble silver from the electrolyte, but are destroyed in the process. (Grafting of functional groups onto the surface of inert plastics such as polyethylene offer some promise.) Considerable effort has been expended in the development of separator materials and other cell components capable of withstanding sterilization temperatures. Inorganic materials meet this requirement, but have high internal resistances, poor energy density because of their thickness, and create serious structural cell-design problems.

Heat evolution rates have been calculated on charge and discharge. Good agreement is obtained between calculated and measured values of the total heat evolved over an entire cycle. Poor agreement was found for heat evolution rates; however, this was due to an inability to determine the division of current between two simultaneous reactions having different heat evolution rates.

Both silver-zinc and silver-cadmium cells can be made with nonmagnetic materials, so that at zero current their residual magnetic fields are negligible. During current flow, however, their magnetic fields are comparable to those of the nickel-cadmium cells unless the batteries are wired to compensate for this effect.

Because of the variation in cell structural details and the consequent performance variations, virtually no parametric performance data exist outside of the manufacturer's hands.

Recommendations.—The most important requirement for improving the secondary performance of the silver-zinc battery is further improvement of the stability and reversibility of the zinc electrode. Continued studies are also needed to eliminate the high-impedance behavior of the silver electrode that occurs during a portion of the charge and discharge cycle. Silver migration and the problems it causes need further study because proposed approaches result in large decreases in the current-carrying capability of the battery. Attempts have been made to solve these problems by the development of better separators; more fundamental approaches should not be neglected.

Packaging methods used for sealed silver-zinc and silver-cadmium cells are based on quick-fix modifications of the vented structures. A

study of the mechanical design of sealed cells could lead to lighter weight, stronger, and more stable structures.

Present difficulties in utilizing silver-cadmium cells effectively stem from high-pressure behavior of individual cells in a series-connected battery due to the divergence of characteristics of individual cells. Intensive attack on this problem requires a standardized product and a much improved method of charge control.

The practicality of standardizing some compromise structure for the large majority of space applications and of accepting the resulting design penalties should be seriously examined. Until such standardization occurs, no general program for gathering parametric data can be undertaken without excessive cost.

HIGH-ENERGY DENSITY SYSTEMS

Much research has been done on systems employing organic solvents and high-activity electrode materials to attain batteries with energy densities greater than 200 W-h/lb. Such systems consist of nonaqueous solvents, compatible electrolyte, lithium anodes, and either inorganic or organic cathodes. Presently no working cells of this type are available for practical application. Reversible cells with inorganic cathodes (energy densities of more than 100 W-h/lb) should be available in a few years.

It will be longer before cells with organic cathodes are practical. Reaction products and mechanisms are not known, and the rapid self-discharge of the cell due to the solubility of such electrode materials in the solvent is a serious problem. No approach to the development of a separator capable of restraining this self-discharge has been evolved. Organic cathode reactions are usually not completely reversible.

When finally evolved, nonaqueous cells constructed in conventional fashion may be expected to be poor in high-current performance, discharging at the 10- to 100-hour rate. This suggests that their usefulness will be limited to relatively low-rate applications. The development of high-rate cells would require the development of aprotic electrolyte solutions with conductivities equivalent to those of aqueous sulfuric acid and potassium hydroxide solutions. This is unlikely; the potential exists for weight savings in both manned vehicle and interplanetary probe secondary-battery applications where some discharge rates may be in excess of 10 years.

High-energy density batteries are being developed by the Army and Air Force for primary batteries in portable field equipment, but there are fewer similar space applications.

The dry-tape battery, in which active materials are stored individually until needed, is an attractive idea for some mission applications, at least until some other type of fuel cell with storable fuel becomes available. Neither the dry-tape battery nor the high-energy battery can currently compete with available fuel cells.

The dry-tape concept must be weighed against fuel-cell capabilities. If a fuel cell with storable fuels can be developed, it would probably be preferable to the mechanically complex dry tape.

CHAPTER 2

Battery Principles

The fundamental electrochemical principles underlying battery operation and many of the operating characteristics of batteries and cells are common to all electrochemical systems. It is the purpose of this chapter to discuss as simply as possible battery design, operation, control, and testing in sufficient depth to provide the battery user with a rudimentary understanding of principles, and to collect, in one chapter, material generally applicable to all batteries. In this way, much repetition may be avoided. In some cases, although the material is generally applicable, specific expository examples have been selected.

In keeping with the desire for simplicity, discussion of basic electrochemistry is avoided entirely, since it cannot be covered in sufficient depth to be of practical use within the scope of this book. Thermodynamics is applied for the purpose of deriving an expression for heat evolution in batteries. For a further discussion of these subjects, the reader is referred to the many available texts on electrochemistry and chemical thermodynamics.

A galvanic cell is an electrochemical device, the ingredients of which can react spontaneously. However, these materials are packaged in such a way that the reaction process, particularly that of electron transfer, cannot proceed unless an external circuit is closed. All electrochemical batteries and fuel cells operate on this principle; i.e., a mutual oxidation-reduction (redox) reaction. This reaction is a chemical change in which there is a transfer of electrons from one reactant to the other. The reactant losing electrons is oxidized, and the one accepting electrons is reduced. When these reactants are mixed, under the proper conditions, the reaction occurs spontaneously with the evolution of heat. However, when these reactants are mounted on current-collecting electrodes and prevented from mixing, immersed in an ionic solution (electrolyte), and connected by an external circuit, the reaction then proceeds at a rate which may be controlled by the circuit's resistance to an electric current. The products of the reaction enter the electrolyte to replace those combined at the electrode of opposite polarity at which the chemical change is completed. The resulting concentration gradients cause diffusion through the ionized fluid. These reaction products are usually compounds or ions (fragments of chemical compounds which have lost or gained electrons and are either negatively or positively charged). Ionized species must be transported in order to carry current between electrodes.

7

The electrolyte solution is usually made up of a solution of some highly ionizable chemical, such as sulfuric acid or potassium hydroxide, in water. The cell's electric conductivity is directly related to the ionic conductivity of the electrolyte; as a result, solutions used as electrolytes have maximum ionic conductivity, i.e., the ability to transport large numbers of ions with small potential drops. Other satisfactory electrolyte solutions may be composed of highly polar, nonaqueous organic solvents containing dissolved electrolytes. Fused salts, solutions of salts in ammonia, and even gases may also act as electrolyte solutions.

A simple electrochemical cell operation for a zinc/mercuric-oxide cell is represented diagrammatically in figure 2-1. Basically, one-half of the electrochemical reaction occurs at the negative terminal, where the zinc is oxidized in the presence of the OH^- ion

$$Zn+4OH^- = Zn(OH)_4^= +2e^-$$
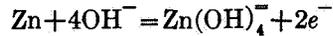
liberating two electrons to the metal in the process.

However, an electrolyte solution saturated with potassium zincate slowly precipitates zinc oxide. The net reaction may then be written

$$Zn+2OH^- = ZnO+H_2O+2e^- \qquad (2-1)$$
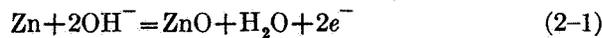
The chemical reaction stops when the half-cell reaction establishes a high enough potential gradient between the zinc and the electrolyte. The reaction continues as long as OH^- ions and zinc are available at the electrode, and the electrons are removed.

At the cathode, the reduction reaction can be expressed by

$$HgO+H_2O+2e^- = Hg+2OH^- \qquad (2-2)$$
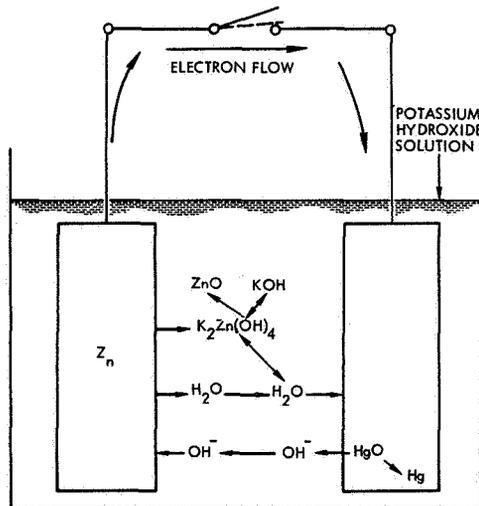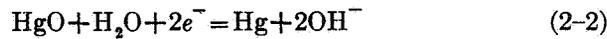
FIGURE 2-1.—Diagrammatic representation of
a zinc-alkali mercuric-oxide cell.

This reaction removes both the water and the electrons generated at the anode and regenerates OH^- ions to replace those consumed at the anode. Thus the net overall reaction is the sum of the two half-cell reactions of equations (2-1) and (2-2). By deleting identical terms from both sides, a simple redox reaction is produced:

$$Zn + HgO = ZnO + Hg$$
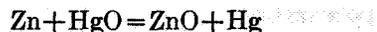
For the reaction in the galvanic cell to progress smoothly, the following processes must occur:

(1) Electrons must find a continuous external path from anode to cathode. The reaction rate may be limited by the rate of this electron transfer.

(2) Water is generated at the anode and consumed at the cathode. This transference of water occurs by diffusion, but in some types of batteries is assisted by fluid convection. The reaction rate may be limited by the mass-transport rate of molecules or ions (below).

(3) The hydroxyl ion (OH^-) is generated at the cathode and consumed at the anode, requiring transport from cathode to anode. Normally, the rate of transport through the bulk of the fluid of materials other than the major current carriers is controlled by diffusion processes, since the influence of the electrical field of the electrodes upon the charged ion extends only a short distance (less than 0.5 millimeter) into the electrolyte.

Some form of mass transport occurs in all batteries. Mass-transport characteristics are important to the behavior of a cell and may be responsible for a significant portion of the energy losses.

Electrochemical systems used in rechargeable or secondary batteries are reversible. After electrical energy has been delivered from the battery, the process may be reversed by pumping electric current through the cell in the opposite direction.

GALVANIC CELL VOLTAGES

The theoretical open-circuit voltage of a galvanic cell is determined solely by the thermodynamics of the reactions and is independent of the quantities of material present in the solid state. Normally, the chemical reactions are written separately as cathode and anode reactions, each characterized by standard electrode potentials. These have been determined for most inorganic electrode reactions. Under standard conditions the cell voltage is the algebraic sum of the standard electrode potentials of the two electrodes.

The reversible or zero current potential, E_{rev}, of a cell varies as conditions depart from the standard state. The value of E_{rev} may be corrected for such departures by use of the appropriate theoretical relationships. In general, where cell reactions and electrode processes are precisely understood, the agreement between measured values and theory is excellent.

POLARIZATION PHENOMENA

When current is withdrawn from a battery (discharge), or is forced into a battery in the reverse direction (recharge), the voltage across the terminals of the battery shifts from the reversible potential. This departure from the reversible potential is known as overpotential, η, and has three major contributory sources, referred to as polarization phenomena. The relative contribution of these three polarization phenomena varies with the system and conditions of use.

Ohmic Overpotential, η_r.—Ohmic losses are the aggregate voltage drops within the battery due to the flow of current through resistances in the leads, electrolyte, electrodes, and resistive films which may have formed on reactive surfaces. Ohmic losses are linear with current:

$$\eta_r = IR$$

where I is current and R is resistance.

Activation Overpotential, η_a.—Activation overpotential is a complex phenomenon associated with the transfer of an ion across an adsorbed barrier layer at the electrode surface, sorption, discharge of the ion, desorption, and/or evolution of gases from the surface. Evaluation of activation overpotentials requires a precise knowledge of the nature and kinetics of the rate-controlling step of the reaction. Activation overpotentials are of major significance in reactions involving gas evolution or consumption at electrode surfaces and may also be significant for other reaction species. At high overpotentials, the activation overpotential usually follows an equation of the Tafel form:

$$\eta_a = A + B \ln i$$

where A and B are constants, and i is current density. At low overpotentials (<50 millivolts), η_a is usually linear with current density (refs. 1, 2).

Concentration Overpotential, η_c.—Concentration overpotential involves a voltage shift which is a function of the variation in concentration of electroactive species in the vicinity of the electrode-electrolyte solution interface. Conduction in the bulk of the electrolyte solution is a function of both the diffusion characteristics of the ionic species involved and the properties of the solvent. After current has passed through the cell for a period of time, a layer of electrolyte solution near the electrode surface becomes depleted in the ionic species which reacts at the electrode, thereby establishing a concentration gradient between the electrolyte solution at the surface of the electrode and the bulk of the electrolyte solution. The concentration (or activity) of the reaction species at the electrode surface is no longer that of the bulk electrolyte and the potential of the electrode shifts. This shift is usually called the concentration overpotential.

All three polarization phenomena result in a shift in voltage from the zero-current value in a direction which impedes the flow of current. On discharge, the cell voltage falls below E_{rev}. When the cell is opposed by a potential equal to E_{rev}, no current will flow.

Polarization data on battery cells are commonly reported as a polarization curve, or plot of current versus voltage. Data are normally taken after both activation and concentration polarization have set in. The slope of the polarization curve, although expressible in ohms, does not represent the true value of the impedance of a battery cell. Impedance measurement is discussed elsewhere.

CALCULATION OF CELL POTENTIALS FROM FREE ENERGY DATA

For any electrochemical system, the reversible potential is calculated from the equation:

$$\Delta G^\circ = -zFE^\circ \qquad (2\text{-}3)$$

where

F Faraday's constant $= 96\ 500$ A-sec/g equivalent

z the number of electrons transferred in the reaction

ΔG° the molar Gibbs free-energy change at standard conditions for the reaction

E° the standard electrode potential.

Standard conditions are defined as 25° C and unit activity of all reactants and products in their normal states. A pure solid at 25° C is in the standard state.

Where conditions are not standard, $\Delta G \neq \Delta G^\circ$, but the equation

$$\Delta G = -zFE_{rev}$$

still applies.

For systems in which the reactants and the products are solids[1] and are slightly soluble in the electrolyte, the free-energy change at any temperature, ΔG, may be calculated from the entropy data:

$$\Delta G = \Delta G^\circ + (T - T^\circ)(\Delta S) \qquad (2\text{-}4)$$

where T° is 298.6° K, the standard condition.

This new value of ΔG may be used for the calculation of cell potentials at temperature T, provided that a change in temperature has not altered the state of the reactants or products.

When the electrolyte solution is consumed in the reaction, or the reactants or reaction products are dissolved in the solvent, ΔG is a function of the activities of the electroactive species involved. Activities are nonlinear functions of concentration, and are experimentally determined for the high concentrations of solute normally used in electrochemical cells. The equations for calculating activities in more dilute solutions (ref. 3) are not useful in working cells using more concentrated solutions. For a reaction

$$mM + nN \rightarrow jJ + kK$$
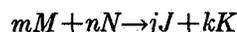
in which the reactants M and N and the products J and K are not at unit activity,

$$\Delta G_{t,p} = \Delta G^\circ - RT \ln\ (a_M)^m (a_N)^n / (a_J)^j (a_K)^k \qquad (2\text{-}5)$$

[1]All solids are considered to be at unit activity.

where

$(a_I)^i$ the activity of material I raised to the ith power

i number of mols of material I participating in the reaction.

Activities of ions in solution as a function of concentration are available in the literature referenced.

In the event that ionic species or solvents are consumed or produced in the reaction (as in the lead-acid cell, $Pb+PbO_2+2H_2SO_4=2PbSO_4 +2H_2O$), the concentrations and activities of ions in solution vary with the state of charge, resulting in a change in both ΔG and E_{rev}.

When gases are produced or consumed at the electrodes, the resulting free energy is a function of fugacity, which is a nonlinear function of pressure. At atmospheric pressure or below, fugacity is approximately equal to the ambient pressure; thus pressure may be substituted for activity in equation (2–5), and reasonable accuracy will still result.

CALCULATION OF HEAT EVOLUTION FROM GALVANIC CELLS

The rate of heat evolution at the electrodes can be estimated if the reversible potential of the cell and the entropy of reaction are known. Using the sign convention that energy added to the electrochemical system is positive, that withdrawn from the system is negative, the enthalpy change, ΔH, resulting from the addition of both heat and electrical work to the system, is

$$\Delta H = Q + W_e \qquad (2\text{--}6)$$

The maximum electrical work which can be removed from the system $\left(W_{e_{max}}\right)$ as a result of the reaction of 1-g equivalent weight of reactants is given by

$$-W_{e_{max}} = \Delta G = -FE_{rev} \qquad (2\text{--}7)$$

If the reaction is performed reversibly and at constant pressure[2] in an electrochemical cell, the heat absorbed, Q_{rev}, is

$$Q_{rev} = \Delta H - W_{e_{max}} = \Delta H - \Delta G = T\Delta S \qquad (2\text{--}8)$$

If the reaction is performed irreversibly at a potential $E \neq E_{rev}$, then the heat absorbed is given by equation (2–6). However,

$$W_{e_{max}} = \int E_{rev} I \, dt \qquad (2\text{--}9)$$

and

$$W_e = \int EI \, dt \neq W_{e_{max}} \qquad (2\text{--}10)$$

Adding $\left(W_{e_{max}} - W_{e_{max}}\right)$ to the right side of equation (2–6):

$$Q = \Delta H + \left(W_{e_{max}} - W_e\right) - W_{e_{max}} \qquad (2\text{--}11)$$

$$= \Delta H + \left(\int E_{rev} I \, dt - \int EI \, dt\right) - \Delta G \qquad (2\text{--}12)$$

$$= \Delta H + \int (E_{rev} - E) \, I \, dt - \Delta H + T\Delta S \qquad (2\text{--}13)$$

---

[2]Except where gases are directly involved, the effects of change in pressure tend to be small.

For consistency with the original sign convention, the sign of current direction used is $+$ for charge (energy added to system), $-$ for discharge. The total heat absorbed in the reaction of 1-g equivalent of reactants in a battery is, therefore

$$Q = \int \Delta E I \, dt + T \Delta S$$

NOTE.—For consistency, ΔS is in J/g-equiv °K, I in amperes, dt in seconds, ΔE in volts $= (E_{rev} - E)$, T in °K.

Differentiating with respect to time,

$$\frac{dQ}{dt} = q = I \Delta E + \Delta S \, \frac{dT}{dt} + T \, \frac{dS}{dt} \qquad (2\text{-}14)$$

Consequently, when the temperature changes slowly

$$\frac{dT}{dt} \cong 0$$

$$q \cong I \Delta E + T \, \frac{dS}{dt}$$

A change in S caused by the reaction of N equivalents of reactants takes place as a result of the flow of NF A-sec of electrical change, spread across a time period, Δt. Since the change in entropy is proportional to the quantity of materials changed

$$\left(\frac{dS}{dt}\right)_I = \left(\frac{\Delta S}{\Delta t}\right)_I = KI \qquad \text{and} \qquad T \, \frac{dS}{dt} = KIT \qquad (2\text{-}15)$$

where K is a proportionality constant equal to $\Delta S/F$.

$$(\Delta S \text{ in J/g-equiv °K})$$

The final equation becomes

$$q \cong (E_{rev} - E)I + KIT \qquad (2\text{-}16)$$

where

q	watts of heat
E	volts
I	amperes
K	4.186 $\Delta S/F$
T	°K
ΔS	cal/g-equiv °K (or entropy units)
4.186	conversion factor, calories to joules.

Equation (2-16) expresses the rate of heat evolution or absorption resulting from any electrochemical process as a function of the voltage at the terminals of the reaction cell, and the current through the cell. If several reactions occur simultaneously, each must be treated separately, and their effects added. For this, the division of current between the two parallel reactions must be known.

The derivation of equation (2-16) assumes constant temperature. Consequently, deviations may be expected from predicted behavior during periods of rapid temperature change. In addition, after transition between charge and discharge or after step changes in current, the heat evolved at the electrodes cannot be measured at the cell exterior until time has been allowed to establish a new steady-state thermal gradient in the cell consistent with the changed conditions.

Thermodynamic data are reported in the literature as free energies and enthalpies of formation and entropies for individual compounds at standard conditions. The thermodynamic quantities for the reactions are derived from the quantities of formation by algebraic addition.

Thus, for a reaction

$$2A + B \rightarrow C + 2D$$
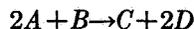
reaction entropy at standard conditions (25° C)

$$\Delta S_r^\circ = 2S_{(D)}^\circ + S_{(C)}^\circ - 2S_{(A)}^\circ - S_{(B)}^\circ \qquad (2\text{-}17)$$

The methods of handling thermodynamic calculations will be found in any classical thermodynamics text (ref. 4). The method of estimation of thermodynamic quantities and the values of these quantities for many aqueous systems are given in references 5 and 6.

BATTERY IMPEDANCE

The large capacitance of the interface between the surface of an electrode and the electrolyte in a cell has led to considering the battery cell in electronic circuit design as a large capacitor in series with small resistances and inductive reactances. Other approximations of battery equivalent circuits in the form of resistor-capacitor networks have been used (ref. 7). Battery impedances have been measured, and data are reported in the appropriate sections.

Electrode behavior is more complex than the resistor-inductor-capacitor equivalent circuit. The changing character of the adsorbed layers of electrolyte with changing overpotential causes the capacitance of the electrodes to vary greatly with the potential across the electrode-electrolyte interface. Thus, capacitive reactances measured with ac signals vary with a change in dc current through the cell, since the dc causes an overpotential to appear.

In addition, with dc flowing, concentration overpotentials appear, and the rate of voltage change with time during establishment of concentration overpotential is not at all like an exponential capacitive decay. As a result, measured impedance values are valid only for the conditions of measurement. Such data should be used with caution in circuit designs in which battery dynamic impedance significantly affects circuit performance.

Similarly, equivalent circuits for batteries can simulate battery dynamic impedance only under limited circumstances. In general, response of batteries to high frequencies can be simulated by a resistor-capacitor-inductor network such as the one in figure 2-2 (ref. 7). Values will vary with the size and type of battery.

GENERAL STRUCTURE

CELL STRUCTURE

The construction of all practical cells is generally the same, consisting of a negative and a positive electrode, an ionically conductive electrolyte, and usually a separator, which prevents contact between negative and positive active materials and acts as a carrier and immobilizer for the
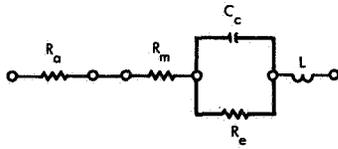
FIGURE 2-2.—Battery equivalent
circuit (ref. 7).

R_a = Electrolyte resistance C_e = Faradaic capacitance
R_m = Metal conductor resistance L = Inductance
R_e = Shunt resistance

electrolyte. All these elements are enclosed in a case. If the case is metallic, the negative and positive terminals must be insulated from one another. Most working cells are built in one of five different basic structures, although considerable variation in details of construction will be found from system to system and from manufacturer to manufacturer.

The prismatic cell is the most common of the larger sizes. It consists of alternately interleaved, flat negative and positive electrodes, set apart by one or more layers of separators in the form of flat sheets (typical automotive battery), bags (silver-zinc and silver-cadmium), or windings. Figure 2-3 depicts the typical wound-separator prismatic nickel-cadmium cell.

The principal advantage of the prismatic structure is its amenability to the design of electrodes of complex structure. Active materials may be enclosed in pockets, tubes, or in materials with a fine pore structure. Close electrode spacing is practical and close control of electrode spacing reasonably convenient.

The spirally wound cylindrical structure is generally used only when the exterior cylindrical shape is desirable, but the nature of the chemical system is such that flat, thin electrodes are required. A sandwich is made of a negative electrode, a separator, and a positive electrode, rolled up and pressed into a cylindrical container. Usually, the negative electrode is allowed to contact the metal case, and the positive electrode is connected to the insulated terminal. Figure 2-4 shows a typical, spirally wound, cylindrical cell.

The button cell consists of a single flat negative and a similar positive electrode each in contact with one end of a metallic case. The case has a low length-to-diameter ratio, and may be cylindrical or rectangular with rounded corners.

Negative and positive electrodes may be held in their respective sections of the case by firmly pressing them in place, or by the elasticity of the separator material. The top and bottom of the case are sealed by an insulating gasket. The principal advantages of the button cell are a simple, low-cost structure and the convenience of assembling high-voltage batteries by stacking the cells end to end. Button cells are usually of a lower capacity than other types. Figure 2-5 shows a typical button-cell structure.
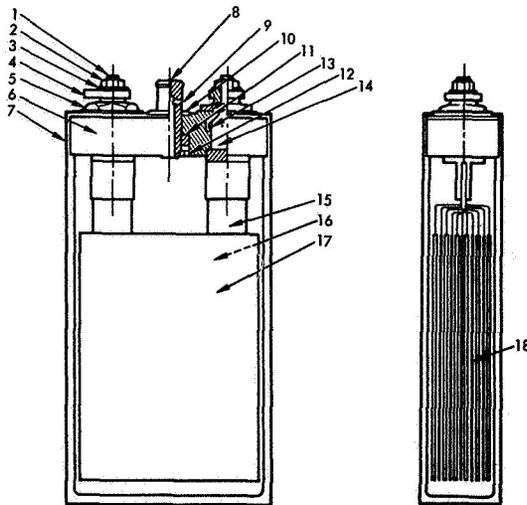
FIGURE 2-3.—Prismatic nickel-cadmium cell.

Parts List

Item no.	Description	No. req'd	Item no.	Description	No. req'd
1	Post_____	2	10	Vent washer	1
2	Post nut, top	2	11	Vent nut____	1
3	Connector		12	Nut seal____	1
	washer___	2	13	Gland_____	2
4	Connector__	_____	14	Post ring___	4
5	Post nut,		15	Plate tab___	_____
	bottom___	2	16	Plate,	
6	Jar cover___	1		positive__	_____
7	Jar_____	1	17	Plate,	
8	Vent plug___	1		negative__	_____
9	Vent ring___	1	18	Separator___	_____

In the concentric cylindrical cell, the active materials are arranged in two concentric cylinders with a separator between them. The outer electrode may be either negative or positive. The inner electrode is brought into contact with the cell top, which is insulated from the case by an insulating washer or gasket. Figure 2-6 shows a typical concentric cylindrical cell structure.

The bipolar electrode cell incorporates the negative electrode of one cell and the positive electrode of the adjoining cell in a single structural element. A battery or "pile" is formed by stacking these elements with interleaved layers of electrolyte (fig. 2-7). The structure is simple in concept, but practical problems are encountered in preventing an electrolyte leakage path between the faces of the bipolar electrode.
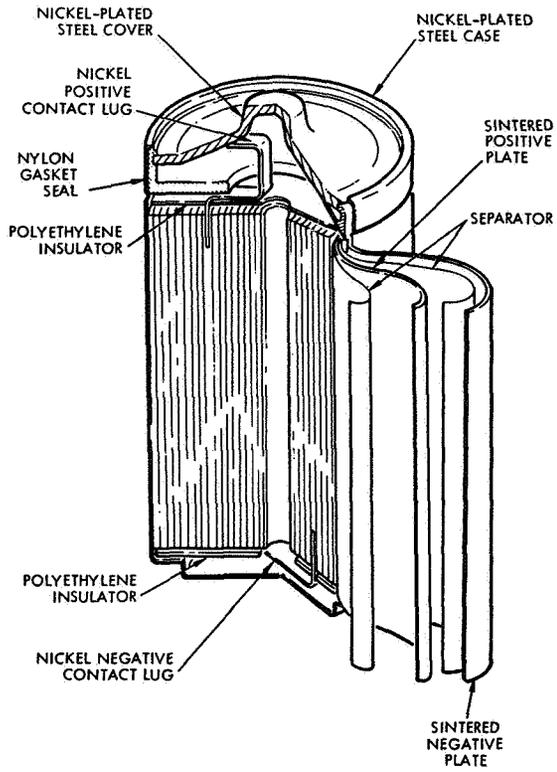
FIGURE 2-4.—Spiral-wound electrodes.
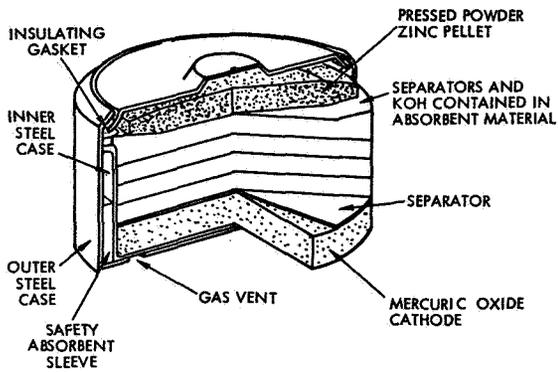
FIGURE 2-5.—Flat pellet or "button" structure "Mallory" alkaline mercuric oxide-zinc cell.
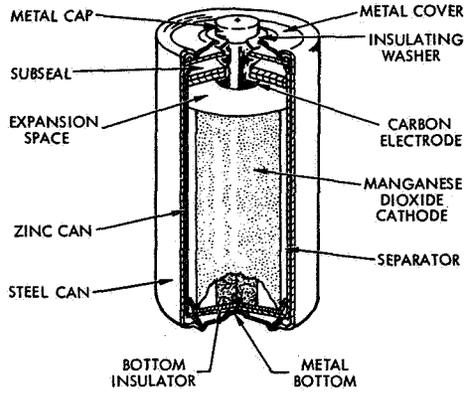
FIGURE 2-6.—Cross-sectional view of an "Eveready" Leclanche concentric cylindrical cell.
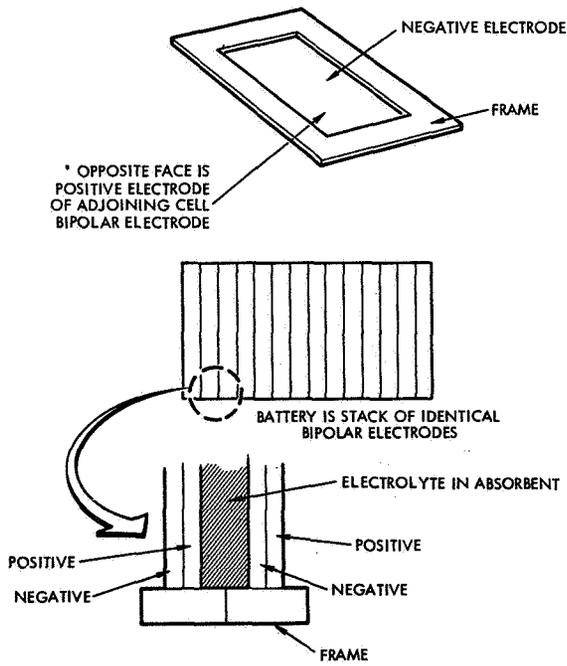
FIGURE 2-7.—Bipolar electrode pile battery.

The advantage of the bipolar electrode pile battery is the extremely low resistance and inductance of the internal metal conductors, enabling the construction of batteries capable of delivering pulses of high current for short periods.

BATTERY STRUCTURE

There are many varieties of battery structure possible; frequently, unconventional methods of battery assembly are used to satisfy special needs. Some of the more common battery structures, however, are as follows.

Prismatic cells are usually assembled in a covered box and connected by cross strapping. Connections are made to exposed cell terminals, if available, or via a connector if the battery case is totally enclosed (fig. 2-8).
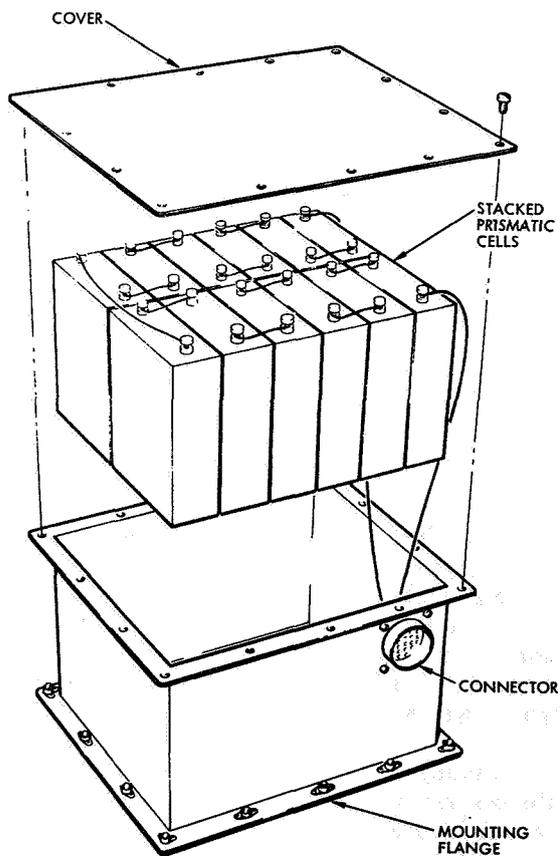
FIGURE 2-8.—Typical prismatic battery structure.

Cylindrical cells may be stacked in rows, or hexagon-close-packed for greater utilization of volume. Normally, the cells are oriented in polarity to minimize the length of interconnecting wires. The volumetric efficiency of packaging cylindrical cells into a rectangular space is never as great as that of prismatic cells. However, certain configurations of hexagon close packing can be more efficient than prismatic cells when packed into a cylindrical battery case (fig. 2-9). Cylindrical structures may offer advantages in applications where convection cooling can be used.
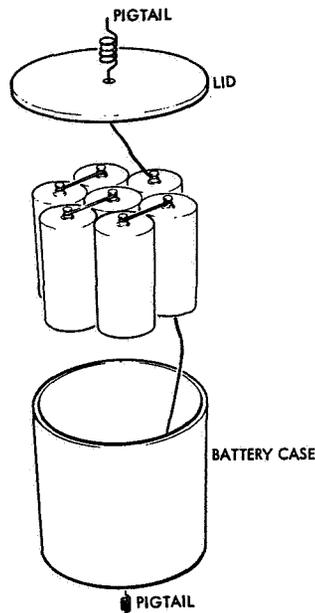
FIGURE 2-9.—Hexagon-close-packed cylindrical battery.

Button cells may be pressure stacked or series connected by welding the positive terminal of each cell to the negative terminal of the succeeding cell, forming a long cylindrical stack of high voltage. These stacks may then be combined into a higher voltage package by assembling them into rows or by hexagon close packing. The use of portable high-voltage batteries has decreased as a result of the invention of lower voltage transistorized equipment. Figure 2-10 shows a typical welded assembly stack of button cells.

The cell tray assembly (fig. 2-11) has the quality of maintaining a rigid structure independent of the structural strength of the cell cases, but it is limited to applications in which neither size nor weight are important. Circuit boards have been used to make the intercell connections.
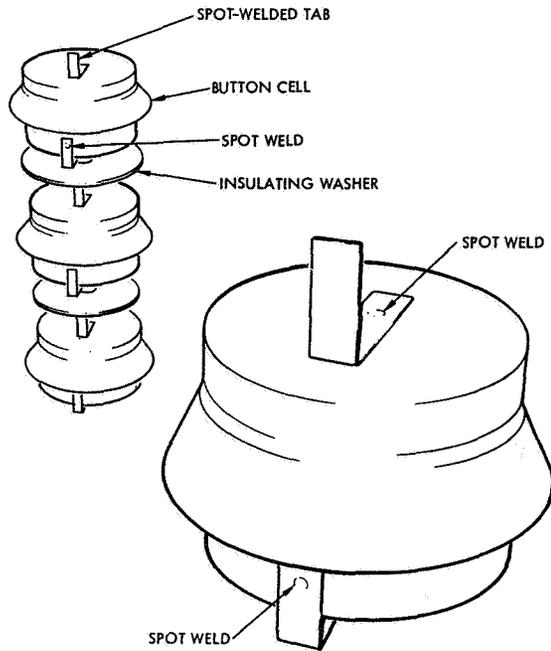
FIGURE 2-10.—Stacked button cells, welded structure.
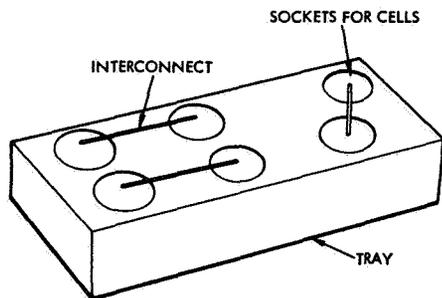
FIGURE 2-11.—Cell-tray battery structure.

BATTERY-CELL OPERATION

CELL DISCHARGE CHARACTERISTICS

Figure 2-12 shows a typical battery-cell discharge curve at constant current.

The initial period A during which the cell voltage decays below the starting voltage may have a combination of causes. Activation or concentration polarization may be developing, concentrations of reaction
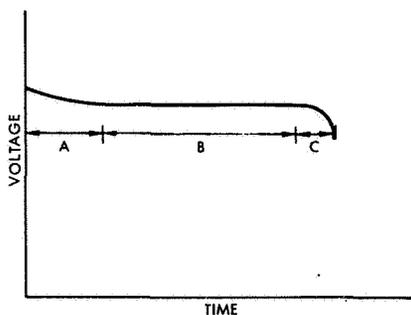
FIGURE 2-12.—Battery discharge curve
at constant current.

products may be changing (causing a shift in the reversible potential), or resistive films or layers may be forming. Occasionally, at high currents, these phenomena occur so rapidly that they are not observed.

When all polarization phenomena have reached a steady state, period B, the discharge plateau, begins. If the chemical reaction is a simple one in which the free energy change per equivalent remains constant and if continued discharge does not increase the resistivity of the electrodes or the electrolyte, this level is relatively flat. If changes occur in the reversible potential or in the resistivity of one of the cell components, this region slopes downward and may curve.

Region C is reached when the cell is almost exhausted. If the knee is well defined and sharp, the decrease in voltage results from a decrease in the quantity of reactants in the solution or on the surface of the electrode as these reactants are changed to the discharged state. This decrease in quantity of reactants causes an increase in current density (current per unit area) at the remaining surface of the charged-state materials and an increase in both concentration and activation over-potentials. If the knee is not well defined, voltage losses are partly caused by the increase of ohmic resistance in the cell.

Although this is the typical behavior of cell discharge, different types of cells deviate in varying degrees. These variations will be discussed in the appropriate sections.

CELL-CHARGING CHARACTERISTICS

A typical battery-charging curve at constant current is shown in figure 2-13.

Region A shows the establishment of polarization, region B the plateau voltage, and region C the exhaustion zone. The causes of the observed phenomena are similar to those of the discharge curve.

OVERCHARGE

If charging current is forced through a fully charged cell, the voltage rises beyond the reversible potential of a new chemical reaction, and stays at this new level of overcharge voltage, E_{ov}.
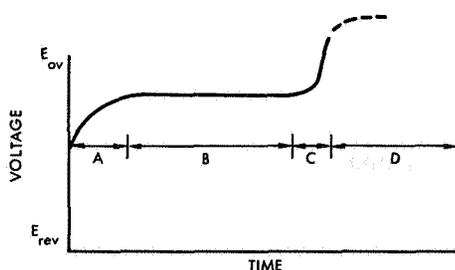
FIGURE 2-13.—Typical cell-charging curves
at constant current.

In cells having an aqueous electrolyte, this overcharge reaction is usually the electrolysis of water,

$$2H_2O = 2H_2 + O_2$$
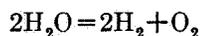
producing hydrogen and oxygen gas. In vented cells, the gases are released and the consumed water is periodically replenished in normal battery maintenance. In sealed cells where the gases are trapped, the cell case ruptures as a result of continued overcharge if no means are provided for coping with the evolved gases and the eventual buildup of pressure. Extended overcharge in the absence of overpressure tends to deteriorate cell electrodes and separators.

TEMPERATURE EFFECTS ON CELL CHARGE-DISCHARGE CHARACTERISTICS

Reversible potential:

$$\frac{dE_{rev}}{dT} = \frac{\Delta S}{zF}$$

Therefore, E_{rev} decreases with a rise in temperature when ΔS is negative and increases when ΔS is positive.

Polarization Phenomena.—Elevated temperatures increase the electrolyte conductivity and diffusion rate and decrease activation overpotentials. This results in an overall decrease in both activation and concentration overpotentials as the temperature rises. Thus, at low temperatures charging voltages increase and discharge voltages decrease, leading to an overall loss in cell reversibility.

EFFICIENCY

Several definitions of efficiency have been used:

Thermodynamic efficiency:

$$\eta_T = \frac{\int_{t_1}^{t_2} EI\ dt}{4.186\ N\ \Delta H}$$

(2-18)

N = number of mols reacted

Electrical work efficiency:

$$\eta_W = \frac{\int_{t_1}^{t_2} EI\,dt}{4.186\,N\,\Delta G} \qquad (2\text{-}19)$$

This expresses the ratio of electrical work obtained to the maximum theoretically obtainable electrical work. The above relationships are valid for all batteries, but are most frequently used in evaluating primary battery efficiency.

Storage battery efficiencies are also expressed as ampere-hour and watt-hour efficiencies for convenience in power system design. For any battery-operating cycle which charges a battery from t_1 to t_2, then discharges from t_2 to t_3, finally returning at t_3 to the state of charge which existed at t_1:

Watt-hour efficiency, $\eta_{W\text{-h}}$, is expressed by

$$\eta_{W\text{-h}} = \frac{\int_{t_2}^{t_3} EI\,dt}{\int_{t_1}^{t_2} EI\,dt} \qquad (2\text{-}20)$$

or the fraction of energy obtainable from the battery per unit of energy used in charging it.

Ampere-hour efficiency, $\eta_{A\text{-h}}$, is expressed by

$$\eta_{A\text{-h}} = \frac{\int_{t_2}^{t_3} I\,dt}{\int_{t_1}^{t_2} I\,dt} \qquad (2\text{-}21)$$

$\eta_{A\text{-h}}$ is significant because it is always unity when the charge-discharge reaction is the only chemical reaction involved. Deviations from unity indicate that nonuseful reactions occur at some time during the charge-discharge process.

BATTERY-OPERATING CONTROLS

CHARGE CONTROL REQUIREMENTS

Any battery charge control must perform the following functions:

(1) Deliver direct current to the battery at a potential equal to or greater than the sum of the reversible potential and the charging overpotential.

(2) Detect a change in the operating characteristics of the battery, signaling the exhaustion of reactive materials in the discharged state, and terminating the charge. In some batteries, the stored energy must be maintained at peak by using a continuous low-level overcharge current (trickle charge).

(3) Control the current delivery to the battery at a level which prevents overheating and/or excessive evolution of gases from the electrodes.

METHODS FOR DETECTING CHARGE COMPLETION

Present methods for detecting charge completion depend upon the detection of phenomena attendant upon the completion of charge or upon the onset of overcharge.

Battery Terminal Voltage.—One of the most popular sensor methods is detection of the voltage rise at the end of charge (zone D of fig. 2–13). There are three ways of using this method.

First, if the charging voltage is clamped at a constant level, the current will fall exponentially to a much lower steady level. This is the taper charge used almost universally in automotive applications. A typical charging curve is shown in figure 2–14, (A) current and (B) voltage.
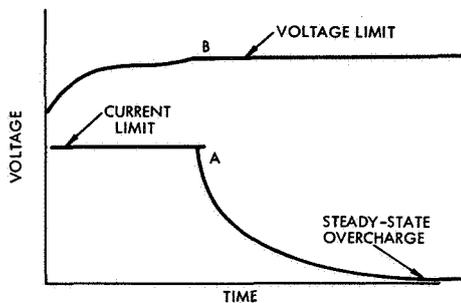
FIGURE 2–14.—Modified constant potential charging (A) current, (B) voltage.

A second, and less common, charge control uses the voltage to terminate charge or to switch to a lower charging current by lowering the applied voltage (fig. 2–15).
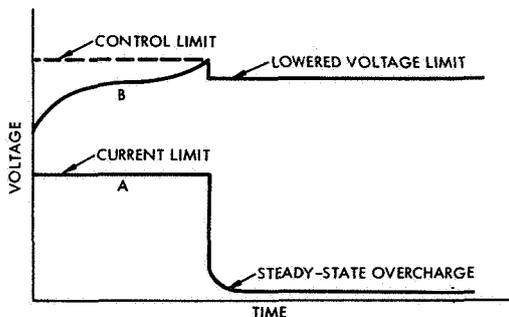
FIGURE 2–15.—Constant current charging with voltage-initiated switchdown.

A third variation of the same method is a stepwise switchdown of the charging current through several preset levels, each step initiated by a sensing of voltage. It is also possible to sense the rapid change in current occurring when the battery voltage reaches the source voltage limit.

Sensing the Presence of Gases.—Overcharge-generated hydrogen and/or oxygen has been used to initiate the termination of charge or the reduction of the charging current. Gas pressure inside a sealed battery cell has been detected by a pressure switch (ref. 8) and measured by auxiliary electrodes having a potential relative to one of the cell electrodes, which varies as a function of gas pressure. Charging is terminated when the auxiliary electrode potential has reached a predetermined level. This is discussed in more detail under the section on auxiliary electrodes. Micro fuel cells may also be used as pressure detectors. (See ch. 6.)

Temperature Sensing.—Temperature has been used as a charge control in those batteries in which heat dissipation rates change significantly at the end of charge (refs. 7, 9). The method is rarely used (except to prevent excessive overheating) because of the possibility of confusing temperature changes caused by changing environmental conditions with those caused by internal heating.

Temperature sensors can also be used to compensate other charge controls for variation in cell or battery characteristics as a function of temperature.

Sensing the Current-Time Integral.—If the battery capacity is predictable or known, an ampere-hour meter can keep a running account of the current into and out of the battery, terminating the charge or reducing-to-trickle charge when the ampere-hour meter indicates that the battery is full. Two types of ampere-hour meters are described: the electronic ampere-hour meter and the coulometer, or electrochemical ampere-hour meter.

The success of the method depends upon how accurately the current integrator represents battery performance.

Slow Charge.—Charging the battery at a current no greater than that which it is able to tolerate for an indefinite period avoids the use of all controls. The success of the method depends upon the battery's tolerance of extended overcharge and the available slow-charge time.

A combination of the charging methods described above may be used. In many cases, only such combinations are effective. The relative merits of the charge controls vary with the battery and the application.

THE DIVERGENCE PROBLEM

As long as all cells in a series-connected battery are matched, i.e., full discharge and full charge are reached at the same moment, a single function or combination of functions may be used to control the battery. If, as is usual, the several cells have different capacities due either to product variations or to use and aging effects, an additional problem is introduced.

If one cell reaches full charge or full discharge first and is not detected by the charge control sensors, the low-capacity cell is subjected to overcharge or overdischarge, and gas evolves. The charge control methods which measure variables such as battery voltage and temperature can easily miss the small change which accompanies acquisition of full charge by one cell, since the effect is masked by the lower voltages of the remaining cells. As the total number of series-connected cells increases, the problem enlarges as a result of the increasing probability of having one cell of divergent capacity and the decreasing sensitivity of detection.

CELL-LEVEL CHARGE AND DISCHARGE SENSORS AND CONTROLS

In an effort to solve the divergence problem, various methods of controlling and/or sensing individual cells have been tried.

Some control methods are a natural result of the sensor design. Pressure controls, either pressure switch or auxiliary electrode, are basically cell sensors and measure the internal pressure of individual cells. Other controls, such as voltage sensors, can be designed to measure individual cell characteristics. Sensing at the cell level increases sensitivity to the anomalous behavior of one cell, and makes it possible to terminate the battery charge on a signal from the first cell to reach a critical state of voltage, pressure, etc. The large number of sensors used tends to decrease system reliability, since a false full-charge signal caused by failure of any one of the sensors can effectively prevent charging of the battery. This may be overcome by voting the sensor outputs, and effecting a compromise between sensitivity and reliability. In this modification, two or more cell sensors must give a full charge signal before battery charging is terminated. At the cell level, controls have been applied in addition to sensing.

STABISTORS

The stabistor consists of two series-connected silicon-diode junctions. Its characteristic forward voltage drop is used to limit the voltage applied to the cell. As cell voltage increases, more of the charging current is diverted to the diode, resulting in a crude form of limited voltage charging. The knee of the stabistor curve is relatively "soft," leading to a wider range of voltage than desirable (ref. 10).

The Amp-Gate[3] diode is a stabistor mounted on a heat sink, with the diode driven almost into thermal runaway. The negative voltage-temperature coefficient of a silicon diode is used to shift the characteristic diode curve to the left, sharpening the knee of the curve (fig. 2–16).

As a result of the "soft" character of the diode knee, current is bypassed from the start of charge; therefore, the stabistor and Amp-Gate diode waste power. Figure 2–17 is an approximation of the energy lost from premature conduction of the stabistor. The amount of energy lost is significant if the system is energy limited, as are most space-power systems.

---

[3]Trademark. P. R. Mallory & Co.
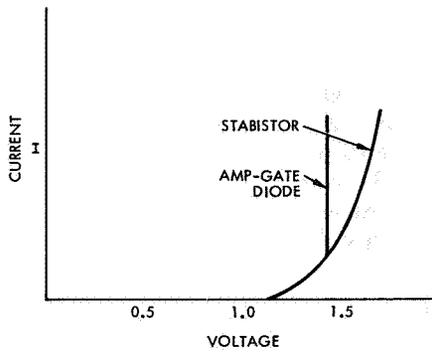
FIGURE 2–16.—Stabistor and Amp-Gate diode
characteristic curves.
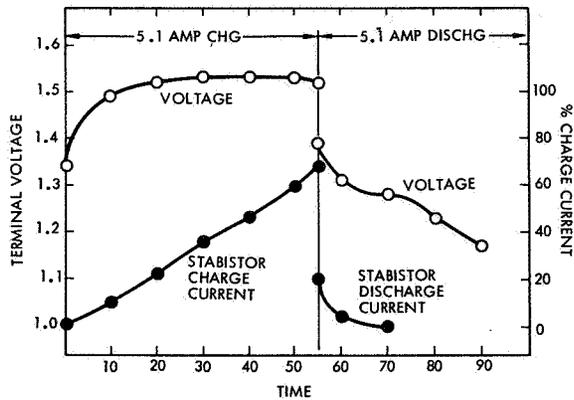
FIGURE 2–17.—Stabistor characteristic curve showing
bypass conduction throughout charge, and losses during
discharge.

The stabistor and Amp-Gate diode do provide a significant protection against overcharge.

TEMPERATURE EFFECTS

The relationship of temperature to charge control is variable from cell system to cell system and is discussed in the appropriate sections.

AUXILIARY ELECTRODES

By use of appropriate catalysts, auxiliary electrodes can be made which permit recombination of either hydrogen or oxygen. These electrodes may also be used as detectors for the presence of these gases.

Two types of auxiliary electrodes have been described for use as charge control sensors in alkaline batteries, particularly nickel-cadmium

cells: a fuel-cell oxygen electrode developed by the General Electric Co. and an adsorption electrode developed by Gulton Industries, called the Adhydrode. These electrodes, both designed for detection and recombination of oxygen, have markedly different properties.

The fuel-cell electrode (refs. 11, 12, and 13) is a proprietary product containing a platinum catalyst which promotes the oxygen recombination reaction.

$$O_2 + 2H_2O - 4e \rightarrow 4(OH)^-$$
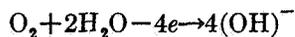
The cell's nickel electrode provides the electrons and water necessary to continue the reaction, and consumes the OH^- ions generated. The voltage response of the fuel-cell electrode to oxygen pressure is nonlinear, reaching full voltage at 60-mm oxygen pressure, after which the voltage is unaffected by further increases in pressure. Its oxygen recombination rate is equivalent to more than 50 mA/cm^2 without significant polarization losses (ref. 12). In addition to oxygen, hydrogen may also be recombined at the fuel-cell electrode at equivalent rates in excess of 100 mA/cm^2 with negligible polarization (ref. 11), allowing overdischarge of the cell and consequent generation of H_2 without overpressure.

The use of two fuel-cell electrodes in each cell has been proposed for charge control of nickel-cadmium cells (ref. 11). A large area electrode, directly connected to the cadmium electrode, is used for oxygen recombination, and a small area electrode, connected to the same terminal through a current sensor, is used for control. The large recombination electrode prevents saturation of the control electrode until a predetermined gas evolution rate has been reached. This prohibits premature termination of the charge due to early initiation of oxygen evolution from the nickel electrode, which has been observed at elevated temperatures (ref. 11). Circuits have been designed with magnetic amplifiers and/or current relay sensors, which terminate charge or reduce charging current to a trickle level when a full-charge signal is given by the electrode of any cell in the battery (refs. 7, 14, 15, and 16). This can be changed by the appropriate adjustment of threshold levels to a voting system, requiring more than one cell to give a full-charge signal.

The rate of heat evolution caused by the overcharge reaction, whether the recombination occurs at an auxiliary electrode or at the cell anode, is equal to the total overcharge power delivered to the cell. Where a load resistor is used in the control electrode external circuit, a small portion of the power is dissipated in the resistor. However, for practical purposes, when a battery is continuously overcharged, all of the energy delivered to it is converted to heat, which is mostly dissipated in the battery.

Repeated cycling of the fuel-cell electrode results in a loss in oxygen pressure sensitivity, and in an apparent false indication of internal oxygen ascribed to saturation of the electrode with oxygen (ref. 15).

Effects of temperature upon fuel-cell electrode characteristics have not been reported, but are essential for integrated system design in environments having limited heat-removal capabilities.

In the second type of oxygen-sensing electrode for alkaline batteries, hydrogen is generated at the auxiliary electrode and held interstitially and by surface adsorption.

$$H_2O + e = OH^- + H_{(ads)}$$
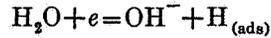
The oxygen then reacts at the electrode surface.

$$4H_{(ads)} + O_2 = 2H_2O$$
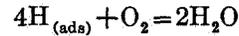
The electrons are supplied by the cell anode. When connected to a cadmium electrode, the Adhydrode has a potential 0.8 volt negative with respect to the normal hydrogen electrode. The Adhydrode current shows a linear response to pressure of oxygen in the range from -10 to $+30$ psig. The slope of the current-pressure line changes with temperature from 0.1 mA/psi at 0° C to 2.5 mA/psi at 40° and 55° C (ref. 17).

Because of this large variation, the Adhydrode oxygen-pressure sensor requires compensation of the pressure-current relationship for temperature (ref. 17).

The operation of both types of electrodes for recombining oxygen and of similar electrodes for recombining hydrogen depends upon the potential of the electrodes with respect to that of the electrolyte. In some cases, the recombination electrodes may be connected to the appropriate cell terminal through a current sensor or load resistor. However, where the positive terminal is greater than $+0.8$ volt relative to the hydrogen-recombination auxiliary electrode, or the negative terminal is greater than -0.8 volt relative to the oxygen-recombination auxiliary electrode, recombination may be inhibited and gas evolution may occur at the auxiliary electrode. In this case, the auxiliary electrode may be clamped at the appropriate potential by use of a resistor-diode network. This recombination technique was used successfully in the development of a sealed lead-acid cell (fig. 2–18) using wetproofed electrodes to prevent flooding. The current through the resistor is small and limited to that required to forward-bias the silicon diode.

Another device for gas detection and recombination is the miniature fuel cell. Two fuel cells are used, one for oxygen recombination with an external hydrogen feed connected, and the other for hydrogen recombination with an external oxygen feed connected (ref. 18). When this device
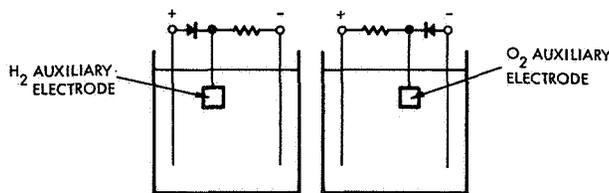
FIGURE 2–18.—Diode clamping of auxiliary electrode potential.

is used in its present form (in a closed system), the water produced causes flooding unless a special reservoir is used. In addition, the operation of the fuel cell is degraded by the presence of a mixture of gases rather than one pure gas. The method does have the advantage of not utilizing the electrolyte of the galvanic cell as the fuel-cell electrolyte, and therefore is instantly adaptable as an add-on charge control, or gas recombiner.

BATTERY-FAILURE MODES

Individual battery systems are subject to individual types of failures. However, a number of failure modes are common to all batteries designed to deliver large amounts of electrical energy (as distinguished from voltage reference cells and other low-current cells).

Separator deterioration is common to most types of batteries. The positive electrodes of a battery contain a powerful oxidant. In the presence of an electrolyte, this chemical reacts with the separator at a rate which increases rapidly with temperature. In an attempt to reduce the rate of deterioration in long-life batteries, plastics or other "inert" materials are used as separators.

Loss of capacity due to crystal growth is present in many types of batteries. Originally, the electrodes of many types of batteries are composed of finely divided reactive materials. If a crystalline substance is immersed in a self-saturated solution, an equilibrium condition is reached in which the rate of solution equals the rate of deposition from solution; therefore, the net solution rate equals zero. However, there is a tendency to dissolve the finely divided particles having a higher surface-energy content and to redeposit this material on the surfaces of the larger particles. In effect, this causes the larger particles to grow at the expense of the smaller particles, the net result being a considerable loss in true surface area. This crystal growth is greatly accelerated by thermal cycling or low-rate charge-discharge cycles. A severe increase in polarization occurs as a result of the increase in current density, making the cell useless.

Loss of active material from the electrodes can occur as a result of one or more of the following mechanisms:

(1) Mechanical separation due to vibration, electrostatic stresses, differential expansion of electrodes and active material.

(2) Erosion of active materials. In the charge-discharge cycling of some secondary batteries, there is a considerable transport of liquids between electrodes. This fluid flow is due to generation and consumption of water at the electrodes and can erode the active materials.

(3) Solution and redeposition of active materials can occur. Although the net amount of active material in the solution may not change, some active material may be dissolved and redeposited in a place out of contact with the electrodes. This relocated material is lost to the cell, unless it can be redissolved and redeposited on the electrode.

Perforation of the separator by dendritic growth of metallic materials can short-circuit the cell. Dendritic growth results from the charging

process and occurs when the active material is electrodeposited preferentially on specific crystal surfaces. The result is a growth of long, slender needles through the separator.

Mechanical damage resulting from mishandling, severe environmental condition or generation of internal pressure can result in cell failure.

Carbonation.—Vented or leaking alkaline batteries are subject to carbonation of the electrolyte. The strong caustic absorbs carbon dioxide from the air and produces potassium carbonate. This process decreases the electrolyte conductivity.

$$2KOH + CO_2 \rightarrow K_2CO_3 + H_2O$$
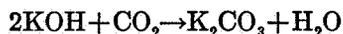
Leaking batteries can be completely discharged by major leaks if the electrolyte forms a continuous conductive path between the terminals of two or more series-connected cells. If the resistance of the leakage path is low enough, the battery may be completely destroyed as a result of internal heat generation occurring during the discharge process. Less severe leaks tend to increase battery resistance and decrease capacity.

Data on battery failures are found in the applicable sections of chapters dealing with the various types of batteries.

SPECIAL TEST METHODS

The NASA-sponsored battery literature contains little in the way of detailed analytical test procedures and special test methods. These will be found for the most part in the literature on analytical chemistry and instrumental analysis. Many of the common analytical and instrumental techniques are of great value in battery analysis and failure mode determination.

Photomicrography is a valuable technique. Dry photomicrography utilizes the common methods of metallographic specimen preparation, and is used to examine seals, electrodes, separators, welds, and most of the solid parts of the battery. Wet photomicrography may be used to study electrode operation. Portions of electrodes are enclosed in a transparent container during the examination process.

Gas-analysis techniques are used for determination of the quantity and composition of the gases generated during wet stand and/or operation of the cell. This may give significant clues to the reaction mechanisms and failure modes. Inert-gas detectors are frequently used for the detection of leaks in cell seals. A small quantity of helium or argon is enclosed in the cell and the gas is detected by mass spectrometry.

X-ray diffraction analysis may be performed on cell electrodes in both the wet and dry state and is used to study the composition of electrodes and the particle size of the active materials present. The capacitance of the electrode double layer is found by measuring the voltage rate of change resulting from the leading edge of a current pulse drawn from an electrode, and calculating the capacitance of the final current divided by the initial rate of change of voltage.

The double-layer capacitance method is used in forming an estimate of the true, or microscopic, surface area of the electrode. Surface area

is also measured by the nitrogen absorption technique (BET), at the temperature of liquid nitrogen.

A series of screening methods for separators in alkaline batteries is given in reference 35. This includes individual papers on determination of dimensional stability, strength, electrolyte retention, pore size, electrical resistivity, degradation by soluble silver, degradation by oxidants and alkaline solutions, electrolyte diffusion, silver diffusion, zinc diffusion, and zinc penetration.

Galvanostatic methods, measuring the response of electrode voltage to a step change in current, and triangular wave voltammetry, measuring the current response of an electrode to a slowly changing applied voltage, are both used in studying the reaction mechanisms and processes occurring at the electrode surfaces.

BATTERY-TESTING METHODS

The determination of the battery-operating characteristics has always been a highly variable art, dependent upon the extent and quality of the information required. To determine the operating characteristics for some secondary and most noncritical primary battery applications, it is only necessary to connect the battery across some kind of load, preferably the one for which it is intended, and see how long it lasts. As the need for a higher system efficiency increases, the demand for amount and quality of information also becomes greater. In some cases, extremely accurate measurement of several battery properties and their variation with service and environmental conditions is necessary.

The lack of data on batteries with very complex behavior makes it difficult to predict electrical characteristics in new environments. In some cases it is common to measure operating characteristics and service life under simulated or actual conditions of service. In a few cases (such as those where environmental test results would be obsolete because of the test time required) it is possible to accelerate the testing program. This, however, implies a knowledge of the mechanisms of the failure processes.

TESTING ACCURACY

Control

Testing accuracy requirements are largely determined by the required accuracy of the design data. These requirements should be consistent. For example, if the battery voltage is influenced by several parameters, there should be no compromise in the accuracy with which the relationships between the various influencing factors and the cell voltage is determined. To illustrate, the normalized current-voltage curves of a nickel-cadmium battery have a slope with an absolute value approximately equal to 0.50/0.08. (See fig. 4-4.) Voltage measurements made within an accuracy of 0.001 volt are not valid to this accuracy level unless normalized current (current/cell capacity in ampere-hours) is controlled to an accuracy of $(0.001)(0.5)/(0.08) = 0.0062$. For instance,

in a 6-A-h cell operating at a discharge current of 3 amperes, the discharge current must be controlled to $(0.5)(0.0062) = 0.0031$ ampere $= 0.10$ percent. If lesser accuracies are required, the accuracy of control of those variables which affect cell voltage may be reduced proportionately. It is important, however, that the level of control be consistent with the accuracy and precision desired of the final data.

The requirement for a specific degree of accuracy in battery testing varies with the use to be made of the data. However, a fairly high degree of accuracy is desirable in any form of battery test because the polarization phenomena which must be measured in order to characterize a battery occur within a range of a few hundred millivolts, but must be measured (in a finished cell) in combination with the cell's electromotive force, which is usually over 1 volt. This degrades the accuracy with which the characteristics of interest are observed.

Temperature control accuracy of nickel-cadmium cells will probably be determined by the relationship between temperature, cell voltage, and the overcharge current. During overcharge, cell voltage has a temperature coefficient of from 1 to 2 mV/°C, which leads to a temperature control requirement of 0.5 to 1.0° C for 1.0-millivolt accuracy. Clearly, the achievement of this accuracy of temperature control at the interior of a cell is impracticable, so if 1-millivolt accuracy is required in the measurements, it must be achieved by careful measurement of temperatures and/or computation of the temperature at cell interior.

Control of applied voltage (where cells are tested under a constant potential or modified constant potential conditions) should have a precision similar to the accuracy of measurement.

Setting accuracy is of equal importance to control accuracy. Voltage settings are made simply with a differential voltmeter or a precision digital voltmeter. Current settings with accuracies of the order of 0.1 percent are somewhat more difficult to achieve, since even a precision shunt is subject to significant errors when operated at high currents unless special precautions are taken for removal of heat or for correction of the measured shunt drop for shunt temperature.

STANDARDS

Continuously monitored secondary standards are highly desirable for the detection and correction of instrument drift, and may be of considerable use in salvaging otherwise useless data resulting from instrument error. Some practical secondary standards include:

Voltage_____ Mercury cell in controlled temperature box. Temperature-compensated zener diode.
Current_____ Precision power supply operating into a shunt with special heat-sink arrangements.
Temperature_____ Thermocouple with both junctions at controlled temperature.

MEASUREMENT

Voltage measurement accuracy is feasible to the 1-millivolt level and below, if required. The measurement of the temperature of circulating

liquids or gases is feasible to 0.1° C, and 1 order of magnitude better than that is achievable by use of expanded-scale thermometers. However, it is much more difficult to measure accurately the temperature of a cell immersed in a circulating fluid, whether liquid or gas, under conditions of heat transfer between the surface and the fluid environment. If the temperature-sensing element is exposed to the fluid environment, it will reach a temperature closer to the temperature of the fluid than of the surface upon which it is mounted. In any case, it will not indicate the interior temperature of the cell. In one method of estimating internal temperature, the thermocouple junction is mounted on the insulated cell terminal, and the entire cell top is enclosed in an insulating material to isolate it from the controlling environment. This technique depends upon conduction of heat along the internal electrode leads of the cell and may result in an appreciable thermal lag because of the poor conductivity and the heat capacity of the leads, terminals, and other mechanical elements. An additional error due to loss of heat along the external connection wires may be minimized by selection of low-conductivity metals and use of a tortuous heat path. This should represent an improved means of cell-temperature sensing without the need for inserting thermocouples into the cell's interior. Figure 2–19 shows a diagram of the measurement setup.
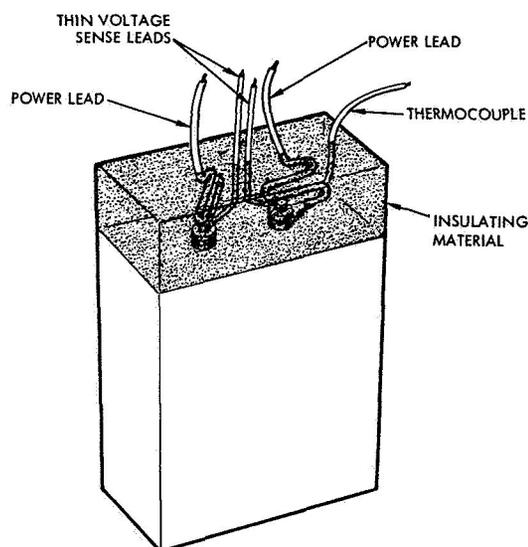
FIGURE 2–19.—Method of measuring cell's interior temperatures.

Each battery system with its unique properties will be sensitive to various environmental and service variables in its own way. In cases where the sensitivity of the battery to these variables is not well understood, it is essential to make certain preliminary measurements to

determine such sensitivities and establish the required accuracy of measurement before a program to measure the electrical characteristics can start. Known sensitivities are discussed in the appropriate chapters.

DISCHARGE CHARACTERISTICS

Discharge characteristics are commonly measured under conditions of constant current, constant resistance, and simulated actual load. Although the constant resistance method is the simplest and least expensive, it varies both the discharge current and voltage with time. This disadvantage makes the interpretation of the data difficult, and the interpolation of electrical property data almost impossible. Constant current discharge holds all variables except voltage constant and makes it possible to simplify the interpretation of electrical characteristic data in terms of voltage as a function of time, with other variables such as temperature, current, and service life as additional variables. A typical constant current discharge circuit is shown in figure 2-20. Simulated or actual load operation is the final proof of design adequacy, but is usually unsuitable for acquisition of parametric design information.
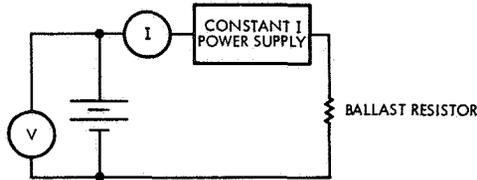
FIGURE 2-20.—Typical constant-current discharge circuit. NOTE.—Ballast resistor must be sized so that, at the regulated current, the voltage across the ballast resistor is always greater than the sum of the maximum possible battery voltage and the minimum usable output voltage of the constant current power supply.

CHARGING CHARACTERISTICS

The charging characteristics of a battery are usually measured at constant current, with the addition of a charge control for protection of the battery against overcharging. The various influential parameters, i.e., temperature, depth of discharge, and charge currents, are controlled for accuracy, and are varied independently. Typical testing circuitry for modified constant potential charging is shown in figure 2-21.

INTERACTION OF CHARGE AND DISCHARGE TEMPERATURES

Occasionally, a situation will be found in which the temperature of the preceding half cycle influences the electrical characteristics of the following half cycle. In this case, the temperature of the cell may be
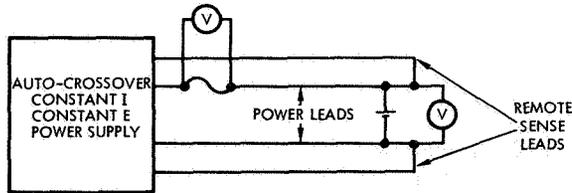
FIGURE 2-21.—Modified constant potential charger.

smoothly or suddenly varied between two levels as a function of time. An experimental setup and control system is shown in figure 2-22.
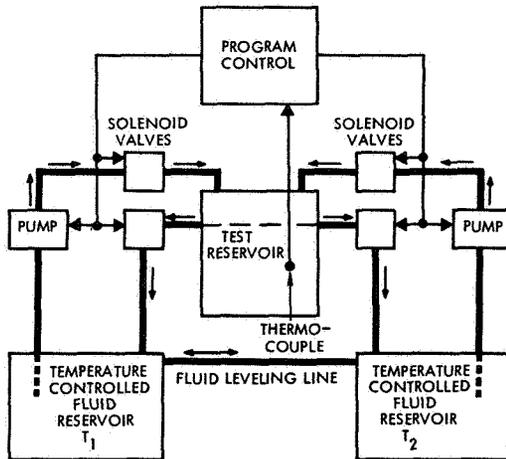
FIGURE 2-22.—Testing system for variation of cell
temperature with time.

OVERCHARGE CHARACTERISTICS

Two methods have been used for determining the relationship between overcharge current and voltage. The cell may be charged until it reaches a limiting potential and held at constant potential thereafter until the charging current falls to a constant value. Several values of potential limit are used. Cells intolerant of extensive overcharge are usually tested this way to prevent damage. A second method, for cells able to tolerate high levels of overcharge, charges the cells at a constant current and waits for the voltage to stabilize. Several values of overcharge current are used. In either case, if the overcharge process generates appreciable quantities of heat, and if the overcharge characteristics are sensitive to temperature, control of the temperature and/or compensation

of the data for the temperature are essential. Frequently, overcharge data will take the form of a straight-line plot of log of current versus voltage.

CAPACITY

Capacity may be determined by integrating the current of the discharge curve over the discharge time period. Usually, capacity is reported to some arbitrary end voltage which represents the minimum acceptable voltage that the system will tolerate.

EFFICIENCY

Efficiency may be determined in several ways. The battery may be operated in a variable depth of discharge mode, starting with a discharged cell, charging it to a fraction of its full capacity, and discharging it again. The integral of discharge current over the discharge period, divided by the integral of the charge current over the charge period, equals the ampere-hour efficiency for that cycle. By varying the total charge-discharge energy, several cycles of varying input ampere-hours are run. Efficiency is then determined by plotting the input ampere-hours on the ordinate versus the output ampere-hours on the abscissa and measuring the slope of the resulting curve. A slope of 1.0 indicates 100 percent current efficiency. A slope of 0 indicates 0 percent efficiency. Extreme caution must be used in determining the endpoint of the discharge cycle and in controlling both charge and discharge currents accurately, since a small error in end-of-discharge voltage or in current can lead to large errors in the efficiency (ref. 9).

Naval Ammunition Depot (NAD), Crane, Ind., measures efficiency in the same manner, but shows a plot of ampere-hour output versus time. Since charge current is not constant in a voltage-limited charging mode, this method shows true efficiency only during the constant current portion of the curve.

Vinal (ref. 19) reports a similar method starting with a fully charged battery discharging a known number of ampere-hours, restoring precisely the same number of ampere-hours, and then discharging at the same current until the end-of-discharge voltage of the second discharge equals that of the first discharge. This method permits efficiency determinations to be taken at a fractional depth of discharge in an operating mode more similar to the probable operating mode of the battery. However, at fractional depths of discharge, the end-of-discharge voltage falls on the plateau of the discharge curve, where the voltage has a very small rate of change with time. Because of this, a minute uncertainty in the voltage measurement can cause large errors in the efficiency.

Another possible approach to the determination of efficiency is the measurement of losses appearing either as heat or as mechanical work. In sealed cells, the only form of mechanical work possible is the pressure-volume work; consequently, measurement of heat losses and pressure should provide a determination of efficiency as a function of time. No concerted effort has been found toward correlating the measured losses with other efficiency measurements, although losses have been measured.

HEAT EVOLUTION

Two basic types of calorimeters have been used for the measurement of heat evolved in battery cells. The adiabatic calorimeter, various forms of which were used by Bruins et al. (ref. 20), Metzger and Sherfey (ref. 21), and Sparks and Bauer (ref. 9), consists of a double-chambered calorimeter. If the cell is in a fluid environment, a thermocouple, stirrer, and precision thermometer occupy the inner chamber. The inner chamber, thermocouple, and heating and cooling apparatus are all enclosed in an outer chamber. The temperature of the inner chamber is measured as it rises or falls in response to the heat evolved or absorbed by the test cell; the outer chamber temperature is controlled by heating or cooling coils to equal the inner chamber temperature. Since inner and outer chambers are equal in temperature, no heat transfer occurs between them. Knowing the heat capacity of the contents of the inner chamber, the rate of temperature change may be used to compute the rate of the heat evolution causing the change.

One disadvantage of the adiabatic calorimeter is the temperature change occurring in the cell under study. If the rate of heat evolution is a function of temperature, or if continuous operation of the calorimeter over longer periods of time is required, the isothermal flow calorimeter is the more attractive instrument. In the flow calorimeter, fluid from a large constant-temperature reservoir passes across the cell whose heat-generation rate is to be measured, and the fluid temperature is measured both before and after it flows across the cell. If the mass flow rate of the fluid (determined by the controlled pumping rate) and the heat capacity of the fluid are known, the rate of heat evolution may be calculated. Figure 2–23 shows the isothermal flow calorimeter used by Foley and Webster (refs. 22, 23) in measurement of heat evolved in battery cells. The primary disadvantages of the isothermal flow calorimeter are a slightly greater timelag between heat evolution and the measured fluid temperature rise, the need for more sensitive temperature-measurement elements to measure the much smaller temperature rise of the fluid stream, and a somewhat higher cost. Beck and Kemp (ref. 24) measured heat evolution from a battery cell by encapsulation of the cell in a foamed insulation and measurement of temperature rise. This is a crude approximation of the adiabatic measurement. Sparks and Bauer (ref. 25) used a combination of flow calorimetry and adiabatic calorimetry in measuring the temperature swings encountered in a simulated satellite environment.

PRESSURE MEASUREMENT

In unfinished cells, pressure is measured routinely by the manufacturers of battery cells simply by attachment of a bourdon gage or pressure transducer to the fill opening of the cell and measuring or recording pressure. Two methods have been devised for measuring pressure in a battery cell without making an opening in the sealed cell. These enable a cell user to measure internal pressure without endangering the cell balance by a loss of oxygen through the gage fittings. Bauer (ref. 26) measured the internal pressure by fitting a cell with a strain gage on its
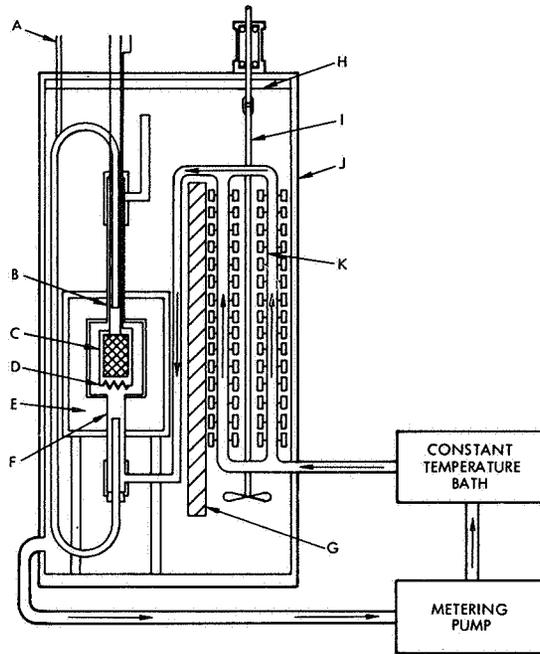
FIGURE 2-23.—Isothermal flow calorimeter used by Foley and Webster in measurement of heat evolved from battery cells.

A. Thermopile leads
B. Hot junction
   thermopile
C. Test cell
D. Calibration heater
E. Air space
F. Cold junction
   thermopile

G. Partition
H. Fluid level
I. Stirrer shaft,
   stainless
J. Thermal ballast tank
K. Heat exchanger

most flexible wall and enclosing it in a hydraulic chamber. As pressure is generated in the cell, the strain-gage output indicates deflection of the wall, and the hydraulic chamber is pumped up until the gage indicates zero or null deflection. The interior and exterior pressures are then equal, and the pressure may be read on a bourdon gage or recorded with a pressure transducer from the hydraulic chamber. The method is precise, but is too unwieldy for routine use with a large number of cells. J. M. Sherfey (private communication) used a load cell (an electrical transducer for measuring force) to measure the internal pressure of prismatic cells. The battery cell and load cell are clamped between metal plates, and the battery cell is charged. The expansive force caused by gas pressure in the battery cell is translated to the transducer and

measured as an electrical output.   The method is affected by the initial clamping force used to hold the cell and transducer, the temperature, and the variations between cells, and shows a slight hysteresis between increasing and decreasing pressures.   Overall accuracy of careful measurements is estimated at ±10 percent.   This method requires direct calibration using both a pressure gage and a load cell and is performed on a typical cell, the same size as those to be measured, except that it has an opening for gas pressurization.

IMPEDANCE

Several methods of measuring cell and battery impedance are currently used.   Brodd and deWayne use a capacitance-resistance bridge, and plot the resulting impedance as capacitive reactance versus resistance. The primary use of this method is the comparison of the diagram with the theoretical impedance analysis based upon electrode kinetics to provide verification of the electrode reaction mechanism (ref. 27).

NAD Crane and Martin-Marietta (ref. 28) measure impedance on the basis of voltage change resulting from a step change in current. Rather than present the entire curve of voltage versus time, a single point voltage at 5 milliseconds after the step change in current is reported; no circuit is shown by NAD Crane.   The impedance is calculated by the equation

$$Z = \Delta E / \Delta I$$

Martin-Marietta uses an impedance testing arrangement such as shown in figure 2-24 (ref. 28).   Willihnganz and Rohner measure battery impedance using both current step-change methods and ac bridge methods,
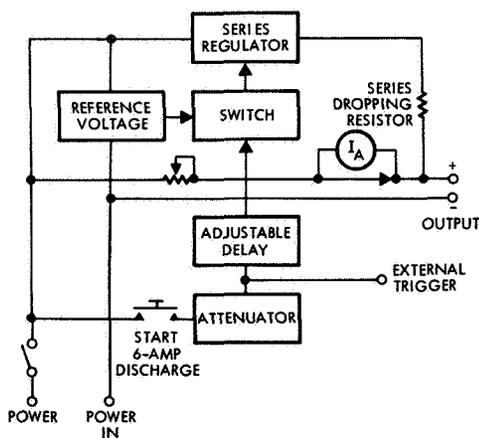
FIGURE 2-24a.—Internal resistance test unit block diagram.
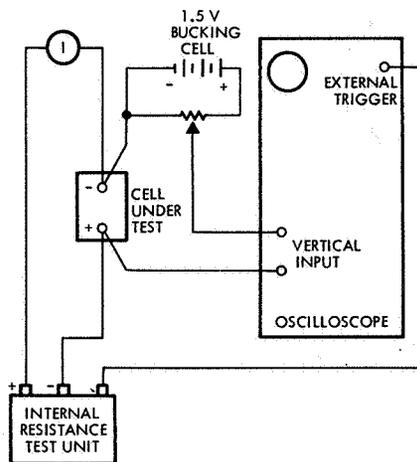
FIGURE 2-24b.—Martin-Marietta imped-
ance arrangement.

and found greater precision and ease of measurement with an ac RLC
substitution Wheatstone-bridge method than with the step-change
method. Separate resistance, inductance, and capacitance measure-
ments were made. Inductance is measured at 5000 hertz, capacitance
at 1000 hertz (ref. 29).

Sparks and Bauer (ref. 9) use a simplified ac bridge method for measur-
ing overall impedance versus frequency.

LEAK TESTING

Leakage tests of battery cells can be made in three ways:

(1) Chemical tests for leakage of an electrolyte will detect gross
leaks from the cells. These tests are performed by spraying the cell
with an indicator solution which changes color upon contact with a
strong alkali or acid, or by wiping the cell with a dampened strip of
paper impregnated with the indicator. Some of the indicators used are
litmus (refs. 30, 31), phenolphthalein (refs. 28, 9), and bromothymol
blue. In general, the tests should be made with the cell short circuited
to prevent a false indication caused by the electrolysis of the indicator
solution and production of traces of alkali or acid at one of the
terminals.

(2) Smaller gas leaks, usually helium, may be detected by a spec-
trometer (ref. 32). If, immediately prior to sealing, the cell is backfilled
with a calibrated quantity of helium, small leaks of the order of 10^{-8}
cc/sec may be detected by means of mass spectrometry. Argon has
also been used, but the test is complicated by the presence of appre-
ciable quantities of argon in the atmosphere at sea level (ref. 9). A
detailed analysis of seal leakage testing is given in reference 32.

(3) Gross leak detection may also be performed by immersion of
the cell in a nonwetting fluid, such as mercury, and evacuation of the

chamber holding both mercury and the cell. Leaks are detected by the formation and rise of bubbles through the mercury.

TRANSIENT VOLTAGE PHENOMENA

The measurement of battery voltage transients resulting from sudden load changes may be necessary if sensitive equipment must be operated from a battery power line which is subjected to large current transients. Such measurements are frequently complicated by switching noises and ringing introduced by the measurement of circuits. R. S. Sawyer (NASA Manned Spacecraft Center, private communication) suggests the use of the circuit of figure 2-24c for measurement of voltage transients without introduction of excess noise.
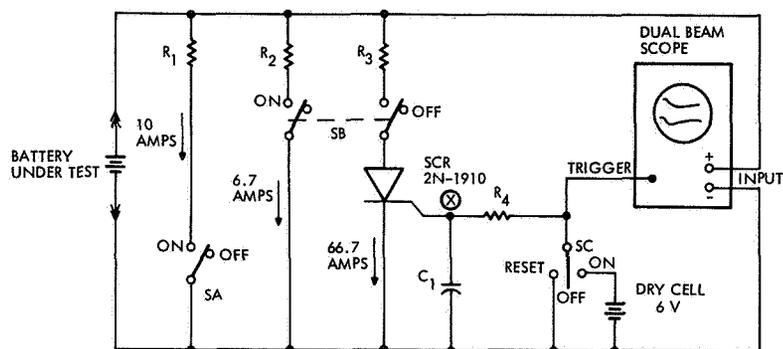
FIGURE 2-24c.—SCR switching circuit for applying battery transients.

Switches SA and SB are positioned to "on." This results in a 16.6-ampere load being applied to the battery (10 amperes through R_1 and SA, and 6.6 amperes through R_2 and one-half of switch SB). The other half of switch SB is closed at the same time the 16.6-ampere load is applied, but the additional 66.7-ampere load is not applied, since the SCR has not been turned on.

After the 16.6-ampere load has been on for 3 minutes, switch SC is placed to the "on" position; this sends a trigger signal to start the scope trace, and a few microseconds later the SCR is turned full on. With the SCR on, an additional 66.7-ampere load is applied to the battery through R_3, one-half of switch SB, and the SCR for a total load of 83.3 amperes. The RC network components R_4 and C_1 are selected so that point X of capacitor C_1 is charged to 3.0 volts in approximately 10 milliseconds. The voltage at point X is also the gate voltage to the SCR, and the maximum gate turn-on voltage is 3.0 volts. The turn-on time of the SCR (90 percent full on) is 1.5 to 2 milliseconds. Therefore, the maximum time delay from scope trigger to SCR full on is approximately 12 milliseconds.

ACCEPTANCE TESTING

The amount of acceptance testing performed on cells and batteries varies with the criticality of the application using the batteries as well as the level of confidence of the battery engineer or system engineer. Typical aerospace acceptance tests generally applied are as follows:

> Weight
> Dimensions
> Capacity
> Charge retention
> Impedance
> Leakage
> Environmental:
>> Shock
>> Vibration

The environmental acceptance testing required on batteries for terrestrial applications is defined in generalized specifications developed by the SAE, ASA, and other agencies and in military specifications for both terrestrial and aircraft applications. However, aerospace testing requirements are not normally established in general specifications, because of the large differences in environment inherent in launch vehicles, and because the lightweight structures tend to develop resonances which amplify the shock and vibration differently in each application. At the present time, each application has environmental test requirements tailored to the application. In general, the approach to acceptance testing of battery cells and batteries has been the measurement of those factors of use in assuring good cell quality, followed by an environmental test which exposes the cell or battery to the anticipated stresses. In addition to the shock and vibration tests, complete batteries are usually exposed to a thermal vacuum test, in which the battery is mounted on a radiating plate and operated while exposed to a combination of the expected thermal environment and a hard vacuum.

Depending upon the environment to which the cell or battery may be exposed, other test requirements may be imposed.

DESIGN QUALIFICATION TESTS

In both the design qualification tests and the environment acceptance tests, the operating battery is exposed to shock, vibration, thermal-vacuum, and any other appropriate test. In design qualification testing, the stress level applied to the battery is higher than in acceptance testing. One or more prototypes are tested using the theory that if they withstand the rigorous environment of the qualification test, identical units will easily survive the less-severe operational environment. Experience has shown that, in general, battery cells have little difficulty surviving the mechanical shock and vibration associated with the typical aerospace environment, but that temperature control of the battery is essential to its survival. Complete batteries and batteries mounted on spacecraft structures may show more frequent mechanical failures, depending upon structural details.

LIFE TESTING

The time of survival of batteries in both nonoperating and operating environments is critical. The nonoperating environment is usually simulated in life tests by storing the cell or battery over a range of temperatures and occasionally removing a specimen for test and evaluation. The operating environment tests usually repeat whatever nondestructive acceptance tests may have been performed, followed by operational tests to determine the deterioration which has taken place over the storage period.

Life tests of secondary batteries may take the form of cycle-life testing, consisting of a series of charge and discharge operations continued until the cell or battery has failed. In both shelf tests and cycle-life tests, an analysis of the causes, mechanisms, and probability of cell or battery failure goes hand in hand with the tests themselves.

Two approaches can be taken to the cycle-life testing of secondary batteries. In the time-of-survival approach, groups of cells are cycled in a predetermined pattern, subjected to an environment or a set of environments characterizing the expected application. A criterion or definition of failure is established. When the individual cell or group of cells pass across the dividing line between success and failure, the test is terminated and the cells dissected to determine the cause of failure. In the parametric variation approach, the electrical characteristics of the cells are measured at the beginning of life, and each variable affecting the characteristics is varied independently to determine the individual effects on electrical characteristics. Having established the performance of new cells, the cells are cycled in accordance with one or more prearranged schemes, and specimens are removed periodically for a repetition of electrical characteristic measurements. The effect of cycle life is established quantitatively in terms of its effect upon the electrical characteristics and upon the variables affecting the electrical characteristics.

The relative merits of the two approaches are easily evaluated. The time-of-survival approach answers the specific question: "If I operate the cell in this specific way, how long will it last?" This approach is relatively inexpensive and readily automated, except for the final analysis of failure. It depends for its success upon the initial definitions of failure and success and upon the judicious selection of test conditions. If these criteria are not carefully chosen, trivial answers will result. For example, if the test conditions are too severe or if the definition of failure is not consistent with the test conditions, immediate failure may result; however, it may be possible to operate the "failed" cell for several years under more reasonable test conditions. The parameter-variation approach provides quantitative measurements of the critical factors which affect cycle life. From these quantitative measurements, it is possible to derive all of the data necessary to predict characteristics under operating conditions other than the specific test conditions, provided that the original range of measurements encloses the operating conditions, or that data extrapolation is practical and has a reasonable basis in theory or experience. The

danger in the parameter-variation approach is that the cell-operating characteristics may be affected by so many variables that the determination of all the effects of the variables may not be feasible without excessive expense. If one of these important variables is uncontrolled and undetermined, the value of the measurements is usually greatly reduced, since the uncontrolled variable will tend to broaden the band of measurements, obscuring the effects of the measured variables. Consequently, an all-or-nothing approach must be taken. All of the important variables must be known and controlled to produce precise, repeatable data.

A number of compromises are possible in achieving a proper balance between the two approaches to cycle-life testing. For example, the number of cells cycled may be considerably larger than those removed for characterization testing, so as to minimize the expense of characterization testing. Similarly, cells need not be subjected to such rigid control of environmental and operational variables during routine cycling as during characterization testing.

ACCELERATED TESTING

Under some circumstances, it is possible to accelerate the rate of cell failure by varying the rate-controlling variables so as to speed up the failure process. In this way, it is possible to estimate the survival time of a battery under more normal operating conditions by a test of relatively short duration. Willihnganz points out in a battery workshop symposium (ref. 33) that the successful use of accelerated-life testing of lead-acid batteries depends upon acceleration of the specific process causing failure under normal operating conditions. If, for example, a degradative process slower than the usual failure mechanism is accelerated to the point at which it controls the service life, the test will give misleading results. The application of accelerated-life testing to batteries therefore requires a thorough knowledge of the mechanisms of all of the failure processes, and the way in which they vary with the accelerating test variables. The approach is common to all cell systems. However, a large volume of field service data is usually needed before it is possible to correlate accelerated test data with actual operating data.

TEST EQUIPMENT

A wide variety of test equipment has been used for testing batteries from simple to complex systems. The equipment used in some of the major aerospace test facilities is described below.

CYCLING TESTERS

The elements of a battery-cycling tester are shown in figure 2–25. The functions of each of these elements is as follows: The power supply delivers controlled power to the cell during charge and controls the discharge current during discharge. If the charge and discharge currents are different, a remotely programed power supply or two separate power supplies may be used to change the current settings.
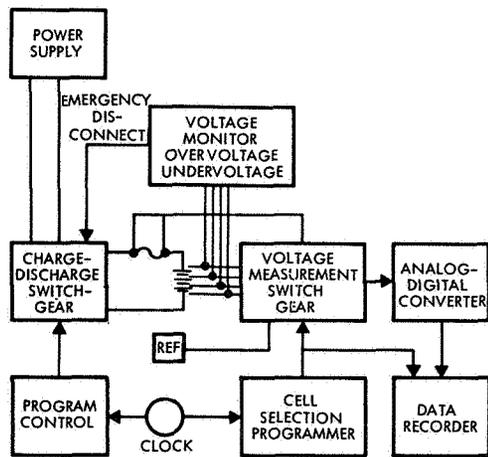
FIGURE 2-25.—Elements of a battery cycling tester.

Electrical switches or relays change the connections of cells, power supplies, current, and voltage programing by switching from charge to discharge, and vice versa. The safety monitor system monitors cell voltages and actuates the switchgear when any cell reaches an operating regime which could damage either cell or equipment.

VOLTAGE MEASUREMENT

Cell voltages are measured or recorded by connecting a precision voltmeter (or analog-to-digital converter) consecutively across each cell through the cell-selection switchgear. The operation of this equipment is coordinated and controlled through a central programer, the complexity of which may vary between manual control through the usual clock-timed programer, to a computer of the process-control type which has output relays for the performance of switching and control operations and which may also do some additional on-line data reduction. A typical example is the NAD Crane test setup. A block diagram of this is shown in figure 2-25 (ref. 34).

One problem associated with the design of large testing setups intended for unattended operation for long periods is the reliability of switches, clocks, and relays. A failure in test equipment can compromise the usefulness of the data, even though the safety monitoring system prevents actual damage to the equipment and test specimens. Other problems are encountered when large, high-speed data acquisition systems are assembled. One of the most frequent is common mode noise due to the presence of ground loops and of stray fields from lighting and other equipment. Ground loops may be eliminated by using single-point grounding techniques. Noise pickup in measuring circuitry may be minimized by the use of guarded input circuitry and by integrating the input over a finite

period of time. Integrating digital voltmeters are generally available. NAD Crane integrates inputs by using the hold-and-read method, in which the voltages are held in precision capacitors and then scanned by a digital voltmeter immediately after having been disconnected from the cells. This integrates the noise over the storage period of 400 milli-seconds, and has the additional advantage of a zero time delay between measurements (ref. 34).

SHUNTS

If accuracies better than 2 percent are desired, the method of obtaining current measurements and settings is usually restricted to the deter-mination of voltage drop across a precision shunt. The design of a shunt for accurate measurement is a compromise between the accuracy of voltage measurement and heat generation. NAD Crane (ref. 34) uses shunts with 100-millivolt full-scale drop, requiring voltage measurement accuracy of 0.1 millivolt to achieve 0.1 percent of full-scale accuracy. On the other hand, shunts with a 1.0-volt full-scale drop have a heat dissipation 10 times greater than the 100-millivolt shunt, making it necessary to consider the possibility that excursions in shunt temperature may affect measurement accuracy. As an example, manganin has a coefficient of resistivity of 0.002 percent/°C. If an overall accuracy of 0.1 percent is desired in which one-half is allocated to shunt temperature variations, and the other half to other uncertainties such as accuracy of calibration, the shunt must operate in a temperature range of $\pm12.5°$ C. This is not impracticable if large open-ribbon shunts are used and if additional cooling can be applied where required.

POWER SUPPLIES

There is a whole spectrum of solid-state, automatic-crossover power supplies available throughout the industry which are ideal for battery-cycling operations. In the automatic-crossover power supply, both a voltage limit and a current limit may be set. The output characteristics of the supply follow the load demands. A large load demands a higher current than the preset current limit permits, so the current is supply limited, resulting in a lower output voltage than the preset value. As the load becomes smaller, the voltage required to force the current through the load increases, the supply automatically crosses over at the preset voltage limit to a voltage-limited mode, and the output current falls. Many of these power supplies have a remote sensing capability, in which the signal voltage may be taken directly from the battery terminals to the voltage-limiting control circuit, rather than at the output of the power supply. This enables accurate control of potential at the battery terminals and eliminates the effect of line drop. In some commercial power supplies, however, the remote sensing circuitry is unable to compensate for very large line drops which may occur as a result of long power runs, and some modification of the power supply is neces-sary. One such modified power supply is the Hewlett-Packard J-11-6274 A.

CELL DROPOUT SWITCHING

When charging cells at a constant current, it may be desirable to measure the voltage of each cell so that a cell reaching the preset limit may be removed from the circuit, while the remaining cells in the series circuit continue to be charged. This is accomplished by the switch connection pattern shown in figure 2–26. However, as the cell and battery
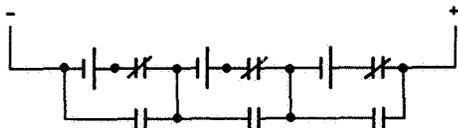
FIGURE 2–26.—Switch connection pattern.

operating currents increase, the availability and cost of reliable switching relays becomes a problem. Consideration should be given to the use of semiconductor switches mounted at or near the test cell group. Low-cost germanium transistors capable of switching more than 30 amperes are readily available.

LINE DROP

Consideration should be given to the line drop, switching voltage losses, etc., in purchasing power supplies. For example, in charging 20 series-connected nickel-cadmium cells, approximately 30 volts are required. However, if cell dropout switching is needed at a distance of 15 feet from the control cabinet, the total line length is 600 feet, and voltage drops of 10 to 15 volts are not impossible.

COMPUTER CONTROL OF TEST OPERATIONS

The advent of low-cost process control computers has made practical the development of computer-controlled testing facilities. These computers have the capability of performing switching operations which may be used to control test parameters with great flexibility. Concurrently, some on-line data reduction can be performed minimizing the amount of stored data required. For large-scale test setups, these centrally controlled systems have advantages in flexibility and in partial data-reduction capability, and also cost advantages. The decision-making capabilities of the computer may be used to perform the safety-monitoring functions and to control the measurement functions, thereby eliminating a great deal of ancillary equipment. Data are recorded at high speed on punched paper or magnetic tape in a format suitable for additional data reduction by a general-purpose computer. One such test facility has been set up by Martin-Marietta Corp. of Baltimore, Md. (ref. 28). The block diagram is shown in figure 2–27. At this time the facility is operating but no data have been published.
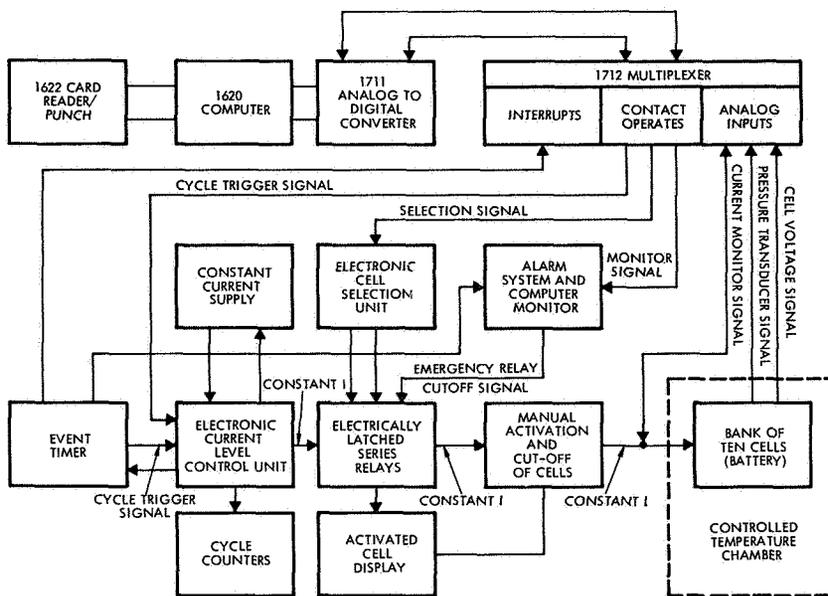
FIGURE 2-27.—General block diagram—computer-operated battery system.

COMPUTER DATA ANALYSIS

The large mass of data produced by long-term battery cycle life testing has led to recording of data on punched paper or magnetic tapes for subsequent analysis by computer. In general, this approach has been relatively unsuccessful, not because of any limitations in the method itself, but because inadequacies in the design of the testing program have resulted in the amassing of large volumes of data which defy analysis by any method whatsoever. So far, published results of computer analysis of battery data have been restricted to nickel-cadmium cells. These results are reported in chapter 4.

EXISTING NASA TEST FACILITIES

Major test facilities financed wholly or in part by NASA, or engaged upon NASA-sponsored test work, are described below.

The NAD Crane facility is the largest and most extensive of the NASA test facilities. A block diagram of the system is shown in figure 2–28. A central 28-volt source supplies electric power to all of the cycling systems. Each cell pack is serviced by its own charge controller, which has current and voltage limit settings within 1 percent accuracy. Control stability is not reported. The charge controller also contains the timing and switchgear for cycling between charge and discharge.

The safety-monitoring system has two parts. An undervoltage monitor continuously monitors the voltage of the entire pack, lighting a warning light and opening the circuit when the pack voltage falls below
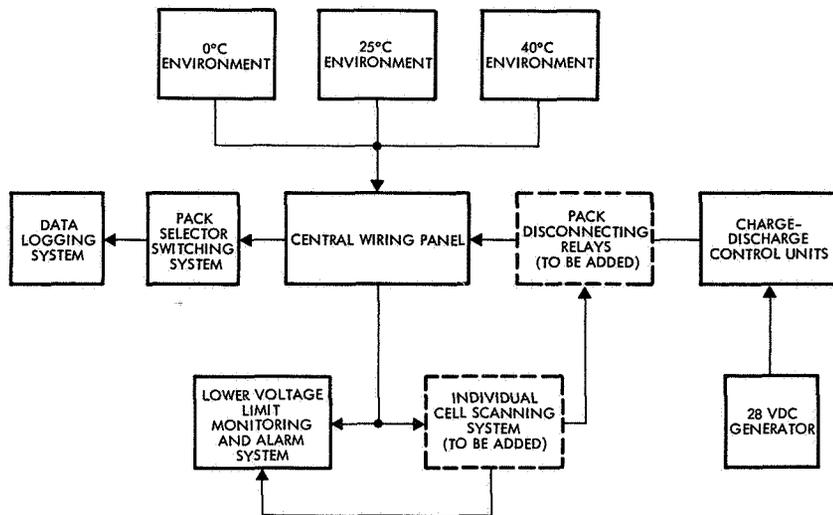
FIGURE 2-28.—Block diagram—NAD Crane test system.

a preset limit. No further automatic action is taken. In addition, the voltages of the individual cells are monitored at intervals and, when any one cell falls outside either the upper or lower limits, an alarm sounds, a light goes on, and the entire pack is disconnected from the charger and left on open circuit. Cells are scanned every 2 minutes with a 900-point crossbar scanner.

The data-logging system has 30 input channels, of which 10 are used for cell measurement, 2 for battery pack voltage measurement, 2 for current (voltage across 100-millivolt shunts), 1 for battery pack identification, and the remainder as thermocouple channels. Cell-voltage-measurement channels have an accuracy of 0.25 percent of full scale, with a full scale of 10 volts. On the basis of a 1.25-volt signal, an accuracy of slightly better than 2.5 percent is achieved. Current measurement accuracy will be determined by the unreported shunt sizing. The current- and voltage-measurement channels are of the sample-and-hold type, integrating the voltages over a period of 400 milliseconds by storage in precision capacitors, and reading by the digital voltmeter after disconnection from the cell. This minimizes noise pickup in the lines.

Voltages are amplified by a high-impedance differential amplifier, where the gain is automatically switched in accordance with the full-scale channel rating, and are converted to a digital signal for recording on punched paper tape.

The Martin-Marietta facility (ref. 28) utilized an IBM-1710 process control computer for control of battery testing. No information is given about the accuracy of the controls or measurements, except the analog-to-digital converter, which is stated to be 0.05 percent of full scale. A block diagram of the system is shown in figure 2-27. This facility is no longer in existence.

REFERENCES

1. KORTUM, G.; AND BOCKRIS, J. O'M.: Textbook of Electrochemistry. Vol. I. Elsevier Publishing Co. (New York, N.Y.), 1951.

2. KORTUM, G.; AND BOCKRIS, J. O'M.: Textbook of Electrochemistry. Vol. II. Elsevier Publishing Co. (New York, N.Y.), 1951.

3. HAMER, W. J.: Compilation of Critically Evaluated Electrochemical Data, Part II. Sixth Quarterly Report for the period Jan. 1 to Mar. 31, 1966. Institute of Basic Standards no. 9047, National Bureau of Standards (Washington, D.C.). No date. (Available as NASA CR-74558, N66-24494.)

4. GLASSTONE, S.: Thermodynamics for Chemists. D. Van Nostrand (New York, N.Y.), 1947.

5. LATIMER, WENDELL M.: The Oxidation States of the Elements and Their Potentials in Aqueous Solutions. Second ed., Prentice-Hall (Englewood Cliffs, N.J.), 1952.

6. ANON.: Circular 500, National Bureau of Standards, 1949.

7. CARSON, W. N., JR.: A Study of Nickel-Cadmium Spacecraft Battery Charge Control Methods. Final Report, General Electric Co., Research and Development Center (Schenectady, N.Y.), Apr. 1966. (Available as NASA CR-62029, N66-36372.)

8. ANON.: The Spacecraft Power Supply System—Relay I. Final Report, Radio Corp. of America, Astro-Electronics Division, 1965. (Available as NASA SP-76, N66-10234.)

9. SPARKS, R. H.; AND BAUER, P.: Nickel-Cadmium Batteries for the Orbiting Geophysical Observatory; Cell Characteristics, Charge Control Concepts, Battery Design. Vol. I. Rept. no. 2315-6005-RU000, TRW Systems (Redondo Beach, Calif.), Apr. 1, 1963.

10. COCCA, F. J.: Charge Control for Secondary Batteries, Part 3, Stabistors— Their Application in Battery Operation. Presented at the 18th Annual Power Sources Conference (Fort Monmouth, N.J.), May 19–21, 1964, p. 65.

11. CATOTTI, A. J.; AND READ, M. D.: Charge Control of Nickel-Cadmium Batteries; Auxiliary Electrodes for Overcharge and Over-discharge Control. Presented at the 19th Annual Power Sources Conference (Fort Monmouth, N.J.), May 18–20, 1965, p. 63.

12. ANON.: Research Study on the Use of Auxiliary Electrodes in Sealed Silver-Cadmium Cells. Final Report, July 1962 to June 1963, General Electric Co., Advanced Technology Laboratories (Schenectady, N.Y.). No date. (Available as NASA CR-55014, N64-12025.)

13. CARSON, W. N., JR.; CONSIGLIO, J. A.; AND MARR, J. W.: Study of the Use of Auxiliary Electrodes in Silver Cells. Final Report, General Electric Co., Advanced Technology Laboratories (Schenectady, N.Y.), Mar. 1966. (Available as NASA CR-405, N66-18430.)

14. CARSON, W. N., JR.: Charge Control for Secondary Batteries, Part I: Auxiliary Electrode for Charge Control. Presented at the 18th Annual Power Sources Conference (Fort Monmouth, N.J.), May 19–21, 1964, p. 59.

15. SIZEMORE, K. O.: Use of the Adsorption Hydrogen Electrode and the Oxygen Fuel-Cell Electrode in Nickel-Cadmium Cells. Rept. no. TM X-55469, Goddard Space Flight Center, Apr. 1966. (Available as N66-24926.)

16. SIZEMORE, K. O.; AND HENNIGAN, T. J.: Auxiliary Electrode Instrumentation for Nickel-Cadmium Cells. Rept. no. TM X-55471, Goddard Space Flight Center, May 1966. (Available as N66-24928.)

17. SEIGER, H. N.; SHAIR, R. C.; AND RITTERMAN, P. F.: Charge Control for Secondary Batteries, Part 2: The Adhydrode in Charge Control. Presented at the 18th Annual Power Sources Conference (Fort Monmouth, N.J.), May 19–21, 1964, p. 61.

18. FRANK, H.; AND STRIER, M. P.: Small Fuel Cell To Eliminate Pressure Caused by Gassing in High Energy Density Batteries. Final Rept. no. SM–48457–F, Douglas Aircraft Co., Inc., Astropower Laboratory (Newport Beach, Calif.). No date.

19 VINAL, GEORGE W.: Storage Batteries: A General Treatise on the Physics and Chemistry of Secondary Batteries and Their Engineering Applications. Fifth printing, John Wiley & Sons, Inc. (New York, N.Y.), 1966.

20. BRUINS, P. F.; CAULDER, S. M.; AND SALKIND, A. J.: Calorimetric Study of the Thermodynamic Properties of the Nickel-Cadmium Cell. Final Rept., Oct. 1, 1964, to Dec. 31, 1965. Polytechnic Institute of Brooklyn, Department of Chemical Engineering (New York, N.Y.). No date. (Available as NASA CR–71408, N66–21663.)

21. METZGER, W. H., JR.; AND SHERFEY, J. M.: Electrochemical Calorimetry, III. Thermal Effects of Nickel-Cadmium Batteries. Electrochem. Tech., vol. 2, no. 9–10, 1964, p. 285.

22. FOLEY, R. T.; AND WEBSTER, W. H.: Research Into Fundamental Phenomena Associated With Spacecraft Electrochemical Devices—Calorimetry of Nickel-Cadmium Cells. Second Quarterly Report, Goddard Space Flight Center, Oct. 31 to Dec. 31, 1966. American Univ. (Washington, D.C.). No date.

23. FOLEY, R. T.; AND WEBSTER, W. H.: Research Into Fundamental Phenomena Associated With Spacecraft Electrochemical Devices—Calorimetry of Nickel-Cadmium Cells. Third Quarterly Report, Goddard Space Flight Center, Oct. 31 to Dec. 31, 1966. American Univ. (Washington, D.C.). No date.

24. BECK, T. R.; AND KEMP, F. S.: Heat Generation in Lunar Orbiter Battery. Rept. no. D2–23612–1, Boeing Co. (Seattle, Wash.), Oct. 1964.

25. SPARKS, R. H.; AND BAUER, P.: Nickel-Cadmium Batteries for the Orbiting Geophysical Observatory: Battery Fabrication, Battery Environmental Qualification, Battery Life and Test Summary, Subsystem Compatibility and Functional Tests, Battery Failure Analysis, Battery Use Criteria, Conclusions. Vol. II. Rept. no. 2315–6008–RU000, TRW Systems (Redondo Beach, Calif.), Feb. 12, 1964.

26. BAUER, P.: Pressure Characteristics of Sealed Nickel-Cadmium Cells. Electrochem. Tech., vol. 3, no. 1–2, 1965.

27. BRODD, RALPH J.; AND DEWANE, HAROLD J.: Impedance of Leclanche Cells and Batteries. J. Electrochemical Soc., vol. 110, 1963, p. 1091.

28. ANON.: Testing of Sealed Nickel-Cadmium Cells. Vol. I. Experimental Design. Rept. no. ER 14543, Feb. 1, 1963, to July 31, 1966, Martin-Marietta Corp., The Martin Co. Division (Baltimore, Md.). No date.

29. WILLIHNGANZ, E.; AND ROHNER, PETER: Battery Impedance: Farads, Milliohms, Microhenrys. AIEE Applications and Industry, vol. 44, Sept. 1959, p. 259.

30. ANON.: Transcript of the Conference on Secondary Space Batteries, Vol. I: Manufacturing and Testing Problems. Report on Interagency Advanced Power Group. Rept. no. PIC–BAT 209/6, Power Information Center (Philadelphia, Pa.), Sept. 1963.

31. ANON.: Transcript of the Conference on Secondary Space Batteries, Vol. II: User's Problems, Conclusions, and Recommendations. Report on Interagency Advanced Power Group. Rept. no. PIC-BAT 209/6.1, Power Information Center (Philadelphia, Pa.), Sept. 1963.

32. JAKOBI, W.: Research and Development Program on Sealed Nickel-Cadmium Cells for Space Use. Final Report, Gould-National Batteries, Inc. (Minneapolis, Minn.), Apr. 30, 1963. (Available as NASA CR-55845, N64-16699.)

33. ANON.: Battery Workshop. NASA Headquarters (Washington, D.C.), Oct. 6-7, 1966.

34. BRUESS, E. C.: Evaluation Program for Secondary Spacecraft Cells. First Annual Report No. QE/C 65-356, Apr. 1962 to Dec. 31, 1964. U.S. Naval Ammunition Depot, Quality Evaluation Laboratory (Crane, Ind.), May 14, 1965. (Available as NASA CR-63424, N65-26408.)

35. COOPER, J.; AND FLEISCHER, A.: Screening Methods. Air Force Aero Propulsion Laboratory (Wright-Patterson Air Force Base, Ohio). No date.

CHAPTER 3

Data Requirements and Format

DATA REQUIREMENTS

The requirements for battery-operating-characteristic data depend upon the electric-power-system design in which the batteries are used. A relatively simple and conservatively designed system generally requires a minimum of detailed operating-characteristic data. As the design becomes more sophisticated and the requirement for high-efficiency storage and utilization of source energy becomes more critical, the requisite amount and accuracy of battery characteristic data increase. The maximum data required for a highly sophisticated power subsystem are:

(1) Discharge voltage as a function of time under the actual load conditions expected.

(2) Charge voltage and current as a function of time under the actual charging conditions expected. If the charging conditions are unknown, the battery data should contain enough information to derive the charging current and voltage required.

(3) Overcharge current requirements.

(4) Quantity of electrical energy available from the battery at certain critical points in the mission, and the assurance that at all other periods the energy availability exceeds the requirements.

(5) Rate of heat evolution as a function of time under the actual charge and discharge conditions expected, and a complete temperature profile of the battery as a function of time.

(6) Impedance and phase-shift characteristics of the battery as a function of frequency.

(7) Efficiency of the battery's energy storage and its associated electronics.

(8) Probability of battery failure as a function of time and conditions of use.

(9) Battery voltage transients for critical load changes.

Most, if not all, of the above data requirements depend upon system-design concepts as well as environmental variables such as temperature, charge and discharge currents, and system-load characteristics and specifications (which vary with the changing spacecraft designs and missions). A consistent format is required for presenting battery data in a parametric form useful for calculating the required system characteristics over a wide range of system designs. If possible, the data should

be in a form which can be interpolated or extrapolated and used in designing power systems for missions with no available direct battery test data. This does not preclude the need for a final measurement of battery-operating characteristics under actual or simulated operating conditions. However, greater accuracy in the initial design stages can drastically reduce the incidence of expensive surprises after much of the system-design work has been completed.

ESTABLISHMENT OF FUNCTIONAL RELATIONSHIPS

To meet the interpolation requirement, the data must be presented as a continuous function. To be extrapolated, the data must be either linear or expressed as a mathematical function which can be evaluated outside the existing measurements. In some cases, this function is already known either from theory or from sufficient data having been taken to permit fitting of a mathematical expression. An example of a function which is known to some degree of confidence is the potential of a nickel-cadmium cell in overcharge.

This potential is described by the theoretically derived Tafel characteristic

$$E = a + b \log i$$

where a and b are constants which vary with temperature. To adequately determine the overcharge characteristics of a nickel-cadmium cell, it is theoretically necessary to make only two measurements at each temperature. In practice, more measurements are required. Lesser known relationships may not follow any conveniently solved equation, making it necessary to measure the various parameters at enough points to establish a continuous, smooth curve. The parameters should be measured at several levels until enough is known about the generality of the relationship.

The variables which influence the characteristics of the specific battery types are discussed in the appropriate sections.

INDEPENDENT VARIATION OF PARAMETERS

In spite of the large number of battery measurements, many of the functional relationships are not known. Furthermore, they can be constructed from the available data only in a limited way because the battery measurements concentrate on typical applications, which consequently confounds several of the variables significantly affecting voltage characteristics. For example, when a battery is operated in a typical 100-minute orbit at two different depths of discharge, the charge current and depth of discharge are varied together, making it impossible to isolate the independent effect of either. In addition, most of the parameters of interest vary with the state of charge, which usually cannot be determined accurately from simple measurements. Better, more accurate data, nevertheless, can be achieved by using carefully constructed test programs which account for and control all important independent variables.

DATA FORMAT

The form in which the data are presented is extremely important to the power-system-design engineer, and may critically affect their utility as design data.   A useful format must be compatible with techniques for the design and analysis of a wide variety of electric-power systems, must be flexible in application, and must have data obtainable by normal measurement methods.   A recommendation for the most desirable format for presenting various types of data is given below.   Where examples are given for unavailable data, the curves are so marked.

CURRENT DATA

Current data should be normalized to minimize the amount of stored data and enable comparison of the performance of cells of different capacity.

Ideally, current data should be standardized by converting it to current density, in amperes/centimeter^2 or amperes/inch^2.   Under these circumstances, electrodes (and cells) of similar construction and thickness should display similar behavior.

Where electrode areas are unknown, it is assumed that the cell capacity is directly proportional to electrode area and the data are converted to normalized current in amperes/ampere-hour.   For cells using electrodes of similar construction and thickness, a reasonably good correlation of behavior should be obtainable.

Whether current density data or normalized currents are used, the accuracy with which the behavior of different-sized cells can be correlated decreases as the difference in cell size increases due to changing edge effects (the uneven distribution of current over the surface of a flat electrode) and thermal conductivity effects.

VOLTAGE DATA

Battery voltage data are reduced to unit cell voltages by dividing by the number of series-connected cells.   This is a common practice among system and battery design engineers.

CURRENT-VOLTAGE CHARACTERISTIC DATA

All data on the performance of electrical equipment, including batteries, are presented as current-voltage characteristics, in which normalized current is plotted on the ordinate and voltage/cell is plotted on the abscissa.   The characteristic curves of equipment other than batteries may then be superimposed upon the battery characteristics.   This is done by dividing the current scale by the battery capacity, and the voltage scale by the number of series-connected cells in the battery.   Alternatively, the battery characteristics can be expanded to true current-voltage characteristics by multiplying current and voltage scales by the battery capacity and the number of series-connected cells in the battery.   Either system works as long as consistent practices are followed.   The advantages of this uniform presentation will become apparent.

Discharge-Voltage Characteristic Data

In keeping with the above practice, discharge-voltage characteristic data are presented as current-voltage curves with the estimated state of charge as the third variable. Additional graphs may be provided at different temperatures. In some cases, the curves will be linear; in other cases, a functional relationship between current and voltage may be found in which a plot of voltage as a function of normalized current[1] will be linear. If such relationships can be found, they should be used, since this format permits extrapolation of data into unmeasured regions in the absence of more dependable data.
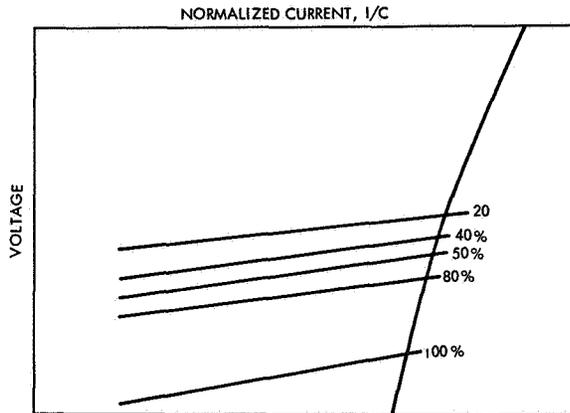
FIGURE 3-1.—Constant-power load line superimposed upon the typical discharge characteristics of a 20-A-h nickel-cadmium cell. Normalized current as a function of voltage/cell. State of charge as a third variable.

An example of this presentation is shown in figure 3-1, in which the discharge characteristics of 20-A-h nickel-cadmium cells are shown as a function of state of charge at 97° F. Using this format, it is possible to construct a discharge curve (voltage versus time) by crossplotting the intersection of the current-voltage characteristics of the cell with the current-voltage characteristics of the load, whether the load is constant current, constant resistance, constant power, or a complex mixture.

In figure 3-1, a typical constant-power load line is superimposed upon the current-voltage characteristics of the battery or cell. All the data are normalized in current.

This presentation can be used to calculate the voltage, current, and state of charge of the cell as a function of time. Voltage, current, and state of charge are all read from the graph at the points where the load

---

[1] Normalized current = current (amperes)/cell capacity (ampere-hours).

current-voltage characteristic intersects the cell characteristic lines. The time at each intersection is calculated by the equation

$$\Delta t_n = (\Delta Q_n)(2)/(I_n + I_{n-1}) \tag{3-1}$$

where

Δt_n is the time required to cross from the $n-1$th intersection to the nth

I_n is the current at the nth intersection

ΔQ_n is the state-of-charge increment between the $n-1$th and the nth intersection

The relationship is valid for all load lines, whether constant power, constant current, constant impedance, or complex.
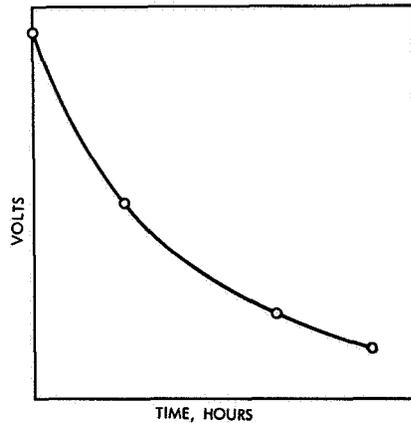
FIGURE 3-2.—Voltage as a function of time as computed from the data of figure 3-1. Constant-power discharge.

In figure 3-2, a typical curve showing voltage as a function of time at constant power is calculated using this method. Note that there is no characteristic discharge plateau. Similarly, curves showing current as a function of time may be plotted and, if desired, the area under the current-time curve integrated to obtain an accurate estimate of depth of discharge under the precise load conditions expected to prevail (fig. 3-3).

This method of calculation gives a more accurate estimate of depth of discharge under actual operating conditions than the usual methods. These methods, based upon the assumption of constant current, are normally too conservative. When using the more accurate method, conservatism in design may be applied consciously, if desired, rather than as a result of inaccurate computation methods.

At constant temperature, cell current-voltage data appear to be linear within the range in which they were measured for several different electrochemical systems. This enables the data to be expressed as linear
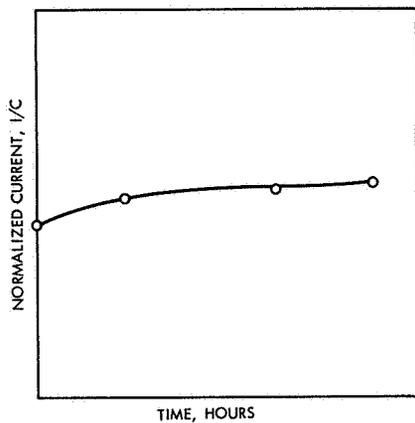
FIGURE 3-3.—Current as a function of time
as computed from the data of figure 3-1.
Integration of the area under this curve
gives depth of discharge.

equations with two empirical constants, which can then be varied with temperature and other perturbing factors.

CHARGE-VOLTAGE CHARACTERISTIC DATA

Charge-voltage characteristics are also readily presented as current-voltage relationships, with state of charge and temperature as additional variables. Again, the advantage of this format is the ease of reconstructing voltage-versus-time and current-versus-time curves for any desired charge-control scheme from the same basic data set. Figure 3-4 shows a typical family of current-voltage curves for a nickel-cadmium battery on charge with state of charge as a third variable. Superimposed upon these curves are the current-voltage characteristics of three charge-control systems: constant current, modified constant potential, and voltage-actuated multistep charging.

In the last method, a battery is charged at constant current until it reaches a predetermined potential (dotted line), then the charge rate is reduced to a new constant value. This reduction in charge current is repeated through one or more preselected levels until the current has been reduced to the final trickle-charge level.

The desired curves of current as a function of time and voltage as a function of time are determined by crossplotting and calculating the time interval required to progress from one state-of-charge line to the next, taking into account the charge efficiency of the battery system.

Over short intervals, η and I may be averaged or assumed to be constant, and the time interval calculated by

$$\Delta t = (\Delta Q)/\bar{\eta}\bar{I}$$

where $\bar{\eta}$ and $\bar{I}$ are average η and I over the interval.
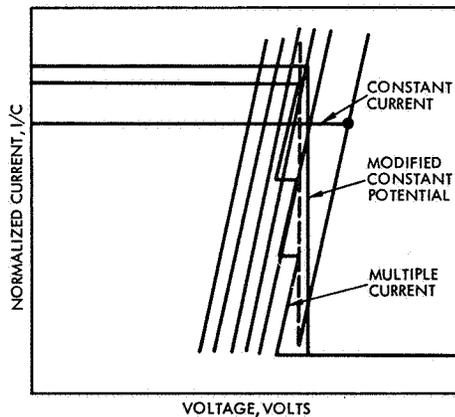
FIGURE 3-4.—Three typical charge-control characteristic curves superimposed upon the typical charge characteristics of a nickel-cadmium cell. Normalized current as a function of voltage/cell. State of charge as a third variable.

Like the discharge-curve example, the method is flexible enough for use when charging current is not constant. An example of this flexibility is found in chapter 13, "Application No. 1," in which the entire interface between solar array, loads, and battery is analyzed graphically.

Like the discharge-voltage-characteristic data, the charging current-voltage characteristics appear to be linear in many cases, and may be handled in the same way. Degradation of electrical characteristics with temperature, age, and other factors may be expressed as changes in the constants of the linear equations for the lines.

CAPACITY DATA

Data on the capacities of galvanic cells are currently reported as functions of cycle life, temperature, current, age, and other factors. Because of the wide variety of testing conditions and criteria of measurement, such as cutoff voltage and end-of-charge voltage, it is often difficult to determine from these data the expected capacity of a cell or battery under an untested set of circumstances. If the electrical characteristics data are properly determined and reported, the available capacity under any set of circumstances can be determined from a knowledge of the standard capacity of the cell and from the variations of the electrical characteristics with the other variables. In this way, the dependence of capacity upon operational variables such as temperature, current, acceptable system voltage variations (which determine maximum charge voltage and discharge cutoff voltage) is determined from an analysis of the cell's electrical characteristics. Variations in standard capacity with cycle life, age, and

other factors can be reported as plots of capacity or fraction of initial capacity versus log of cycle life, time, etc. A better presentation would be the variation of electrical current-voltage characteristics with these factors, so that the complete discharge curve can be reconstructed as required.

EFFICIENCIES

Efficiencies of primary batteries are best reported as the electrical work efficiency as a function of current, temperature, and other variables. (See ch. 2.) The efficiencies of secondary batteries vary in characteristics, depending upon the particular reaction mechanisms causing the loss in efficiency. The means of reporting efficiency is treated in the chapters dealing with each galvanic system. It is important to note, however, that where the ampere-hour efficiencies of the cells are not equal to 1.0, these data are vitally important to the calculation of several essential characteristics of the system, such as available capacity or state of charge, battery heat-evolution rate, and temperature.

OVERCHARGE CHARACTERISTICS

Battery and cell overcharge characteristics are currently being reported in the proper format, a plot of the log of overcharge current versus cell voltage with temperature as a third variable. Accurate reporting of temperature is essential, including a statement of the accuracy of measurement and the point at which the temperature was measured.

IMPEDANCE

Two types of impedance measurements have been made. Where impedance data are to be used only for an assessment of the condition of the cell, a single value may be reported and correlated with the cell conditions. Where impedance data are to be used in power-system design and analysis, the impedance should be reported as a function of frequency from 1 hertz to 50 kilohertz. (See ch. 4, fig. 4–16.) It would also be desirable to report phase shift throughout the same range.

SPECIALIZED DATA RELATED TO THE SILVER ELECTRODE

The silver electrode as used in the silver-cadmium and silver-zinc cells has a discontinuity in both the charge and discharge curves due to a change in the chemical reaction as the process proceeds. In the charge curve, this transition is marked by a change in the voltage level of the cell, and by a peak in the voltage (at constant current) which must be passed before the transition is complete. (See ch. 5, "Electrical Characteristics.") This intermediate peak occurs at a varying state of charge in the neighborhood of 30 percent and its amplitude varies both with current and with temperature. To define accurately the location and amplitude of this phenomenon, it is convenient to show the data as a current-voltage curve as seen in figure 3–5 (ignoring the fact that the state of charge is not constant) which varies as a function of temperature, and a family of curves which show the state of charge at which the inter-
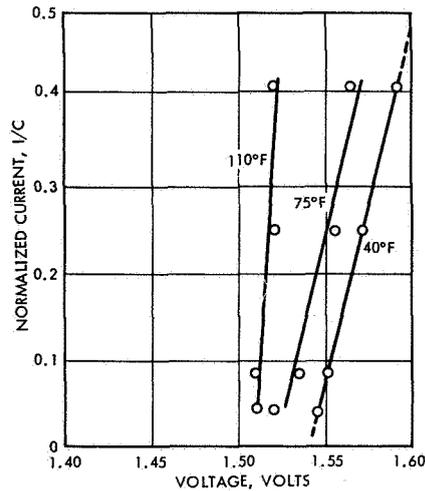
FIGURE 3-5.—Typical presentation of
silver-electrode transition voltage
peak. Current as a function of volt-
age. State of charge is not constant.
Temperature as a third variable. Am-
plitude of intermediate peak in silver-
cadmium cells temperature as third
variable.

mediate peak occurs as a function of temperature, with current as the
third variable (fig. 3-6). When these data are added to the usual
current-voltage characteristics, they complete the characterization of
silver-electrode cells.

STATE-OF-CHARGE INFORMATION

While the system-design engineer usually requires data expressed as a
function of time, the properties of the battery can be referenced only to
the state of charge. If battery data are expressed as a function of time,
and the state of charge at critical points in the charge-discharge cycle is
not accurately known, the electrical characteristics are based upon a
drifting reference point and are essentially unpredictable. This gives
rise to the complex and unwieldy form of data as it is currently reported
in the literature, and creates serious problems for the system designer.

For this reason, all those characteristics which vary with state of
charge are plotted in this work as functions of the true state of charge.
Time is eliminated as an independent variable and the variation of
electrical characteristics in specific applications as a function of time are
calculated from state-of-charge data using the appropriate equations.
Because of the lack of data on the standard capacities of the cells from
which the data were taken, state of charge is usually shown as a per-
centage of the nameplate capacity. For the purposes of design accuracy
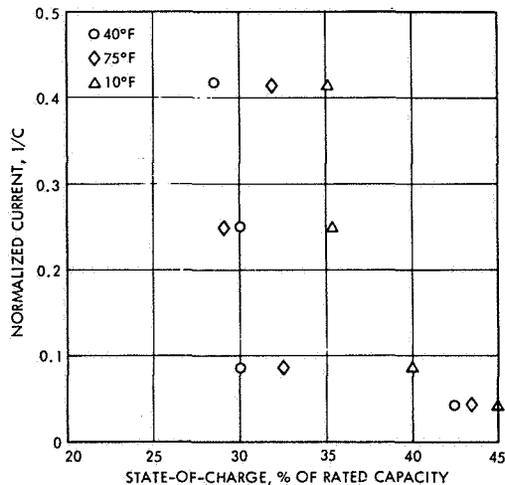
FIGURE 3–6.—State of charge at which transition
peak amplitude is a maximum, as a function of
current. Temperature as a third variable.

and convenience, the data would be better expressed as a percentage of
the standard capacity. (See "Definitions," ch. 4.)

METHODS OF APPLYING DATA TO DESIGN

The basic methods of applying the data as expressed in the recom-
mended format have already been shown. Additional refinements of
method, and the techniques for calculating the required battery capacity,
recharge power, battery heat-evolution rates, voltage-limit settings,
temperature-compensation curves, etc., may be found in chapter 13,
containing the analyses of three typical applications and illustrating the
calculation methods.

SERVICE-LIFE DATA

Currently, data on survival of secondary batteries are usually reported
as a relationship between the log of cycle life and the depth of discharge,
without consideration of the mode of failure. Conditions of operation
such as current and temperature are usually reported as additional
variables, or are confounded statistically with depth of discharge.

In view of the lack of data on the rates of the various failure processes
in aerospace cells, no improved data format can be defined at this
time. The general line of investigation which should be pursued,
however, is the independent identification of each of the processes going
on within the cells leading to failure, a determination of the rate with
which the process occurs, and its relation to the operational and environ-
mental variables which affect the rate. Once these have been deter-
mined, a logical format can be devised.

A great many variables have been determined to affect service life; others have been suggested as having some impact upon life. Among the variables suggested as being of primary importance are cell size, structure, manufacture, maximum charge voltage and minimum discharge voltage, temperature, operating currents or rates, extent and rate of overcharge, depth of discharge, and the effects of isolated occurrences such as excessive overcharge or overdischarge.

DEFICIENCIES IN AVAILABLE DATA

There are insufficient available data on the electrical characteristics of the nickel-cadmium system. Parametric data are needed to estimate cell and battery performance prior to conducting tests to prove design and service life. Such data must be based upon estimates of the state of charge of the cell or battery. Because of the peculiar characteristics of the nickel electrode, such estimates are difficult to make accurately. At the present time, the available data cannot be readily assembled into a coherent picture of cell performance, nor are the current or proposed testing programs likely to elicit such information. A new approach is required involving a study of all of the factors, and their interactions, which influence cell performance.

Specifically, this requires the systematic acquisition of electrical characteristics while holding constant all but one of the variables which affect the electrical characteristics of the nickel-cadmium cell. At the present time, the following variables are known to affect the voltage of a nickel-cadmium cell:

Variable	*Sensitivity*
Current_____	0.1 to 0.2 volt-A-h/A[1]
Temperature_____	0.001 to 0.002 mV/F. In the overcharge region. Insufficient data elsewhere.
State of charge_____ ⎫	
Current of prior half cycle_____ ⎪	
Temperature of prior half cycle___ ⎪	
Age_____ ⎬ Insufficient data.	
Depth of discharge_____ ⎪	
Number of cycles_____ ⎪	
Number of cycles since last reconditioning_____ ⎭	

[1] Derived from the slope of the normalized current-voltage lines. To obtain the conventional figure in ohms, divide by the cell capacity in ampere-hours.

If all of the above variables, exclusive of age effects, are of critical importance in the electrical characteristics, the measurement experiment would be an 8×8×3, and would require 192 cycles. This would lead to confounding of age effects with some of the other effects being examined. However, by judicious selection of tests, and cautious application of statistical techniques, it should be possible to reduce the number of measurements to a more manageable level. Certainly, once the data have been taken for one type of cell, spot checks will be sufficient

to determine whether or not some of these data are transferable to other similar cells.

More data are needed on the rate of onset of the memory effect and on the means of reconditioning batteries on a battery basis. Current cell-reconditioning arrangements are satisfactory in the laboratory and in prototypes, but the complexity of the electronics required for remote reconditioning reduces system reliability.

Resolution is required of the differences in overcharge characteristics between vendor data and other published data. If possible, these data should be normalized to unit capacity (rated or measured) and a standard deviation of values should be determined. Greater measurement accuracy is necessary for the acquisition of overcharge data than has previously been used. This is because the current is extremely sensitive to applied voltage, a tenfold change in current resulting from a change of 20–30 millivolts in cell terminal voltage. These data are essential for the design of overcharge current-limiting circuitry.

Of vital importance is a means of predicting the thermal balance of a nickel-cadmium battery from a proposed charge-discharge cycle. Because of the difficulties in predicting the state of charge of the battery or cell, the thermal balance, which is dependent upon state of charge, is also extremely difficult to predict.

This points out the need for a carefully conceived and controlled experiment in which the rates of each of the simultaneous reactions are determined or estimated independently. The work done at American University by Foley and Webster (see ch. 4, "Heat Evolution") is an excellent beginning, but requires additional measurements to expand its utility. These measurements might include gas evolution rates as a function of nickel-electrode potential both on charge and at rest, the cadmium-electrode potential as a function of gas recombination rate, and improved estimates of the reversible potential of the nickel electrode as a function of state of charge. Several measurements of enthalpy have been made, with moderately good results, but additional entropy data are required. Improvements in entropy data are likely to be difficult because of the irreproducibility of the nickel electrode's reversible potential, the temperature coefficient of which is used to calculate the entropy.

Impedance data as presently measured are adequate for detecting defective cells and for estimating overall power-system impedance when the battery is floating on the line. Frequently, however, cases arise in which a knowledge of the impedance characteristics of a battery are required as a function of frequency, and a carefully designed testing procedure should be developed for measuring this characteristic. Phase-shift data would also be desirable in some cases. Impedance and phase-shift data are vital in the analysis of voltage regulator stability.

Efficiency data are of vital importance in calculating the state of charge, which is a critical reference point for all other data. With the exception of the data shown in chapter 4, virtually no efficiency data are available in the published literature. Moreover, the efficiency data

presented in chapter 4, although the best available, were collected from varied sources and manipulated to achieve internal consistency. The result, while usable, is unsatisfactory. Acquiring efficiency data is therefore of critical importance.

Efficiency data also require extreme accuracy in experimental measurement and control. Of greatest importance is the accurate control of current, temperature, and cutoff voltage. The accuracy of efficiency data is especially sensitive to cutoff voltage because of the low slope of the voltage-time curve.

Data on the effects of high current pulses lasting up to 50 msec on the battery voltage, and on voltage fall and rise times associated with such high-current pulses, are required for analysis of the effect of engine-starting and ordnance-firing operations. Published data are conspicuously lacking, and acquisition would be low in cost and of great value.

Cycle-life and failure-mode data derived from NAD Crane tests are of some value in their present form. However, more data could be obtained from the cycled cells, which represent a very large investment in testing costs. The division of the cells into 10-cell packs, and the presumption of pack failure when one-half of the cells of any pack have failed, automatically deprives the tester of one-half of the data. Having invested from several months to several years in testing 10 cells, data are collected only from 5. In addition, it would appear advisable to retest the original definition of failure by performing an extensive series of reconditioning and electrical tests on the failed cells to determine their actual capabilities after having failed to perform the assigned mission. This involves a slight risk of compromising the accuracy of some of the failure analyses, but offers a valuable cross-check on the original definition of failure. Cells which have undergone physical failures such as internal short circuits are unlikely to recover, but remain susceptible to failure analysis.

Charge control of nickel-cadmium cells has been extensively investigated. Two advanced methods show great promise. The auxiliary electrode method, which actually combines modified constant potential charge, compensated for cell temperature, and a switchdown-to-trickle charge on receipt of a signal from the auxiliary electrode, appears to be a useful method for most applications. Data have been accumulated showing the response of the system to variations in temperature. The remaining task for development of this method is a demonstration of the charge control at a continuously varying temperature. The coulometer method appears very promising but has one serious deficiency. This method is unable to compensate for the inefficiency of the nickel electrode at elevated temperatures. Further investigation is needed to determine the upper limits of temperature and the lower limits of current at which the cadmium-cadmium coulometer represents a useful predictor of nickel-cadmium-battery state of charge.

Test data are inadequately reported. Considerable emphasis is placed upon accuracy of measurement, but reporting of control accuracy is usually incomplete. The large volume of data generated by cycling tests

is not susceptible to useful reduction and summarization. For power-system designs, current programs are taking the direction of computer control and on-line data reduction to minimize the amount of printed data. Aside from descriptions of the capabilities of the data acquisition systems, little has been written to show the direction the test programs are to take. On-line data reduction, with all of its advantages in brevity of stored data, has the characteristic of discarding raw data in favor of reduced, or summarized, data. This means that if the correct decisions are not taken at the beginning, critical pieces of information could be discarded automatically. The advent of computer-controlled testing and data acquisition into the battery field requires that a careful analysis of the test programs be conducted prior to their inception to assure that an apparently insignificant omission does not compromise the accuracy, validity, or utility of the data taken.

Present methods of normalizing data divide current by rated capacity so as to develop a generalized relationship for cells of different capacities. Differences exist, however, in cells of similar rated capacity due to variations in structure, electrolyte content, true and projected surface areas of the electrodes, and loading of electrodes with active materials. These differences have a significant effect upon the electrical performance. If data are not available from the vendor on these and other significant characteristics, because of a reluctance to disclose proprietary information or for any other reason, measurements should be made, and an effort made to correlate these data with electrical characteristic measurements.

CHAPTER 4

Nickel-Cadmium Batteries

INTRODUCTION

Two basic varieties of nickel-cadmium batteries are available: the pocket-plate type and the sintered-plate type. In the pocket-plate type, the active materials are mixed with conductive metals or graphite and are loaded into nickel-plated steel tubes or pockets. In the sintered-plate type, porous electrode plaques are fashioned of sintered-nickel powder, and the active materials are introduced into the electrode pores by immersion in the nitrate or chloride solution of the metal, i.e., $Ni(NO_3)_2$ or $Cd(NO_3)_2$, followed by electrolysis of the impregnated plaque in alkali. All data and discussion in this report refer to the sintered-plate sealed nickel-cadmium cell.

The electrodes of the sintered-plate cell are damp but are not immersed in a pool of electrolyte. This unusual feature leaves enough electrode surface available for a gas evolution-recombination process to occur, allowing continuous low-level overcharge of a hermetically sealed cell without excessive internal pressures.

HISTORY (Refs. 1 and 2)

The nickel-cadmium couple was first investigated in 1890 by Waldemar Jungner, a Swedish chemist, who received the initial patents in 1899 and 1901. Thomas Edison was awarded a British patent for a nickel-cadmium couple in 1900, but he did not actively use the system because it had a relatively low depth-of-discharge capability. Jungner was joined by K. L. Berg, and by 1904, they were in pilot-line production of batteries for shallow-cycle and standby operation. In 1906, they formed the New Jungner Ackumulator Co.

These early batteries had two basic problems: (1) The negative electrode was a mixture of cadmium and graphite contained in perforated sheet nickel pockets and it lost capacity rapidly as a result of compaction and loss of porosity. (2) The positive electrode used in both the nickel-iron and nickel-cadmium cells swelled and lost capacity. Edison controlled this problem by using a tubular design; Jungner solved the problem by using nonswelling black-nickel hydroxide. At first, the negative capacity loss was prevented by using coprecipitated iron instead of graphite as the conductive material in the negative electrode, but on deep discharge the iron went into solution as a ferrite, migrated to the positive electrode,

69

and reduced its capacity. Today, electrodes are made with a less-soluble form of iron.

Additional improvements in the nickel-cadmium cell were the use of cobalt traces for extending life (1924 to 1934); the addition of nickel strips for increased electrical conductivity (British, late 1920's); the use of thinner and higher conductivity electrodes (British, German, early 1930's); the development of the sintered, high-performance electrode (German, early 1930's); and the development of the technology for the sealed cell (German, mid-1930's). The manufacture of the pocket and tubular nickel-cadmium cell has been carried out in Germany since the 1920's; in England, France, and Belgium since the 1930's; and in the United States since 1946. The Allied Powers acquired the technology of producing sintered electrodes as a part of World War II reparations, and began their manufacture in the early 1950's. The Japanese and Soviets also produce nickel-cadmium cells.

The advent of the hermetically sealed nickel-cadmium cell capable of tolerating moderate amounts of overcharge has been a major factor in the development of long-life, compact, high-performance electrical equipment from electric toothbrushes and razors to satellites.

ELECTRODE REACTIONS

The reactions of the nickel-cadmium cell have been studied extensively (refs. 3, 4, 5), particularly the nickel-electrode reactions.

CHARGE-DISCHARGE REACTIONS

At the negative electrode:

$$Cd + 2OH^- = Cd(OH)_2 + 2e^-$$
$$E_{rev} = -0.809 - 0.059 \log a_{(OH^-)} \tag{4-1}$$
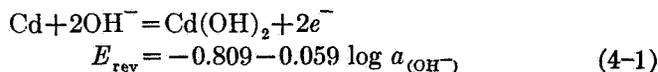
The reactions of the positive electrode are still in some doubt. Falk (ref. 4) suggests:

$$2NiOOH + 2H_2O + 2e^- = 2Ni(OH)_2 + 2OH^-$$
$$E_{rev} = 0.480 + 0.059 \log \frac{a_{(H_2O)}}{a_{(OH^-)}} \tag{4-2}$$
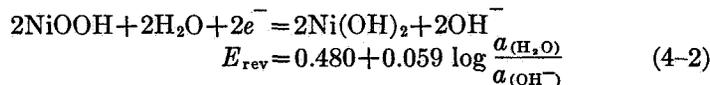
but shows a deviation from the theoretical of the measured emf as a function of KOH concentration. In cells using a 26-percent KOH electrolyte, the negative-electrode potential was independent of the state of charge, while the positive-electrode potential varied with the state of charge. This was interpreted as resulting from the formation of solid solutions of NiOOH and $Ni(OH)_2$ (ref. 4). The emf may be expressed as a function of the H_2O activity in the electrolyte.

$$2NiOOH + Cd + 2H_2O = 2Ni(OH)_2 + Cd(OH)_2$$
$$E_{rev} = E° - 0.059 \log a_{(H_2O)} \tag{4-3}$$
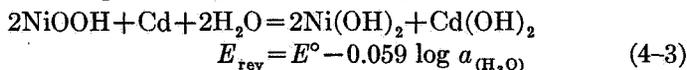
As a result, in a cell operating in a starved condition, the quantity of water consumed is large in proportion to the amount available in the electrolyte, and changes occur in both the activity and the emf of a nickel electrode in relation to the cell state of charge. Reference 4 shows

TABLE 4-I.—*Thermodynamic Data for Nickel-Cadmium Cells With 32% KOH Electrolyte*

Units	ΔH kcal/equiv	ΔF kcal/equiv	dE/dT V/°K	S cal/°K equiv	Ref.
Cd electrode___	[a][b]−22.7	[a]−20.8	−1.4×10⁻⁴	[b]− 6.45	4
Ni electrode___	[a][b]− 8.75	[a]− 8.2	−0.4×10⁻⁴	[b]− 1.84	4
			−1.8×10⁻⁴	[b]− 8.29	4
Total cell___	[a][b]−31.45	[a]−29.0	−2.3×10⁻⁴	[b]−12.0	3
				[c]− 9.95	9
Total cell___	−33.15	[a]−29.4	---------	---------	6
Total cell___	−33.0	---------	---------	---------	11
Total cell___	−32.2	---------	---------	---------	} 10
	−33.7	---------	---------	---------	

[a] Computed from the emf measurements and activity coefficients of KOH.

[b] Computed from dE/dT measurements.

[c] S of NiOOH estimated by the contribution of ions to entropy (Dulong and Petit method).

measurements of emf at half charge totally immersed in various concentrations of an electrolyte. Reference 6 measures the emf of a fully charged electrode at 43.3° C (110° F), as a function of time during which the emf decayed. The table below shows the emf of nickel-cadmium cells (32% KOH electrolyte). The E versus log t lines were extrapolated to an arbitrary time point. The quantity of electrolyte in each cell was not reported.

emf	*Ref.*
1.270_____	6
1.255_____	4

Infrared spectroscopic data (ref. 5) show the discharged form to be $Ni(OH)_2$ with a small amount of water in the crystal lattice. The charging process produces an unidentified hydrogen-bonded structure, which has greater Ni-O symmetry than $Ni(OH)_2$. Although discrete mixtures of compounds were observed, no solid solutions were found.

Excellent summaries of the extensive work on the reactions of the alkaline nickel electrode are found in references 4 and 5, with references to the most significant work. The work summarized in references 5, 6, and 7 proposes more complex reaction mechanisms; this indicates the existence of several nickel oxides in the charged state, and also suggests the formation of compounds with the electrolyte (ref. 8).

Thermodynamic data for the charge-discharge reaction of nickel-cadmium cells are summarized in table 4-I (refs. 3, 4, 6, 9, 10, and 11).

GAS EVOLUTION AND RECOMBINATION

A number of electrode reactions involving the evolution of gases can occur in a nickel-cadmium cell.

At the nickel electrode, the following overcharge reaction occurs in cells which are positive limited. (The capacity of the cadmium electrode exceeds that of the nickel electrode.)

$$4OH^- = O_2 + 2H_2O + 4e^-$$
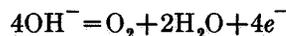
After charge has been terminated, gas evolution continues by decomposition of the active material

$$2NiOOH + 2H_2O = 2Ni(OH)_2 + O_2$$
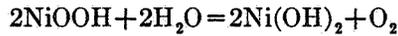
increasing in rate as the temperature rises. This process continues at measurable rates until the cell is totally discharged. At the cadmium electrode or auxiliary electrodes in a charging cell

$$O_2 + 2H_2O = 4OH^-$$
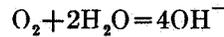
After charge termination

$$2Cd + 2H_2O + O_2 = 2Cd(OH)_2$$
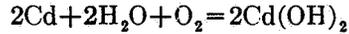
recombining oxygen on open circuit.

The presence of nitrates induces the "nitrogen shuttle" cycle of cell self-discharge.

$$NO_3^- + H_2O + Cd = NO_2^- + Cd(OH)_2$$
$$NO_2^- + 3Cd + 5H_2O \rightarrow NH_3 + 3Cd(OH)_2 + OH^-$$
$$NH_3 + 6NiOOH + H_2O + OH^- \rightarrow 6Ni(OH)_2 + NO_2^-$$
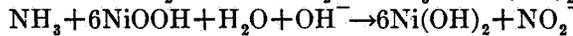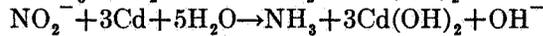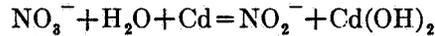
This continues until the cell is totally discharged, or until the ammonia is deactivated by the alternate reaction

$$2NH_3 + 6NiOOH = N_2 + 6Ni(OH)_2$$
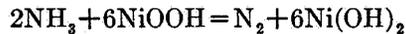
leaving a permanent nitrogen pressure within the cell. Since the processes involved in forming the electrodes usually use the nitrates of nickel and cadmium as the sources of active materials, it is necessary to reduce the nitrogen content of the electrodes to an absolute minimum.

If the capacity of the positive electrode exceeds that of the negative and the cell becomes negative limiting, hydrogen can evolve at the negative electrode during overcharge.

$$2H_2O + 2e^- = H_2 + 2OH^-$$
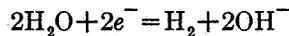
In the absence of catalytic recombination devices, this reaction is almost irreversible, and a long-lasting internal pressure results. Cells manufactured with an excess negative capacity may become negative limiting after extended cycling, or after extended periods on the shelf because of the loss of active surface at the negative electrode. Such behavior generally results from a growth in size of the cadmium hydroxide crystals, which reduces the true surface area of the negative-electrode active material. Oxygen lost from the cell through a microscopic leak can also cause a cell unbalance.

If current is forced through the cell in the discharge direction after the cell is completely discharged, the potential of the cell will reverse and the cell is overdischarged. Hydrogen, oxygen, or both, can be evolved during overdischarge. At the nickel electrode

$$2H_2O + 2e^- = H_2 + 2OH^-$$
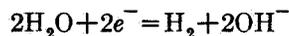
and at the cadmium electrode

$$4OH^- = O_2 + 2H_2O + 4e^-$$
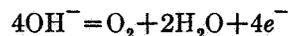
oxygen may recombine in subsequent charging processes, but hydrogen cannot recombine at useful rates without a catalyst. The above gas-evolution reactions can significantly affect cell performance.

The oxygen-evolution rate at the positive electrode during charge is controlled by the current associated with the oxygen-evolution reaction. During the early stages of charge, little or no oxygen evolves. As the cell approaches full charge, its potential rises and the rate of oxygen evolution increases exponentially with rising potential. Unfortunately, at higher states of charge, the O_2 evolution reaction may become preferential to the charging reaction (ref. 12) because there is not enough uncharged active material to accept the charge. Figure 4-1 shows the relationship between the oxygen-evolution and charge-reaction rates at room temperature (25° C) (ref. 12). Since the oxygen-evolution reaction is more temperature sensitive than the charge reaction, oxygen evolution begins at earlier states of charge as the temperature increases (ref. 13).
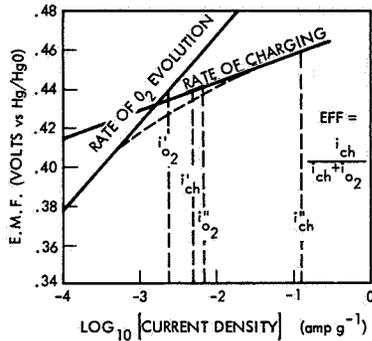
FIGURE 4-1.—Relationship between
O_2 evolution and charge reaction
rates.

The oxygen-recombination rate is controlled by the availability of reaction sites and by the ability of the gas to penetrate to the cadmium electrode. Flooding the electrodes reduces the recombination rate below usable levels. Consequently, rigid control of electrolyte content is essential and should be specified. Cell operation on continuous overcharge at high rates is believed to have adverse effects upon service life, and is not recommended even at steady-state pressures well within the tolerable level. Carson (ref. 14) suggests that the loss in service due to overcharge is proportional to the integral of an undefined overcharge rate function.

Gas evolution due to overdischarge and the prevention of overdischarge are discussed in the sections on battery-operating control.

EFFECTS OF ADDITIVES UPON ELECTRODE PERFORMANCE

Carson (ref. 15) studied the addition of various forms of spinels to the nickel-hydroxide electrode in an effort to improve reversibility and increase working potentials. The charged nickel electrode can decompose in the presence of the peroxyl ion by the following reaction:

$$2NiOOH + H_2O + HO_2^- = O_2 + 2Ni(OH)_2 + OH^-$$
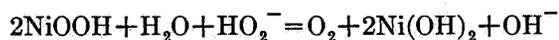
Since the potential of the peroxyl radical is lower than that of the nickel electrode, peroxyl is readily formed. The reaction is autocatalytic; traces of peroxyl increase the peroxyl formation rate at the nickel-electrode surface. Spinels act as decomposition catalysts for the peroxyl radical by reducing the concentration of peroxyl and blocking its further formation. Cobalt additions improve charge retention and capacity, but have no appreciable effect upon reversibility. Scandium additions of 20 atom-percent improve the reversibility by approximately 35 millivolts, and raise the midpoint charge and discharge voltages. This advantage is offset, however, by a loss in utilization efficiency of 30 to 40 percent, leading to a lower-than-normal capacity-to-weight ratio. Ten percent didymium additions had no effect upon reversibility, but produced unexplained increases in utilization efficiency which provided high capacities in a single impregnation. This effect was not observed in multiply impregnated electrodes and was not investigated further. The remaining materials produced either negligible or detrimental effects. Table 4–II, taken from reference 15, shows the C/3 rate performance of the various additive-containing electrodes. Tests at other charge and discharge rates parallel the results in this table.

Ritterman et al. (ref. 16) studied the addition of Li, Na, Be, Mg, Co, and Mn to the nickel electrodes in 5, 10, and 20 atom-percent quantities in an attempt to improve charge retention. Of the materials tested, only cobalt and manganese showed significant improvement in charge retention. Manganese additions decreased charge acceptance, whereas cobalt was observed to improve capacity approximately 14 percent after a 7-day stand at 65° C.

MATERIALS AND METHODS OF CONSTRUCTION

The general structure of sealed nickel-cadmium cells and batteries is described in chapter 2. Several variations in structure may be found in cells from different manufacturers, and in different product lines. Both the nickel and the cadmium electrode are fabricated by most manufacturers in much the same way. Finely divided nickel powder, produced by the thermal decomposition of nickel carbonyl (a vaporizable compound which decomposes from the vapor state at elevated temperatures forming spherical particles of nickel metal), is spread evenly over a current collector grid of nickel or nickel-plated steel, and is sintered in place at a temperature just below the melting point of nickel. A plaque is formed and coined to prevent shorting by strengthening the edges and the place where the current collector tab emerges from the plaque. When finished, the plaque has a porosity between 60 and 80 percent. Immersion in an aqueous solution of the appropriate metal nitrate (nickel nitrate for the positive electrode, cadmium nitrate for the negative) impregnates the finished plaque with active materials. Immersion in a solution of sodium hydroxide in the presence of a polarizing current precipitates the hydroxides. Electrolysis of the electrode in sodium hydroxide solution decomposes nitrates. Ammonia evolves in the process. The impreg-

TABLE 4–II.—*Effect of Nickel-Electrode Additives Upon Utilization Factors and Reversibility; C/3 Cycling Tests*

Code	Name	Utili- zation —	Midpoint voltage versus Hg–HGO		Difference
			Charge	Discharge	
A	None[a]	0.81	0.470	0.370	0.100
B	10 Co	.76	.460	.350	.110
	20 Co	.76	.440	.340	.100
C	10 Sc	.53	.490	.380	.110
	15 Sc	.45	.490	.410	.080
	20 Sc	.42	.490	.440	.050
D	10 Mg	.79	.490	.400	.090
	20 Mg	.58	.490	.400	.090
E	10 Mu	.68	.445	.320	.125
F	10 Ce	.84	.470	.375	.095
G	10 Fe	.40	.480	.370	.110
H	10 Cr	.78	.470	.380	.090
I	10 Al	.70	.470	.390	.080
	20 Al	.96	.460	.370	.090
J	10 Di	2.10	.490	.380	.110
K	10 Ln	.57	.470	.360	.110
L	10 Mo	.66	.480	.380	.100
	20 Mo	.74	.470	.380	.100
M	10 VO	1.25	.460	.360	.100
N	10 Y	.74	.460	.360	.100
	20 Y	.70	.480	.370	.110
O	10 Co Al	.89	.460	.370	.090
	20 Co Al	.95	.440	.350	.090
P	10 Ag Mo	.51	.420	.350	.070
Q	10 Cd Zr	.88	.470	.360	.110
R	10 Mg Al	.67	.470	.375	.095
	20 Mg Al	.69	.490	.390	.100
S	1 Os	.92	.480	.360	.120
T	1 Rh	.39	.510	.420	.090
U	1 Pd	.89	.460	.360	.100
V	1 Pt	1.10	.470	.370	.100
W	1 Ru[b]				
X	10 Co Mo X[c]	.84	.480	.380	.100
Y	10 Cu W X[c]	.74	.460	.360	.100
Z	10 Zn Ti X[c]	.72	.500	.400	.100
AA	10 Co Al X[c]	.92	.470	.360	.110
AB	10 Mg Al X[c]	.91	.425	.380	.095
AC	10 Li Al X[c]	.91	.490	.380	.110
AD	10 Cd Zr X[c]	1.20	.480	.380	.100
AE	10 Co Cr X[c]	.85	.480	.380	.100
AF	10 ScR[d]	.50	.470	.380	.090
AG	15 ScR[d]	.51	.470	.390	.080
AH	20 ScR[d]	.52	.480	.430	.050
AI	10 Ga	1.04	.460	.360	.100
AJ	1 IR[x]	1.14	.460	.350	.110

[a] Standard electrode for comparison.

[b] Not run because of severe degradation of electrode plaque.

[c] Preformed spinels added as fine powder to nickel nitrate impregnation solution.

[d] Rerun of this additive.

nation process is repeated several times until the correct amount of active materials is loaded into the plate.   The electrodes are carefully washed, dried, and set aside for assembly.

McCallum et al. investigated a process for increasing the internal surface area of the electrode current collectors, using electroformed nickel grids of microscopic-pore dimensions, stacked and heat bonded to form electrodes with controlled pore shape and size (ref. 17).   This process has the major advantage of producing electrodes considerably thinner than the commercial sintered plaques, yielding electrodes of improved high-rate performance when using straight-through pore configurations.   McCallum also developed a new method of impregnating the electroformed negative electrodes, utilizing molten salts rather than aqueous solutions, and permitting the use of two-step impregnation rather than the usual four.   The advantages of this were offset by the need for several formation cycles to bring the electrode to its optimum working efficiency.

The immediate value of this work lies in the higher operating currents obtainable through the use of the electrode structure.   Most aerospace applications, however, are capacity limited rather than current limited, and this electrode structure has no capacity advantages.

SEPARATOR MATERIALS

Early nickel-cadmium cells were manufactured with a combined separator-absorbent made of a felted or nonwoven cellulose fabric with excellent absorbent properties.   These cells proved to be limited in service life because of the relatively rapid deterioration of cellulose in an alkaline oxidizing environment (ref. 18).

Efforts to improve separator materials led to programs for screening separator materials for chemical inertness, absorbency, conductivity, mechanical strength, and other significant properties, followed by cell construction and electrical performance evaluation of the resulting cells. Of the more than 50 materials tested, unwoven nylon provided adequate chemical inertness and good electrical characteristics, with nonwoven polypropylene a close second.   Voyentzie (ref. 19) investigated a series of inert separator materials with surface characteristics modified by radiation grafting of reactive compounds.   In this way, it was hoped to improve the wetting and absorbency properties of the separator materials, and to induce ion-exchange properties.   None of the materials tested showed a distinct advantage over the nonwoven polypropylene used in the control cells.

SEALS

A tight seal is vitally important to the nickel-cadmium battery because of the tendency of the cell to unbalance if oxygen generated during overcharge escapes. If this occurs, the balance between negative and positive electrodes changes, and the negative electrode eventually becomes the limiting electrode.   At this point, instead of the cell generating oxygen at the positive electrode and recombining at the negative, a burst of hydrogen gas is given off each time the cell reaches full charge,

and pressure builds up. Whether or not the pressure becomes destructive depends upon the size of the leak. Nickel-cadmium cells use both the glass-to-metal and the ceramic-to-metal seal. An excellent discussion of the technology of both glass-to-metal and ceramic-to-metal seals is given in reference 20, including a discussion of the stresses involved in the formation of seals and the effects of thermal gradients upon seal performance in vacuum tubes.

While the details of the ceramic-to-metal seals are proprietary to the cell or seal manufacturer, all of those currently used depend upon an active alloy seal like that described by Kohl (ref. 20). This involves sensitizing a ceramic body with a titanium or zirconium compound, forming a solid solution with the ceramic at high temperatures. Titanium or zirconium is applied as the hydride suspended in a nitrocellulose lacquer, which is brushed onto the ceramic. When heated in the presence of the brazing alloy, the hydride dissociates and the metal enters into a chemical reaction with the ceramic, simultaneously leaving a clean metallic surface with which the brazing metal can alloy.

Both glass-to-metal and ceramic-to-metal seals present problems. Sealing glasses are attacked by strong alkalis, and silver brazes used in ceramic-to-metal seals are corroded by the electrolytic action of the cell potential through the electrolyte, resulting in premature failures. Improperly designed seals, without sufficient stress relief, may be unable to bear the mechanical loads imposed upon them by the development of internal gas pressures. Seal failure modes are discussed in the section under "Failure Modes."

Voyentzie (ref. 19) reports testing 16 materials for ceramic-to-metal and glass-to-metal seals, and selecting 96 percent alumina as the material with the greatest resistance to attack by KOH solutions. Silver brazing alloy was superior to a previously used 82 percent gold–18 percent nickel brazing alloy because of the greater ductility of silver. Leak rates of less than 10^{-9} cc/yr of air are claimed for both glass-to-metal and ceramic-to-metal seals.

Other types of seals have been proposed or are being investigated, but reports are not available. These include bonded rubber and neoprene seals and graded cermets.

OPERATING CHARACTERISTICS

It is difficult to predict accurately the electrical properties of the nickel-cadmium cell. To a great extent, the problems involved are inherent in the nature of the chemical system, whose properties vary with the history of the cell in the cycles of operation immediately preceding the measurement being taken. This variability is real, and is based upon the properties of the electrodes.

The negative electrode functions during discharge by dissolving the cadmium metal, and reprecipitating cadmium hydroxide as fine crystallites in the pores of the electrode plaque. Similarly, during charge, cadmium hydroxide dissolves and is redeposited at the electrode surface

as cadmium metal. The size of the deposited crystallites depends upon the conditions of deposition: high currents and low temperatures give a finely divided deposit; low currents and high temperatures give a coarser deposit of larger crystals. The discharge characteristics of the negative electrode depend upon the microscopic surface area of the electrode-active materials. As the charging current and temperature change, the characteristics of the subsequent discharge voltage curves vary, even though the state of charge and the discharge conditions are the same. Thus, a battery charged at high temperature, when cooled and discharged, delivers a lower output-voltage discharge wave than the same battery charged at low temperature and discharged under the same conditions. Similarly, a cell discharged under conditions conducive to formation of low surface-area deposits (low current and high temperature) charges at a higher potential than the same cell discharged in another way.

The positive electrode is also unpredictable in behavior, depending upon the temperature and the current at which it is charged. Unlike most battery electrodes, the nickel hydroxide electrode undergoes oxidation and reduction in the solid state; the reaction occurs preferentially at the surface and diffuses inward. Therefore, the surface composition, which determines the electrode potential, differs from the interior composition. The degree of difference is controlled by the difference between rates of oxidation (controlled solely by the current) and of diffusion (controlled solely by the temperature). As a result, the capacity, or state of charge, of the electrode is not a single-valued function of electrode potential. Variations in electrode potential greater than those experienced at end of charge can occur because of the above phenomena.

While these phenomena have been observed qualitatively, no specific data have come to light adequately describing all of these effects or detailing the variables significantly affecting cell performance.

Because of the multiplicity of chemical reactions going on within the nickel-cadmium cell, often simultaneously, the variables influencing the cell's electrical characteristics are inseparable from one another. Ignoring the effects of age and cycle life, the discharge curve of a new cell depends upon temperature, charge mode, efficiency, discharge current, capacity, and state of charge at the beginning and the end of discharge. As a result, although the individual properties of the cell are discussed in separate paragraphs, an understanding of the interdependency of the various factors is essential to the prediction of cell performance. For this purpose, a set of arbitrary definitions is essential for semantic clarity.

DEFINITIONS

The standard capacity of a cell is defined as the measured ampere-hour output of a cell under an arbitrarily defined set of standard conditions. This text uses the following standard conditions for measuring capacity:

Discharge temperature	25° C.
Discharge current	Rated capacity/5.
End-of-discharge voltage	1.000 volt (at the cell terminals).
State of charge at start of discharge	100 percent.

The rated capacity of a cell is that capacity in ampere-hours assigned by the manufacturer as the nominal or nameplate capacity.

The inherent capacity of a cell under a specific set of discharge conditions (different from the standard conditions) is the output of the cell in ampere-hours to an end-of-discharge voltage of 1.000 volt, and starting from a 100-percent state of charge.

The measured capacity of a cell is the output of the cell in ampere-hours to an end-of-discharge voltage of 1.000 volt.

The state of charge of a cell is the fractional ampere-hour capacity remaining in the cell under standard discharge conditions. (It is arbitrarily assumed that the standard charge preceding the standard discharge brings the cell to a 100-percent state of charge, and that, at the end of the standard discharge, the cell is at 0 percent state of charge.)

The charging efficiency is that fraction of the instantaneous charge current being used to charge the cell (as contrasted with the current which may have been diverted to other chemical reactions simultaneously taking place within the cell).

The relative state of charge is the fraction of ampere-hour capacity remaining in the cell, relative to that at the beginning of discharge.

DISCHARGE CHARACTERISTICS

The discharge characteristics of nickel-cadmium cells have been widely measured and reported with varying accuracy and completeness. A typical set of constant-current-discharge curves is shown in figure 4-2.
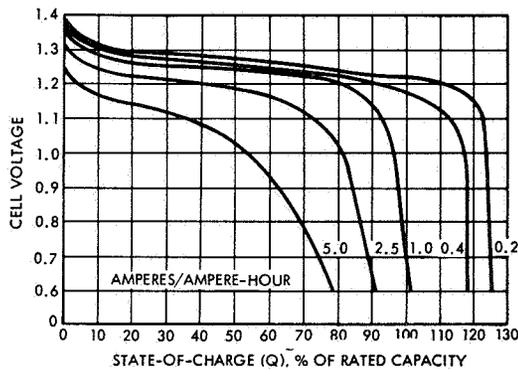
FIGURE 4-2.—Typical discharge characteristics of 20-A-h sealed rectangular nickel-cadmium cell at 75° F. Normalized current (I/C) as additional variable.

These show a great similarity to the generalized or idealized curves shown in chapter 2, the major difference being a significant and measurable slope of the plateau region of the nickel-cadmium discharge curve.

The current-voltage relationship of the nickel-cadmium cell is approximately linear in the range of values measured. Figures 4-3, 4-4, and 4-5
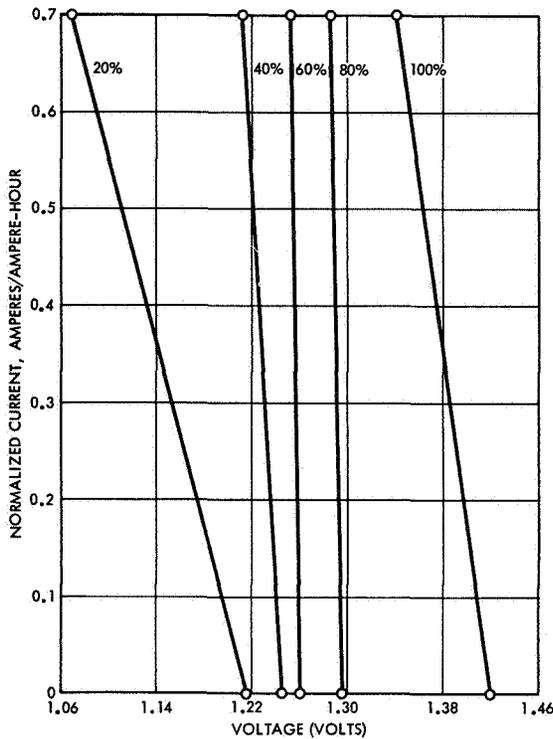
FIGURE 4-3.—Family of normalized current-voltage
lines with state of charge as a third variable (59° F).

show a family of normalized current voltage lines with state of charge
as a third variable based upon data taken at TRW on 20-A-h cells held at
constant exterior temperature in a circulating oil bath. Other data were
reduced, but they are not shown here because the assumptions required
for their reduction make them of limited validity.

If it is assumed, based upon the above data, that the voltage-current
relationship is linear within the normal range of interest, the data taken
by NAD Crane (refs. 21–29) may be plotted on a similar linear scale,
and the characteristics of a wide variety of cells may be established over
a fairly wide range of conditions. The data were taken in this testing
program at only two discharge rates. Consequently, no information can
be derived regarding the conformance of these data to the linear relation-
ship proposed. Reference 30 shows polarization curves that are linear in
the range of C/3 to 2.5C, but depart from linearity at lower currents.
Linearity is achieved by extrapolation of the plateau of the discharge
curve back to the zero intercept E^*, averaging the plateau voltage, $\bar{E}$,
and plotting $E^* - \bar{E}$ versus log I. This presentation, however, is not
directly useful for calculation of discharge curves under complex load
conditions.
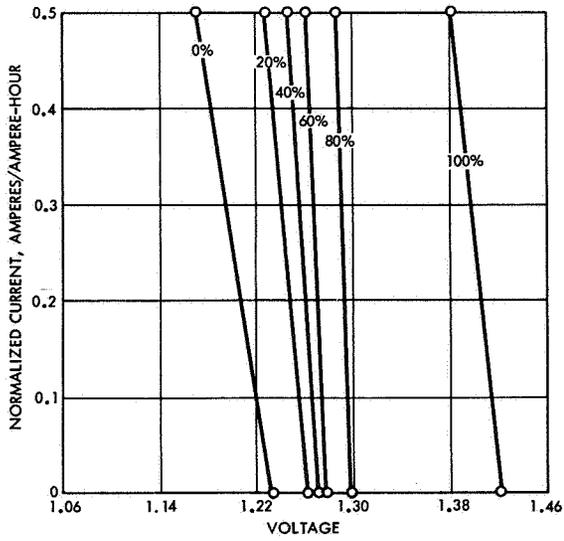
FIGURE 4-4.—Family of normalized current-voltage lines with state of charge as a third variable (78° F).
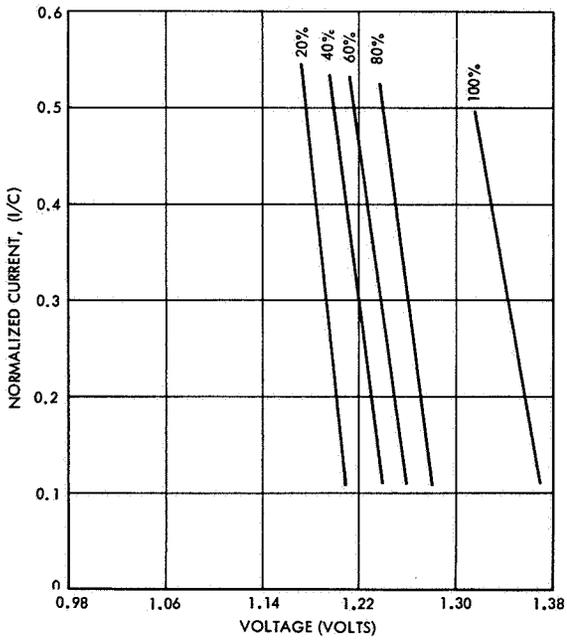
FIGURE 4-5.—Family of normalized current-voltage lines with state of charge as a third variable (97° F).

Typical current-voltage curves derived from portions of the NAD Crane data are shown in figures 4–6 through 4–8 with state of charge and temperature as additional variables. Reduction of these data requires a number of assumptions. Firstly, it is assumed that the inherent capacity of the cell does not differ from the standard capacity under all conditions.
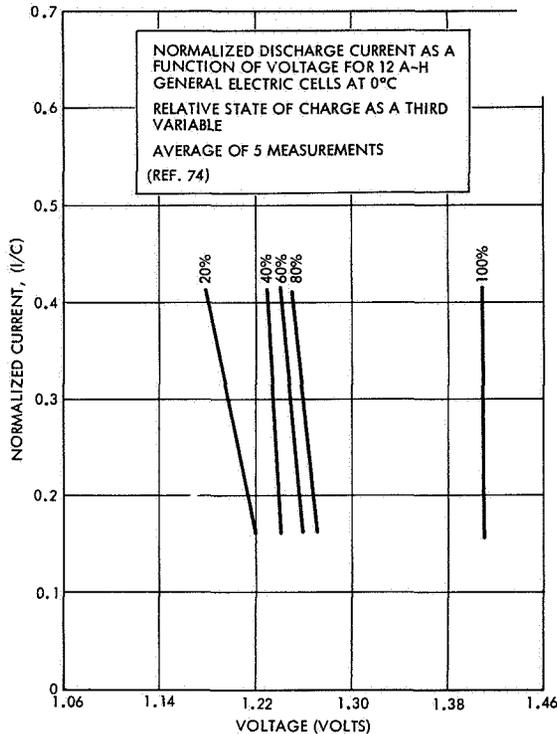
Figure 4–6.—Curves derived from portions of the NAD Crane data.

(See "Definitions," above.) Secondly, it is assumed that the loss of capacity at the high-temperature discharge is due entirely to the lower charging efficiency at elevated temperatures, so that the state of charge of the cell at the beginning of discharge is a fraction equal to the measured capacity divided by the standard capacity. At the low temperatures, it is assumed that the state of charge at the beginning of discharge is 100 percent (not an unreasonable assumption with the charge-control method used), and that the loss in capacity shown is due to the incompleteness of discharge alone, rather than to any difference between standard capacity and inherent capacity. These assumptions establish a basis for estimating the nickel-cadmium-cell state of charge at each point on the discharge curve, since it is not necessarily true that

The figure shows a graph titled:

NORMALIZED DISCHARGE CURRENT AS A FUNCTION OF VOLTAGE FOR 12 A-H GENERAL ELECTRIC NICKEL-CADMIUM CELLS AT 25°C

RELATIVE STATE OF CHARGE AS A THIRD VARIABLE

AVERAGE OF 5 MEASUREMENTS

(REF. 29)

Y-axis: NORMALIZED CURRENT, (I/C) from 0 to 0.7

X-axis: VOLTAGE (VOLTS) from 1.06 to 1.46

Curves labeled 20%, 40%, 60%, 80%, 100%
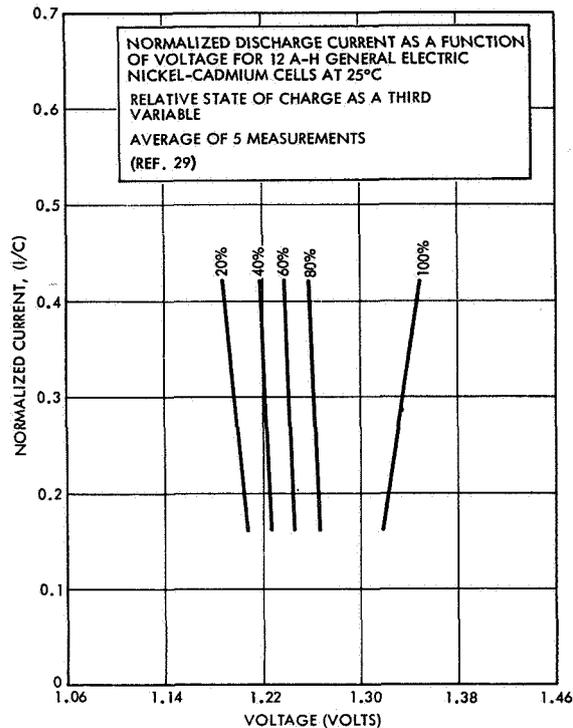
FIGURE 4-7.—Curves derived from portions of the NAD Crane data.

the cell is fully charged at the end of charge or fully discharged at the end of discharge.

An examination of the current-voltage curves produced by reduction of the NAD Crane data shows several general characteristics. Data are more widely scattered than the TRW characteristics data, or the manufacturer's data, probably because of uncertainty in the temperature of the cells. (Only the environmental temperatures are reported.) Cell temperatures are not reported except as maxima during a group of cycles and these are of doubtful accuracy due to the measurement method used. Scatter of the data is widest at the beginning and end of discharge, and smallest about the midpoint. This probably results from the negligible temperature coefficient of voltage in the neighborhood of the discharge midpoint which was observed in nickel-cadmium cells (ref. 31) and to the variability of the cells in capacity. Considerable uncertainty exists regarding the state of charge of the measured cell because of the combined lack of temperature control, efficiency data, and charge current data. This necessitates using the preceding set of assumptions to estimate the cell's state of charge. The result of these combined uncertainties makes the reported data questionable for prediction of operating characteristics in other cycles by extrapolation or interpolation.
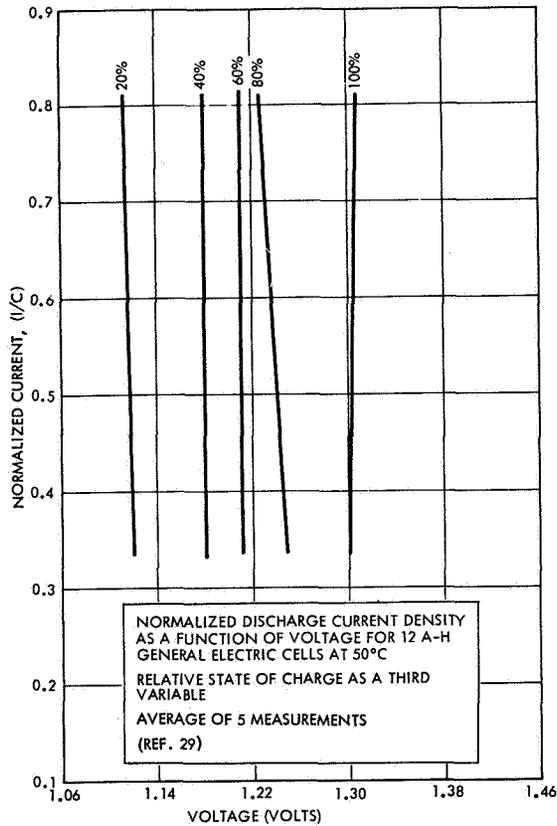
FIGURE 4-8.—Curves derived from portions of the
NAD Crane data.

The TRW data are somewhat more precise, although considerable
uncertainty exists regarding the state of charge of the cell, and no infor-
mation is available regarding the voltage-temperature coefficient at points
along the curve other than the midpoint.

OVERCHARGE CHARACTERISTICS

During overcharge, little or no input energy is stored, and essentially
all input is converted to heat. Under these conditions, electrical charac-
teristics of the cells are different than during active charging; i.e., during
the charging phase where a large fraction of input energy is stored.

Most data available for overcharge behavior have been taken from
measurements of overcharge current as a function of cell voltage and
temperature on individual cells or small packs of cells, rather than on
full-scale batteries. Data from different sources conflict because special
precautions are usually not taken to induce uniform behavior within cell
groups, different methods of controlling temperature are used for different

tests, and different charge methods are used. The last two factors are the most probable sources of variation. The behavior of a cell is a function of the average internal cell temperature; at a given voltage, a 10° F change in internal temperature in the region of 80° F produces approximately a 100-percent change in overcharge current. The internal cell temperature is seldom measured directly; instead, the cell-case temperature or the ambient temperature is measured and/or controlled. When temperature is so measured, incorrect assumptions may be made about the relationship of the measured temperature to the true average cell temperature.
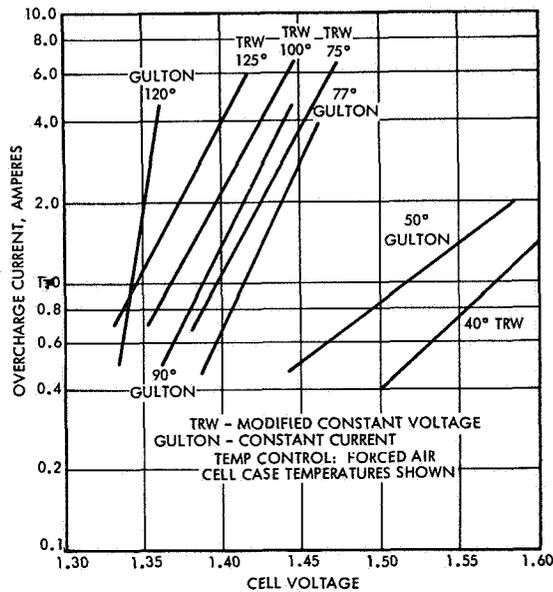
FIGURE 4-9.—Overcharge performance data for Gulton 20-A-h cells.

Overcharge performance data for Gulton nickel-cadmium cells have been taken by Gulton and by TRW on various in-house studies. The Gulton data were obtained on 20-A-h cells, using forced air as a temperature medium. Temperatures shown on Gulton plots are cell-case temperatures measured by attaching thermocouples to the cell case. The cells were charged at the C/10 rate (2 amperes) for 24 hours prior to the overcharge measurements. TRW data and smoothed Gulton data are shown in figure 4-9.

Most overcharge data generated at TRW (ref. 31) derive from tests charging the cells by a modified constant-potential method, rather than by the constant-current method Gulton used. The temperature of the cells was controlled in forced air ovens, and the cell-case temperature

measured by attaching thermocouples to the cell case. Both the slopes of the lines and the overcharge current values at a given voltage and temperature differ considerably in the two sources. TRW currents are generally higher than Gulton's in the range from 60° to 90° F. The TRW tests may not have run long enough to reach the true overcharge current level, or the overcharge current basically differs for different charge methods, or for variations in cell manufacture. At the present time, it is not possible to evaluate the relative accuracy of the two data sources.

The temperature sensitivity of the overcharge measurements may be determined by crossplotting the log I versus E curves at constant current for various temperatures. At 75° F and higher, and at a current of C/10, the TRW data show a slope of 1 mV/°F, while the Gulton data show a slope of 2 mV/°F. Below 75° F, the characteristic is nonlinear.

NAD Crane took overcharge data measurements (refs. 21 to 29), on different cells from several manufacturers, but left cell environment uncontrolled, and only reported cell temperatures above 80° C, making the analysis of the independent effects of temperature and current impossible. The resulting voltage curves fluctuate widely, probably because of environmental fluctuations and internally generated heat. Cell temperatures vary from the reported environmental temperature as much as 50° C. Consequently, the sole value of the data reported is in giving assurance that the cell survived the conditions to which it was exposed.

CAPACITY

The measured capacity available from a nickel-cadmium battery depends greatly upon the manner of operating the battery. Loss of measured capacity may result from one or from a combination of factors.

If the battery is fully charged and is discharged at a higher current or a lower temperature than that of the capacity measurement standard, increased polarization causes the terminal voltage to reach the minimum acceptable level (cutoff) sooner. In these circumstances, the residual capacity is still in the battery and may be withdrawn without further charging by reducing the current or raising the temperature. The capacity is not lost, but operating conditions demand the application of a derating factor. If the battery is charged at a lower current, a higher temperature, or a shorter time than those of the measurement standard procedure, an apparent loss in measured capacity occurs. In effect, reduced efficiency at low currents and high temperatures causes a lower time integral of the product of charge current and efficiency than measurement standard, and results in an apparent loss in capacity. Actually, the inherent capacity of the battery is unchanged; the charge-control system has failed to recharge the battery to full capacity. In addition, the combined conditions of a low charging current and a high temperature tend toward the formation of lower surface area crystallites, which, on subsequent discharge, increase polarization and cause further losses in measured capacity. To some extent, the effects of an increase in

temperature may be overcome by increasing the charge current, thereby increasing efficiency and decreasing crystallite size. Similarly, the effects of a decrease in charging current may be partially offset by a decrease in the operating temperature. Once the efficiency of conversion from electrical to chemical energy has decreased to zero, however, charging for longer periods of time cannot overcome the charging efficiency losses due to decreases in current or to rise in temperature. Failure to charge a battery completely may also occur when the charge-control logic is unrepresentative of actual battery performance.

Typical data on fresh-battery capacity shows a broad peak about room temperature, with a loss in capacity at both low and high temperature. The extent of this capacity rolloff at temperature extremes depends upon the specific operating conditions. Lower discharge currents raise the low-temperature end of the curve, while higher charge currents raise the high-temperature end of the curve (fig. 4–10). The capacity available
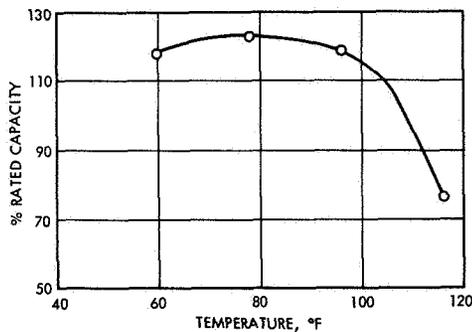
FIGURE 4–10.—Available capacity versus temperature (7-amp discharge), Gulton 20-A-h cells, modified constant potential charge mode.

from a nickel-cadmium cell also depends upon the method used for charge control. At low temperatures, for example, the amount of electrical energy a battery takes up at constant current before reaching the maximum tolerable voltage may be considerably less than the amount necessary for recharge. Under these circumstances, charging must continue at a lower current (either by step changes or by limiting the applied potential) to achieve the fully charged state. In applications such as the low-level orbits, insufficient time is available for completion of charge, and the capacity of the battery must be derated at the low temperatures.

For the most part, the available capacity data make no distinction between the inherent capacity of a cell under specific operating conditions and the measured capacity under the same set of conditions. Failure of the system to charge or discharge the cell or battery completely affects

the measured capacity. Because the battery's electrical and thermal characteristics depend upon the battery state of charge, prediction of the performance characteristics without the state-of-charge information leads to confusion. As a specific example, a nickel-cadmium cell, having a capacity which is limited by the positive electrode, and operating under typical charge control at a temperature of 100° F and with a low-to-moderate charge current, may reach a charge efficiency of zero at a 60-percent state of charge (60 percent of the positive-electrode active materials are in the charged state, 40 percent are in the discharged state). The capacity is 60 percent of the standard measured capacity. At the start of discharge, however, the cell is already 40 percent discharged, and its electrical characteristics best compare with those of a cell discharging from 60 percent to the final required depth of discharge. NAD Crane reports measured capacity data as a function of the temperature of the testing environment but does not report cell-temperature data.

EFFICIENCY

Bauer and Sparks reported ampere-hour efficiencies of nickel-cadmium cells (ref. 31) for 20-A-h and 12-A-h cells, and NAD Crane reported the ampere-hour efficiencies for cells of various sizes from different manufacturers (refs. 21 to 29, and 32). Watt-hour efficiencies are the product of ampere-hour efficiencies and the discharge/charge voltage ratio. Both cases used modified constant-potential charging, but applied different voltage-limit settings. Efficiency data are obtained from a series of partial charges and discharges of varying depth, starting with a fully discharged cell and plotting the ampere-hour output against the ampere-hour input (ref. 31) or against charging time (NAD Crane). Bauer and Sparks went one step further by assuming that the curve ran through the origin (no output for no input) and measuring the slope of the input-versus-output curve at intervals. A slope of 1 indicates 100 percent efficiency; a slope of zero indicates 0 percent efficiency. When the Crane data are handled in a similar manner, the results are not always consistent internally. Figure 4-11 shows a typical NAD Crane input-versus-output curve. Even ignoring the extrapolated portion of the curve, the results are not consistent with known heat-evolution rate data, oxygen-evolution rate data, and other efficiency data, nor are efficiencies of greater than 100 percent theoretically achievable. The appearance of the inflection resulting in these discrepancies is fairly common in the Crane data. A partial explanation is the wide discrepancy between the temperatures of the cells and the reported environmental temperature, and probable inaccuracies in the measurement of the end-of-discharge voltage cutoff.

Carson (ref. 14) reports the variation of the rate of evolution of oxygen from the positive electrodes as a function of state of charge. Since the oxygen-evolution reaction is the principal, if not the only, cause of ampere-hour efficiency loss in nickel-cadmium cells, the curve is an inverted image of the efficiency curves. The conversion efficiency of the cell approaches 100 percent during the early states of charge, when oxygen
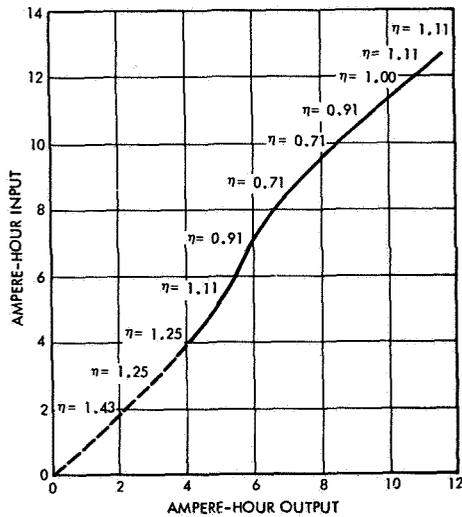
FIGURE 4-11.—Typical NAD Crane input-output curve for a 12-A-h nickel-cadmium cell extrapolated back to the origin. Efficiencies (η) computed from the slope of the curve (ref. 31).

evolution is not significant in rate. As the cell approaches full charge, the oxygen evolution-recombination cycle takes over and the efficiency approaches zero. Ampere-hour efficiency rises with increasing charge current and decreasing temperatures, provided that the cell-terminal voltages do not exceed the level at which evolution of hydrogen from the negative electrode occurs.

Figures 4-12 through 4-15 show ampere-hour efficiencies of nickel-cadmium cells as a function of state of charge, with temperature and charge rate as additional variables. These data were derived from measurements on the OGO cells (ref. 31) and from unpublished measurements taken by Grumman Aircraft and by TRW Systems, in connection with OAO and other programs. The data have been smoothed, and are based upon cycling the cell to 100 percent depth of discharge. There are currently insufficient data for an efficiency determination at lesser depths of discharge; however, there are indications that the decreasing depth of discharge sharpens the knee of the efficiency curves and increases the overall efficiency. There also appears to be justification for the belief that the efficiency of charge at a low rate is increased if the early stages of charge are performed at a high rate. Thus, the use of these efficiency data in design will result in conservative estimates of the state of charge.

IMPEDANCE

Battery dynamic impedance is of critical importance in the design of compact electric-power systems. If the impedance characteristics are
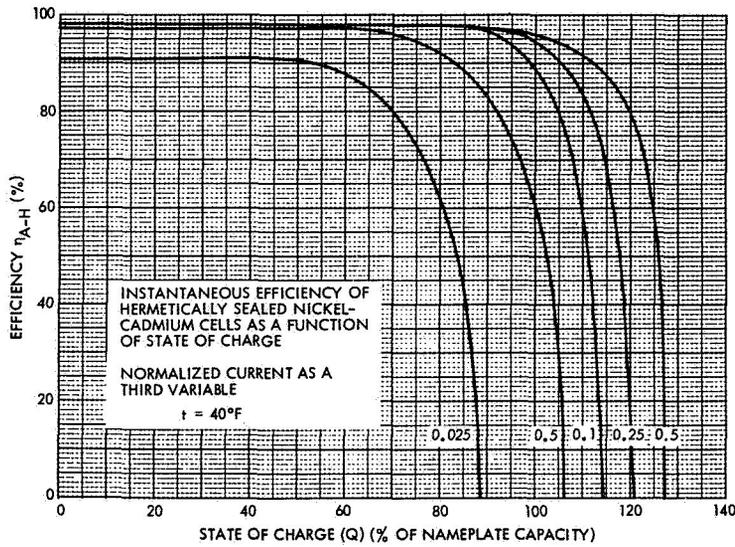
FIGURE 4-12.—Ampere-hour efficiencies of nickel-cadmium cells as a function of state of charge, with temperature and charge rate as additional variables.
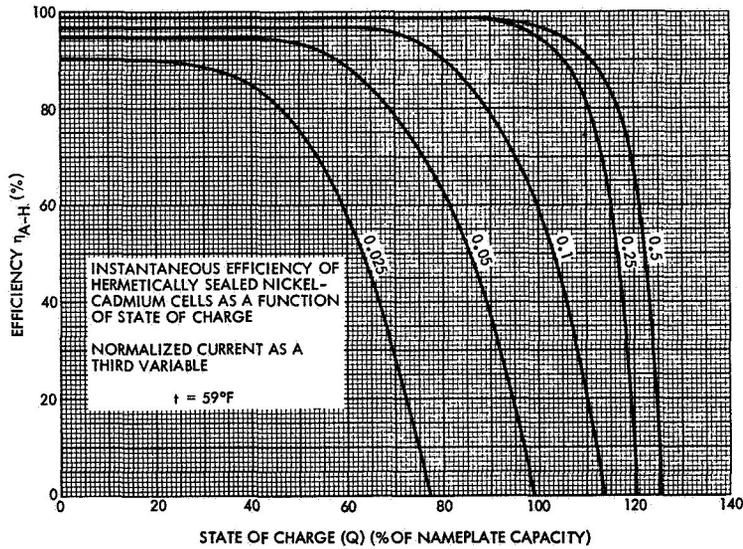
FIGURE 4-13.—Ampere-hour efficiencies of nickel-cadmium cells as a function of state of charge, with temperature and charge rate as additional variables.

INSTANTANEOUS EFFICIENCY OF
HERMETICALLY SEALED NICKEL-
CADMIUM CELLS AS A FUNCTION
OF STATE OF CHARGE

NORMALIZED CURRENT AS A
THIRD VARIABLE

t = 78°F
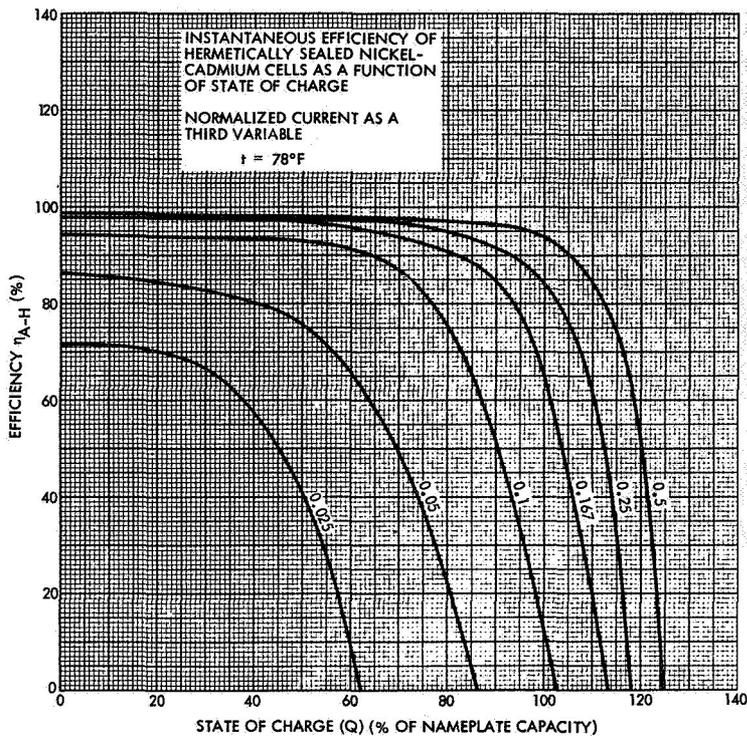
FIGURE 4-14.—Ampere-hour efficiencies of nickel-cadmium cells as a function of state of charge, with temperature and charge rate as additional variables.

known, the battery may be used as a filter for the power subsystem. In addition, impedance measurements are useful in detecting potential battery-cell failures.

Brodd and DeWane (ref. 3) measured the ac impedances of nickel-cadmium cylindrical and button cells, using a capacitance bridge, and reported the results in the form of Argand diagrams (plot of reactance versus resistance). These results did not agree completely with theoretical predictions from electrode kinetics (ref. 33), the deviations being interpreted as resulting from interference by physical factors. In general, the results indicate a decreasing resistive and capacitive reactance as a function of increasing frequency, until reaching a frequency at which the reactance approaches zero. At this point, a net inductive reactance appears and resistance again increases. Impedance increased suddenly at end of discharge. Bauer and Sparks (ref. 31) measured alternating current impedance as a function of frequency and found slight indications of a decrease in open-circuit impedance with increasing frequency in the
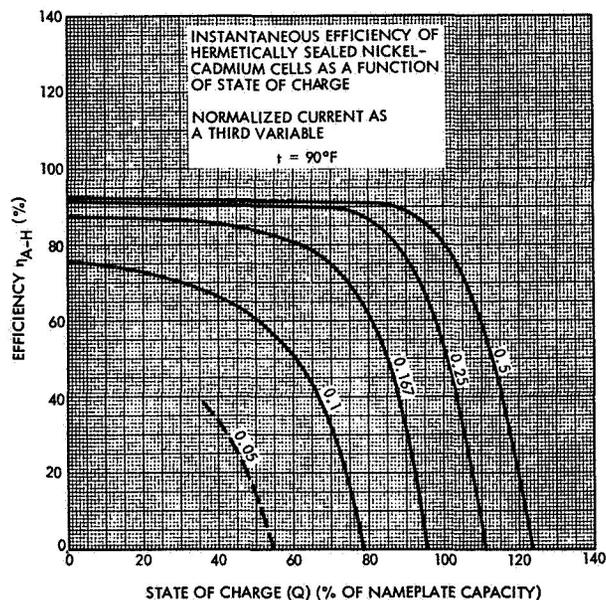
FIGURE 4–15.—Ampere-hour efficiencies of nickel-cadmium
cells as a function of state of charge, with temperature and
charge rate as additional variables.

lower frequency range. The magnitude of the measured impedance,
however, in relation to the capacity of the cell, is an order of magnitude
higher than expected if the electrode processes were the controlling factor.
It seems probable, therefore, that the ohmic resistances of the current
conductors and electrolyte overshadow the electrode processes in the
larger size prismatic cells. Figure 4–16 shows the measurements of im-
pedance as a function of frequency on open circuit and during charge and
discharge. NAD Crane measured the impedance of nickel-cadmium cells
by measuring potential 5 milliseconds after a step change in current
(galvanostatic method) (refs. 21 to 29). These data are plotted, showing
the relationship of impedance to capacity (fig. 4–17, refs. 34 to 37). To
minimize the effects of scatter in the data, averages of five impedance
values are plotted.

The NAD Crane data show an increase in cell impedance with in-
creasing size in cylindrical cells, in contrast with Brodd and DeWane's
(fig. 4–18) decrease in impedance with increasing size. The data are
scattered, possibly because of variations in structure of the cells from
different manufacturers.

Gulton Industries reported additional impedance data in their cell
characteristics data sheets (fig. 4–17), measured by the galvanostatic
method.
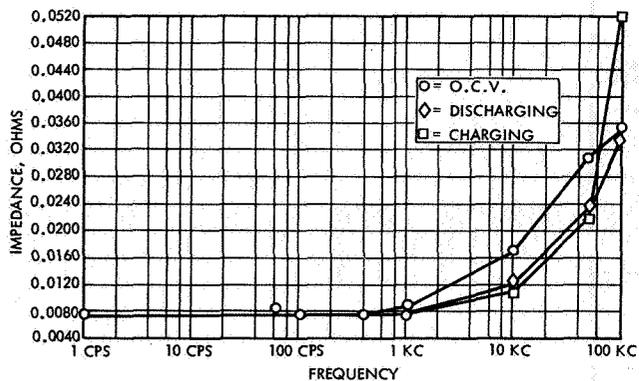
FIGURE 4–16.—Cell impedance versus frequency; Gulton VO–20 HS cell (sine-wave measurement method).
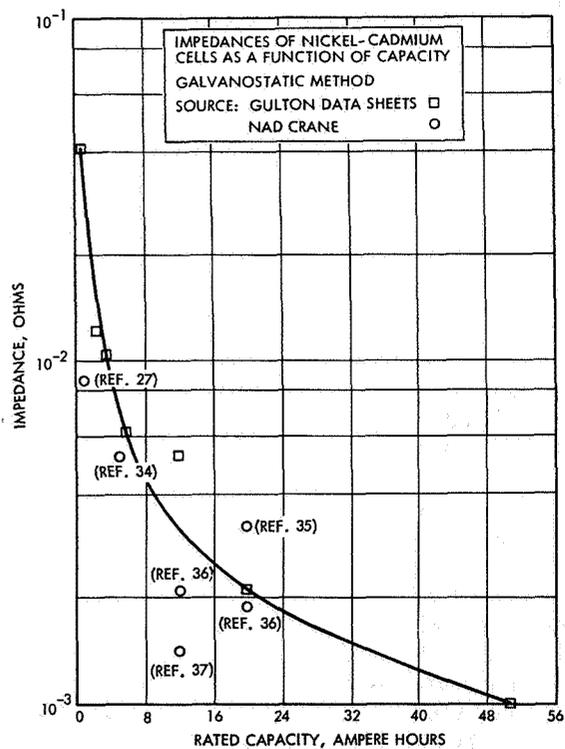
FIGURE 4–17.—Impedance of nickel-cadmium cell versus capacity; galvanostatic method. (Sources: Gulton data sheets; NAD Crane.)
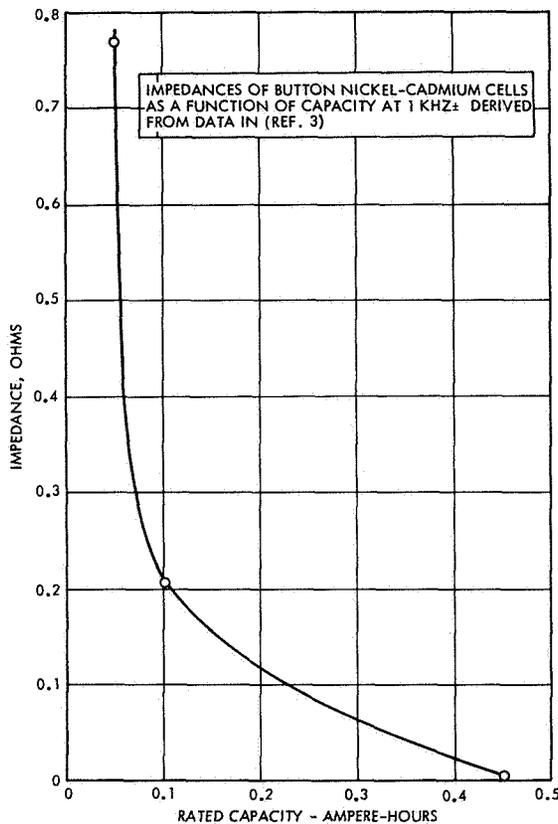
FIGURE 4-18.—Impedance of button nickel-cadmium
cells versus capacity at 1 kHz.

Variation of impedance due to changes in temperature is reported by
Brodd and DeWane, who found significant increases in cell impedance
with increasing temperature.   Increases in cell resistance tend to over-
shadow those in capacitive reactance.

An overall qualitative interpretation of the available data suggests
that in the small, simply structured, button cell, having a low-inductance
configuration, the bulk resistivity of the electrolyte and the kinetics of
the electrodes control the impedances at low frequency.   As cell structure
changes to the spiral or prismatic configuration, and simultaneously
increases in surface area, the contribution of the electrode kinetics to
impedance becomes less significant, and that of the inductance and
electrical resistivity of the internal conductors and current collectors
becomes the overriding factor in determining impedance.   The increase
in impedance with increasing capacity shown by the Crane data on
cylindrical cells (fig. 4-19, refs. 38 to 44) has not been explained.
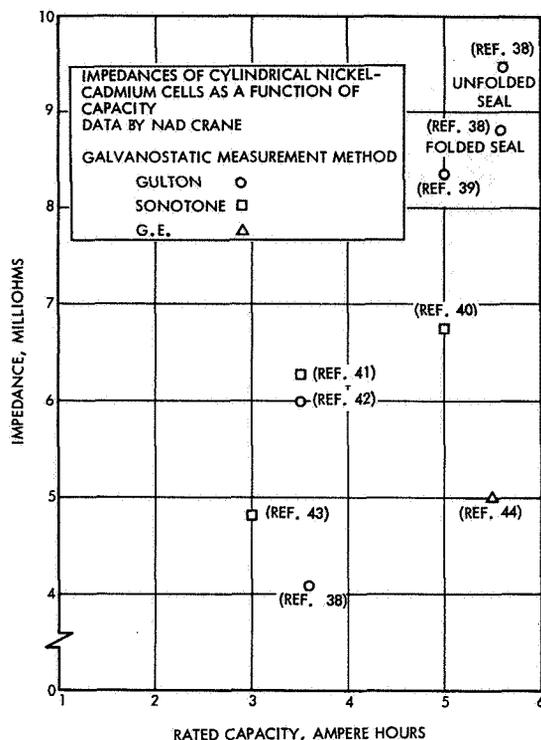
FIGURE 4-19.—Impedance of cylindrical nickel-cadmium cells versus capacity; data by NAD Crane (galvanostatic measurement method).

HEAT EVOLUTION

From the system-design standpoint, the heat-evolution rate in nickel-cadmium batteries is of tremendous importance in aerospace applications. The limited heat-rejection capability of satellites and spacecraft, and the narrow range of temperatures in which the battery can operate with both high-efficiency and high-performance characteristics, require detailed knowledge of the heat-evolution rate of the batteries throughout their operating cycle. As yet, no fully adequate method exists for predicting heat-evolution rates as a function of time.

Theoretically, if the rate of each reaction in progress within the cell is known, equation (2-16) can be used to estimate the heat evolution caused by each reaction. By adding their effects, the total instantaneous heat-evolution rate can be estimated. For the charge-discharge reactions, the thermodynamic data are used to calculate the reversible potentials and substituted into the general equation with measured entropies, voltages, and currents. A problem arises when the overcharge reaction begins to

parallel the charge reaction, since, in order to evaluate the heat effects of these reactions, an estimate is required of the current devoted to each of them.   Several approaches are possible.   If the potential of the nickel electrode can be measured relative to some standard, it might be possible to estimate the rate of gas evolution, from which the current supporting the overcharge reaction can be calculated.   Experimental verification could be obtained for equation (2–16) by making simultaneous measurements of current, voltage, nickel-electrode potential relative to a standard electrode, gas pressure, and heat evolution, during a charge-discharge cycle.   Such an experiment would fail to account for the heat effects because of spontaneous generation of oxygen by decomposition of the nickel electrode after terminating charge.

A reasonable approximation of the heat-evolution rate on charge may be obtained using the expression:

$$q = (I\Delta E + ITK)\eta_{A\text{-}h} - IE(1 - \eta_{A\text{-}h}) \qquad (4\text{-}4)$$

where η is the ampere-hour efficiency as obtained from figures 4–12 through 4–15, and is used as an estimate of the fraction of current which is used in the charging reaction.   This expression does not account for the delayed energy stored as oxygen pressure on charge and later released as heat during the early stage of discharge, or for the heat effects of spontaneously generated oxygen.

Beck and Kemp (ref. 45) measured the heat-evolution rate of cells for the Lunar Orbiter battery in terms of a synthetic parameter $E_{\Delta H}$, a "voltage associated with the enthalpy of the reaction," which varies with temperature and combines both the free energy and the entropy terms of the classical thermodynamic equation.   An empirical equation computed the total heat generated over an entire cycle, including average discharge voltage, average charge voltage, current, and efficiency terms.   Over the complete cycle, the reversible heat term (included in the $E_{\Delta H}$ parameter) is eliminated, since the cyclic integral of any thermodynamic property such as entropy equals zero.   The prediction of heat-generation rates is reported to be impractical because of inadequate efficiency information. Metzger and Sherfey (ref. 11) establish heats of reaction for the charge-discharge reaction and for oxygen recombination at 33.0 and 30.43 kcal/equivalent, respectively, calculating these values from measurements of heat generation in nickel-cadmium-sealed cells.   Bruins et al. (ref. 6) measured heats of reaction of the charge-discharge reaction from calorimetric measurements on sealed nickel-cadmium cells and on cells containing lithium-hydroxide electrolyte additives or didymium-hydroxide additions to the positive electrode.   Changes in the heats of reaction with LiOH additions led to the conclusion that the system depends on an electrolyte concentration.   Foley and Webster (refs. 10, 46, 47) measured the heat evolved on repetitive cycling of a 6-A-h nickel-cadmium cell using an isothermal flow calorimeter (fig. 4–20).   They also report concurrent voltage measurements and pressure data derived from auxiliary electrode potential measurements.   Additional data, including the relationship of cell potential to oxygen evolution from the positive
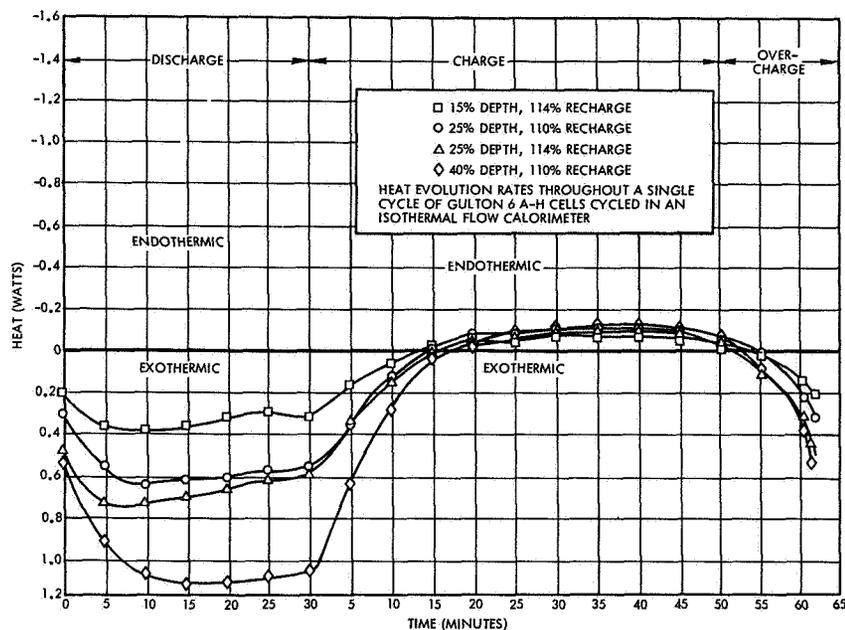
FIGURE 4–20.—Foley and Webster measurement of heat evolved on repetitive cycling on a 6-A-h nickel-cadmium cell using an isothermal flow calorimeter.

electrode, are required to assemble a complete picture of the heat-generation rates as a function of current, time, and state of charge; and to allow a theoretical comparison with measured heat-generation rate data. Tafel curves showing such data were measured under experimental conditions widely different from those in the calorimeter and, consequently, are not compatible with the calorimetric data. Reproducibility of the measured data is good. Current plans call for extending measurements to the 12-A-h and 20-A-h sizes.

MAGNETIC PROPERTIES

The varying magnetic field created by a battery disturbs the experimental instruments designed to measure low-intensity magnetic fields. Nickel-cadmium batteries are composed largely of ferromagnetic materials having a strong residual magnetism and, as current-carrying devices, also produce an induced magnetic field which increases exponentially with current.

Voyentzie (ref. 19) measured the magnetic field of a 10-cell nickel-cadmium battery using spiral-wound cylindrical cells, and found that the influence of the external wiring on the magnetic field generated by the battery exceeded the influence of the battery cells by an order of magnitude. He proposes a low-magnetic wiring pattern as shown in figure 4–21. Unpublished magnetic-field measurements made at TRW on a
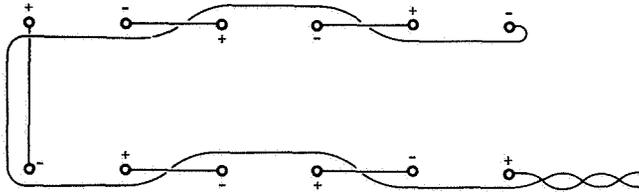
FIGURE 4–21.—Wiring pattern for low magnetic fields.

12-A-h nickel-cadmium battery of 22 series-connected cells had a maximum intensity magnetic field, as shown in the following table:

Condition:	Maximum magnetic field intensity, gamma (at 1 ft)
Open circuit_____	500 to 3000.
1-A discharge_____	200 to 700.
5-A discharge_____	1000 to 3000.

The residual magnetic field is peculiar to the nickel-cadmium battery. Other batteries made only of nonmagnetic materials have negligible residual fields. However, the magnetic field intensities of nonmagnetic batteries with current flowing are comparable to those of the nickel-cadmium battery.

MEMORY EFFECT AND RECONDITIONING

The memory effect in a nickel-cadmium cell occurs when the cell cycles at a constant depth of discharge, and is characterized by progressive decreases in the voltage of the discharge curve with increasing cycle of cell operation. Carson et al. (ref. 14), Bauer and Sparks (ref. 48), and others describe this effect, and attribute it to the reduction in surface area by crystal growth of unused materials. The magnitude of the memory effect varies with the depth of discharge and with the log of the number of cycles of operation, based upon cycle-life data. (See data under "Cycle Life.") When cells are operating at random depths of discharge, the memory effect does not appear to a significant extent in approximately 500 cycles (ref. 49).

A "memorized" cell may be reconditioned and a large part of its original capacity restored by fully discharging the cell and allowing it to remain under load for a time after it has fallen below its minimum acceptable output voltage. Bauer and Sparks (ref. 31) and Halpert (ref. 50) observed this. Carson (ref. 14) suggests using several reconditioning cycles for complete restoration of capacity. Hennigan and Sizemore described automatic nickel-cadmium reconditioning circuits (ref. 51) in which the cells are discharged through individual transistors connected across them after discharging the battery through its own discharge transistor (fig. 4–22).

NAD Crane reconditions with a capacity measurement discharge to 1 volt/cell (or 0.5 volt on any 1 cell) and suggests this partial reconditioning is only temporary (refs. 32, 52). Unpublished TRW data on a
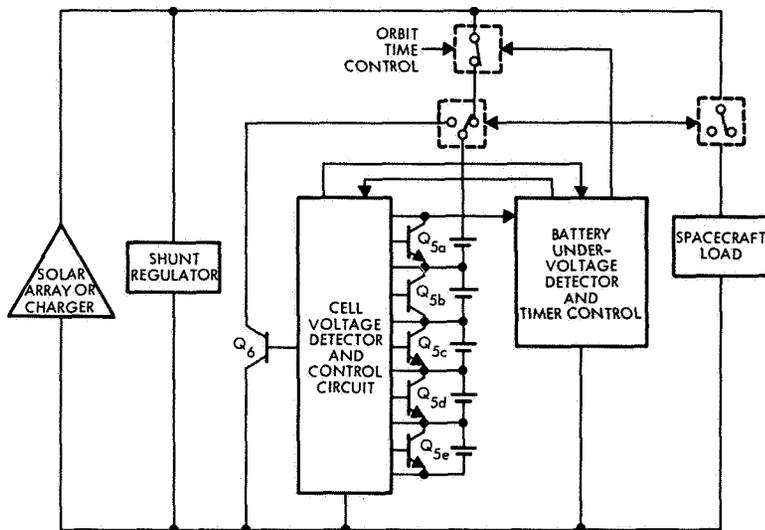
FIGURE 4-22.—Nickel-cadmium battery reconditioner system.

22-cell battery reconditioned by full discharge every 50 cycles show a net gain in postreconditioning capacity after 700 cycles of operation at 75 percent depth of discharge, although slight intermediate losses did occur. The capacity gain is still unexplained (fig. 4-23).

SERVICE LIFE

The two basic criteria used in evaluating the service life of a battery cell are deterioration in performance characteristics and failure. With the exception of the memory effect, which may be reversed by reconditioning, and of performance changes immediately preceding a failure, the nickel-cadmium cell usually shows no significant performance changes throughout its life. In other words, an unfailed cell, properly reconditioned prior to characteristic measurement test, has essentially the same performance characteristics after many thousands of cycles as when new and recently reconditioned. This does not imply that the cells have infinite life, but after reconditioning, the performance characteristics are unaffected until failure actually occurs or is imminent. The use of failure as a criterion of service life must be evaluated in terms of the service conditions to which the cell is subjected, since most of the observed failures have been due more to the use of improper charge controls, inadequate system designs, and a failure to recognize the impact of these factors upon cell and battery survival.

Two major NASA programs for life testing a variety of nickel-cadmium cells have been implemented, one at the Inland Testing Laboratories (refs. 53, 54) and one at NAD Crane (refs. 28, 32, 52). The five referenced reports are summaries of these two large testing efforts.
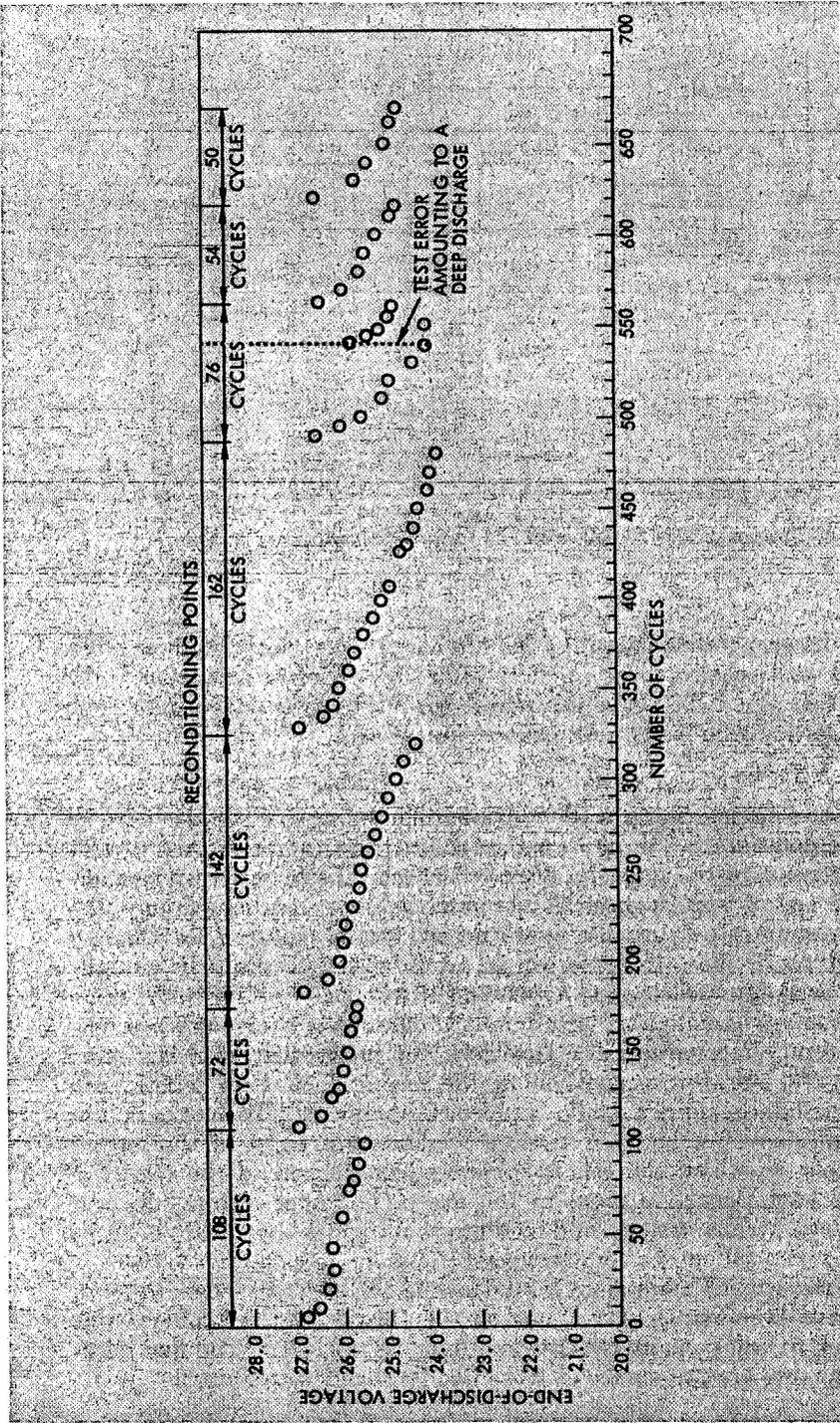
FIGURE 4-23 —Typical nickel-cadmium battery behavior on reconditioning (24-hour synchronous orbit cycles).

The Inland Testing Laboratories performed cycling tests at $-10°$, 25°, and 40° C, varying the depth of discharge between 10 and 40 percent. The current required to replace the discharged energy in a typical 100-minute orbit situation, multiplied by an overcharge factor which varied with the temperature (115 percent at $-10°$ C, 125 percent at 25° C, and 150 percent at 40° C), determined the charging currents. The preset voltage limits varied with the type of cell. Both voltage and overcharge factors were selected on the basis of undescribed preliminary tests. The average end-of-charge and end-of-discharge voltages and representative charge and discharge curves are reported; temperatures of cells are not reported. Failures are usually recorded as the cell's inability to deliver power at 1 volt or higher throughout the discharge cycle (later reduced to 0.9 volt), although other failure symptoms, such as electrolyte leaks, gas pressure bulge, and separator puncture by a grid wire, are listed. For the most part, however, the failure mode and mechanisms are not identified. Examinations of the charge curves of many of the cells operating at 25° and $-10°$ C showed individual cells' end-of-charge potentials as high as 1.7 volts, although the test conditions specify an applied potential limit of 1.54 volts per cell. Assuming that the testing equipment functioned properly, divergence in cell characteristics is to be suspected, since no attempt at matching the cells in capacity to minimize divergence was reported.

NAD Crane conducted a 3-year series of life-cycling tests on 23 combinations of sizes of nickel-cadmium cells and charge-control concepts. Reference 28 describes the testing procedures and equipment, and reference 32 summarizes the cumulative results of these tests. Reference 52 is an intermediate report, but the later document includes all of the data. The description of the various failure modes of the nickel-cadmium battery and the identification, insofar as possible, of these failure modes in the batteries on test constitutes the primary contribution of the Crane life-cycling tests to battery technology. The section on "Failure Modes" details the analysis of failure in the various battery cells. A brief correlation of the incidence of failure of each type of cell with cycle life is shown, but the contributions of the various failure modes are neglected, partially robbing the correlation of significance.

Each type of cell was cycled in a test program at three temperatures: 0°, 25°, and 40° C (tests began at 50° C but changed when rapid failures occurred).

Two typical orbital situations were flown, the 1.5- and the 3.0-hour orbit.

Voltage limits were set at 1.41 volts/cell at 40° C, 1.49 volts/cell at 25° C, and 1.55 volts/cell at 0° C.

The extent of recharge was 115 percent at 0° C, 125 percent at 25° C, and 160 percent at 40° C. In establishing the extent of recharge, no compensation was allowed for variations in the charge current between the 1.5- and the 3-hour orbit situations. These nominal percent recharge limits were reduced automatically if the cell reached its voltage limit, reducing the charging current. Since charge curves are reported as hours

of charge, the actual ampere-hours of cell input are not visible, leading to the conclusion that some failures possibly resulted from a failure to recharge the cell.

In addition to the standardized tests described above, there is a series of tests on nickel-cadmium cells using specialized charge-control techniques, including auxiliary electrodes, coulometer, stabistor, a two-step charge regulator, and the Sherfey "upside-down cycle," in which the cells cycle between a state of full discharge and partial charge. For the most part, this testing of specially controlled cells is not advanced enough to permit a judgment regarding the effects of the controls on cycle life.

From the Inland Testing Laboratories data, Clark and Ingling (ref. 55) established cycle life as a logarithmic function of depth of discharge (fig 4-24). The seriously reduced cycle life shown at the lower temperatures is attributable to the establishment of unsatisfactory operational conditions rather than to any failure of the cell itself.
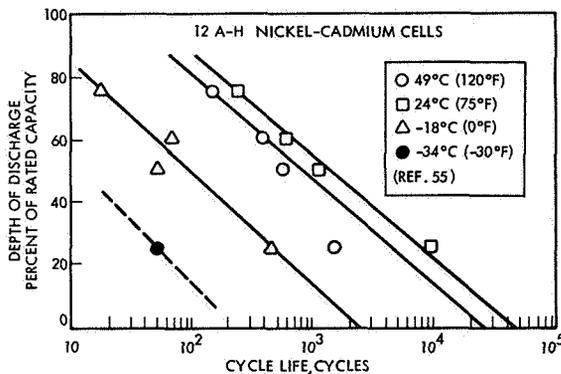
FIGURE 4-24.—Logarithmic plot of cycle life as a function of depth of discharge.

Francis (ref. 56) summarizes cycle-life data as a function of the depth of discharge (fig. 4-25), using the classical log-cycle-life versus depth-of-discharge plot. The data on low-temperature cycles depart considerably from the usual logarithmic relationship, not because of any failure of the cell itself but because the cells were operated under an unsatisfactory regime. Since the data summarized by Francis and those correlated by Clark and Ingling do not account for periodic reconditioning of the cells, they must be considered pessimistic when applied to systems using reconditioning. Carson et al. (ref. 49) show no correlation between cycling and failure when using a random-depth cycle.

The Martin-Marietta Corp. performed a statistical regression analysis and calculated multiple correlation coefficients between the observed cycle life and the results of four acceptance tests (ref. 57). Their final
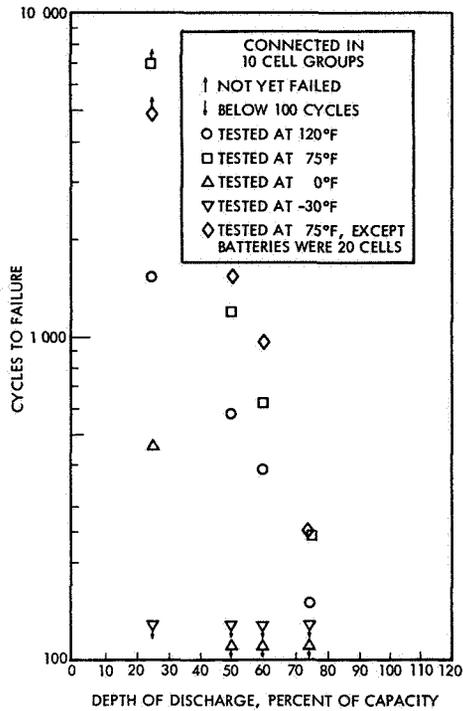
FIGURE 4-25.—Cycle life of nickel-cadmium
cells; 12-A-h nominal capacity, 90-minute
orbit.

product was an empirical equation containing linear regression coefficients
between cycle life and acceptance test data.

$$Y = -4351 + 3057X_1 - 10387X_2 - 5.3X_3 - 772X_4 \qquad (4-5)$$

where

X_1 cell capacity (measured)
X_2 end-of-charge voltage
X_3 end-of-charge pressure
X_4 internal resistance
Y the predicted life of the cell in cycles

To use the same data for prediction purposes, the predicted life of the
individual cells was based upon the mean life of the cells in the battery
by the equation

$$Y - \overline{Y} = b_0 + b_1(X_1 - \overline{X}_1) + \cdots b_4(X_4 - \overline{X}_4) \qquad (4-6)$$

where $\overline{Y}$ is the observed mean life of the cells in the battery and $b_0, b_1 \ldots$
b_4 are the intercept and regression coefficients.

Relating the observed mean life to predicted individual cell life permits
normalizing or compensating the data for differences in operating con-
ditions affecting cell life.

While the above statistical analysis shows a correlation between the factors observed and the cell life, this method of predicting cell and battery life is of little value in itself, because of the necessity of testing and determining the observed mean life before computing the predicted life. Furthermore, the effect of the various factors upon cell life shown by the regression equation does not agree in a physical sense with other known facts.

Equation (4–5) also shows that increasing internal resistance increases service life linearly, when, in fact, high impedances indicate a defective cell to both manufacturers and users. A high-impedance cell has a higher charging voltage and a lower discharge voltage, leading to premature cell failure.

To match the mean capacity of the batteries and simplify the statistical calculations, the capacities of the individual cells in each battery were deliberately mismatched. The capacity of the battery, however, is that of its lowest capacity cell. This established ideal conditions for divergence failures of the lower capacity cells and weighted the final equation heavily in favor of small capacity changes resulting in large improvements in service life.

Mauchly and Waite (ref. 58) established methods of predicting failures in specific nickel-cadmium cells by comparing the electrical characteristics on cycling with the electrical characteristics of similar cells which have failed. Two methods are used to reduce data.

The superimposed curve profile method combines all data curves which can be accurately superimposed upon each other, and retains only one curve specimen. This eliminates large masses of redundant data without losing important information. A quantitative computer process correlating failures with different charge-discharge curve patterns resulted in the following list of failure symptoms:

> End-of-charge voltages above 1.60
> End-of-discharge voltages below 1.18
> Erratic voltage behavior

These conclusions do not represent any new knowledge. More detailed conclusions are reached regarding the end-of-charge voltage band (not less than 1.40 nor more than 1.60), the minimum charge limiting voltage (1.45 volts/cell), the voltage dispersion during charge (less than 0.08 volt/cell), and a drop in cell voltage on charge-voltage limiting of the battery pack (less than 0.6 volt).

From the data on voltage dispersion, a second computer program used to predict failure of specific cells processes the voltage data from five charge-discharge cycles and generates a frequency distribution histogram of the differences between each two consecutive voltage measurements. The computer makes a bar graph, using the magnitude of the difference in voltage measurements as the ordinate, and the frequency with which this difference occurs as the abscissa. A gaming program assigns weights to the various differences in the histogram patterns and correlates the resulting information with actual failure data. The voltage differences are divided into three groups, representing small (DV-low), medium-sized

(DV-mid), and large (DV-high) differences. A set of rules provides a quantitative basis for failure prediction. This is called the "first difference histogram method."

The discharge failure symptoms are—

(1) A DV-high frequency of occurrence equal to or greater than 9.

(2) A DV-high greater than one-fourth that of DV-low.

(3) A DV-low frequency of occurrence differing from that of DV-mid by 15 or more.

(4) A DV-mid frequency of occurrence exceeding that of DV-low one-fourth.

The charge failure symptoms are—

(1) A DV-low frequency of occurrence of four or more times larger, or one-fourth less than DV-mid.

(2) A DV-high frequency of occurrence of more than one-half that of DV-low.

(3) A DV-mid frequency of occurrence more than twice or less than one-half that of DV-mid (discharge).

Each of these failure symptoms carries weighted demerits against the cell. Cells having the highest count fail earliest. Again, the first difference histogram method described shows no new failure symptoms. Larger changes in voltage and large differences in the slopes of the charge and discharge curves are known to precede failure. The primary advantage of this approach is the quantization of the analytical process.

The results of the failure prediction processes, using the unpublished NAD Crane data recorded on punched paper tape, are unsatisfactory, requiring almost 1500 cycles of operation before failure can be accurately predicted by the first-difference histogram method. Mauchly and Waite describe some deficiencies of the NAD Crane testing methods and make specific recommendations for improved data acquisition which, if applied, should lead to earlier failure prediction. However, their analysis of the required improvements does not place sufficient emphasis upon the control of the operational and environmental factors largely responsible for the erratic behavior of the cells.

CHARGE AND DISCHARGE CONTROLS

IMPACT OF CHARGE CONTROLS UPON SERVICE LIFE

A charge control for nickel-cadmium batteries primarily protects the battery from overpressure and overtemperature damage due to improper charging conditions. Ineffective control within any part of the operating regime of the battery can lead to premature failure. Basic methods of charge control are discussed in chapter 2. Carson (ref. 14) reviewed various methods for control of nickel-cadmium battery charging; he considered not only charge controls but system interface problems and the effect of orbit variables upon the selection of control methods. This excellent review qualitatively explores the strengths and weaknesses of each control method and gives each method a preference rating based upon

the author's judgment, after a cursory consideration of some of the system interface problems. A more detailed consideration of such system problems would, however, exert a great influence upon the order in which the methods are rated.

DETECTION OF CHARGE COMPLETION

A basic problem in charge control of nickel-cadmium batteries is the detection of charge completion. The methods discussed in chapter 2 apply, but the problem is complicated by the very small difference between the charging potential, and the next higher overcharge potential, corresponding to oxygen evolution from the nickel electrode. Voltage sensing methods must be applied with a great deal more care than with other electrochemical systems, in which the difference between charge and overcharge potentials is larger and more easily detected. As a result, other methods and combinations of methods have been investigated and are summarized below, with a critique of their applicability in various types of electric power systems.

The constant-current, charge-control system does not sense state of charge. Instead, it uses the oxygen overcharge cycle to prevent a buildup of destructive pressures within the cells, limiting the charge current to that which the cells will tolerate on continuous overcharge. Nominally, commercial nickel-cadmium cells accept a continuous overcharge of C/10; however, this varies with the history of the cell and with the temperature. At low temperatures, the overcharge acceptance without pressure buildup in the cell may be below C/20. At high temperatures, the charging efficiency at low-current rates is poor (see figs. 4–12 through 4–15), and the maximum achievable state of charge is limited. This requires oversizing the battery to obtain the necessary capacity and oversizing the charge-power source to compensate for the decreased efficiency. As a result of these considerations, the constant-current system is attractive for nickel-cadmium batteries only when neither charge time nor total charge energy is severely limited, and when charging power is naturally limited by the source or can be conveniently limited by a system element. The ATS-1 satellite had a separate battery-charging power source with limited current capability, and used constant-current charging. In effect, Nimbus I (ref. 59) and Relay (ref. 60) used constant-current charging since both had current limiters. Both Nimbus I and Relay had bus voltage limiters, but the voltage level was set too high to protect the battery effectively from the effects of overvoltage (1.74 volts/cell for Nimbus, and 1.65 volts/cell for Relay).

In addition, Relay had an overpressure trip switch set at 500 psi on one cell.

Aerospace applications have never used true constant potential charging because of source current limitations. To hold the potential constant demands tremendous currents from the source at the beginning of charge. Another disadvantage of this charging method is that a burst of hydrogen may be generated from the negative electrode of a fully discharged cell at the beginning of charge.

Modified constant potential charging is less effective with nickel-cadmium cells and batteries than with other types. (The standard automobile dc voltage regulator is a modified constant potential charge control, with an undervoltage disconnect to prevent motoring the generator.) This ineffectiveness is due to the small voltage rise at the end of charge and the large change in end-of-charge voltage as a function of temperature, making detection of the fully charged state difficult. If a nickel-cadmium battery charges at a constant current to a limiting potential of 1.47 volts/cell and holds at that potential thereafter, the additional heat generated at the end of charge will raise the battery temperature, thus decreasing the potential of the overcharge reaction and allowing a higher overcharge current to flow. The result is a thermal runaway condition in which increased heat causes increased overcharge, which in turn increases heating. Use of a much lower potential limit minimizes thermal runaway, but may not permit effective charging at lower temperatures. Two approaches are used to overcome these flaws. One approach compensates the voltage limit with the temperature. This was used in Pegasus satellite (ref. 61), ATS-4 (ref. 62), made available in OGO through the command selection of two voltage-limit levels (ref. 31), and has been proposed by Sparks and Wright (ref. 63) as a part of a generalized integrated electronic battery control system. The second approach employs an overtemperature protection device to reduce charge current to a preset trickle level; it has been used as an additional protection on virtually every satellite flown.

A principal requirement of the temperature-compensated, voltage-limit method is an accurate knowledge on the part of the designer of the heat-generation characteristics, efficiency, and the relationship between the voltage and overcharge current of the battery as a function of temperature. These data are necessary to select the proper functional limits. To date, in spite of the uncertainties in the available data (a factor of 2 in the overcharge Tafel curves, for example), the method has been used effectively in many applications.

A modification of the above method is modified constant potential with switchdown to trickle charge. Several sensor outputs have been used to accomplish this transition, including temperature (see above), voltage, pressure, and the output of an auxiliary electrode or of a coulometer.

By using the battery temperature as the switchdown initiator, a partial temperature control of the battery is possible, independent of the thermal-control system of the spacecraft. The amount of overcharge decreases with increasing temperature as a result of the lower efficiency at the higher temperatures, and the lesser amount of heat required to bring the battery to the switchdown temperature. The extent of overcharge under conditions of low charging current availability may be quite large, particularly if the heat-removal capability of the system is high. No immediate damage results, but the long-term life of the battery is expected to deteriorate by extended overcharge. The method was used effectively in OGO (ref. 31).

The effective use of a temperature-compensated voltage sensor as an initiator for switchdown to trickle charge is more dependent upon the availability of good electrical characteristics information than modified constant potential charging. Voltage limits are determined as a function of temperature. This system is effective over a narrow temperature range because the low-temperature voltage limit must be set at a level high enough to insure complete charging, but not high enough to permit the evolution of hydrogen gas. Any error in setting will result either in pressure development or inadequate charging. At the high temperatures, the same narrow dividing line between inadequate charge and excessive heating must be negotiated. The effective temperature range in which all four of these requirements can be satisfied is narrow.

Pressure sensing has been extensively investigated, using the auxiliary electrode cells of both the fuel-cell type and the adsorption-electrode type. Both Sizemore (ref. 64) and Bauer (ref. 13) found that the fuel-cell type of electrode gave a premature full-charge signal under some circumstances. Sizemore (ref. 64) used the adsorption hydrogen electrode to control several series-connected nickel-cadmium cells, allowing the first cell signaling full charge to terminate battery charging by switching to trickle charge. Compensation for variation of temperature was achieved by varying either the signal voltage at which full charge is assumed or the load resistance across the auxiliary electrode. Sizemore found an increased auxiliary electrode sensitivity over the first few months of operation, leveling off to constant characteristics thereafter. In addition, the adsorption hydrogen electrode gave a false full-charge signal at the beginning of charge immediately following discharge, resulting in a brief period of trickle charge prior to commencement of normal charging. Hennigan and Sizemore (ref. 51) use electronic charge-control circuitry to implement adsorption hydrogen electrode control of nickel-cadmium batteries, including temperature compensation curves for voltage and load resistance (fig. 4–26).

Lerner and Seiger (refs. 65, 66) and Carson and Hadley (refs. 67, 68) suggest using two auxiliary electrodes in each cell. One, a high recombination-rate platinum catalyst fuel-cell electrode, connects directly to the negative electrode and acts as a recombination or "scavenger" electrode, maintaining low-oxygen pressures in the cell until the electrode is saturated. When the current through the scavenger electrode reaches the saturation level, the pressure rises, and a lower sensitivity signal electrode senses this pressure rise and terminates charge. The signal electrode may be the adsorption hydrogen electrode (refs. 65, 66), or a silver spinel catalyst electrode (refs. 67, 68).

Stroup (ref. 69) studied coulometric control of charging, using nickel-nickel and cadmium-cadmium coulometers, rejecting the nickel-nickel type in favor of the more reversible cadmium-cadmium coulometer. The coulometer consists of two cadmium electrodes, immersed in a potassium hydroxide electrolyte and having a capacity similar to that of the controlled battery. Prior to use, the coulometer cell, closed by a pressure relief fitting, is charged in both directions at the oxygen plateau
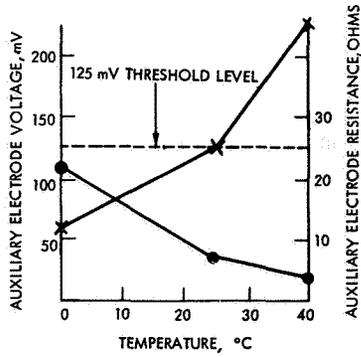
FIGURE 4-26.—Auxiliary electrode temperature compensation requirements. (X) Threshold level of auxiliary electrode (mV) versus temperature for R_s=6.8 ohms. (●) Auxiliary electrode resistance (R_{s-}) versus temperature for 125-mV threshold.

level (1.45 volts) until the hydrogen potential (1.55 volts) is reached. After this formation cycle, the residual gas is pumped out and the cell sealed. Oxygen leakage into the formed cell will unbalance the coulometer. In operation, the voltage drop across the cell remains at approximately 50 millivolts until the coulometer is fully polarized in the charge direction, then the voltage drop increases to a level greater than 1 volt. This signal increase is used to switch from full charge to trickle charge, bypassing the trickle current around the coulometer cell. To prevent gas evolution due to excessive potentials across the coulometer, the trickle current is bypassed by a silicon or germanium diode or other junction device, with a forward voltage drop limiting the potential applied to the cell. At voltages below 1.0 volt, the current through a polarized coulometer is less than C/1000. Coulometer capacity drifts downward by 10 to 15 percent during the first 100 cycles, then remains constant for at least 3000 cycles. Simple circuit approaches are shown. Stroup limits the applicability of the coulometer to temperatures of 25° C and below, presumably because of the lack of information on the ability of the coulometer to track the cell at high temperatures, and because of capacity deterioration in the battery. NAD Crane tested a battery pack with coulometer control beginning at 80 percent depth of discharge and decreasing depth of discharge by increments of 10 percent until reaching stability. The coulometer maintained the battery at 30 percent depth of discharge, and logged over 6500 cycles. A second battery, operating at 40 percent depth of discharge, completed 805 cycles. More recent data (Stroup, NASA GSFC, private communication) disclose that the coulometer control has undergone operational testing and flight qualification for the proposed RAE satellite, which uses coulometers with

0.010-inch interelectrode separation.   Testing failures have been reported in models with 0.005-inch spacing.

Chapter 2 contains a general discussion of stabistor control of nickel-cadmium cells.   NAD Crane tested stabistor control at temperatures ranging from −20 to +40° C and at 25 and 40 percent depth of discharge. At 40° C and 40 percent depth of discharge, cell efficiency was too low for satisfactory cycling, and the pack was changed to 15 percent depth of discharge.   Several cell failures occurred at the low temperatures, because the very soft characteristic of the stabistor allowed the cell voltages to reach gas-generation levels.

NAD Crane also tested cells cycled in the Sherfey upside-down cycle. In this system, the fully discharged cells charge to about 60 percent of their capacity, and discharge 40 percent.   After five such cycles, the cells are discharged fully through individual resistors, and the sequence is repeated. In this way, the cells are operated below the 100-percent-capacity mark and avoid overcharge.   In addition, the repetitive deep discharges avoid the formation of the memory effect.   After 1864 cycles, no failures have occurred, although deposits (presumably caused by leakage) and bulging due to high pressure were observed.   Some of the leaking cells reached voltages at end of charge of 1.62 volts, suggesting severe cell unbalance due to oxygen loss, drying of the electrolyte, or both.

Charge-control system circuits and block diagrams for nickel-cadmium cells are shown by:

(1) *Ford and Liwski* (ref. 70).—Shunt regulator designed to clamp the battery bus voltage at one of two levels, both of which are functions of temperature.   The voltage level is selected on the basis of the output of an auxiliary electrode, the higher level occurring with a small output of the auxiliary electrode.

(2) *Graff* (ref. 61).—Modified constant potential charger with a voltage limit varied inversely with temperature and a separate two-level trickle charger with a constant current output set on command at either C/60 or C/12, the higher current compensating for the effects of high battery temperatures.

(3) *Liwski (U.S. Marine Engineering Laboratory)* (ref. 71).—Two-mode bench-test charge controller.   The first mode charges at constant current until the auxiliary electrode reaches a potential of 125 millivolts, then the current decreases linearly with the increasing electrode potential until the battery reaches trickle charge at 250 millivolts.   In the second mode, a 5-minute time delay continues constant current charge after reaching the initial 125-millivolt electrode potential before decreasing charge current.

(4) *Yagerhofer* (ref. 72).—Circuitry for a modified constant potential charger for 100-minute orbit applications, using both a current limit and a voltage limit.   Automatic battery transfer due to undervoltage is used to switch in a standby battery.

(5) *Hennigan and Sizemore* (ref. 51).—Circuitry for modified constant potential charging of a battery, followed by switchdown to a trickle-charge level when any one of the battery-cell auxiliary electrodes reaches

a predetermined potential which varies as a function of temperature. Hennigan and Sizemore also show a reconditioning circuit.

(6) *Carson and Hadley* (ref. 67).—Sensing circuits of several types for the monitoring auxiliary electrode potentials.

(7) *Sparks and Wright* (ref. 63).—Block diagrams of a complete integrated electronic control system, including system logic, temperature-compensated modified constant potential charging, cell bypass for over-discharge protection, and reconditioning. Voltages are sensed at the cell level, and are compensated for cell temperature, rather than average battery temperature by means of temperature-sensitive elements of the voltage-sensing circuits.

OVERDISCHARGE PROTECTION

Under some circumstances, deep discharge of a battery causes gas evolution in cells of a lower capacity than the remaining battery cells due to a reversal of potential in the low-capacity cell. (See Ch. 2, "The Divergence Problem.")

Three methods for ameliorating the effects of overdischarge in nickel-cadmium cells were investigated. Dassler (U.S. Patent No. 2,934,581) proposed using an antipolar mass consisting of deposits of cadmium hydroxide in the nickel electrode. Under conditions of limited over-discharge, this antipolar mass protects against the formation of hydrogen gas until the conversion of all cadmium hydroxide to metallic cadmium. In practice, the antipolar mass is effective only at extremely low current densities. At useful current densities, hydrogen generates simultaneously with cadmium hydroxide reduction (ref. 73). Bypassing the cell with a low-voltage-drop semiconductor minimizes the reverse-voltage drop across the cell, and consequently the reverse current through the cell. Alliegro et al. tested germanium diodes as bypass elements (ref. 74) and found them of limited value in delaying the effects of overdischarge.

A method for lessening the effects of overdischarge was introduced by Sparks and Wright (ref. 63), who proposed a solid-state low-output voltage converter at each cell, clamping the voltage at 0.8 volt. This converter is normally off, turning on only when the cell enters under-voltage. The method is complex, and further complications are introduced if protection against electronic component failure is required. Ritterman and Seiger (ref. 75) designed and tested a cell capable of both overcharge and overdischarge. The capacity of the cell is limited by that of the cadmium electrode. This assures that oxygen is generated on overdischarge. The auxiliary silver electrode recombines the oxygen and is oxidized to Ag_2O in the process. The silver electrode is regenerated on charge. A diode is connected across the terminals of the cell to clamp the overdischarge voltage. An Adhydrode was used for over-charge control. The cells survived more than 250 overdischarge cycles without failure, except those due to silver migration within the cells, causing the Adhydrode control electrode to short-circuit. Another cell capable of both overcharge and overdischarge developed by Catotti and Read (ref. 76) uses a hydrogen-recombination cycle with two fuel-cell

electrodes in each cell, one for overcharge control of oxygen generation, and one for overdischarge control of hydrogen. Both are true gas-recombination electrodes. On cycling, the cells accepted limited over-discharge at relatively high currents. In the cycles used, pressures as high as 78 psi were generated within the cell (50 percent overdischarge per cycle for 200 cycles of operation). The hydrogen pressure fell, however, when oxygen was generated on overcharge.

THERMAL INTERFACE PROBLEMS

The problems associated with integrating the battery into the thermal-control system of a spacecraft are important enough to warrant a discussion, independent of the other system-interface problems. Spacecraft electronic equipment consists of silicon semiconductors, metal film or composition resistors, tantalum capacitors, and inductors, plus other plastic and metal components. The heat dissipation of these components can be predicted from the conditions of operation, and a relatively simple "worst-case analysis" can be used to determine the maximum and minimum temperatures of properly mounted components. The components themselves operate over a wide range of temperatures without damage or intolerable deterioration of their electrical characteristics. Batteries, on the other hand, vary in heat dissipation over their charge-discharge cycle, depending upon the state of charge. The rates of heat evolution or absorption are nonlinear with cell voltage. A nickel-cadmium battery can be operated with high performance over a temperature range of approximately 0° to 40° C, but this wide temperature range introduces design complications. As a result, the battery temperature has a profound influence upon the thermal-control subsystem of the spacecraft, and may be a primary factor in the determination of thermal-control-design concepts.

The criticality of the thermal interface between battery and spacecraft grows with increasing power demand by the spacecraft. In general, spacecraft with body-mounted solar arrays tend to be less critical in their characteristics, since all the solar energy falling on the spacecraft ultimately becomes heat (except for that actually radiated by communications antennas) and is reradiated by the solar array in such a way as to stabilize the average temperature at approximately room temperature. However, spacecraft with external appendages for gathering electrical energy from the Sun may have a higher power input than their available radiating surface area can handle conveniently, unless an active thermal-control system is used. Large variations in the heat output of the battery further increase the need for the heavier, more complex, and less reliable active thermal-control systems.

Bauer and Sparks (ref. 48) simulated the thermal interface between a nickel-cadmium battery and the OGO spacecraft, measuring the heat evolution and absorption during simulated orbital operations, finding battery-temperature variation from 75° to 100° F with the control system used. (Modified constant potential charging with 95° F temperature switchdown to trickle.)

SYSTEM INTERFACE PROBLEMS

Beyond the thermal-interface problem discussed above, and the possibility of interference with magnetic measurements, the nickel-cadmium battery presents no unusual system-interface problems to the design engineer. General system-interface problems common to all batteries are discussed in chapter 12.

FAILURE MODES

Nickel-cadmium battery failure modes may be divided into four general categories:

(1) Cell failures due to inadequate design or improper quality control.

(2) Cell and battery failures due to improper operation. (These are discussed under "Battery Operating Controls," ch. 2.)

(3) Cell and battery failures due to divergence of cell properties or characteristics.

(4) Cell wearout.

Design and quality control failures were summarized by Stroup (ref. 69) as belonging to four categories.

A chemical or electrolytic attack of the sealing alloy or glass may cause leakage of the seals.

The deposition of conductive silver-based compounds across the terminal insulator results in cell short circuiting. References 48 and 77 describe this phenomenon in more detail. The metallic silver, used as the brazing alloy in the ceramic-to-metal seal of the positive terminal, is electrolytically attacked, forming silver oxide (Ag_2O). Silver oxide is soluble in the potassium-hydroxide electrolyte, and migrates or diffuses to the negative terminal where it is redeposited, probably as metallic silver. This deposit gradually extends across and short-circuits the insulator. Cells having a single insulated terminal (the negative electrode being common with the case) short-circuit more than cells having two insulated terminals, because in the two-terminal cell the potential is divided between the two insulators, lowering the driving potential for corrosion of the silver alloy. Scott, Mainz, Sparks, and others discuss this type of failure mode in a workshop symposium (ref. 77) (also see Bauer and Sparks, ref. 31). The battery and power system is considered to have failed if the battery fails to meet the requirements of the system design by allowing the end-of-discharge voltage to fall below the minimum acceptable level. (See further discussion under "Memory Effect and Reconditioning," above.)

Migration of the negative active electrode material has also been observed (refs. 31, 52, 77). NAD Crane Ordnance Laboratories describes migration as a uniform dark coating on the separator material, occasionally penetrating the separator to produce a high-resistance short circuit. In places of severe penetration, burned spots are found on the separator (refs. 28, 32, 52). According to Bauer and Sparks (ref. 31), the formation of nodular growths on the negative electrode gives it a burned appearance.

NAD Crane describes separator deterioration (refs. 28, 32, 52) as a thinning of the separator, loss of tensile strength, and an adhesion to the negative electrode. Bauer and Sparks (ref. 48) describe a similar adhesion to the negative electrode accompanying the burned appearance which indicates the presence of migration.

Blistering of the positive electrode is described as a result of characterization test charges at the C/1 rate (ref. 50) and as a result of cyclic operation (refs. 28, 32, 52). Separator deterioration in the area of the blister was observed (ref. 52). Blistering and separator deterioration increase in severity toward the center of the core of cylindrical cells using spirally wound electrodes.

Loosened or extraneous active material crumbled from the edges during assembly, or areas of electrode materials separated from the current-collecting grid during winding of the cylindrical cells (refs. 28, 32, 53).

FAILURE RATES

Little useful data are available to form conclusions regarding failure rates. Sparks and Wright (refs. 63, 77) list failure rates as varying with time, but do not show the basic data or the means of derivation. They do distinguish, however, between the different modes of failure.

Service-life data are usually presented as plots of the log of the number of cycles as a function of the depth of discharge. Accumulated service-life data are shown with different failure modes not distinguished from each other (ref. 57). The NASA battery-testing program at NAD Crane (refs. 28, 32, 52) makes it possible to correlate failure data by failure mode. In an initial attempt at failure-rate determination, the failures may be divided into three categories, each of which is assumed to occur independently of the others.

Premature failure can result from a charge-control defect or from mechanical defects in cells. Included in this category are failures caused by separator puncture and localized heating resulting from defective welds. The rate of cell failure is unpredictable because the severity of the initial cell defect determines the number of cycles that the cell will survive. Since these defects may appear slowly, they are handled as random phenomena and are evaluated statistically.

The next category includes cell failures resulting from separator deterioration, migration of the active materials, and other wearout effects.

The final cell failure involves a cell inability to deliver the current at the minimum acceptable voltage. However, this deteriorated performance cannot be attributed to a particular physical failure mode, and is therefore categorized separately.

Initially, the data from cells containing mechanically caused defects are eliminated. The unexplained failures were tentatively attributed to the memory effect and handled separately, and the separator deterioration and migration failures were tentatively combined. Figures 4–27 through 4–29 illustrate the results; the circles of figure 4–27 represent the
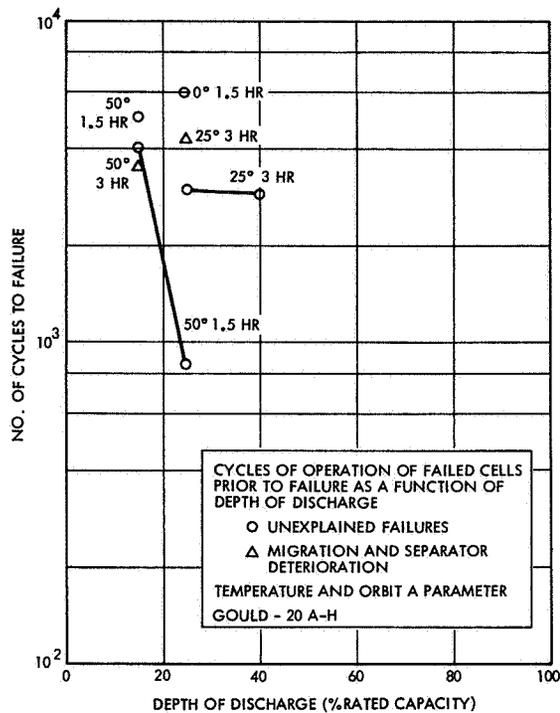
FIGURE 4-27.—Cycle life of Gould 20-A-h nickel-cadmium cells.

memory effect or unexplained failures, and the triangles represent the migration-separator deterioration data.

The following conclusions were reached from an examination of figures 4-27 through 4-29. The data derived from the unexplained failures and attributed to the memory effect deviate from the usual log-cycle-life versus depth-of-discharge relationship. The service life and the slopes of the lines (arbitrarily drawn as straight lines on semilog paper) vary greatly in different cells operating at the same temperature. Considering the scattered data, no reasonable conclusion can be derived other than that service life increases while temperature decreases in the range from 40° to 0° C. Even this conclusion is only qualitative, and may be confounded by the possibility that failures may be partly due to inadequate recharge of the battery.

There are several possible explanations for the erratic behavior of the cells.

(1) The unexplained failures may not be due to the development of the memory effect alone. Instead, the failures may result from several types of unexplained failure mechanisms occurring at different rates in the various cells.
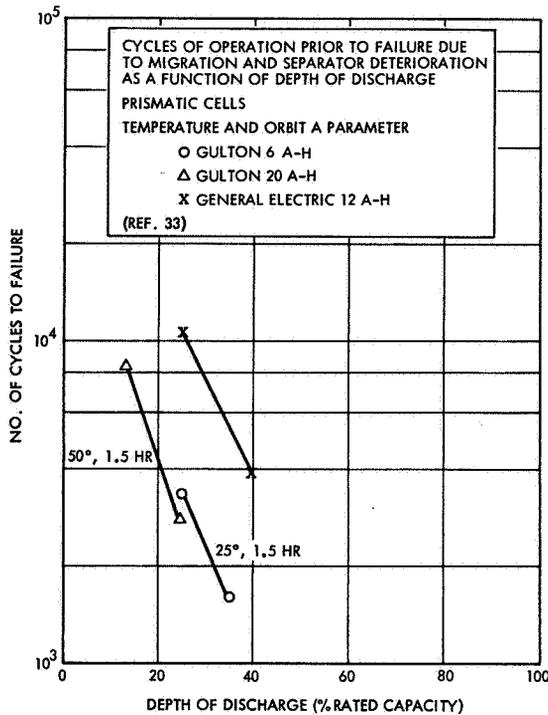
FIGURE 4-28.—Cycle life of prismatic nickel-cadmium cells.

(2) The unexplained failures may be due to the memory effect, but the relationship between memory effect and failure rate is masked or disturbed. In view of the nature of the reconditioning cycle being used, this is quite possible. The Crane Ordnance Laboratories reconditioning cycle consists of a discharge of the battery to a terminal voltage of 1.0 volt per cell, followed by a long overcharge and a second discharge 1 volt per cell. Under this method, only partial reconditioning can take place, and the restoration of capacity tends to be uneven from cell to cell, since cell voltages vary considerably when the total battery voltage averages 1 volt per cell.

The data on migration and separator deterioration are more consistent. When all extraneous failure modes are eliminated from consideration, the curves showing log cycle life versus depth of discharge fall into several distinct groups. Data on cylindrical cells fall in a very wide band of lines at 40° C, and the prismatic cells are closely grouped. The steeper slopes of the lines suggest that the prismatic cells tend to wear out faster with increasing depth of discharge than some types of the cylindricals. The same relationship appears to be true at 25° C. However, there are insufficient data available for any useful correlation at 0° C.
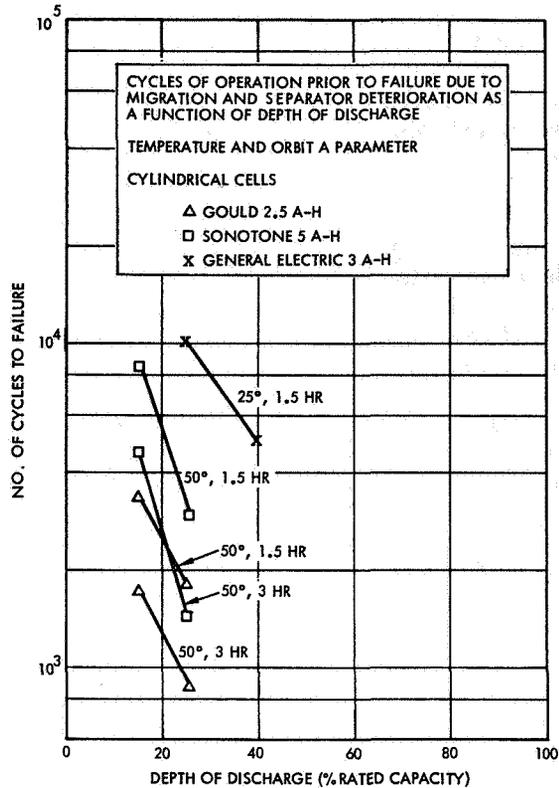
FIGURE 4-29.—Cycle life of cylindrical nickel-cadmium
cells.

Various types of cells appear to differ in sensitivity of separator and migration failures to the depth of discharge. However, the conclusions regarding this difference may not be valid, since they were based upon limited data. However, the results are sufficiently consistent to suggest further analyses of this kind.

The data on the rate of occurrence of short circuits across the cell terminals due to deposition of silver or silver compounds are scattered, and apparently show no relationship with depth of discharge. Theoretically, the rate should increase with the applied voltage. Scott (ref. 77) has suggested accelerating this effect by applying higher-than-normal voltages to cell terminals in the presence of an electrolyte. However, a change in brazing alloy has since made these data obsolete.

Gas-pressure failures are discussed under "Charge Control."

Epstein and Waite (ref. 78) used cryptanalytical techniques on the NAD Crane data to pinpoint the failure modes associated with specific battery manufacturers to enable them to evaluate and improve the product. This method, which determines the combinatorial frequency of occurrence of three coded failure characteristics, identifies single- and

triple-failure modes, and identifies the individual manufacturer responsible for each type and combination of failures. Many of the conclusions reached in this analysis are both self-evident and trivial. However, the method does make it possible to expose unsuspected combinations of failures when they occur with unusual frequency.

Wet Stand

When nickel-cadmium batteries stand open circuited in the fully charged condition, they slowly lose their charge and decay in open-circuit voltage. Both phenomena occur linearly with the logarithm of time (ref. 6). Bourgault and Conway (ref. 79) investigated this self-discharge phenomenon by measuring the oxygen-evolution rate from the nickel electrode as a function of time and electrode potential. They determined that the self-discharge process occurs on open circuit with a simultaneous change in electrode potential and an evolution of oxygen. The potential decay curves show two linear regions (versus log of time) having different slopes. The potential at which the transition between the two rate-determining processes occurs depends upon the concentration of potassium hydroxide in the electrolyte. Either of two mechanisms proposed for the self-discharge process suggested can explain the slopes of the decay curve adequately.

The self-discharge phenomenon increases in rate with rising temperature. The decay in potential following the Tafel relationship

$$E = E' - b \log (t + \gamma)$$

where γ is an empirically determined constant, and the slope b is

$$b = \frac{K_1 RT}{K_2 F}$$

where

R	gas constant
$K_1 + K_2$	integers
F	Faraday's constant
T	absolute temperature

Therefore, the variation in rate is directly proportional to absolute temperature.

In addition to the self-discharge process, a slow deactivation of the negative electrode occurs, causing a cell on constant-current charge after a period of shelf storage to exhibit higher-than-normal end-of-charge voltages (refs. 31, 80). If charging voltages are permitted to exceed the appropriate limits (approximately 1.5 volts at room temperature), hydrogen gas is generated in the cell, causing permanent internal pressures. The phenomenon occurs randomly, with increasing probability of occurrence and increasing end-of-charge potential as the storage time lengthens. It appears only on the first charging cycle after shelf storage, and may be avoided by subjecting the cell after storage to continuous overcharge at low currents, gradually increasing the current until the desired overcharge current is reached at safe voltages.

ENVIRONMENTAL FACTORS

MECHANICAL ENVIRONMENTS

Modern nickel-cadmium cells are capable of withstanding most mechanical environments to which they may be exposed in the manufacture, transportation, assembly, launch, and flight of aerospace vehicles. Generally, the internal structure of a cell is able to tolerate these stresses; any failures which occur are usually found in the battery-packaging elements or are due to poor design of the battery structure. The environmental test data are not summarized here because of the lack of general applicability.

THERMAL ENVIRONMENTS

Nickel-cadmium batteries are sensitive to variation in thermal environment. This sensitivity takes the form of large variation in the electrical characteristics and service life and is discussed in the appropriate sections.

STERILIZATION

Sterilization of all spacecraft components is required to avoid contaminating planetary bodies (other than the Moon) with living organisms from the Earth, at least until the presence or absence of rudimentary forms of life has been established. While many methods of sterilization have been examined, including chemical surface decontamination with ethylene oxide and assembly under sterile conditions (ref. 81), heating the finished spacecraft assembly to 145° C for 36 hours and repeating this heating cycle three times seems to be the most practical system.

Nylon nickel-cadmium battery separators will not withstand this sterilization heat cycle. Liska (ref. 82) investigated the sterilization problem of Gulton nickel-cadmium batteries in both the charged and discharged condition, varying separator materials. Preliminary tests of separator materials showed that several promising materials, including asbestos cloth, polypropylene and a polypropylene-nylon mixture, underwent large dimensional changes in heated potassium hydroxide solutions, but were dimensionally stable thereafter. These materials were used after a high-temperature pretreatment. Sterilization of only the negative electrode resulted in a loss of recombination capability, but no loss in capacity. Sterilization of only the positive electrode led to a loss in capacity, but not in recombination capability. Sterilization of both positive and negative electrodes separately led to low capacity, but no loss of recombination capability. This last test result was unexplained.

Sterilization of complete cells in the discharged condition showed that in several cases a modest loss in capacity occurred after three sterilization cycles, and that the output voltage of the cells fell somewhat. In most cases, the tolerance of the cell to overcharge was considerably impaired, leading to additional problems in charge control. Sterilization of the cells in the charged condition, with a trickle current flow maintaining them at full charge during the sterilization process, resulted in large permanent capacity losses.

Richards (ref. 83) investigated the sterilization resistance of Sonotone cylindrical 4-A-h cells in the charged and discharged condition.

Sterilization of fully discharged cells led to a capacity loss of approximately 25 percent in the first cycle after sterilization. Capacity losses on further cycling of the sterilized cells, however, were not as rapid as that of a control group. After 300 days of cyclic operation, no significant difference was found between the capacities of the control cells and those sterilized in the discharged state. No significant decline in discharge-plateau voltage was observed, but a significant rise in charge voltage occurred after sterilization. Sterilization of cells in the charged condition led to immediate failures in a significant proportion of the cases.

Long overcharge (60 milliamperes for 118 days) of cells sterilized in the discharged condition apparently had an additional deteriorating effect upon cell capacity.

RADIATION EFFECTS

Argue et al. studied the effects of gamma, electron, and neutron radiation on nickel and cadmium electrodes in an experimental cell immersed in a liquid electrolyte, using commercial electrodes (ref. 84). A similar study on the effects of high-energy proton irradiation was also performed (ref. 85). The effects of radiation are summarized below.

Gamma.—Voltage: The polarization characteristics of the electrodes were unaffected; however, after 8×10^7 rads, a 10-millivolt drop in open-circuit voltage was observed. Since this occurred after 62 hours at relatively high temperatures induced by the deposition of energy within the cell, it is reasonable to suppose that this is a normal decay in open-circuit voltage due to time and temperature.

A serious loss of capacity in the cadmium electrode was observed at a 75-percent state-of-charge irradiation, but very little loss at 25, 50, or 100 percent state of charge. This loss was repeated in several runs and appears to be statistically supportable, although no explanation is given. Irradiation during shallow cyclic operation of the cell in the neighborhood of 75 percent of full charge appears to have a worse effect than open-circuit irradiation.

Cell balance was affected and the cell became negative limiting after 3×10^8 rads. No explanation is advanced. (The shift in balance could have been partially caused by losses in oxygen gas from the system during cycling or irradiation; no information is provided about possibility of such losses.) Active material was lost from the negative electrode at a rate which is a function of the integrated dose and of the dose rate. This is attributed to the scrubbing action of gas bubbles generated by radiolysis of the electrolyte. The quantity of active material lost was insufficient to account for the negative limiting after irradiation.

Electron.—A voltage depression was observed, and was interpreted as being due to high temperatures. When electrodes were directly irradiated, no loss in active material occurred. However, when the electron beam impinged upon the electrolyte, material was lost from the negative electrode at a level consistent with the losses due to gamma irradiation

TABLE 4-III.—*Summary: Typical Nickel-Cadmium-Battery Applications*

Application	Orbit period	Average power (eclipse), W	Depth of discharge, percent	Charge-control method	Notes	Refs.
ATS-4	24 hr	100	14-25	Temperature-compensated modified constant potential switchdown to trickle on signal from auxiliary electrode.		62
IMP	12	35		Modified constant potential switchdown to trickle on low charge current.		60
Nimbus	104 min	160	20	Temperature-compensated modified constant potential switchdown to trickle on over-temperature or undervoltage.	7 or 8 battery modules.	86
Pegasus	100 min	40	13	Current limited temperature compensated modified constant potential, 2 command trickle levels.		61
UK-1	100 min	5-7	5	Temperature compensated modified constant potential.		87, 72
Telstar			to 40	Constant current.		88
OGO (Pogo)	100 min	250	37	Modified constant potential switchdown to trickle on overtemperature, command select V limit, I limit.		31, 49
(EGO)	42 hr	250	84 (max)	Same as Pogo.		31, 48

doses within 1 to 1.5 orders of magnitude. This lends support to the electrolyte radiolysis mechanism theory of material removal.

Fast Neutron.—After a total dose (gamma plus fast neutron) of 7.4×10^5 rads, no loss of active material from any electrode occurred, although some elemental transmutation reactions occurred. It was concluded that fast neutrons were not more damaging than gamma radiations.

High-Energy Proton.—Any discernible effects of radiation were obscured by an uncertainty in the capacity measurements.

THERMAL CONDUCTIVITY

Gulton Industries (ref. 89) measured the thermal conductivity of nickel-cadmium prismatic cells, finding that the thermal conductivity increased proportionally with increasing overcharge current. This enabled overcharge of the cells at high rates with small thermal gradients between interior and exterior.

TYPICAL NICKEL-CADMIUM-BATTERY APPLICATIONS

As a rule, nickel-cadmium batteries have been employed where long cycle life, nonleaking, secondary batteries are required. In satellite applications, the discharge rates have varied from approximately the 1-hour to the 5-hour rate, but the actual envelope of the system's capability is somewhat wider, since it may be used at currents as high as the 10-minute rate. The minimum rate at which the nickel-cadmium system may be used is determined by the self-discharge rate, which varies considerably with temperature. Rates of several hundred hours are quite plausible.

Nickel-cadmium batteries are less frequently used in applications requiring a limited number of cycles and limited survival times. Table 4–III shows a number of typical satellite applications with pertinent characteristics data.

REFERENCES

1. ANON.: Encyclopedia of Chemical Technology. Vol. 3. Second ed., Wiley (New York, N.Y.), 1936.
2. ATKINSON, G. S.: A Short History of the Jungner-Nife Nickel-Cadmium Battery. Electrochem. Tech., vol. 4, no. 7–8, 1966, p. 431.
3. BRODD, R. J.; AND DEWANE, H. J.: Impedance of Sealed Nickel-Cadmium Dry Cells. Electrochem. Tech., vol. 3, no. 1–2, 1965, p. 12.
4. FALK, S. U.: Investigations on the Reaction Mechanism of the Nickel-Cadmium Cell. J. Electrochem. Soc., vol. 107, no. 8, 1960, p. 661.
5. KOBER, F. P.: Analysis of the Charge-Discharge Characteristics of Nickel-Oxide Electrodes. J. Electrochem. Soc., vol. 112, no. 11, 1965, p. 1064.
6. BRUINS, P. F.; CAULDER, S. M.; AND SALKIND, A. J.: Calorimetric Study of the Thermodynamic Properties of the Nickel-Cadmium Cell. Final Report, Oct. 1, 1964, to Dec. 31, 1965. Polytechnic Institute of Brooklyn, Dept. of Chem. Engineering (Brooklyn, N.Y.). No date. (Available as NASA CR-71408, N66-21663.)

7. ALKE, P. E.; CASEY, E. J.; DUBOIS, A. R.; AND MOROZ, W. J.: Effects of Foreign Ions on Nickel Hydroxide and Cadmium Electrodes. J. Electrochem. Soc., vol. 112, no. 4, 1965, p. 371.

8. KOBER, F. P.; AND LUBLIN, P.: Potassium Distribution in Nickel-Oxide Electrodes. J. Electrochem. Soc., vol. 113, no. 4, 1966, p. 396.

9. LATIMER, W. M.: Oxidation Potentials. (Oxidation States of the Elements and Their Potentials in Aqueous Solutions.) Second ed., Prentice-Hall (Englewood Cliffs, N.J.), 1952.

10. FOLEY, R. T.; AND WEBSTER, W. H.: Research Into Fundamental Phenomena Associated With Spacecraft Electrochemical Devices—Calorimetry of Nickel-Cadmium Cells. First Quarterly Report, Jan. 1 to Sept. 30, 1966, American Univ. (Washington, D.C.). No date. (Available as NASA CR–81350.)

11. METZGER, W. H., JR.; AND SHERFEY, J. M.: Electrochemical Calorimetry, III. Thermal Effects of Nickel-Cadmium Batteries. Electrochem. Tech., vol. 2, no. 9–10, 1964, p. 285.

12. CASEY, E. J.; HENDERSON, H. S.; AND KING, T. E.: Canadian Research on Secondary Batteries. Presented at the 16th Annual Power Sources Conference (Fort Monmouth, N.J.), May 22–24, 1962, p. 108.

13. BAUER, P.: Characteristics of Three-Electrode, Sealed, Nickel-Cadmium Cells. Proc. IEEE Trans., vol. AS–2, 1964, p. 784.

14. CARSON, W. N., JR.: A Study of Nickel-Cadmium Spacecraft Battery Charge Control Methods. Final Report, General Electric Co., Research and Development Center (Schenectady, N.Y.), Apr. 1966. (Available as NASA CR–62029, N66–36372.)

15. CARSON, W. N., JR.: Study of Additives To Improve Nickel Hydroxide Electrode Behavior. Final Report, General Electric Co., Advanced Technology Laboratories (Schenectady, N.Y.), Mar. 15, 1964.

16. LERNER, S.; RITTERMAN, P.; AND SEIGER, H. N.: Investigation of Battery Active Nickel Oxides. Final Report, Gulton Industries, Inc. (Metuchen, N.J.), Sept. 12, 1966. (Available as NASA CR–72128, N67–15153).

17. FAUST, C. L.; McCALLUM, J.; SCHAER, G. R.; AND TREVETHAN, D. G.: Development of Large-Internal-Surface-Area Nickel Metal Plaques. Final Report, Battelle Memorial Institute (Columbus, Ohio), Sept. 30, 1965. (Available as NASA CR–54831, N66–14376.)

18. GREENLER, P. H.: Study of Sonotone Corporation Nickel-Cadmium Size F Battery Cells. Final Report No. 2303–0003–RU000, TRW Systems (Redondo Beach, Calif.), Apr. 1961.

19. VOYENTZIE, P. R.: Improving Performance and Reliability of Sealed Secondary Type Nickel-Cadmium Storage Batteries for Satellite and Space Application. Final Report, Jan. 10, 1961, to Jan. 11, 1963. Sonotone Corp., Battery Division (Elmsford, N.Y.). No date. (Available as NASA CR–53258, N64–17492.)

20. KOHL, W. H.: Materials and Techniques for Electron Tubes. General Telephone & Electronics Technical Series. Reinhold Publ. Corp. (New York, N.Y.), 1960.

21. ANON.: Evaluation Program for Secondary Spacecraft Cells, General Performance Test on Gulton Industries, Inc., 20.0 Ampere-Hour Sealed Cells. Rept. no. QE/C 64–5, U.S. Naval Ammunition Depot, Quality Evaluation Laboratory (Crane, Ind.), Apr. 16, 1964. (Available as NASA CR–58202, N64–27902.)

22. ANON.: Evaluation Program for Secondary Spacecraft Cells, General Performance Test on General Electric Co., 3.0 Ampere-Hour Cells. Rept. no. QE/C 64-1, U.S. Naval Ammunition Depot, Quality Evaluation Laboratory (Crane, Ind.), Jan. 6, 1964. (Available as NASA CR-55630, N64-46104.)

23. ANON.: Evaluation Program for Secondary Spacecraft Cells, General Performance Test on Gould National Batteries, Inc., 3.5 Ampere-Hour "D" Cells. Rept. no. QE/C 64-7, U.S. Naval Ammunition Depot, Quality Evaluation Laboratory (Crane, Ind.), Jan. 2, 1964. (Available as NASA CR-55631, N64-16105.)

24. ANON: Evaluation Program for Secondary Spacecraft Cells, General Performance Test on Gould National Batteries, Inc., 20.0 Ampere-Hour Cells. Rept. no. QE/C 64-4, U.S. Naval Ammunition Depot, Quality Evaluation Laboratory (Crane, Ind.), Feb. 28, 1964. (Available as NASA CR-53639, N64-19621.)

25. ANON.: Evaluation Program for Secondary Spacecraft Cells, General Performance Test on Sonotone Corporation, 5.0 Ampere-Hour "F" Cells. Rept. no. QE/C 64-2, U.S. Naval Ammunition Depot, Quality Evaluation Laboratory (Crane, Ind.), Feb. 4, 1964.

26. ANON.: Evaluation Program for Secondary Spacecraft Cells, General Performance Test on Gulton Industries, Inc., 6.0 Ampere-Hour Cells. Rept. no. QE/C 64-3, U.S. Naval Ammunition Depot, Quality Evaluation Laboratory (Crane, Ind.), Mar. 2, 1964.

27. ANON.: Evaluation Program for Secondary Spacecraft Cells, Acceptance Test on Gulton, 1.25 Ampere-Hour Cells With High Overcharge Capabilities. Rept. no. QE/C 66-120, U.S. Naval Ammunition Depot, Quality Evaluation Laboratory (Crane, Ind.), Feb. 28, 1966. (Available as NASA CR-71296, N66-20898.)

28. BRUESS, E. C.: Evaluation Program for Secondary Spacecraft Cells. Rept. no. QE/C 64-274, U.S. Naval Ammunition Depot, Quality Evaluation Laboratory (Crane, Ind.), June 15, 1964. (Available as NASA CR-58179, N64-27383.)

29. ANON.: Evaluation Program for Secondary Spacecraft Cells, General Performance Test on General Electric Co., 12.0 Ampere-Hour Cells. Rept. no. QE/C 64-6, U.S. Naval Ammunition Depot, Quality Evaluation Laboratory (Crane, Ind.), Apr. 8, 1964. (Available as NASA CR-53923, N64-19925.)

30. RUSSELL, C. R.; AND SELIS, S. M.: An Analytic Representation of the Discharge Characteristics of Commercial Secondary Batteries. Electrochem. Tech., vol. 1, no. 3-4, 1963, p. 77.

31. BAUER, P.; AND SPARKS, R. H.: Nickel-Cadmium Batteries for the Orbiting Geophysical Observatory: Cell Characteristics, Charge Control Concepts, Battery Design. Vol. I. Rept. no. 2315-6005-RU000, TRW Systems (Redondo Beach, Calif.), Apr. 1, 1963.

32. BRUESS, E. C.: Evaluation Program for Secondary Spacecraft Cells. Second Annual Report, Jan. 1 to Dec. 31, 1965. Rept. no. CE/C 66-304, U.S. Naval Ammunition Depot, Quality Evaluation Laboratory (Crane, Ind.), May 13, 1966. (Available as NASA CR-76034, N66-29760.)

33. BRODD, R. J.: Electrical Properties and Kinetics of Electrode Reactions. J. of Research, National Bureau of Standards, A. Physics and Chemistry, vol. 65A, no. 4, 1961, p. 275.

34. ANON.: Evaluation Program for Secondary Spacecraft Cells, Acceptance Test on Gulton 6.0-Ampere-Hour Adhydrode Cells. Test Rept. no. QE/C 65-536, U.S. Naval Ammunition Depot, Quality Evaluation Laboratory (Crane, Ind.), July 28, 1963. (Available as NASA CR-64617, N65-33222.)

35. ANON.: Evaluation Program for Secondary Spacecraft Cells, Acceptance Test on Gulton 20.0 Ampere-Hour Cells. Test Rept. no. QE/C 63-317, U.S. Naval Ammunition Depot, Quality Evaluation Laboratory (Crane, Ind.), June 14, 1963. (Available as NASA CR-55627, N64-16103.)

36. ANON.: Evaluation Program for Secondary Spacecraft Cells, Acceptance Test on Gulton 12 and 20 Ampere-Hour Adhydrode Cells. Test Rept. no. QE/C 67-1, U.S. Naval Ammunition Depot, Quality Evaluation Laboratory (Crane, Ind.), Jan. 21, 1967.

37. ANON.: Evaluation Program for Secondary Spacecraft Cells, Acceptance Test on Gulton 12 Ampere-Hour Cells. Rept. no. QE/C 65-124, U.S. Naval Ammunition Depot, Quality Evaluation Laboratory (Crane, Ind.), Feb. 16, 1965. (Available as NASA CR-57470, N65-19868.)

38. ANON.: Evaluation Program for Secondary Spacecraft Cells, Acceptance Test on Gulton 3.6 and 5.6 Ampere-Hour Cells With Vulcanized Neoprene Terminal Seals. Rept. no. QE/C 66-69, U.S. Naval Ammunition Depot, Quality Evaluation Laboratory (Crane, Ind.), Jan. 28, 1966. (Available as NASA CR-70852, N66-19094.)

39. ANON.: Evaluation Program for Secondary Spacecraft Cells, Acceptance Test on Gulton 5.0 Ampere-Hour Nimbus Cells. Rept. no. QE/C 65-460, U.S. Naval Ammunition Depot, Quality Evaluation Laboratory (Crane, Ind.), June 23, 1965. (Available as NASA CR-63912, N65-29145.)

40. ANON.: Evaluation Program for Secondary Spacecraft Cells, Acceptance Test on Sonotone 5.0 Ampere-Hour Cells. Rept. no. QE/C 65-583, U.S. Naval Ammunition Depot, Quality Evaluation Laboratory (Crane, Ind.), Sept. 2, 1965. (Available as NASA CR-67350, N65-35357, or NASA CR-67713, N66-11672.)

41. ANON.: Evaluation Program for Secondary Spacecraft Cells, Acceptance Test on Sonotone 3.5 Ampere-Hour Sealed Cells. Rept. no. QE/C 66-340, U.S. Naval Ammunition Depot, Quality Evaluation Laboratory (Crane, Ind.), June 6, 1966. (Available as NASA CR-76520, N66-31895.)

42. ANON.: Evaluation Program for Secondary Spacecraft Cells, Acceptance Test on Gulton 3.5 Ampere-Hour Sealed Cells With the Plitt Seal. Rept. no. QE/C 66-709, U.S. Naval Ammunition Depot, Quality Evaluation Laboratory (Crane, Ind.), Nov. 18, 1966.

43. ANON.: Evaluation Program for Secondary Spacecraft Cells, Acceptance Test on Sonotone 3.0 Ampere-Hour Triple Seal Cells. Rept. no. QE/C 65-612, U.S. Naval Ammunition Depot, Quality Evaluation Laboratory (Crane, Ind.), July 23, 1965. (Available as NASA CR-64353, N65-31031.)

44. ANON.: Evaluation Program for Secondary Spacecraft Cells, Acceptance Test on General Electric 5.0 Ampere-Hour Nimbus Cells. Rept. no. QE/C 65-459, U.S. Naval Ammunition Depot, Quality Evaluation Laboratory (Crane, Ind.), June 23, 1965. (Available as NASA CR-64687, N65-33221.)

45. BECK, T. R.; AND KEMP, F. S.: Heat Generation in Lunar Orbiter Battery. Rept. no. D2-23612-1, Boeing Co. (Seattle, Wash.), Oct. 1964.

46. FOLEY, R. T.; AND WEBSTER, W. H.: Research Into Fundamental Phenomena Associated With Spacecraft Electrochemical Devices—Calorimetry of Nickel-Cadmium Cells. Second Quarterly Report, Goddard Space Flight Center, Oct. 1 to Dec. 31, 1966. American Univ. (Washington, D.C.). No date.

47. FOLEY, R. T.; AND WEBSTER, W. H.: Research Into Fundamental Phenomena Associated With Spacecraft Electrochemical Devices—Calorimetry of Nickel-Cadmium Cells. Third Quarterly Report, Goddard Space Flight Center, Jan. 1 to Mar. 31, 1967. American Univ. (Washington, D.C.). No date.

48. BAUER, P.; AND SPARKS, R. H.: Nickel-Cadmium Batteries for the Orbiting Geophysical Observatory. Vol. II. Rept. no. 2315-6008-RU000, TRW Systems (Redondo Beach, Calif.), Feb. 12, 1964.

49. CARSON, W. N.; CONSIGLIO, J. A.; AND NILSON, R. R.: Characterization of Nickel-Cadmium Electrodes. Final Report, Goddard Space Flight Center, July 1, 1963, to Dec. 31, 1964. General Electric Co., Advanced Technology Laboratories (Schenectady, N.Y.). No date. (Available as NASA CR-63916, N65-29148.)

50. HALPERT, G.: Some Factors To Consider in Determining the Capacity of a Nickel-Cadmium Cell. Rept. no. TM X-55610, NASA, Goddard Space Flight Center, Aug. 1966. (Available as NASA N67-11393.)

51. HENNIGAN, T. J.; AND SIZEMORE, K. O.: Auxiliary Electrode Instrumentation for Nickel-Cadmium Cells. Rept. no. TM X-55471, Goddard Space Flight Center, May 1966. (Available as NASA N66-24928.)

52. BRUESS, E. C.: Evaluation Program for Secondary Spacecraft Cells. First Annual Rept. no. QE/C 65-356, Apr. 1962 to Dec. 31, 1964. U.S. Naval Ammunition Depot, Quality Evaluation Laboratory (Crane, Ind.), May 14, 1965. (Available as NASA CR-63424, N65-26408.)

53. ANON.: Testing and Evaluation of Nickel-Cadmium Spacecraft Type Cells. Final Report, Cook Electric Co., Inland Testing Laboratories, 1965. (Available as NASA CR-63181, N65-25404.)

54. ANON.: Testing and Evaluation of Nickel-Cadmium Spacecraft Type Cells. Final Rept. no. 9PD-4667-2, Jan. 1 to Nov. 1, 1965. Cook Electric Co. (Dayton, Ohio). No date.

55. CLARK, W. W.; AND INGLING, W. G.: Evaluation of Secondary Batteries. Presented at the 17th Annual Power Sources Conference (Fort Monmouth, N.J.), May 21-23, 1963, p. 122.

56. FRANCIS, H. T.: Space Batteries. Armour Research Foundation, 1964. (Available as NASA SP-5004, N64-18052.)

57. ANON.: Testing of Sealed Nickel-Cadmium Cells. Vol. III. Study of Relationship Between Acceptance Test Data and Nickel-Cadmium Cell Life. Rept. no. ER 14473, Martin-Marietta Corp., The Martin Co. Division (Baltimore, Md.), Jan. 1967.

58. MAUCHLY, J. W.; AND WAITE, J. H.: Computer Methods for the Reduction, Correlation and Analysis of Space Battery Test Data. Final Report, Goddard Space Flight Center, May 1 to Dec. 31, 1966. Mauchly Systems, Inc. (Montgomeryville, Pa.). No date.

59. MacKENZIE, C. M.: Solar Power Systems for Satellite in Near-Earth Orbits. Rept. no. X-716-67-77. Goddard Space Flight Center, Mar. 1967.

60. WHITNEY, C. B.: Design and Development of a Hermetically Sealed 12 Ampere-Hour Silver-Cadmium Cell in a Non-Magnetic Metallic Case. Rept. no. D2-90023, Yardney Electric Co. (N.Y.), Aug. 1961 (rev. Feb. 21, 1962).

61. GRAFF, C.: The Electrical Power System for the Pegasus Satellite. Rept. no. TM X-53419, Marshall Space Flight Center. No date. (Available as NASA N66-32609.)

62. MOSES, E. G.: Design Techniques for an ATS-4 Power System. Rept. no. X-716-67-59, Goddard Space Flight Center, Feb. 1967.

63. SPARKS, R. H.; AND WRIGHT, W. H.: Integral Electronic Charge Controls for High Performance Secondary Batteries. Presented at Aerospace and Electronic Systems Conference (Los Angeles, Calif.), Oct. 3-5, 1966.

64. SIZEMORE, K. O.: Use of the Adsorption Hydrogen Electrode and the Oxygen Fuel-Cell Electrode on Nickel-Cadmium Cells. Rept. no. TM X-55469, Goddard Space Flight Center, Apr. 1966.

65. LERNER, S.; AND SEIGER, H.: Characterization of Recombination and Control Electrodes for Spacecraft Nickel-Cadmium Cells. Third Quarterly Report, Goddard Space Flight Center, Dec. 9, 1966, to Mar. 9, 1967, Gulton Industries, Inc. (Metuchen, N.J.). No date.

66. LERNER, S.: Characterization of Recombination and Control Electrodes for Spacecraft Nickel-Cadmium Cells. First Quarterly Report, Goddard Space Flight Center, June 9 to Sept. 9, 1966, Gulton Industries, Inc. (Metuchen, N.J.). No date.

67. CARSON, W. N.; AND HADLEY, R. L.: Auxiliary Electrode Space Cells. AIAA no. 64-752. Presented at Third Biennial Aerospace Power Systems Conference (Philadelphia, Pa.), Sept. 1-4, 1964.

68. ANON.: Study Papers on the Auxiliary Electrode. Rept. no. PIC-BAT 209/9. Power Information Center (Philadelphia, Pa.), Sept. 1-4, 1964. (Available as NASA CR-67987, N66-11765.)

69. STROUP, E. R.: Analysis of Cadmium-Cadmium Coulometers Used for Charge Control in Nickel-Cadmium Space Batteries. Rept. no. TM X-59021, Goddard Space Flight Center, Sept. 1966. (Available as NASA N66-39923.)

70. FORD, F. E.; AND LIWSKI, P. P. M.: Control Devices and Circuitry for Use With Spacecraft Batteries. Rept. no. 93/66, U.S. Navy Marine Engineering Laboratory (Annapolis, Md.), Apr. 1966. (Available as NASA CR-74787, N66-24963.)

71. LIWSKI, P. P. M.: Control Devices and Circuitry for Use With Spacecraft Batteries. Rept. no. 25/65, U.S. Navy Marine Engineering Laboratory (Annapolis, Md.), Apr. 1965. (Available as NASA CR-62959, N65-24894.)

72. YAGERHOFER, F. C.: Design of the United Kingdom Scientific Satellite Solar Power System. No. 2498-62. Presented at American Rocket Society Space Power Systems Conference (Santa Monica, Calif.), Sept. 24-28, 1962.

73. CATOTTI, A. J.; AND READ, M. D.: Charge Control of Nickel-Cadmium Batteries; Auxiliary Electrodes for Overcharge and Overdischarge Control. Presented at the 19th Annual Power Sources Conference (Fort Monmouth, N.J.), May 18-20, 1965, p. 63.

74. ALLIEGRO, F.; BELOVE, L.; AND VOYENTZIE, P.: High Capacity Sealed Nickel-Cadmium Batteries. Presented at the 16th Annual Power Sources Conference (Fort Monmouth, N.J.), May 22-24, 1962, p. 99.

75. RITTERMAN, P.; AND SEIGER, H. N.: Hermetically Sealed Cells Capable of Overdischarge as Well as Overcharge. Final Report, Goddard Space Flight Center, Gulton Industries, Inc. (Metuchen, N.J.), May 1964.

76. CATOTTI, A. J.; AND READ, M. D.: Development of a Nickel-Cadmium Storage Cell Immune to Damage From Overdischarge and Overcharge. Final Report, General Electric Co., Battery Business Section (Gainesville, Fla.), June 21, 1965. (Available as NASA CR-62019, N65-34228.)

77. ANON.: Battery Workshop. NASA Headquarters (Washington, D.C.), Oct. 6-7, 1966.

78. EPSTEIN, S. D.; AND WAITE, J. H.: Computer Methods for the Reduction, Correlation and Analysis of Space Battery Test Data. First Quarterly Report, Jan. 1 to Apr. 30, 1967, Goddard Space Flight Center, Mauchly Systems, Inc. (Montgomeryville, Pa.). No date.

79. BOURGAULT, P. L.; AND CONWAY, B. E.: The Electrochemical Behavior of the Nickel-Nickel Oxide Electrode, Part I. Kinetics of Self-Discharge. Canadian J. of Chem., vol. 37, 1959, p. 292.

80. BAUER, P.: Pressure Characteristics of Sealed Nickel-Cadmium Cells. Electrochem. Tech., vol. 3, no. 1-2, 1965, p. 43.

81. LORSCH, H. G.: Biocontamination Control. Space Aeronautics, vol. 46, no. 6, Nov. 1966, p. 82.

82. LISKA, J.: Investigation of Sterilization of Secondary Batteries. Final Report, June 26 to Oct. 26, 1966, Gulton Industries, Inc. (Metuchen, N.J.). No date.

83. RICHARDS, R. N.: Heat Sterilization Testing of Nickel-Cadmium Cells. Final Rept. no. 06030-6001-R000, TRW Systems (Redondo Beach, Calif.), Oct. 1966.

84. ARGUE, G. R.; MACKENZIE, D. E.; MCCOLLUM, W. A.; AND RECHT, H. L.: The Effects of Radiation on Nickel-Cadmium Battery Electrodes. Final Rept. no. AI-65-66, North American Aviation, Inc., Atomics International Division (Canoga Park, Calif.), Apr. 15, 1965. (Available as NASA CR-62796, N65-24491.)

85. KELCHNER, R. E.; NICHOLSON, M. M.; AND RECHT, H. L.: Effects of High-Energy Protons on Selected Cells. Final Rept. no. AI-66-149, June 1966 to Aug. 1966, North American Aviation, Inc., Atomics International Division (Canoga Park, Calif.). No date.

86. CHERDAK, A. S.; GREENBLATT, R. C.; AND MACKENZIE, C. M.: Nimbus Power Systems. Rept. no. X-450-66-333, Goddard Space Flight Center, June 1966.

87. STROUP, E. R.: The Battery for the International Ionosphere Satellite, Ariel I. No. 2510-62. Presented at the American Rocket Society Space Power Systems Conference (Santa Monica, Calif.), Sept. 25-28, 1966.

88. BOMBERGER, D. C.; AND MOOSE, L. F.: Nickel-Cadmium Cells for the Spacecraft Battery. Rept. no. SP-32, Goddard Space Flight Center. Telstar I, vol. 3, June 1963, p. 1687. (Available as NASA N64-11082.)

89. SHAIR, R. C.; ET AL.: Hermetically Sealed Sintered Plate Nickel-Cadmium Secondary Batteries. Final Report, Gulton Industries, Inc. (Metuchen, N.J.), July 1963. (Available as NASA CR-60819, N65-17518.)

CHAPTER 5

Silver-Cadmium Batteries

Although the silver-cadmium couple has been known for some time, it has been intensively developed only since World War II. It has been viewed as a compromise between the short-life, high-energy density silver-zinc cell, and the long-life, low-energy density nickel-cadmium system. It is presently the only system which can make cyclic orbital satellite applications free of residual magnetic properties. It has been flown in a number of satellites, generally with good success. The silver-cadmium cell is available in both sealed and vented configurations, the sealed type being most common in aerospace applications.

CHEMISTRY

The chemistry of the cadmium electrode is nearly identical in both the silver-cadmium and nickel-cadmium cells. (See ch. 4.) A significant exception is the lower O_2 recombination rate at the pressed powder cadmium electrode. Hennigan (NASA GSFC, private communication) states that observed recombination rates are one-twentieth of those observed in sintered electrodes. The chemistry of the silver electrode is identical with the positive electrode of silver-zinc cells. (See ch. 6.)

STRUCTURE

Cell geometry, materials, and methods of construction of both the silver electrode and the separators is similar to that of the silver-zinc cell. (See ch. 6.) The cadmium electrode, however, usually has a different construction than the nickel-cadmium cell.

Although other methods have been used, including the porous nickel plaque found in the nickel-cadmium cell, most silver-cadmium cells employ pressed powder or pasted cadmium electrodes.

Finely divided precipitated cadmium hydroxide is mixed with water and a binder to form a heavy paste, which is applied to a silver mesh. The pasted electrode is then dried, wrapped in a thin layer of porous paper, and pressed into the mesh to insure good contact.

ELECTRICAL CHARACTERISTICS

Although the electrical characteristics of the silver-cadmium and silver-zinc cells are similar, the silver-cadmium cell operates at a lower

voltage. These characteristics combine the highly reversible properties of the cadmium electrode with the two-step characteristics of the silver electrode.

DISCHARGE CHARACTERISTICS

Figure 5–1 shows a typical discharge curve for a silver-cadmium cell, and illustrates the significant portions of the curve. As described in chapter 2, regions A and B are typical of the onset of polarization and of the discharge plateau. Region C is the transition between the upper and lower discharge plateaus. The voltage of the upper plateau is characteristic of the reduction of divalent silver to the monovalent state, and the voltage of the lower is characteristic of reduction of monovalent to metallic silver. In an ideal cell, starting at the fully charged state, this transition region would be expected to occur at the 50-percent state of charge. In practice, the upper plateau rarely occupies more than 20 to 30 percent of the discharge capacity of the cell, and may disappear entirely under some circumstances. In figure 5–1, both reactions are occurring simultaneously at the lower plateau voltage.
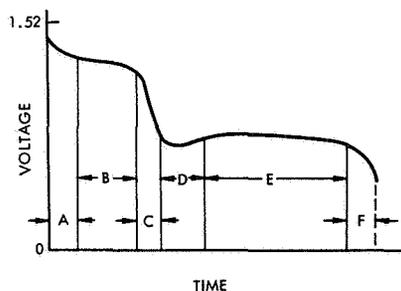
FIGURE 5–1.—Typical discharge curve
for a silver-cadmium cell.

Region D, known as the dip, often appears at the start of the lower plateau at the temperature of test. With continued discharge, however, the plateau voltage rises to the level of region E due to internal temperature increases and the increasing conductivity of the silver electrode as metallic silver replaces the relatively poorly conductive Ag_2O. At low discharge rates, the dip is not observed. The amplitude of the dip will also vary with the structure of the electrodes. Region F is the usual exhaustion region.

The literature provides several sources of discharge-characteristic data, each related to a different cell and not directly comparable to other cells due to the practice of the cell manufacturers of optimizing a cell for its application by varying the type and number of layers of separators and absorbents; the amount and concentration of the electrolyte; the number, composition, and structure of the electrodes; and other variables. Data

are reported by Stafford on Yardney 3-A-h and 5-A-h cells (ref. 1) and by Biess on 12-A-h cells (ref. 2). Similarly, Whitney (ref. 3) reports on 3-A-h cells specially designed for operation in a 100-minute orbit. No structural details are given. Imamura (ref. 4) reports on the Yardney YS 12 S-1 and YS 12 S-2, which differ in that YS 12 S-2 contains additional absorbent layers and omits the use of a polyvinyl alcohol film separator adjacent to the silver electrode. This results in cells of improved performance but degraded resistance to silver migration. The Imamura data are shown in current-voltage form in figures 5-2 and 5-3.
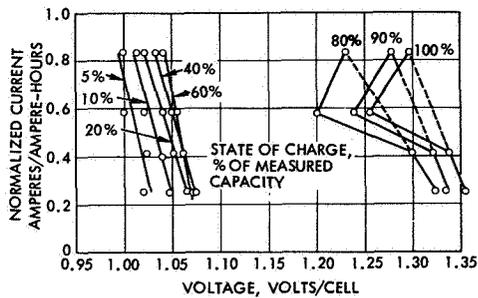
FIGURE 5-2.—Current-voltage discharge characteristic of Yardney YS 12 S-1 silver-cadmium cell at 75° F. State of charge as third variable.
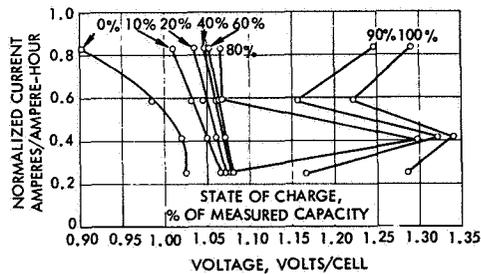
FIGURE 5-3.—Current-voltage discharge characteristic of Yardney YS 12 S-2 silver-cadmium cell at 75° F. State of charge as third variable.

All of the data examined show very erratic behavior of the cell, and considerable variation from cell to cell in the region of the upper plateau, in spite of the similarity of performance in the lower plateau region. Apelt and Hennigan (ref. 5) have observed a complete suppression of the

upper discharge plateau after long periods of trickle charge.   As a result, it is usually not practical to design systems dependent upon the availability of energy at the upper plateau voltage.
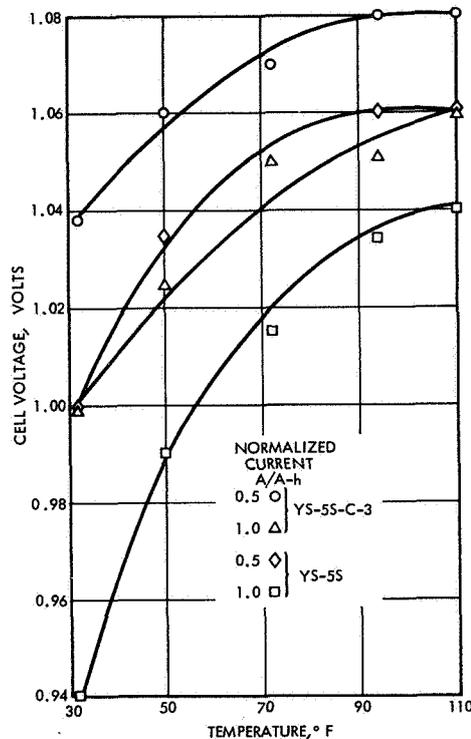

FIGURE 5-4.—Discharge voltage plateau as a function of temperature. Normalized current as third variable.

Variation of discharge characteristic with temperature is manifested in several ways, and Stafford et al. (refs. 1 and 2), Kemp and MacLean (ref. 6), Banks et al. (ref. 7) observed that the upper voltage plateau decreases in duration as the temperature increases.   Charkey (ref. 8), however, found that the upper plateau disappeared when the cell was discharged at low temperature (−10° C).   Stafford et al. (refs. 1 and 2) measured the shift in plateau voltages with temperature and with current, and Banks et al. (ref. 7) give parametric data on the variation of plateau voltage as a function of current with temperature as a third variable. Figure 5-4 shows the variation in discharge plateau voltage as a function of temperature according to Stafford.

A variation in capacity as a function of temperature and charge rate is reported by Stafford et al. (refs. 1 and 2) and Imamura (ref. 4).   This

variation is due, however, to the inability to return the cell to the fully charged state at low temperatures and high charge rates. Banks et al. give parametric data on the recharge of silver-cadmium cells, showing the maximum state of charge achievable under various conditions of charge, current, and temperature.

CHARGE CHARACTERISTICS

Except for a somewhat lower voltage, the charging characteristics of the silver-cadmium cell are similar in nature to those of the silver-zinc cell. Figures 5-5 through 5-7 show current-voltage characteristics
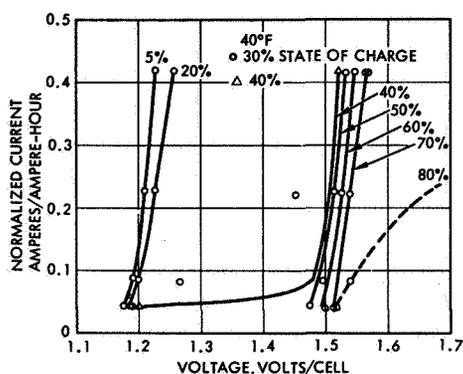
FIGURE 5-5.—Current-voltage charge characteristic of Yardney YS 12 S-2 silver-cadmium cell at 40° F. State of charge as third variable.
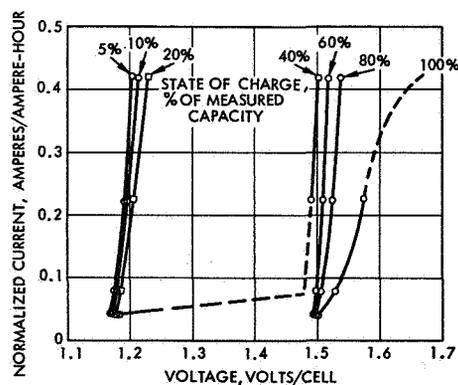
FIGURE 5-6.—Current-voltage charge characteristic of Yardney YS 12 S-2 silver-cadmium cell at 75° F. State of charge as third variable.
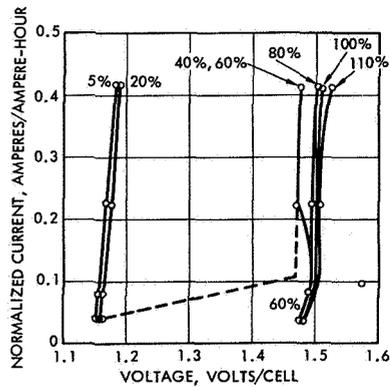
FIGURE 5-7.—Current-voltage charge
characteristic of Yardney YS 12 S-2
silver-cadmium cell at 110° F.
State of charge as third variable.

of the YS 12 S-2 cell on charge at different temperatures. A typical
charge curve showing voltage at constant current as a function of charge
time is given in figure 5-8. At a state of charge of approximately 30
percent, the transition between the lower and upper plateau occurs. The
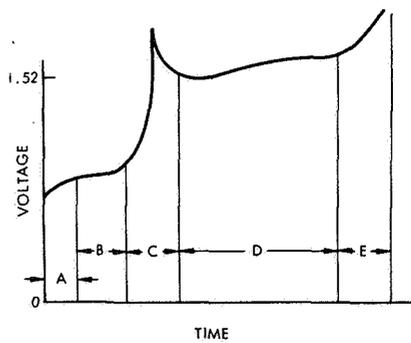
FIGURE 5-8.—Typical silver-cadmium
constant-current charge curve.

terminal voltage of the cell goes through a well-defined peak (region C)
before falling to the level of the upper plateau. The magnitude of the
intermediate peak changes with current and temperature and under
some circumstances can be great enough to interfere with charge control.
Stafford (ref. 1) has characterized the 3- and 5-A-h cell in the upper and
lower plateaus and in the region of the intermediate peak (fig. 5-9) and

shows data on the variation of these characteristics with current and temperature. Imamura performed extensive charge-characteristic measurement with current and temperature as independent variables. The results of this measurement are shown in the form of the current-voltage curves of figures 5-5 through 5-7 and as a temperature compensation curve of figure 5-10.
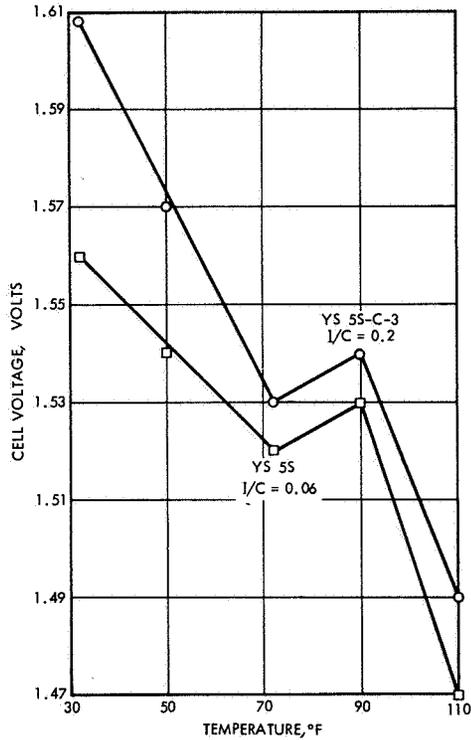
FIGURE 5-9.—Peak charge voltage versus temperature.

Voltage variation with temperature at constant current and state of charge appears to be linear in the YS 12 S-2 cell and the YS 5 S C-3 cell, but nonlinear in the YS 5 S cell (ref. 1). Stafford (ref. 1) shows a temperature coefficient of 0.52 mV/°F, and an analysis of the Imamura data shows a coefficient between 0.62 and 1.2 mV/°F, depending upon the state of charge of the cell.

The slopes of the current-voltage curves, which are equivalent to 0.004 ohm from 40° to 110° F, do not vary with temperature in the upper plateau region. They do appear to vary, however, in the lower plateau region, decreasing with increasing temperature from 0.009 at 40° F to 0.006 ohm at 110° F. (YS 12 S-2 cell, Imamura data.)
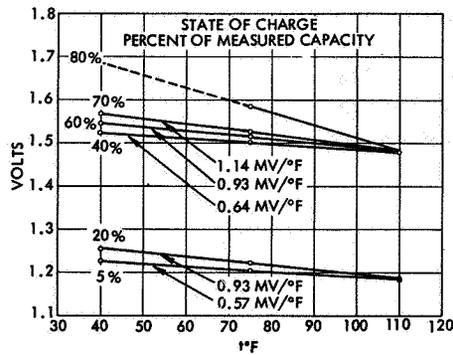
FIGURE 5-10.—Variation of voltage with temperature at constant current. $(I/C = 0.42)$ Yardney YS 12 S-2 cell. State of charge as third variable.

OVERCHARGE CHARACTERISTICS

Unlike the nickel-cadmium system, the silver-cadmium cell will tolerate only limited amounts of overcharge. Precise data on the relationship between current, voltage, temperature, and pressure are not available. Biess et al. (ref. 2) measured the effects of temperature on voltage and current but did not report cell pressures, so that it is not possible to evaluate the effects of long periods of constant potential float, or constant current overcharge using these data. Charkey and Dalin (ref. 9) show a buildup of hydrogen pressure to 50 psi during the first 100 days of overcharge of the negative electrode at a current density of 0.1 mA/in.^{2}, followed by a falloff in pressure. This, however, was in an experimental cell with no free electrolyte, making the available recombination surface higher than that normally found in the silver-cadmium cell.

EFFICIENCY

Stafford (ref. 1) measured the ampere-hour efficiencies of silver-cadmium cells of two types, finding average efficiencies of 0.946 and 0.994. The lower efficiency cell was a cell of 3-A-h capacity in a 5-A-h case, designed for high-rate operation. No explanation is given for the deviation of efficiency from the theoretical 1.000. In all probability, the deviation is due to the generation and recombination of small amounts of oxygen gas on overcharge. In any event, the ampere-hour efficiency of the silver-cadmium system may, for practical purposes, be taken to be 1.0, and the watt-hour efficiency is then equal to the ratio of output voltage to charge voltage.

NAD Crane (ref. 10) measured the overall efficiencies of 4-A-h silver-cadmium cells developed by the Electrochimica Corp., Menlo Park, Calif., operating at 65 percent depth of discharge. After the initial cycles,

which showed efficiencies greater than 100 percent, expressing a change in the average state of charge for each cycle, the measured efficiencies stabilized at a level between 86.1 and 96.8 percent. Lower efficiencies appear to be associated with higher charge currents, but, because of variations in the test, it is difficult to assign causes to the variation in efficiency.

IMPEDANCE

The impedance of silver-cadmium cells varies considerably with the state of charge, in a manner similar to that of silver-zinc cells, going through a large peak during the transition between upper and lower plateaus. Imamura (ref. 4) measured impedances of the YS 12 S–1 and –2 series cells as a function of frequency throughout the discharge period using the ac bridge method. Figure 5–11 shows the impedance of a two-cell YS 12 S–2 battery superimposed upon a battery-discharge curve.
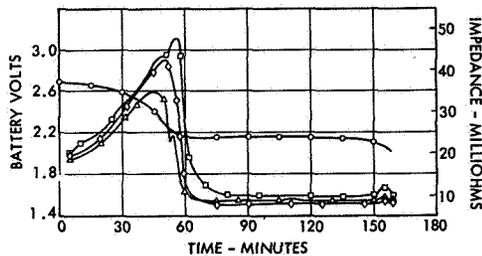
FIGURE 5–11.—Impedance characteristics of two series-connected YS 12 S–2 cells during 4-amp discharge.

○ Two-cell voltage ◊ Impedance at
400 cps
□ Impedance at △ Impedance at
10 cps 2461 cps

It is to be expected that the impedance will go through a similar peak on the charge cycle. This high impedance peak, coincident with the transition between upper and lower plateaus, is popularly ascribed to the high resistivity of Ag_2O in comparison with that of AgO and metallic silver. The transition region is therefore the point of highest bulk resistivity of the electrodes. Much of the AgO has been consumed and the amount of metallic silver has not yet increased to the extent necessary to improve the conductivity of the active material.

HEAT EVOLUTION AND ABSORPTION

The basic principles governing heat effects in batteries as stated in chapter 2 apply to silver-cadmium cells. However, the peculiarities in

the thermal behavior of these cells result from the irreversible behavior of the silver electrode, and are very similar to those encountered in the silver-zinc cell. Consequently, heat effects in both types of cells are discussed here.

The ampere-hour efficiency of both silver-zinc and silver-cadmium cells is approximately unity when they are neither overcharged or over-discharged. Consequently, equation (2–16) is valid for both charge and discharge cycles. However, because two simultaneous reactions can occur at the silver electrode throughout a significant portion of either the charge or discharge periods, predictions of heat rate may be in error, based upon the assumption of the division of current between the two reactions.

If the cell were on the upper plateau of discharge or the lower plateau of charge, and if only one reaction were in progress, a reasonable prediction of heat rate could be obtained from equation (2–16). If, however, the true transition point between the upper and lower plateaus is assumed to occur at 50 percent state of charge, and the reactions to occur sequentially (when, in fact, they occur simultaneously throughout much of the cycle), the predicted heat-evolution rate will be high during the early stages of the cycle and low beyond the 50-percent mark. The total heat evolved during the entire cycle, represented by the area under the curve, will be fairly accurately determined. Heat evolution in a silver-cadmium battery was computed in this manner by Banks et al. (ref. 7) as a part of a computer battery design program. Rowlette (ref. 11) computes the heat evolved in the silver-zinc Surveyor battery by the equation

$$q = I(E_H - E_I)$$

where E_r is the terminal voltage of the cell, and $E_H = -\Delta H/zF$.

This translates directly to equation (2–16) in that

$$E_H = E_{\text{rev}} + T\Delta S$$

where ΔS is in volts/degree K.

Figures 5–12 and 5–13 show typical predicted versus actual heat output curves resulting from this work.
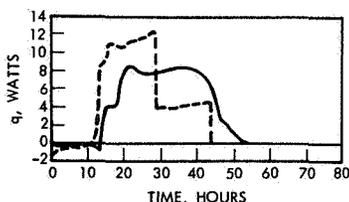

FIGURE 5–12.—Heat-generation rates of silver-zinc Surveyor battery on 3-amp charge.
————— Calculated curve (heat generation)
————— Measured curve (heat dissipation)
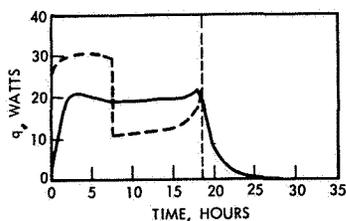
FIGURE 5-13.—Heat-generation
rates of silver-zinc Surveyor
battery on 7-amp discharge.
— — — Calculated curve
(heat generation)
——— Measured curve
(heat dissipation)

Gross (ref. 12) shows a combination of flow calorimeter and space-craft system simulator designed to measure the heat-generation rates and temperatures of complete batteries by measurement of heat rejection to a water-cooled baseplate. No data have been produced as yet. Also see reference 13.

STERILIZATION

Because the materials used in the silver-cadmium cells, including cases, separators, electrolyte, and silver electrodes, are similar to or identical to those used in the silver-zinc cell, all tests on individual materials other than the cadmium electrode are reported under silver-zinc (ch. 6).

Tests on the cadmium electrode were performed by Jet Propulsion Laboratory on cadmium electrodes manufactured for the purpose by the Electric Storage Battery Co. (ref. 14). Cadmium electrodes sterilized in 40 percent KOH electrolyte at 145° C in the charged state lost all of their capacity during the sterilization cycle. This loss was attributed to oxidation by the residual air in the sterilization chamber. Attempts at recharging the sterilized electrode failed because only about 20 percent of the theoretical capacity was attainable.

Discharged electrodes sterilized under the same conditions exhibited similar behavior. However, when the limiting potential applied by the charger was raised, the electrode accepted charge at the higher voltage, and subsequently at normal charge voltages. It was concluded that the sterilization process induced high-resistance behavior in the cadmium electrode, which reverted to normal after a single formation charge.

MAGNETIC PROPERTIES

The Eagle-Picher Co. (ref. 15) reports the use of silver grids and stainless-steel current leads between grids and terminals. Attempts at

using 18 percent nickel silver and cupro nickel as grid alloys were un-
successful because of excessive resistance. Stainless steel was also not
usable as a grid because excessive work hardening made the material
too difficult to use. Annealing in inert gas left a hard oxide coating on
the stainless steel.

The Yardney Electric Corp. (ref. 16) attempted the development of
a metal-encased nonmagnetic silver-cadmium cell. An interim design
using tin-coated brass was unsuccessful because the soldered joints failed
to provide a hermetic seal.

Cells were constructed using 310 stainless-steel cases over inner plastic
cases, but subsequent tests (ref. 6) showed an excessive failure rate
associated with leaking and loss of capacity.

Measurements on the magnetic field of a battery, consisting of 22 series-
connected 12-A-h cells in two rows of 11, are reported by W. H. Scott
(TRW Systems, private communication). The wiring was laid out in a
single loop. The maximum field strength, reported in the table below,

Condition:	*Magnetic field, gamma at 1 ft from center*
Open circuit_____	10–23
1-A discharge_____	200–250
3-A discharge_____	2000–3000

occurred in a direction normal to the plane of the wiring loop. Hennigan
(NASA GSFC, private communication) reports less than 8 gamma at
18 inches with 3 amperes flowing. The large difference is probably due to
differences in wiring or in loop orientation.

SERVICE LIFE

The expected service life of silver-cadmium cells has so far defied
rational prediction, largely because the cells tested and the test conditions
have varied so widely that no correlation seems possible among them.
Frink (ref. 17) summarizes the cycle life of silver-cadmium batteries
in tabular form, but provides no references to the original data. Francis
(ref. 18) summarizes the cycle life of silver-cadmium batteries in the
form of a plot of log showing cycle life as a function of depth of discharge.
However, most of the data are based upon tests in progress, and must be
considered as preliminary.

The available NASA-sponsored data on the service life of silver-
cadmium cells consist of two series of tests conducted for the Boeing
Co. and one series conducted by NAD Crane. The Boeing (refs. 3 and 6)
tests were on three-cell batteries at several depths of discharge, in a 100-
minute orbit, and using a solar-array simulator which applies a poorly
regulated modified constant potential charge control to the battery.
NAD Crane (ref. 19) conducted tests in several different types of cells in a
24-hour orbit at a 20-percent depth of discharge and varying temperature.
Tests for Boeing were conducted (ref. 6) on 12-A-h silver-cadmium cells
packaged in an inner plastic case surrounded by an outer metal case,
operated at 35 percent depth of discharge in a 100-minute orbit. A few

additional scattered tests of different types of cells are also found (refs. 10 and 15). These data are summarized in figure 5–14, which shows the initial failure and, where available, the failure range of cells in a 100-minute orbit. Clearly, it has not been possible to duplicate the promise
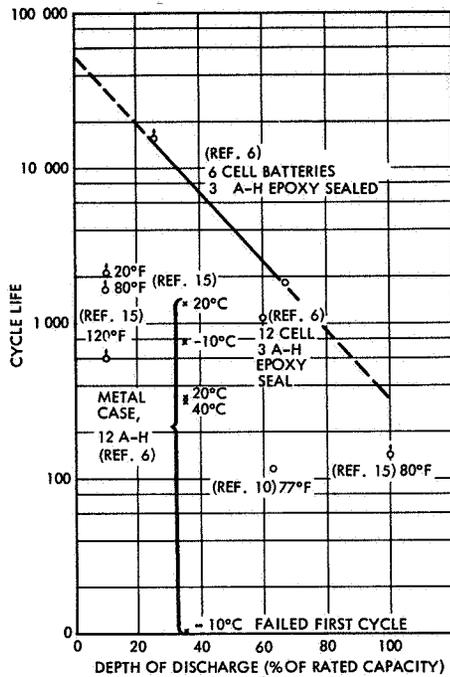
FIGURE 5–14.—Cycle life of silver-cadmium cells.

of these early data on cycle life. Cycle life in the 24-hour orbit at 20 percent depth of discharge has been found to fall between 34 and 200+ cycles at a 20-percent depth of discharge. It is not clear why operation in a longer orbit with its slower charge should decrease life. Since NAD Crane (ref. 19) used a limit of 1.50 volts per cell, compared with the Boeing limit of 1.60 volts per cell, differences in charge-voltage limit and consequent failure to recharge may be partially responsible.

WET- STAND- TIME

No test data on wet stand-time of silver-cadmium cells was found. Manufacturers' claims are for stand times of up to 3 years, but it is not stated whether fully charged or discharged. Hennigan (NASA GSFC, private communication) reports 23 percent loss of capacity after 1.5 years at 25° C in the charged condition.

CHARGE AND DISCHARGE CONTROLS

The sensitivity of the silver-cadmium cell to the charge-control method is somewhat greater than that of the sealed nickel-cadmium cell, due mainly to the lack of tolerance of the silver-cadmium system for extended overcharge. The manufacturers recommend charging of vented cells to an end voltage of 1.55 to 1.70; the higher value offers maximum capacity, while the lower offers minimum maintenance.

Impact of Charge Controls Upon Service Life

The requirement for sealing cells for operation in a space environment imposes severe problems in control of charge to the battery. Excessive overcharge leads to generation of gases, followed by mechanical failure of the cell cases due to overpressure, since the presence of excess electrolyte prevents the use of negative-electrode surface for recombination at useful overcharge rates. In common with most cells, the most convenient means of eliminating excessive overcharge is to limit the voltage which is applied to the cell to some value at which the rate of evolution of oxygen from the silver electrode is small enough to enable recombination. Failure to do this will seriously limit the service life of the cell. At the same time, unless a long time is available for charging the battery, it is necessary to raise the end-of-charge voltage limit above the level reached by the intermediate peak (between lower and upper plateaus). If this is not done, on modified constant potential charging, the battery will undergo a period of slow charge until the intermediate peak is passed. Under some circumstances, this period can be several hours long. In short-time orbits, such as the 100-minute orbit, the battery will fail to recharge and a premature system failure will result. This is not a battery failure in the sense that, after failure, the battery may then be operated successfully in another charge control mode.

Detection of Charge Completion

Two methods have been proposed for detection of charge completion: measurement of battery or cell voltage, and measurement of oxygen pressure with an auxiliary electrode. Although systems have been selected for several spacecraft, only one documented instance was found in the NASA-sponsored literature of a study of alternative charge-control procedures, and selection of the optimum based upon the best knowledge at the time. Biess et al. (ref. 2) studied the characteristics of the silver-cadmium system, and concluded that the optimum charge-control system for the 100-minute orbit case was the modified constant potential method, compensated for temperature in accordance with the equation

$$V = 38.40 - 0.024 \ (T - 30)$$

where
  V voltage of a 24-cell battery
  T battery temperature in degrees F

During long periods of continuous sunlight, the battery, after charging, remained open circuited until an undervoltage occurred, upon which it

was automatically switched in to supply the loads. Constant potential float was avoided for long periods to prevent oxidation of the metallic silver current collectors and consequent failure of the battery. The temperature-compensation relationship was determined by measurement of the intermediate charging peak, and setting the voltage level at each temperature high enough to prevent interference with battery charging. Current was controlled to a limiting value of 2 amperes. Batteries employing this charge-control method failed after 3 to 6 months in orbit because of cell divergence. Hennigan (NASA GSFC, private communication) reports a survival time in orbit of more than 400 days for a silver-cadmium battery in the FR-1 satellite. Charge control for the 17-percent depth of discharge, 100-minute orbit period mission was modified constant potential, using a temperature-compensated voltage limit which varied from 1.5 volts per cell at 40° C to 1.6 volts per cell at 0° C.

Carson et al., in a compendium (ref. 20), investigated the use of auxiliary electrodes for charge control of silver-cadmium cells, finding that the operation of cells in which a platinum-catalyzed electrode was connected to the cadmium electrode failed due to the growth of silver dendrites from the silver electrode to the auxiliary electrode. The auxiliary electrodes were wetproofed to prevent flooding by using Teflon as a binder for the catalyst and current collector materials. Hennigan (NASA GSFC, private communication) states that the formation of dendrites is due to severe overcharging; subsequent cells made at GSFC and subjected to little overcharge lasted for 2 years. Cells were three-fourths flooded.

The use of auxiliary electrodes in silver-cadmium cells appears less attractive than their use with nickel-cadmium cells because of the requirement for flooded operation of the silver-cadmium system. In a gravitational field, this disadvantage may be overcome by proper design and orientation in the field so as to leave the auxiliary electrode in the airspace above the electrolyte. In zero-G operation, however, the unpredictability of location of the electrolyte makes necessary alternative means of assuring that the electrode is not completely immersed in the electrolyte, and thus isolated from the gas.

CELL DIVERGENCE

The problems of cell divergence in the silver-cadmium cell are similar to those described in chapter 2, but the difficulties in charge control caused by such divergence are far more severe than those encountered in unsealed cell systems or in the sealed nickel-cadmium system. This situation results from the lack of tolerance of extended overcharge of the silver-cadmium cell, and from the unpredictability of placement in the charge cycle of the transition between lower and upper plateaus. Many of the cases in which failure has been observed have coincided with the appearance of one or more divergent cells.

TRW concluded from an analysis of telemetered data and laboratory test data that the failure of several silver-cadmium batteries was due to severe divergence of the characteristics of one or more cells from that of the others (ref. 21), permitting cell voltage on charge to exceed normal

levels. Similar phenomena were also noted in tests conducted for Boeing Co. (refs. 3 and 6) on silver-cadmium cells.

THERMAL-INTERFACE PROBLEMS

The thermal-interface problems encountered in the use of the silver-cadmium system are similar in character to those described earlier. Because of the lack of tolerance of overcharge, the likelihood of thermal runaway as encountered in the nickel-cadmium system is slight, although it is theoretically possible. Heat evolution during charge and discharge is greater than in the nickel-cadmium system because of the large difference between reversible potential and operating potential during the middle half of the charge and discharge periods.

Charge control of the silver-cadmium cell is highly sensitive to the effects of temperature in spite of the large increase in potential at the end of charge because of the sensitivity of the magnitude of the intermediate peak to temperature variations.

SYSTEMS-INTERFACE PROBLEMS

The large difference between charge voltage and discharge voltage of the silver-cadmium cell results in poorer regulation than with any of the other common types of battery. A 20-cell system, designed so that the silver-cadmium battery controls the voltage of the main power bus, would vary in voltage from 20 volts at end of discharge to 32 volts at end of charge. System regulation can be improved by the use of boost charging, boost discharging, and other methods (all of which introduce switching problems), or by the use of a postbattery regulator, which imposes an efficiency penalty in some cases. Since all secondary batteries impose a penalty either in system regulation or in complexity or efficiency, the silver-cadmium system has no serious system penalties other than those of charge control and thermal control, discussed previously.

FAILURE MODES

Silver-cadmium cells can fail in several ways. Silver migration and reaction with the separator are discussed under silver-zinc cells (ch. 6) and will not be repeated here. Mechanical failures such as perforation of the separator, poor welds, leakage of electrolyte or gases from imperfect seals can also occur. (See ch. 2.)

Whitney (ref. 3) presents data which illustrate clearly the occurrence of cell divergence in a three-cell battery. Kemp and MacLean (ref. 6) also show data in which low voltages of a few cells of a battery result in application of excessive voltages to some of the companion cells. The low-voltage cells failed first, often accompanied by leaks. These data, taken on cells with an exterior steel case covering the plastic one, may not be directly applicable to the plastic-cased cells.

TRW Systems performed a comprehensive failure analysis on the silver-cadmium battery in OGO II, which failed after 1027 revolutions. It was concluded that the failure was due to open circuiting of one cell of the battery by loss of electrolyte. The mechanism proposed is that of divergence in cell characteristics resulting in overcharge of one of the cells at excessive voltages, generation of high internal pressures, and opening of the plastic case. The phenomenon was reproduced in the laboratory (ref. 21).

A similar battery (ref. 21) on life test did not fail in this way, but instead failed due to an internal short circuit in one of the cells (although divergence symptoms were also seen).

The Boeing Co. (ref. 6) has observed a slight depression in the discharge curve of cells which have been cycled at constant depth of discharge for long periods, and suggests the possibility that this may be comparable to the memory effect in nickel-cadmium cells. Since the cadmium electrodes are of entirely different structure in the two types of cells, this possibility cannot be ruled out.

REFERENCES

1. STAFFORD, W. T.: Silver-Cadmium Cell Evaluation Study. Interim Report on Goddard Space Flight Center Contract no. NAS 5-899 and NAS 5-3900, Rept. no. 2315-6002-KU000, TRW Systems (Redondo Beach, Calif.), May 16, 1962.
2. BIESS, J. J.; STAFFORD, W. T.; AND WRIGHT, W. H.: OGO Silver-Cadmium Battery Study. Final Report on Goddard Space Flight Center Contract no. NAS 5-899 and NAS 5-3900, Rept. no. 2314-6001-RU000, TRW Systems (Redondo Beach, Calif.), May 1963.
3. WHITNEY, C. B.: Design and Development of a Hermetically Sealed 12 Ampere-Hour Silver-Cadmium Cell in a Nonmagnetic Metallic Case. Rept. no. D2-90023, Yardney Electric Co. (New York), Aug. 1961 (rev. Feb. 21, 1962).
4. IMAMURA, M. S.: Evaluation of New Silver-Cadmium Cells for Use in OGO Batteries for Polar Orbit Missions. Engineering Report on Goddard Space Flight Center Contract no. NAS 5-899 and NAS 5-3900, Rept. no. 7062.7-2, TRW Systems (Redondo Beach, Calif.), May 1966.
5. APELT, A. O.; AND HENNIGAN, T. J.: Use of a Sealed Silver-Cadmium Battery on Explorer XII. Goddard Space Flight Center, Rept. no. TN D-1543, Jan. 1963. (Available as NASA N63-11741.)
6. KEMP, F. S.; AND MACLEAN, J. T.: Design and Development of a Hermetically Sealed 12 Ampere-Hour Silver-Cadmium Cell in a Nonmagnetic Metallic Case. App. A to Final Report on Goddard Space Flight Center Contract no. NAS 5-2115, Rept. no. D2-20496-1, Yardney Electric Co. (New York). No date. (Available as NASA CR-60574, N65-16322.)
7. BANKS, H. O., JR.; BAUER, P.; BINCKLEY, W. G.; RIESS, H.; AND ROBINSON, R. L.: Spacecraft Electric Power System Sizing and Analysis Computations. Final Report on Jet Propulsion Laboratory Contract no. BK 3-211739, Rept. no. 8584-6001-RU000, TRW Systems (Redondo Beach, Calif.), Mar. 15, 1964. (Available as NASA CR-60357, N65-15711.)
8. CHARKEY, A.: Research and Development Study of the Silver-Cadmium Couple for Space Application. Final Report on Goddard Space Flight Center Contract no. NAS 5-9106, Yardney Electric Co. (New York). No date.

9. CHARKEY, A.; AND DALIN, G. A.: Research and Development Study of the Silver-Cadmium Couple for Space Application. Final and Fifth Quarterly Report on Goddard Space Flight Center Contract no. NAS 5-3452, July 1 to Sept. 30, 1964, Yardney Electric Co. (New York). No date. (Available as NASA CR-62010, N65-23275.)

10. ANON.: Test and Evaluation Program for Electrochemical Cells Developed on NASA/GSFC Contracts. Report on Goddard Space Flight Center Contract no. S-23404-0, Rept. no. QE/C 65-123, U.S. Naval Ammunition Depot (Crane, Ind.), Feb. 18, 1965. (Available as NASA CR-57109, N65-18487.)

11. ROWLETTE, J.: Heat Generation in the Surveyor Main Battery. Abstract no. 47, Electrochem. Soc., fall meeting (Chicago, Ill.), vol. 2, Oct. 1967.

12. GROSS, S.: Development and Fabrication of Advanced Battery Energy Storage System. Midterm Report on Manned Spacecraft Center Contract no. NAS 9-6470, Sept. 27, 1966, to Mar. 26, 1967, Boeing Co., Space Division (Seattle, Wash.), Apr. 10, 1967.

13. BAUER, P.; AND SPARKS, R. H.: Nickel-Cadmium Batteries for the Orbiting Geophysical Observatory. Vol. II. Rept. no. 2315-6008-RU000, TRW Systems (Redondo Beach, Calif.), Feb. 12, 1964.

14. BODAMER, G. W.: Heat Sterilizable, Impact Resistant Cell Development. First Annual Report on Jet Propulsion Laboratory Contract no. 951296, Rept. no. 67-218, Sept. 24, 1965, to Dec. 31, 1966, Electric Storage Battery Co., Carl F. Norberg Research Center (Yardley, Pa.), Apr. 21, 1967.

15. ANON.: Design and Development of Silver-Cadmium Storage Batteries. Final Report on Goddard Space Flight Center Contract no. NAS 5-1318, July 1, 1961, to June 30, 1962, Eagle-Picher Co. (Joplin, Mo.). No date. (Available as NASA CR-78069, N66-87335.)

16. ANON.: Design and Development of a Hermetically Sealed 12 Ampere-Hour Silver-Cadmium Cell in a Nonmagnetic Metallic Case. Final Report on Goddard Space Flight Center Contract no. NAS 5-2155, Yardney Electric Co. (New York). No date. (Available as NASA CR-60026, N65-14597.)

17. FRINK, A. M., JR.: Sealed-Cadmium Silver-Oxide Batteries. Paper presented at the 17th Annual Power Sources Conference (Fort Monmouth, N.J.), May 21-23, 1963, p. 114.

18. FRANCIS, H. T.: Space Batteries. Armour Research Foundation, NASA Rept. no. SP-5004, 1964. (Available as NASA N64-18052.)

19. BRUESS, E. C.: Evaluation Program for Secondary Spacecraft Cells. Rept. no. QE/C 66-304, Jan. 1 to Dec. 31, 1965, U.S. Naval Ammunition Depot, Quality Evaluation Laboratory (Crane, Ind.), May 13, 1966. (Available as NASA CR-76034, N66-29760.)

20. ANON.: Study Papers on the Auxiliary Electrode. Rept. no. PIC-BAT 209/9, Power Information Center (Philadelphia, Pa.), Oct. 1965. (Available as NASA CR-67987, N66-11765.)

21. ANON.: Investigation of OGO-II Malfunctions, Vol. II—Silver-Cadmium Battery. Final Rept. no. 2360-6005-R0000, TRW Systems (Redondo Beach, Calif.), May 17, 1966.

CHAPTER 6

Silver-Zinc Primary and Secondary Batteries

The silver-zinc couple, one of the earliest battery systems, was used as a source of power as early as 1800. Alessandro Volta made use of a series-connected string of vessels, each containing a silver and a zinc rod in dilute acid solution. In 1899, additional interest was generated in the rather expensive curiosity by Junger; however, it was not until 1910 that Morrison patented the first silver-zinc alkaline cell. The first practical silver-zinc cell was developed by Henri André in the late 1920's. André was able to reduce the effect of solubility of the electrodes by using a semipermeable membrane to prevent migration of the active materials and the consequent rapid deterioration of the negative electrode. Development of the silver-zinc system was accelerated as the need for high-energy density batteries increased during World War II. Batteries were developed for primary, limited cycling, and extended cycling applications.

CHEMISTRY (Refs. 1 and 2)

POSITIVE ELECTRODE REACTIONS

The silver-zinc alkaline cell is characterized by two distinct voltage plateaus on charge and discharge. Open-circuit voltages of these plateaus are approximately 1.60 and 1.86 volts. The reaction occurring at the silver electrode at the lower voltage plateau is

$$
\begin{array}{lll}
\textit{Charged} & & \textit{Discharged} \\
Ag_2O + H_2O + 2e^- & = & 2Ag + 2OH^- \\
E_{rev} = 0.34 - .059 \log a^2(OH)^- & & \quad (6\text{-}1)
\end{array}
$$
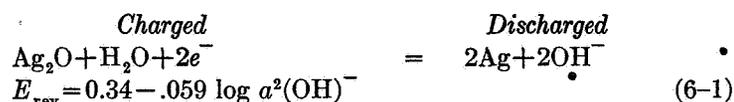
and that at the higher voltage plateau is

$$
\begin{array}{lll}
\textit{Charged}^1 & & \textit{Discharged} \\
2AgO + H_2O + 2e^- & = & Ag_2O + 2OH^- \\
E_{rev} = 0.57 - .059 \log a^2(OH)^- & & \quad (6\text{-}2)
\end{array}
$$
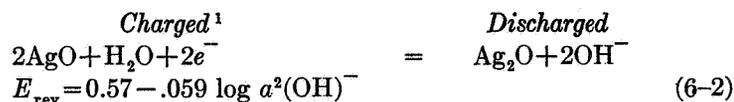
On charge, the reactions occur in the direct opposite to that written. As can be seen from equations (6-1) and (6-2), the charge and discharge processes of the silver electrode occur in two discrete steps, each with a unique reversible potential. Butler (ref. 3) studied the

---

[1] There is some doubt as to the precise structure of the charged-state compounds.

charging processes at the silver electrode. The initial stage of charge, beginning with a silver electrode containing no silver oxides, was examined at constant potential. After an initial unexplained decrease, the current rose for a brief period. This rise was attributed either to an increase in the effective surface area of the electrode as the solution penetrated the pores of the oxidized surface, or to changes in the overpotential of the electrode engendered by changes in the surface. The rest of the charging process was studied at constant current. The potential rises rapidly at first, leveling off at the plateau voltage corresponding to the production of Ag_2O. At the end of the first plateau, the potential rises again, going through a distinct peak and then falling to a plateau higher than the first, corresponding with the oxidation of monovalent silver oxide (Ag_2O) to divalent silver oxide (AgO). (The intermediate peak between the lower and higher plateaus of the charging curve appears in the charging curves of working cells, and may cause difficulties, since it interferes with charge control.)

Butler summarizes the theories advanced to account for this intermediate peak. The two principal theories are: (1) the high resistance of Ag_2O; and (2) passivation resulting in high-current densities as the last of the available surface silver is oxidized. He suggests studying the effects of surface area to find a resolution between the two theories. Such studies are now being conducted by Blackman and Butler (ref. 4). To elucidate the processes in the alkaline silver electrode, Blackman and Butler (ref. 4) have plotted equipotential maps from which the distribution of current densities across circular electrodes may be determined.

Data on the oxidation and reduction of silver in a potassium-hydroxide solution were obtained by the triangular potentiostatic sweep method, and are presented in reference 5. In this method, a sweep is applied in which voltage is varied with time as a triangular function and the corresponding current is recorded. Peaks in the current plot result from the opposing effects of an increasing rate of electron transfer and a depleting of electroactive species at the electrode surfaces.

The surface area work done by Blackman and Butler (ref. 4) led to studies of electrode gassing on pyrolysis. These studies found that varying amounts of carbon monoxide and carbon dioxide were evolved in oxygen, while ethane and ethylene were evolved in hydrogen. This demonstrates that a carbonaceous deposit is present in commercially prepared sintered silver electrodes, attributed to organic binders used in electrode production. Considerable variability was found in carbon content from plate to plate of a single manufacturer and between different manufacturers.

Experiments with electrodes containing argentic-oxysalt compounds (ref. 6) showed the feasibility of using these compounds which deliver higher half-cell potentials and higher energy densities than AgO. Polarization and temperature-voltage curves were developed. Utilization efficiencies between 94 and 100 percent were found in experimental cells. High polarization losses and somewhat difficult electrode preparation limit the applicability of argentic-oxysalt electrodes. Thermodynamic

and weight comparisons between argentic-oxysalt electrodes and AgO are presented in tables 6-I and 6-II.

TABLE 6-I.—*Thermodynamic Values for Silver Oxides at 25° C*

Reactants	dE/dT, V/°K	Enthalpy, ΔH, kcal	Free energy, ΔF, kcal	Entropy, ΔS, eV
$2[2Ag(AgO_2)_2 \cdot AgNO_3] + 4Zn$	-2.26×10^{-3}	-496.0	-371.2	-83.3
$2(6AgO \cdot AgNO_3) + 2KOH + 6Zn$	1.01×10^{-4}	-434.4	-442.8	28
$2AgO + Zn$	5.70×10^{-5}	-84.8	-85.6	2.68
$7Ag_2O + 7Zn$	-1.69×10^{-4}	-533.4	-518.0	-51.7

TABLE 6-II.—*Molecular Weight—Coulombic Content Equivalent Weight of Silver-Oxygen Compounds*

Compound	Molecular weight	Coulombic content, electrons/ molecule	Open-circuit voltage against Zn anode in 45 percent KOH	Equiva-lent weight, g/eV electrons/ molecule	Coulombic content experi-mentally deter-mined, electrons/ molecule
$2Ag(AgO_2)_2 \cdot AgNO_3$	945.3	17	2.01	55.6	17
$2Ag(AgO_2)_2 \cdot Ag_2SO_4$	1087	18	2.01	60.2	18
$2Ag(AgO_2)_2 \cdot AgSO_4$	979.4	18	----------	54.4	----------
$2Ag(AgO_2)_2 \cdot AgF \cdot HF \cdot 1\frac{1}{2}H_2O$	949.3	17	2.01	55.8	17
AgO	123.9	2	1.85	62.0	2
$2Ag_3O_4 \cdot AgClO_4$	982.8	17	----------	57.8	----------
Ag_2O	231.8	2	1.60	115.9	----------
$6AgO \cdot AgNO_3$	913.3	13	1.60	70.3	15

NEGATIVE ELECTRODE REACTIONS

The reaction occurring at the zinc electrode is

Charged		*Discharged*	
$Zn + 2OH^-$	$=$	$ZnO + H_2O + 2e^-$	(6-3)
or	$Zn + 4OH^-$	$=$	$Zn(OH)_4^- + 2e^-$

$$E_{rev} = 1.22 - \frac{0.059}{2} \log \frac{a_{(ZnOH)_4}}{a^4(OH)^-} \qquad (6\text{-}4)$$

Work is being conducted at Idaho State University (ref. 7) to determine which reaction is valid. As written, reaction equation (6-4) results in a relatively high solubility of the zinc oxidation product in a potassium-hydroxide solution. The zincate then undergoes very slow decomposition

to zinc oxide. This characteristic is a major drawback in the zinc electrode.

The self-discharge reaction of the electrode may be written

$$Zn + 2OH^- + 2H_2O = Zn(OH)_4^{--} + H_2 \qquad (6-5)$$

The reaction proceeds slowly because of the high hydrogen overvoltage on zinc (approximately 0.5 volt). By adding mercury to the negative plate, the overvoltage can be maintained at a high level (ref. 8). Thermodynamic values for the reversible reactions are given in table 6–I.

The solubility of zinc oxide in potassium hydroxide is one of the major limitations to the extended operation of silver-zinc cells. The dissolution and replating of zinc during cycling of cells has been the object of extensive investigation. Through a literature search and experimentation, the Electric Storage Battery Co. (ESB), Raleigh, N.C. (ref. 9), compiled data on the following:

    (1) Conductivity of potassium hydroxide solutions.

    (2) Dissolution of zinc in potassium hydroxide at various temperatures.

    (3) Solubility of zinc oxide in potassium hydroxide as a function of concentration and temperature.

    (4) Solubility of zinc oxide in potassium hydroxide at elevated temperatures.

    (5) Vapor pressure of potassium-hydroxide solutions.

This information is useful in calculating diffusion constants and cell performance, and in optimizing operation under various environmental conditions.

GAS EVOLUTION AND RECOMBINATION

General

Hydrogen and oxygen gas may be evolved in the silver-zinc cell during charge, discharge, and stand. In vented cells (normally found in missile systems and short-duration space applications), the evolution of gases at low rates does not present a serious problem. However, in sealed-cell operation (longer duration space applications, secondary space batteries), the evolution of gas may result in premature cell failure due to case rupture.

Gassing on Charge

When all available active materials have been consumed on charge, the overpotential increases until gassing occurs. In a balanced cell, oxygen is evolved at the silver electrode and hydrogen at the zinc electrode. Since the most common form of cell construction includes an excess of zinc-active material, oxygen is the only gas normally evolved on completion of charge and on overcharge.

The oxygen generated at the silver electrode diffuses to the negative electrode where it combines with metallic zinc to form zinc oxide. On continued charging, this is reconverted to zinc metal. If an equilibrium

is reached between gas generation and recombination rates, no pressure buildup occurs. Dalin et al. (ref. 10) report a recombination rate for oxygen at a rotating electrode, equivalent to 8.4 μA/cm^2.

Any hydrogen generated on overcharge may recombine at an exceedingly low rate (the equivalent of 1.0 μA/cm^2 under ideal conditions at 25° C at an Ag$_2$O electrode). The rate appears to decrease with time. Higher gas-generation rates result in pressure buildup in a sealed cell. Carson et al. (ref. 11) discuss the possibilities of using an auxiliary electrode which can recombine small amounts of hydrogen.

GASSING ON DISCHARGE

Since the silver-zinc system is an extremely efficient electrochemical couple, almost all the stored energy is converted to electrical output and practically no gas is generated on normal discharge. If one cell in a battery is depleted before other cells and is force discharged, hydrogen gas will evolve at the positive electrode. If the overdischarge is continued, the negative electrode eventually becomes depleted and oxygen gas will also evolve. Excessive overdischarging will result in venting or cell case rupture.

GASSING ON STAND

During charged stand, the negative electrode will self-discharge according to equation (6-5), generating hydrogen. Lander and Snyder (ref. 12) observed that the gassing rate varied inversely with electrolyte concentration and the mercuric-oxide content of the negative-electrode material, and directly with temperature. It was also found that saturation of an electrolyte with zinc oxide and amalgamation of the current collector grid had little effect on the gassing rate. To minimize self-discharge at temperatures up to 125° F, use of a 40- to 45-percent potassium-hydroxide electrolyte and between a 2- and 4-percent mercuric-oxide additive in the negative-electrode materials was recommended. (See the section on "Modification of Reaction Chemistry by Additives," below.)

During extended periods of stand, it has been observed (ref. 7) that a decomposition reaction occurs as follows:

$$2AgO = Ag_2O + 1/2O_2 \qquad (6\text{-}6)$$

This reaction proceeds slowly at room temperature and below, and rapidly at 140° C and above.

Dalin et al. (ref. 10) found that silver oxide reacts with the hydrogen generated at the negative electrode during self-discharge. The reaction rate appears to be first order, increasing with temperature. Cells stored at 71° C showed no pressure rise on charged stand, indicating a self-discharge rate equal to or less than the recombination rate for the given electrode construction, cell geometry, and temperature. Additional work using rotating disk and polarographic methods continues to study rates of reaction and reaction order. The usefulness of this recombination process also may be limited by the rate of diffusion of hydrogen through the electrolyte to the silver electrode. In cells operating in a

gravitational field, part of the electrodes may be designed to protrude above the electrolyte, allowing free surface for recombination. In a gravity-free environment, this is not always practical.

Gas evolution or its deleterious effects may be minimized by proper charge-discharge controls, use of electrode additives, auxiliary electrodes, and by proper cell design. Each of these items is discussed in the following sections.

MODIFICATION OF REACTION CHEMISTRY BY ADDITIVES

Materials other than silver-silver oxide, zinc-zinc oxide, and potassium hydroxide have been added to the silver-zinc couple to improve the operating characteristics. In many cases, the exact nature of the interaction between additive and basic material is not clearly understood.

ZINC-ELECTRODE ADDITIVES

The two most common additives to zinc electrodes are a mechanical binder and a self-discharge suppressor. Secondary zinc electrodes are most commonly manufactured in the discharged state; i.e., as powdered zinc oxide, to which is added a mechanical binder for improving mechanical strength. Polyvinyl alcohol (PVA) is the most commonly reported binder (refs. 8, and 13 to 19).

In operation, the zinc electrode undergoes a change in shape caused by solution and reprecipitation of zinc oxide as the cell cycles between charge and discharge. In a gravitational field, the deposits move toward the lower part of the electrode, thickening it, and reducing the total available surface area. Dalin and Sulkes (ref. 20) studied the addition of various binders to the zinc electrode to reduce the rate of this shape-change process. Carboxymethylcellulose, polyvinyl alcohol, and polyethylene oxide used in 1 to 3 percent concentrations of negative mix by weight did not improve cycle life. Polyvinyl alcohol was found to agglomerate with cycling. Carboxymethylcellulose in concentrations above 0.5 percent decreased cycle life by migrating toward the positive electrode, where it reacted with silver oxide to deposit reduced silver on separators. An addition of 1.7 percent Teflon to the zinc-oxide powder was found to double cell-cycle life. A disadvantage of the Teflon additive was that it reduced the oxygen recombination rate by 35 percent on open circuit and by 15 percent on overcharge.

The self-discharge reaction (eq. (6–5)) is suppressed by raising the hydrogen overvoltage through the addition of mercury (normally as mercuric oxide added to the zinc-oxide powder). However, it was found (ref. 21) that mercuric oxide will adversely affect the performance of heat-sterilized cells. (See section entitled "Heat Sterilizable Cases," below.)

The Electric Storage Battery Co. (ref. 21) claims a reduction in the amount of gas generated by the negative electrode through the addition of an unspecified compound (code no. 323–43), found to withstand heat sterilization without adversely affecting cell performance.

The addition of mercury to the zinc electrode has also been used to control the growth of zinc dendrites (long needles of zinc growing through

the separator causing short circuits).   (See the section on "Electrode Degradation Processes," below.)

SILVER ELECTRODE ADDITIVES

The addition of palladium (1 percent by weight) to the silver electrode of cells specifically designed for heat sterilization (ref. 13) minimized the 50-percent loss in capacity resulting from the presence of separator degradation products.   However, cells containing palladium exhibited poor stand life.   Lander (ref. 22) reports that palladium increases the monovalent (lower) silver plateau to about 50 percent of charge time in contrast to the 5 to 20 percent normally expected, and reduces polarization on charge at low temperature (15° F) improving discharge voltage. The mechanism by which palladium improves reversibility is not understood.

Cadmium was added to the silver electrode to promote gassing protection in the event of cell reversal.   Cadmium acts to combine the oxygen gas evolved at the zinc electrode, thereby limiting gas-pressure buildup in sealed cells (ref. 10).

ELECTROLYTE ADDITIVES

The most common additive to the potassium-hydroxide electrolyte is zinc oxide.   Zinc oxide forms the zincate ion $(Zn(OH)_4^-)$ in caustic solution.   Normally, sufficient zinc oxide is added to saturate the potassium hydroxide.   The addition of zincate ion permits operation at higher current densities because of diffusion phenomena occurring between the electrode-electrolyte interface and the bulk electrolyte.   A good discussion of the mechanism is presented by Shaw (ref. 2).

ELECTRODE DEGRADATION PROCESSES

Three processes other than gas evolution have been identified as being responsible for the deterioration in performance of the silver-zinc cells.   The electrode shape-change phenomenon involves a redistribution of the active material of the negative or zinc electrode, with a consequent change in current density, and an increase in polarization, thereby decreasing performance.   This was discussed under "Electrode Additives."

Oxides of silver have been shown to dissolve in the electrolyte, forming argentate ions, which, upon contact with the zinc electrode, deposit metallic silver on the zinc.   This forms a shorted zinc-silver cell, which then evolves hydrogen gas from the zinc electrode.

An empirical approach to the prevention of silver deposition on the zinc electrode, used by most battery manufacturers, is the interposition between silver and zinc electrodes of layers of separator designed to prevent the dissolved silver compounds from reaching the negative electrode.   Usually, these consist of layers of cellulose or cellulose derivatives which react with the silver compounds, reducing them to metallic silver.   The cellulose is oxidized in the process.   A more detailed discussion will be found in the section titled "Separator."

One of the major failure modes in the silver-zinc cell is the development of short circuits as a result of the growth of zinc dendrites which penetrate the separator. Dendrite growth through cellulosic separators occurs by electrodeposition within the membrane rather than by mechanical perforation. Thus, a separator which resists zincate diffusion would limit dendrite growth.

Stachurski, Dalin, and McBreen (refs. 23 to 28), Arouet and Blurton (ref. 29), and Oxley (refs. 30 and 31) studied zinc-electrode performance under varying charge rates to develop methods and processes for improving the life of silver-zinc cells. Stachurski's work was theoretical in nature, resulting in the derivation of a diffusion equation. Limited experimentation was conducted using a rotating electrode and a specially constructed dendrite growth-studying apparatus. Stachurski's later work investigated the electrode-electrolyte-separator interface and zinc growth into and through the separator. The work of Arouet and Blurton and the earlier work by Oxley was empirical, and placed considerable emphasis on half-cell experiments under varying conditions.

It was found that the growth of zinc dendrites through the separator material occurs by the following mechanism:

During charge, zinc is deposited on the negative electrode in various forms, depending on temperature, overvoltage, and current density.

At low overvoltages (approximately 20 millivolts), a fine filament or mossy growth with a density 2 to 8 percent that of solid zinc is formed. Measurement of the filament surface area by the double-layer capacitance method indicates that a zinc-hydroxide film covers most of the filament surface. Growth occurs mainly at the ends of the filament, with the rate of solution and deposition being equal along the filament body.

When the overvoltage is increased to approximately 100 millivolts, elongated, branched, and hexagonal dendrite crystals form. Over 100 millivolts, the separator limits growth and the dendrite growth fills in the space between electrode and separator, forming a heavy sponge which appears nodular.

Completely smooth deposits were obtained using rotating-disk electrodes (resulting in a high Reynolds number for convection of electrolyte past the electrode) at overvoltages below 150 millivolts.

Polarization curves indicate that mossy growths form at potentials where activation polarization controls the plating reaction, while dendrites form at potentials where diffusion limitation starts.

Stachurski developed a theory to account for the changing zinc deposits. At low overpotential (below 100 to 150 millivolts), zincate can diffuse readily to regions near the ends of filaments, but is exhausted before it can penetrate the moss. Thus, deposition is activation controlled at the filament tips and diffusion controlled within the mossy region. In intermediate region near the filament tips, deposition is both activation and diffusion controlled.

When the overvoltage is raised above the critical value of 100 to 150 millivolts, the intermediate region disappears because the deposition rate at the filament tips increases. The diffusion layer moves out beyond the

plane of the filament tips and the entire deposit becomes diffusion controlled, causing a change from mossy to dendritic form.

Arouet, Blurton, and Oxley (refs. 29 to 31) studied deposition at various current densities and temperatures and found that deposition above a critical current is diffusion controlled. Under diffusion-controlled conditions, the initial deposit appears compact but additional deposition is dendritic. Figure 6-1 shows the empirically derived relationship between current density, temperature, and deposit morphology. This work also established the adherence of zinc deposits at various current densities, charge methods, temperatures, and electrolyte additive. The experimental results are plotted parametrically as percentage of adherent deposit versus total deposit (expressed as coulombs/centimeter^2).
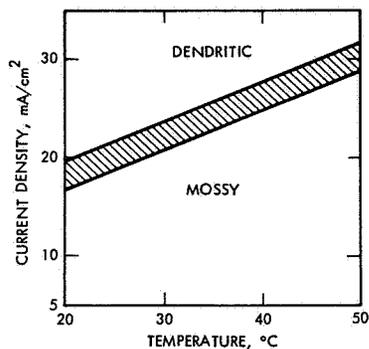

FIGURE 6-1.—Variation of critical current density (shaded area) with temperature within experimental limits.

Examination of the data shows that intermittent charging, low temperature (25° C), high-current density, and the presence of lead ions in the electrolyte favor adherent deposits of zinc. These plots are discussed at length in reference 32.

Recommendations to minimize dendrite growth are as follows:

(1) Electrolyte volume should be minimal.

(2) Zinc electrodes should be framed in a nonporous insulating material if fast charging is desired.

(3) Small amounts of lead should be added to the zinc electrode or to the electrolyte.

(4) The battery should be charged by a pulsed dc current with a sufficiently long offtime to allow zincate ions to diffuse to the electrode surface. Current density for charging should be as high as possible without permitting diffusion control.

Stachurski (ref. 25) used the deposition theories to explain cell-capacity degradation by loss of active material from the negative electrode.

He noted that the overvoltage in the galvanostatic charging of a plate which has lost active material is greater than expected from the decreased geometric area. The following process was presented in explanation. A minor decrease occurs in surface area by active material loss. This results in an increase in current density, which in turn causes an increase in overpotential. Conversion from mossy to dendritic deposits occurs as a result of the higher overpotential. This in turn leads to further loss of surface area, and the process snowballs.

The work completed to date offers an understanding of zinc-electrode processes. To apply these experimental results to practical cells requires additional work. In their final report (ref. 29), Arouet and Blurton recommend additional studies on silver-zinc batteries. Both fundamental and applied work are necessary for a fuller understanding of the negative electrode.

In an attempt to reduce the rate of dendrite growth (a principal mode of premature cell failure), electrodes have been amalgamated using a mercuric-chloride and potassium-bromide solution (ref. 30). As a result, the dendrite growth rate was reduced a small degree; however, those dendrites which did form tended to be thicker and more numerous. This reduces cycle life because of an increased incidence of short circuits. On discharge, thicker dendrites are harder to dissolve, increasing the likelihood of early failure by puncturing the separator.

The following electrolyte additives are thought to be preferentially adsorbed on dendrites:

 (1) Tetramethyl ammonium-hydroxide pentahydrate
 (2) Tin as Sn^{++}
 (3) Thiourea
 (4) Ethylenediamine

The beneficial effects of preferential adsorption on surface protrusions (dendrites) is the inhibition of further growth at these points. At present, there are no conclusive results except that tin (as Sn^{++}) appears to be promising in minimizing dendrite growth.

The following electrolyte additives have been tested (ref. 19) and found to have no effect on extending useful cell life:

 (1) Kaolin
 (2) Polyethylene oxide
 (3) Lithium hydroxide
 (4) Polyvinyl acetate (PVA)

Sodium silicate was found to be detrimental. Aluminum hydroxide may improve capacity retention over extended cycling. In heat-sterilized cells (ref. 13), aluminum hydroxide did not appear to improve performance.

STRUCTURES

GENERAL

Silver-zinc batteries may be divided into two broad categories: primary and secondary. Primary batteries are those used for one, or at the most, two discharges. A primary battery is often manufactured in

the dry-charged condition and electrolyte is added just prior to use. Such batteries are extensively used in launch-vehicle applications, but have only limited use in space vehicles.

A secondary silver-zinc battery may be recharged a number of times. The available cycle life is limited by design parameters. Secondary batteries are manufactured either vented or sealed. Space application of vented-cell batteries is limited to short-mission times. A pressurized and sealed canister is used to maintain a suitable environmental pressure higher than the electrolyte vapor pressure. Missile and booster vehicle primary batteries are commonly made from vented cells in a sealed canister, and may be automatically activated.

Sealed rechargeable silver-zinc cells and batteries have the greatest potential for space applications. Most of this discussion is directed toward sealed secondary silver-zinc cells.

CELL GEOMETRY

A detailed description of cell geometry may be found in chapter 2. Silver-zinc cells have been produced in prismatic, button, and spirally wound cylindrical shape. The most common shape is the prismatic.

Recently, a cylindrical cell was developed in an attempt to produce a heat-sterilizable battery. This cell uses a formed ceramic-cup separator in a concentric cylindrical structure similar to that of a Leclanche cell with a cylindrical silver cathode, powdered zinc anode, and stainless-steel canister (ref. 33). The design is not suitable for high-rate applications.

The dry-tape cell is a recent, novel approach to primary construction. A silver-zinc cell was constructed using a silver-peroxide-impregnated tape, an electrolyte-impregnated tape, and a zinc-block electrode. The tapes are kept separate until used and are driven by an electric or spring-wound motor. The dry-tape concept is discussed in detail in chapter 10.

AUTOMATICALLY ACTIVATED SILVER-ZINC BATTERIES

Silver-zinc batteries for primary, high-rate discharge applications are frequently designed with separate electrolyte reservoirs. In the dry state, the batteries have long storage lives. When the electrolyte is transferred from the reservoir to the cells through a distributing manifold, the battery is ready to operate within seconds. Pressure for the electrolyte transfer or activation process is usually provided by a pyrotechnic gas generator which is ignited remotely by an electric current pulse. In low-temperature environments, the heat generated by the pyrotechnic device may be used to warm the electrolyte.

MATERIALS AND METHODS OF CONSTRUCTION

SILVER ELECTRODE

Early silver electrodes, made of pressed, dry silver powder, were weak and performed poorly. The development of the pasting and sintering processes improved this cell.

Pasting is a popular method of silver-electrode construction today. A paste is made from silver or silver oxide and water, and a binder. This is spread over either a silver or nickel grid or molded into sheets, then pressed into the grid. The pasted plates are then sintered, during which the silver oxide is converted by thermal decomposition to silver, and organic additives are burned off. For primary-cell usage, the plates are charged in formation tanks against inert counterelectrodes. Grid thickness, silver density, and plate thickness are varied to suit the intended usage. The effect of varying these parameters will be discussed under the section on "Electrical Characteristics."

A recently developed dry process lends itself to continuous operation. A continuous strip of silver grid is coated with a water solution of carboxymethylcellulose (CMC), after which silver-oxide powder is pressed onto the grid. The strip is then punched to size. Apparently, the CMC results in good adhesion between the grid and powder. This method is best suited for primary batteries. No direct comparisons were made between wet-pasted and sintered electrodes (ref. 34).

Current collection from sintered-silver electrodes is normally accomplished by coining an area of the sintered plate and spot welding a silver strip or wire lead. On pasted plates, connection is made by spot welding or twisting the lead to the supporting grid.

Charkey and Goodkin (ref. 35) observed that cells subjected to low-rate discharges (c/8–c/80), followed by reasonably high-rate (c/8) charges, undergo severe capacity loss. The problem was isolated to the silver electrode. The electrode surface area, as measured by the double-layer capacitance (DLC) and BET nitrogen adsorption methods, was sharply reduced on low-rate discharge, and it was postulated that a slow plating of silver from solution during the reduction of Ag_2O to Ag was responsible for an increased crystallite size and a reduced active surface area. Placing a highly absorbent material against the positive electrode and incorporating inert materials into the electrode were found to improve performance. The additive, usually magnesium oxide, is gradually dissolved out, ultimately losing its effect. The inert additives are thought to aid in maintaining small crystallite size and increase the active surface area by dissolving to form new pores in the electrode.

ZINC ELECTRODE

Zinc electrodes may be made by pasting a mixture of zinc and potassium hydroxide onto a metal grid. Such electrodes are fragile. Present production methods commonly dry-press a mixture of zinc oxide, binder, and additives onto a grid placed in a mold conforming to the plate dimensions. Often, a loosely woven support fabric is pressed into the plate at the same time.

Another method of plate manufacture, most often used for primary cells, is electrodepositing zinc onto a suitable support, then rolling or pressing the plate to the required thickness. Connection to electrodes is similar to that made for positive plates—either with a welded strip or with a mechanically fastened wire. Plate thickness and porosity (or

density) are related to performance. This will be discussed under the section on "Electrical Characteristics."

AUXILIARY ELECTRODES

Auxiliary electrodes have been used in experimental sealed silver-zinc cells to control internal gas pressure. The principal use of auxiliary electrodes is hydrogen recombination. Without auxiliary means, hydrogen recombination proceeds slowly at the silver electrode, whereas oxygen combination at the zinc electrode proceeds somewhat more rapidly.

Carson et al., in a compendium (ref. 37), developed several auxiliary electrodes and methods of construction. Cell-test results to date are inconclusive and work is continuing. The primary concern in using auxiliary electrodes is the poisoning of the zinc electrodes by the catalyst (usually platinum). Tests indicate that problems are minimal.

Hydrogen-recombination electrodes connected to the positive electrodes have taken the form of small electrodes placed at the cell pack top (in the airspace) or at the side or edge of the cell pack, suitably placed to avoid flooding the electrode with an electrolyte. A recombination rate of up to 50 mA/cm^2 is possible. Operating temperatures to 110° C are possible, but life is shortened above 65° C. Performance at 0° C is about 60 percent of performance at room temperature.

The use of auxiliary electrodes for recombination permits operation of the silver-zinc cell at a continuous overcharge without undue pressure buildup. In practice, however, continuous overcharge is avoided because the separator and electrodes are degraded. In space applications, particularly on short-orbit regimes where some overcharge may occur, the auxiliary electrode may prove useful for internal cell pressure control.

For proper operation, the auxiliary electrode must be wetted and in electrolytic contact with the cell pack. However, if flooding occurs, the electrode will not operate efficiently. In space applications, it is necessary to design cells with a minimum amount of electrolyte and highly absorbent separators to allow gas to reach the auxiliary electrodes.

SEPARATOR

The separator in a silver-zinc cell must—

(1) Provide strong mechanical separation between the positive and negative electrodes.

(2) Prevent migration of particles and dissolved silver compounds between the positive and negative electrodes.

(3) Have minimum resistance to the flow of electrolyte and ions.

(4) Be wetted easily by the electrolyte and maintain sufficient electrolyte contact with the electrodes to permit current flow.

(5) Provide minimal degradation of the separator (degradation products should not interfere with cell operation over the anticipated temperature range).

(6) Have sufficient mechanical strength so that no damage will occur during handling and cell assembly.

(7) Be dimensionally stable.

There are three broad categories of separators: cellulosics, noncellulosic synthetic materials, and inorganic separators. Separators may serve specialized functions as silver-migration limiters, zinc-penetration limiters, and electrolyte absorbers. To establish the merit of any candidate separator material, a series of tests (often called screening tests) is conducted to determine the separator value in relation to established materials in use. A good summary of screening methods is contained in reference 38.

SEPARATOR APPLICATION

Separators normally are combined to make use of the best properties of more than one type. One of the most common separator combinations consists of layers of cellulosic or low-resistivity synthetic material, separated from the positive electrode by one or more layers of highly absorbent synthetic separator capable of withstanding oxidation by silver oxides. The separator layers closest to the negative are usually of cellulose or sausage casing, which are both relatively resistant to zinc-dendrite growth. This combination was found most effective in references 15 to 19.

Hennigan (ref. 39) has collected information on test cells, conducted at NASA Goddard Space Flight Center and elsewhere, evaluating separator improvements made by ESB and by the Borden Co. Comparison of test results from various sources is difficult because of construction differences (electrode area, particularly). The data are scattered and the need for more uniform materials was emphasized.

SEPARATOR PROPERTIES

Separator properties are often reported qualitatively. It is impossible now to correlate data presented by the various sources. This does not mean that one data source is superior to any other, but rather that each researcher has chosen test conditions and methods which differ in some respect from those used by others. Tests are often selected which show a particular separator in its best light. No mutually agreed upon (standard) set of test methods exist (although the Cooper and Fleischer methods are a good start). If standard test methods for direct comparison of separator materials existed, the battery designer could then select the best material, based on interpretation of uniform test results. Some representative properties for typical separators are presented with each particular report summary. Descriptions of the separator are presented with test results or qualitative statements regarding separator utility.

The ESB Norberg Research Center (ref. 40) has conducted screening tests on about 40 separator materials. This is expected to reduce the need for extended testing in experimental cells. The most useful tests were measurements of rate of silver reaction and diffusion, rate of zinc-dendrite growth, and electrical resistivity. A few representative test results are presented in table 6-III.

Test results indicate that the effectiveness of a separator in preventing silver diffusion is a function of its reactivity with silver. Materials which resist oxidation allow diffusion. Small pore diameter does not

TABLE 6-III.—*Properties of Separator Materials*

Source	Material description	Oxidation loss in KMnO₄, 25° C, percent	Percent weight loss, 50° C	Tensile strength, dry thickness			Spec. res., ohm-cm	Average pore diam., A	Tort. factor	A Wet thickness, cm×10⁻⁴	B Zn penetration time, min	Ratio, B/A, min/cm×10⁻⁴
				In.	Dry	Wet						
224 1	Cello PUDO (300) (Du P)	69	-----	0.001	20 000	6 000	8.5	200	2.6	71	117	1.6
2	Cello PUDO (600) (Du P)	63	75	.0016	17 000	5 300	8.4	400	2.5	102	158	1.6
7	Sausage casing (Avisco)						7.4	450	2.1	216	1336	6.2
										178	207	1.1
8	Fibrous sausage casing (Avisco)		38	.0035	14 570	6 800	8.2	450	2.1	178	425	2.4
9	Silvered S.C. (Avisco)			.0031	17 750	9 350	5.9	200	1.9	214	1242	5.8
10	Permion 300 (RAI)		23	.0011	12 330	6 300	34.8	75	7.5	36	117	3.2
11	Permion 600 (RAI)		41	.0015	9 550	5 430	38.6	80	5.5	79	158	2.0
14	Polypore WA (Niemand Bros.)			.0031	15 660	12 750						•
15	PMA 80/20		10				63.5	300	4.7			
16	PMA 83/17		10				39.6	350	5.4	152	367	2.4
17	PMA 95/5		10				22.3	300	3.2	191	190	1.0
18	Mipor 12 CN (medium porosity)		1.2	.0048	840	840						
19	Mipor 13 CN (high porosity)		.8	.0048	520	520						
20	Mipor 34 CN (high porosity, true pore)		1.5	.0038	1 180	1 180				147	64	.4
21	Mipor 34 PN (high porosity, coarse pore)		.9	.0060	1 330	1 330						
22	Cello 111-1 (Du P) (experimental)	32		.0012	20 000	6 670						
23	Cello 111-2 (Du P) (experimental)	60		.0012	14 570	6 800	10.0	240	2.6	76	261	3.4
24	FSC (Visking)		38									
25	Cello PUDO 300 + m-phenylene diamine		0				7.8	110	2.4	64	135	2.1
26	Acropar WZ (Gelman Instr.)					3 200	11.0		2.7	127	26	.1
27	Cello PUDO 300 + tolylene diisocyanate									97	118	1.2
28	PUDO 300 + hydroquinone									79	120	1.5
29	PUDO 300 + Zn₂									79	139	1.8
30	C-19-300 (Yec)						8.3	460	2.8	79	153	1.9
31	C-19-600 (Yec)						8.5	400	2.6	114	310	2.8
33	Permion 1000 (RAI): 15 m		19									
	40 m		8							76	84	1.1
39	Cello PUDO 300 (20.3% glycenol)									58	63	1.1

appear to prevent diffusion. Pore diameter appeared to have a relationship to the ability of a separator to resist zinc penetration, but this relationship did not hold in all cases.

Regenerated cellulose appeared to be the material with greatest resistance to silver migration. Migration is arrested by reaction with silver compounds, but the cellulose is consumed in the progress. Addition of antioxidants (*m*-phenylene diamine and diisocyanates) to cellulose also appears promising.

Cellulose sausage casing appeared to be the most effective material in stopping zinc penetration when placed with its smooth side facing the zinc electrode.

The Norberg Research Center separator evaluations used many of the test procedures discussed in Cooper and Fleischer (ref. 38). Data are not reported for all tests with each separator type tested; thus complete comparison of all materials tested is not possible.

CASES

Three types of cases (often referred to as cell jars) are used. These are plastic, metal, and a combination of plastic and metal. Any case used on sealed silver-zinc cells must be resistant to chemical attack from silver oxide (a powerful oxidizer) and concentrated potassium hydroxide; must contain any internal pressure generated; and must maintain structural integrity throughout the anticipated environmental range. Table 6–IV presents the advantages and disadvantages of the three case materials.

TABLE 6–IV.—*Characteristics of Cell Case Types (Ref. 1)*

Type	Advantages	Disadvantages
Plastic_____	No potential on case. Corrosion resistant.	Strength. Crazing. Heat transfer. Sealing of cover to case. Terminal seal. Shock sensitive. Temperature limitations.
Metal (stainless steel)___	Strength. Heat transfer. Sealing cover to case (welding). Acts as pressure vessel (in cylindrical cells). Temperature range. Shock resistant.	Potential on case (must insulate case from battery container). Requires insulated terminals.
Combination outer metal case and inner plastic case.	No potential on outer case. Strength. Temperature range. Shock resistant. Provides additional terminal seal.	Difficult inner seal.

PLASTIC CASES

The majority of silver-zinc cells are produced with plastic cases. The plastic normally used is an acrilonitrile-styrene copolymer. This material is relatively clear (for observation of cell interior) and can be easily sealed by solvent cement, catalyzed cement, or epoxy.

White cycolac (T2502) acrylonitrile-butadiene-styrene (ABS) polymer was used successfully in a sealed-cell design. ABS was chosen because it is nonmagnetic, easily sealed, inert to attack by electrolyte, and strong enough to support the expected internal pressures anticipated (ref. 41).

SEALING

For space applications, a sealed cell may be defined as one in which neither gas or liquid leaks can be detected at measurable rates. Sealing thus prevents drying out of an electrolyte, particularly during overcharge, and maintains electrode balance by containing any gases evolved.

The typical plastic case silver-zinc cell will have two seals: one at the case-to-cover closure, and the other at the terminal-to-cover interface. The case-to-cover plastic-to-plastic seal is commonly made with solvent or catalyzed cement, epoxy cement, or by heat welding.

Terminal seals have been a major problem. Early seals were plastic or rubber under compression, and leaked because of extrusion of the sealing material. The use of epoxies and integrally molded terminals have reduced sealing problems somewhat.

Another method used for sealing cells and batteries is potting or encapsulation. The battery is cast into a solid block of epoxy resin, with the electrical and control leads emerging through a hermetically sealed connector. This approach results in heavy batteries, and has been supplanted by more sophisticated sealing methods (ref. 1).

HEAT STERILIZATION OF SILVER-ZINC BATTERIES

The major obstacle to the heat sterilization of silver-zinc batteries is the rapid reactivity of the separator with the electrolyte and/or electrode materials at elevated temperatures. Sterilization of silver-zinc cells in the charged or partly charged state has been unsuccessful because of the increase in the rate of reaction between dissolved silver compounds and the cellulosic separator materials. Most of the work in sterilizing these cells has been done in the development of new and more resistant separator materials. These must be capable of withstanding a temperature of 135° to 145° C for more than 60 hours without excessive deterioration. A more complete description of requirements and tests may be found in reference 42.

Bogner (ref. 13) indicates that heat sterilization of discharged zinc electrodes is feasible. However, it was found that a polyvinyl alcohol (PVA) binder caused pressure buildup during sterilization. Subsequent tests indicate that equivalent performance could be obtained from electrodes without PVA binder. In addition, it was noted that Viscon paper wrap contributed slightly to pressure buildup with only slight degradation.

Cells containing mercuric oxide in the negative electrode suffered permanent capacity losses on sterilization. Examination of the positive electrodes revealed that mercury compounds had dissolved in the electrolyte and migrated from the negative to the positive electrode. On charge, the mercury converted to mercuric oxide which plugged the porous silver-electrode structure (refs. 9, 21, and 43).

HEAT-STERILIZABLE CASES

Sterilization temperatures of 135° to 145° C are too severe for most common plastics which lose their physical strength at about 100° C. Five materials have been found suitable for heat-sterilizable cells. These materials are polysulfone (PS), polyphenylene oxide (PPO), Celcon acetyl copolymer, Zytel high-temperature nylon, and Penton chlorinated polyether. Fluorocarbons are sufficiently stable at high temperatures, but present severe fabricating and sealing problems; thus, these materials have not been given serious consideration.

Bogner (ref. 13) evaluated nylon, Penton, and Celcon under controlled conditions and in a cell environment. He found that Penton was slightly attacked (surface crazing) by electrolyte, but Zytel-38 nylon and Celcon were not attacked. The liquor from controlled sterilization testing of each material, when used for activation of test-cell components, had no effect on cell performance.

HEAT-STERILIZABLE SEALS

The high-temperature plastics used for encasing sterilizable cells present sealing problems. Most of these materials are inert to common solvents used in solvent cements. In addition to the high sterilization temperature, the seal must withstand any internal pressure generated during sterilization. In the absence of gassing, sterilizable cells will generate an internal pressure of at least 30 psi because of the vapor pressure of potassium-hydroxide solution (40 percent) at 145° C.

Bogner (ref. 13) produced usable seals in Zytel-38 cell cases. The best cover-to-case seal used an 88-percent aqueous phenol cement. Heat sealing, epoxy, and a combination nylon-solvent cement all proved ineffective. A tight fit and application of uniform pressure during bonding was needed for a good seal.

Terminal-to-cover seals were made by molding a pin into the cover. Nylon, Zytel-38, was found to provide the best seal. Nylon filled with glass fibers, and Celcon and Penton were weaker than unfilled nylon. The poor performance of Celcon and Penton may have been due, in part, to the use of a mold and design optimized for nylon.

ESB Norberg Research Center (ref. 21), working with polyphenylene oxide 531-801, found that Dow epoxy DEN 438-EK85 with a DMP 30 catalyst made a satisfactory seal. Solvent sealing was found to cause crazing and hot-gas welding did not produce a good seal.

Himy (ref. 33) reported some encouraging results for ultrasonic and hot-gas welding of polysulfone and polyphenylene-oxide cases. In addition, limited success was obtained with BR-92 (American Cyan-

amid) and Allbond (Allaco) epoxies. Since the work was on a limited scale, no definite conclusions were reached.

There appears to be a need for additional work to develop a suitable sealing method for the case-to-cover seal in heat-sterilizable cells. Most programs have attempted to use existing designs rather than optimizing the joint to be sealed for material, temperature, and sealing method.

Bogner (ref. 13) tested several separator materials. Fibrous sausage casing No.7 (Union Carbide), Permion 600 (RAI), and Dynel (Kendall Co.) were tested. Each separator was sterilized in potassium hydroxide and the liquor used to activate fresh silver-zinc cells. Comparison was made between controls and the cells with degradation products in the electrolyte.

The three materials tested were fragile after sterilization. Degradation products had the following results on cell performance:

Material	Voltage	Capacity
Permion	Equal to control	20 percent loss.
Dynel	No Ag^{2+} voltage	Little effect.
Fibrous sausage casing	Poor	Poor.

An ammoniacal odor was detected in the degradation products of Permion and Dynel. Tests of an electrolyte containing ammonia resulted in poor cell performance.

Improved separators were also tested. Screening tests (resistivity, silver diffusion, zinc penetration, and dimensional stability in potassium hydroxide) gave little indication of ability to withstand heat sterilization. The following results were obtained from controlled cell experiments:

Material	Performance after sterilization
Teflon with acrylic acid graft	Early shorting.
Teflon with methacrylic acid graft	Early shorting.
Teflon with sulfonated styrene graft	Too brittle for cell assembly.
Crosslinked high-density polyethylene with—	
Acrylic acid graft	Better than controls.
Methacrylic acid graft	Better than controls.

Radiation Applications, Inc. (RAI) (ref. 44), prepared various crosslinked polyethylene-acrylic acid-grafted separators by crosslinking with electron beam irradiation or divinyl benzene and cobalt-60 irradiation. Previous crosslinked separators were degraded by sterilization and the degradation products adversely affected cell performance. Candidate separator samples were tested for resistivity, dimensional change in caustic, initial exchange capacity (a measure of grafting and crosslink), and performance in cells. All acceptable samples had a high degree of crosslinking and a high level of acrylic acid graft.

The best separator materials had the following properties:

Sample designation	Thickness, cm		AC resistance, ohm-cm	Tensile strength, psi
	Dry	Wet		
116	0.035	0.038	76–100	800–1800
110	.035	.043	40–55	800–1100

These separator materials appear most promising.

The preparation of grafted and crosslinked polymers presents special problems in process and quality control. Because the processes are sensitive to minor variations in control parameters, careful control of these variables is essential to the uniformity of the product. Southwest Research Institute's (SWRI) (ref. 45) attempts at producing Radiation Applications, Inc., 116 by chemical synthesis led to nonuniform products as a result of the lack of process control and facilities to evaluate product variability (ref. 45). Lockheed-Georgia (ref. 46) successfully prepared RAI 116 separator material, varying their process until an infrared spectroscope pattern of the product material matched that of an original sample provided by RAI. The two materials also matched in performance.

ESB Norberg Research Center (refs. 9, 21, and 43) is currently testing heat-sterilized cells with RAI and SWRI separator materials. Preliminary test results indicate that higher poststerilization pressures are developed with the RAI 116 chemically crosslinked separator than with the RAI 110 radiation crosslinked separator. The SWRI material is presently being evaluated.

The Narmco Division of Whittaker Corp. (ref. 47) is presently working on aliphatic polyalkylenebenzimidazoles which possess most of the properties necessary for a heat-sterilizable silver-zinc battery separator. Some surface modifications are being made by attachment of carboxyl groups to improve the materials.

ELECTRICAL CHARACTERISTICS

The electrical characteristics of the silver-zinc cell are similar to those of the silver-cadmium cell, except that the voltage is higher in the silver-zinc cell. They combine the characteristics of the silver electrode with those of the zinc electrode, which, in spite of its solubility problems, is electrochemically reversible. See chapter 5 for a description of the general shape and characteristics of the charge and discharge curves of silver-zinc and silver-cadmium cells.

The open-circuit potentials of the upper and lower plateaus of the silver-zinc cell are 1.86 volts and 1.60 volts, respectively.

DISCHARGE CHARACTERISTICS

Such data as are available in the literature are usually reported as plots of cell voltage as a function of capacity delivered or of time. Figures 6–2 and 6–3 represent typical data. From these data current-voltage curves can be constructed with temperature and state of charge as additional variables, as shown in chapter 3. Knowing either cell capacity or electrode area, the current scale may be normalized with rated or measured capacity, or reduced to current density.

The electrical characteristics of silver-zinc batteries vary considerably, depending upon the structure of the electrodes, the number of layers and type of materials used in the separator, the concentration of KOH in the electrolyte, and other factors. As an example of the extent to
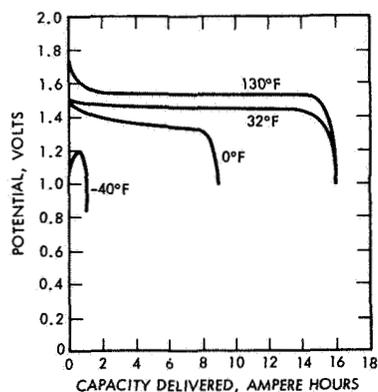
FIGURE 6-2.—Typical 40-hour rate
discharge curves, temperature as a
third variable.

which this variation can be carried, typical characteristics of low-rate
secondary cells and high-rate primary cells are presented.

Discharge data taken by Bogner (ref. 13) were used to prepare three
parametric plots of current density as a function of voltage at various
states of discharge for an experimental secondary cell.

Figures 6-4, 6-5, and 6-6 present these parametric plots at 0°, 25°,
and 38° C, respectively. Voltage varies inversely with current density
and directly with temperature and depth of discharge. The exception
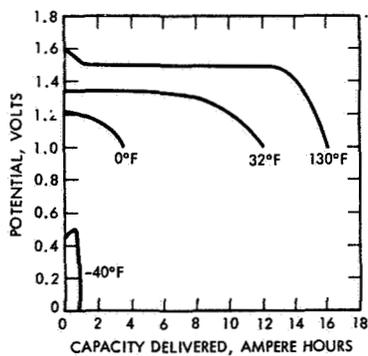
FIGURE 6-3.—Typical 6-hour rate
discharge curves, temperature as a
third variable.
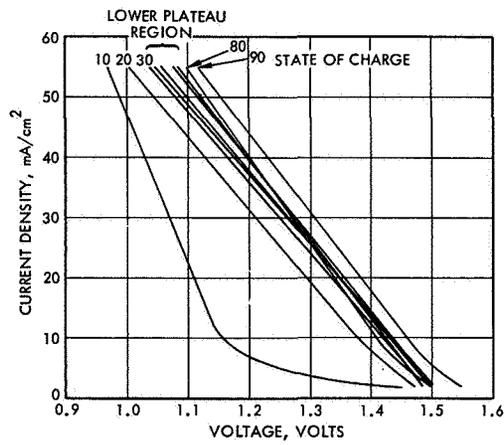
FIGURE 6–4.—Current density versus voltage, 55-A-h Delco-Remy experimental cells at 0° C, state of charge as third variable. NOTE.—Data smoothed, unknown number of measurements, positive electrode thickness 0.073 in., separator —positive wrap, 3-layer fibrous sausage casing, 45 percent KOH.
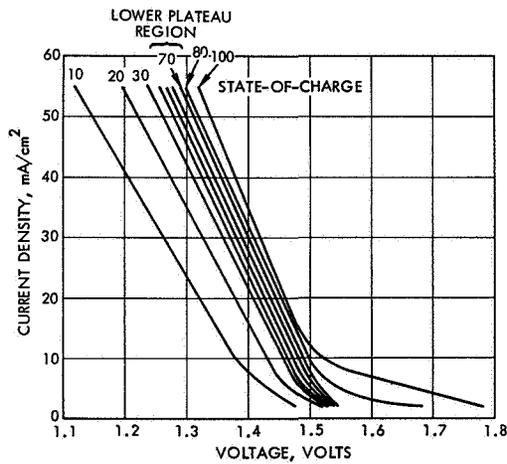
FIGURE 6–5.—Current density versus voltage, 55-A-h Delco-Remy experimental cells at 25° C, state of charge as third variable. NOTE.—Data smoothed, unknown number of measurements, positive plate thickness 0.073 in., separator— positive wrap, 3-layer fibrous sausage casing, 45 percent KOH.
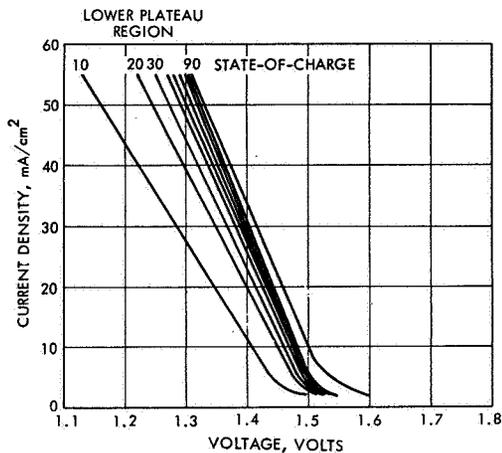
FIGURE 6–6.—Current density versus voltage, 55-A-h Delco-Remy experimental cells at 38° C, state of charge as third variable. NOTE.— Data smoothed, unknown number of measurements, positive plate thickness 0.073 in., separator—positive wrap, 3-layer fibrous sausage casing, 45 percent KOH.

to these rules may be seen on the 0° C plot where constant depth of discharge lines cross. This phenomenon, called "the dip," is observed during constant-current discharges, and is due to competition between cell polarization and internal heating. It is represented by region D of figure 5–1. At lower temperatures (below 20° C) and higher current densities (above 40 mA/cm²), the electrodes polarize and the voltage drops. Because of the polarization and internal resistance losses, considerable heat is generated which raises the cell temperature, and the cell voltage rises. At discharges of 40 mA/cm², cell internal temperature may rise as much as 15° C.

These data may be compared with figure 6–7, in which similar typical data are plotted for a high-rate primary cell. The curves of figure 6–7 are composites of data from various sources, and must be considered approximations.

VARIATION IN PERFORMANCE WITH STRUCTURAL CHANGES

Considerable study has been given the effect of various structural and composition changes upon cell performance. Most of these investigations have concentrated on the separator.

The porosity of the silver electrode will affect cell performance. As porosity (and hence actual surface area) increases, a point is reached at which such increases reduce the quantity of active materials so that capacity is reduced. Figure 6–8 shows the effects of positive electrode porosity (or density) on charge capacity at the 3- and 16-hour rates.
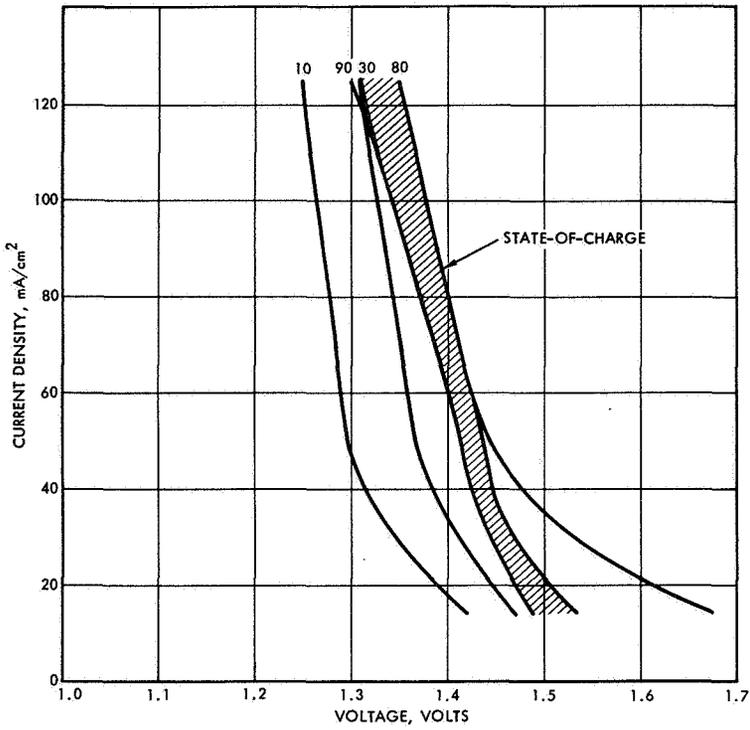
FIGURE 6-7.—Estimated current density versus voltage, 20-A-h primary cells at 25° C, state of charge as third variable.
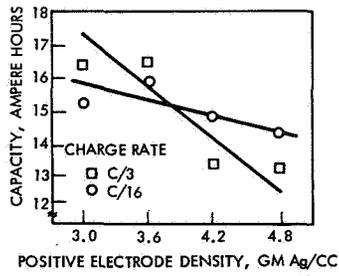

FIGURE 6-8.—Effect of silver-electrode porosity upon cell performance.

The effect of electrode density at higher currents (and hence current densities) is greater as seen by the steeper slope at the 3-hour charge rate.

Zinc-electrode porosity will affect cell performance to a large extent, particularly in high-rate applications. Figure 6-9 (ref. 48) shows the variation of capacity and average ampere-hour efficiency with porosity.
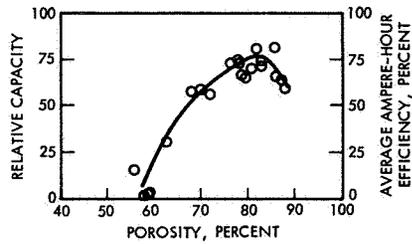
FIGURE 6-9.—Effect of zinc-electrode porosity on capacity and efficiency, 20° C, 40 percent KOH, 730 mA/cm².

The separator system used in a silver-zinc cell has a marked effect on discharge voltage; the effect becomes more severe at high discharge current densities. Cell voltage varies with the resistivity of the separator material used. Figure 6-10 illustrates the change in cell voltage with increasing layers of cellophane separator material. At a discharge rate of 120 mA/cm², voltage decreases 200 millivolts per layer of separator.
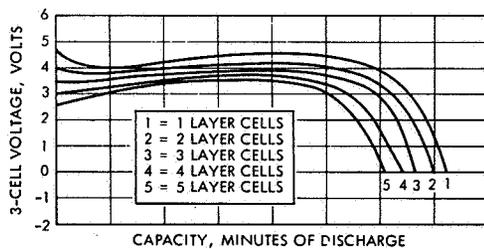
FIGURE 6-10.—Effect of semipermeable membrane layers on discharge voltage.

FACTORS AFFECTING CELL PERFORMANCE

Temperature affects battery charge and discharge characteristics. Figures 6-4, 6-5, and 6-6 illustrate the rapid deterioration of capacity with decreasing temperature at several discharge rates. By comparison of figure 6-5 with figure 6-4, it can be seen that at high rates, low-temperature electrical performance suffers more than at lower rates.

The variation of total energy yield as a function of temperature at various current densities is graphically illustrated in figure 6-11. Energy yield is a maximum at approximately 70° F, because at lower tempera-
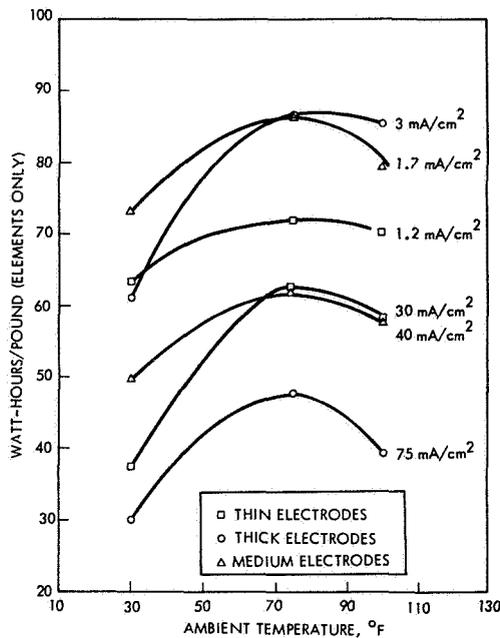
Figure 6-11.—Effects of current density, temperature, and electrode thickness upon cell performance.

tures output voltage is lower due to high polarization losses, and at higher temperatures the small increase in output voltage is offset by a loss of the peroxide portion of the discharge curve (particularly after a period of stand at higher temperature where self-discharge is appreciable).

Efficiency

The ampere-hour efficiency of the silver-zinc system (defined as A-h output/A-h input) under normal operating conditions is close to 100 percent. The watt-hour efficiency (W-h output/W-h input) is about 70 percent under normal conditions because of the difference between the charge and discharge polarization potentials. Charging silver electrodes at high rates (65 to 105 mA/in.^{2}) may result in an ampere-hour efficiency below the normally expected 100 percent.

Dirkse offered three explanations for this lowered efficiency (ref. 49):

(1) The electrode accepts charge, but on discharge, pockets of Ag_2O are left because of favorable current paths being set up (more active areas). Butler found that discharged silver plates appear to be preferentially discharged in the vicinity of grid wires and discontinuities, and at points of stress. In addition, growth of reduced areas seems to occur at the silver oxide-silver interface. These studies are continuing and may yield some understanding about favorable current paths (ref. 50).

(2) A side reaction may occur in which oxygen is formed and sub-
sequently absorbed or recombined.

(3) Some silver oxides are lost by dissolving in the electrolyte
and by reaction with separator. Except at very high temperatures, this
cannot account for more than a very small capacity loss.

Rhyne (ref. 8) reported relative ampere-hour efficiencies (100 percent
being defined as the ampere-hour capacity of a cell with electrolyte ratio
of 0.6 discharged at 1.0 ampere at 75° F) as a function of electrolyte
volume ratio, mercuric oxide content of negative, cell-fit ratio, and
material ratio. This definition of efficiency does not agree with preceding
definitions (ch. 2), and is not comparable with them. Rhyne defines
efficiency as a material utilization fraction based upon an empirical
standard.

WET STAND

During stand periods, activated silver-zinc cells lose energy by self-
discharge as represented by equations (6-5) and (6-6). Since divalent
silver is converted to monovalent, the duration of the upper plateau
decreases. In primary-cell designs, where the cells are not designed
for long stand times, voltage may be seriously affected by stand time.

Where stand times are short, and the electrolyte has not had sufficient
time to penetrate the separator completely, low voltages may occur as
a result of high internal resistance.

Hawkins (refs. 14, 19, and 51) investigated the effect upon wet-stand
time of several different separator combinations in a silver-zinc cell
designed for high-rate applications and limited cycle life, but activated
stand in excess of 2 months.

Figure 6-12 (ref. 14) shows the variation of electrical characteristics
as a function of stand time. The low initial voltage is due to a combina-
tion of poor penetration of the electrolyte into the separator, and low
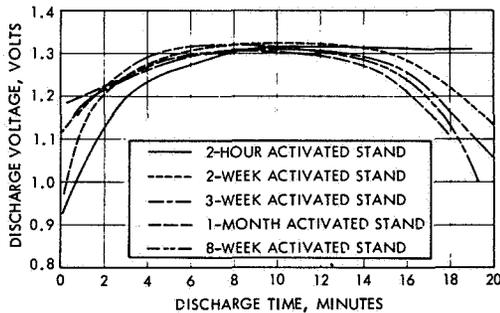
FIGURE 6-12.—Primary zinc-silver-oxide stand
characteristics discharged at 0.8 A/in.²

starting temperature. As the cell discharges, the electrolyte penetrates
the separator and electrodes, and the cell heats internally, increasing
voltage output. The effects of stand time are not entirely consistent,
suggesting that other experimental variables may be affecting electrical

characteristics. Hawkins concluded (ref. 51) that the interposition of a porous layer of inert material between the silver electrode and the cellulose membrane extended the life of the cell, and at the same time added moderate recharge capabilities.

Wylie (ref. 52) reported variation in capacity retention on 160° F wet stand with various separator systems. Table 6–V presents the test results. The shorting failure mechanism is not discussed.

IMPEDANCE

Impedance of silver-zinc cells and batteries is not often reported. The lack of data is due to the difficulty of obtaining repeatable measurements. No adequate impedance data as a function of frequency or of state of charge were found. A discussion of the factors affecting impedance of both silver-zinc and silver-cadmium cells will be found in chapter 5.

PRESSURE EFFECTS

Internal cell pressure does not appreciably affect the electrical performance of a silver-zinc cell. Structural damage may result from excessive pressure buildup.

HEAT GENERATION

Heat effects in silver-zinc batteries are similar to those in silver-cadmium batteries, and are discussed in chapter 5.

OVERCHARGE ACCEPTANCE

The overcharge acceptance of sealed silver-zinc cells is generally conceded to be poor. However, in space-probe operations, a sealed silver-zinc battery is often used in an overcharge mode during the cruise portion of flight. Cells specifically designed for extended overcharge have been developed for this application. Rhyne (ref. 8) developed a sealed silver-zinc cell capable of continuous overcharge for at least 15 days at the 200-hour rate (equivalent to 0.05 mA/cm^2). Pressure buildup with 2 percent mercuric oxide in the negative electrode mix was approximately 10 psig at 140° F. At room temperature there was no pressure buildup. Average float voltage of these cells is shown in figure 6–13. As temperature is increased, float voltage decreases.
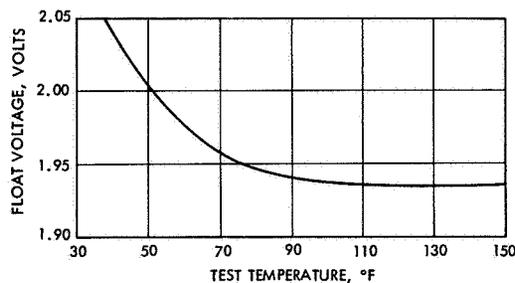

FIGURE 6–13.—Average float voltage of SSC–43C
cells as a function of temperature.

TABLE 6–V.—*Stand Life and Capacity Retention at High Temperature*
(Ref. 52)

Separator system (listed from positive to negative)	Time at 160° F, days	Number of cells	Percent capacity retention	
			Positive	Negative
1 layer 0.008″ Synpor_____	14	9	74–77_____	65–83
2 layers 300 PUD–0 cellophane____	29	6	47–53_____	50–76
	42	1	48_____	46
2 layers 0.008″ Synpor_____	3	9	Shorted____	_____
2 layers 0.008″ Synpor_____	14	3	69–71_____	53–70
2 layers 300 PUD–0 cellophane____	28	3	52_____	60
	42	2	50_____	50
	28	1	Shorted____	_____
1 layer 0.008″ Synpor_____	10	9	Shorted____	_____
1 layer 100–0 PMA_____	_____	_____	_____	_____
1 layer 0.008″ Synpor_____	14	3	60–68_____	65–68
2 layers 100–0 PMA_____	24	3	64–65_____	57
2 layers 300 PUD–0 cellophane___	42	2	46–48_____	*0–45
	4	1	Shorted____	_____
Polypor WA on Saran_____	8–10	2	Shorted____	_____
2 layers 300 PUD–0 cellophane____	_____	_____	_____	_____
1 layer EM 309 Dynel_____	3– 7	12	Shorted____	_____
1 layer Polypor WA on 0.005″ nylon_____	_____	_____	_____	_____
2 layers 300 PUD–0 cellophane___	_____	_____	_____	_____
1 layer EM 309 Dynel_____	6– 8	3	Shorted____	_____
1 layer 0.009″ Porothene_____	_____	_____	_____	_____
2 layers 300 PUD–0 cellophane___	_____	_____	_____	_____
1 layer EM 309 Dynel_____	7–10	3	Shorted____	_____
1 layer 0.007″ PMA 100–1_____	14	1	78_____	83
2 layers 300 PUD–0 cellophane___	_____	_____	_____	_____
1 layer EM 309 Dynel_____	14	3	77_____	81
1 layer 0.008″ Synpor_____	29	3	52_____	58
2 layers 300 PUD–0 cellophane___	_____	_____	_____	_____
2 layers RAI polyethylene_____	29	2	50_____	45
2 layers 300 PUD–0 cellophane___	42	2	22_____	18

*One of these cells dried out on storage and the negative plates may have burned up.

Rhyne concludes that a relationship exists between capacity, cell pressure, and concentration of mercuric oxide originally in the negative mix. It is quite possible that capacity and pressure buildup are related, but at best it can be a tenuous second-order relationship. The work of Lander and Snyder (see section titled "Gas Evolution and Recombination," above) clearly indicates the relationship between gas evolution and mercuric oxide concentration.

Grun (refs. 53 and 54), working to the same basic cell requirements as Rhyne, developed a sealed silver-zinc cell capable of operating on continuous overcharge. A cell operating at 0.02 mA/cm² developed a maximum pressure of 36 psig at 140° F and 13 psig at 70° F. Problems were encountered in battery potting at 140° F. Capacity variation (a fair indication of product control) varied from ±3.5 percent on the best design to ±25 percent on the poorest design for five-cell samples.

Electric Storage Battery Co. (refs. 55 to 57) developed several cell types for use on the Mariner program, requiring a battery to withstand at least 14 days of continuous overcharge. Cells, operated at overcharge rates from 0.1 mA/cm² to 1 mA/cm², performed satisfactorily on controlled tests. A small number of cells short circuited after more than 20 days of overcharge. In tests using a spacecraft-charge simulator, however, high pressures were encountered in one or more cells, necessitating premature termination of tests. On repeated tests it was noted that a cell which had developed high pressure on one cycle would not necessarily be the pressure-limiting cell on the next cycle. Mechanical and materials problems seemed to be more difficult to solve than electrochemical problems.

Frank and Strier (ref. 58) utilized a small fuel cell to recombine gases evolved on extended overcharge of sealed silver-zinc cells. Pressure rise in cells with fuel cells was limited to 10-psig maximum, while a single test, using a standard silver-zinc cell with pressure gage attached, showed a pressure in excess of 15 psig. No comparison was attempted between sealed cells equipped with fuel cells and properly designed sealed silver-zinc cells on extended cycling regimes. The small fuel cell seems to offer a unique method for limiting pressure rise in sealed cells on extended overcharge. However, this advantage must be weighed against the added problems of supplying hydrogen and oxygen to the fuel cells.

Service Life

Service life is affected by separator system, depth of discharge, temperature, and electrolyte concentration. Battery degradation, and thus service life, starts when electrolyte is added. Deterioration of separator and dissolution of the negative electrode begin immediately and continue with time, regardless of cycle life, until end-of-service life.

Numerous reports contain data on capacity versus cycle life, but compilation of this mass of information into parametric form has not been possible because of the large number of uncontrolled variables in each test. Presently, the only practical way to determine cycle life or service

life for a particular application is to actually simulate the time, temperature, and load profiles experienced with a sufficient number of cells or batteries to establish a reliability figure.

Lander (ref. 22) reported life in a simulated 2-hour orbit regime as a function of several variables in cell structure, composition, and operation. Figure 6–14 presents the variation of cycle life with two selected variables.
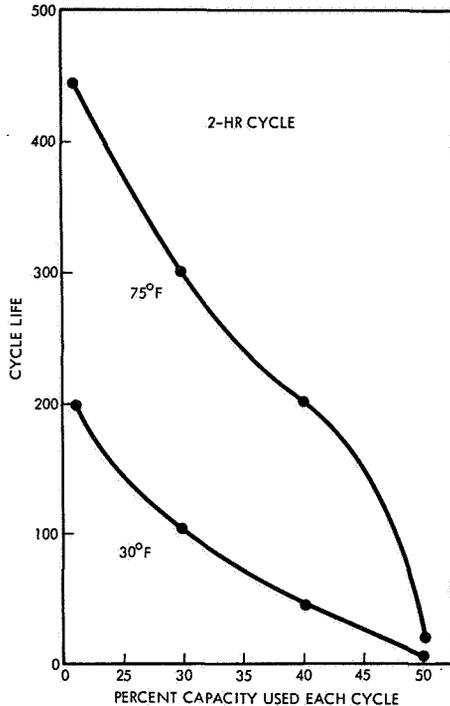

FIGURE 6–14.—Cycle-life performance, effect of depth of discharge, and temperature.

This chart shows decreasing cycle life with increasing depth of discharge and decreasing temperature, although, because of the 2-hour cycle, both charge and discharge currents are varied simultaneously with depth of discharge, and the independent effects of neither can be determined. Other similar data show decreasing cycle life with increasing zinc electrode HgO content, decreasing ratio of ZnO to silver, and decreasing concentration of KOH in the electrolyte solution (fig. 6–15).

A typical analysis of separator for the variation of cycle life with separator characteristics was prepared by Hoyt and Pfluger (ref. 59). Plots were prepared of capacity in ampere-hours (for a particular temperature, discharge rate, and an end-of-discharge voltage) as a function of the number of cycles prior to failure. Separator materials which per-
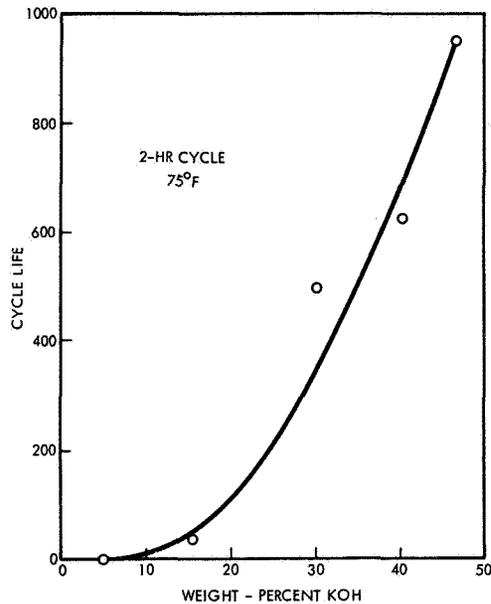
FIGURE 6-15.—Effect of electrolyte concen-
tration.

mitted early shorting or rapid loss of capacity were considered poor
candidates for use in cells. Variations in separator resistivity affect
cell-output voltage, so that separator systems with high resistivity will
compare poorly in this test with low-resistivity systems. Nevertheless,
cells employing high-resistivity separators are valuable in applications
such as in interplanetary space probes, where discharge rates are low
and long life is important.

CHARGE CONTROLS

Brooke (ref. 60) described several charge methods that were con-
sidered for battery charging in the Mariner II spacecraft. Constant
current charging with automatic (or ground-controlled) start-and-stop
action was rejected because of available power limitations and because
malfunction could possibly occur in the start-or-stop circuitry which
would result in battery depletion or severe overcharge.

Constant potential charging was also considered, but was rejected
because of limitations in the power available for charging. The final
charger was of the modified constant potential type consisting of a voltage
regulator and current limiter in series with the battery. Figure 6–16
shows the charger-operating limits for an 18-cell silver-zinc battery.
The upper limit is the boundary of maximum available power and maxi-
mum acceptable voltage; the lower limit line represents the minimum
current-voltage relationship to assure a fully charged battery. No
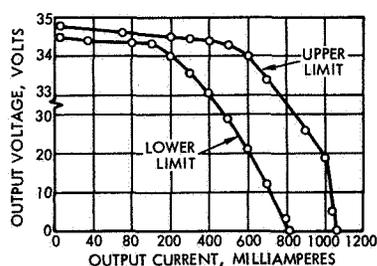
FIGURE 6-16.—Mariner II flight
charger characteristics.

consideration is reported of compensation of charge characteristics for charging temperature.

To prevent premature battery failure, two basic constraints must be imposed during charging of silver-zinc batteries. The polarization of the zinc electrode must be limited to less than 100 millivolts to avoid formation of zinc dendrites. The voltage must be limited to a value of approximately 1.96 volts per cell at room temperature to avoid generation of excessive quantities of O_2 gas. This value should probably be compensated for temperature unless the required range of operating temperature is narrow. After the cell has been fully charged, if its use is not anticipated for a long period of time, charging should be terminated, if possible, and the cell returned to charge from a few hours to a day prior to expected use.

FAILURE ANALYSIS

Failure analysis of silver-zinc cells is difficult because subtle failure patterns and incipient failure are not readily observed. Visible shorts due to separator failure or negative electrode "shape change" can be identified as causes of failure.

Brooke (ref. 60) described the failure analysis of Mariner II batteries in qualitative terms. A decision to increase the separator system, from four turns of cellophane to five turns, was based upon the general appearance of the separator and upon presence of shorted plates after laboratory operation of cells.

Lander (ref. 61) described a failure analysis technique used in examining silver-zinc cells. A failed cell is charged and where possible discharged, including a brief high-rate pulse to determine internal resistance. The discharged cell is opened, the free electrolyte drained out, and the quantity is measured. A sample of the free electrolyte is retained for determination of carbonate content, caustic concentration, and foreign materials.

The electrode assembly is extracted from the case and examined for mechanical failures. A visual examination is made for zinc at the tops and edges of the separator wrap. Where possible, the separator is removed layer by layer from the electrodes and visually examined for

the presence of metallic zinc between separator layers. Samples of the separator, analyzed layer by layer for silver content and their resistance, are measured.

The silver electrode is examined visually for color (zinc oxide imparts a pinkish cast to the plate). Optionally, it may also be weighed and subjected to X-ray or controlled discharge against inert counterelectrodes. The zinc electrode is visually examined for "shape change" and degree of oxidation, is weighed, and is analyzed for silver and foreign materials. The negative current collector grid is examined for the presence of mercury. A cross section of the electrode may be taken by potting in an epoxy resin, sectioning, and polishing.

CORRELATION OF FAILURE ANALYSIS WITH OPERATING VARIABLES

The literature surveyed contained few failure analyses and little effort has been made to correlate failure analysis information with operating variables. Correlation is difficult because of the difficulty in separating the effects of operating variables and because of the limited number of observations available to any single researcher.

Hennigan (ref. 39) has correlated qualitative failure analyses during controlled separator evaluation testing to determine the superiority of one separator over another. Hennigan noted, however, that the unpredictable performance of cells with cellulosic separators created a problem in evaluating typical cell performance.

PRESSURE BUILDUP

Excessive overcharge or overdischarge can result in pressure buildup in silver-zinc cells.

SILVER ELECTRODE

Charkey and Goodkin (ref. 35) studied the capacity loss of cells on low-rate discharge, high-rate charge regimes, and found a reduction of the measurable actual silver-electrode surface area. It was postulated that a slow plating of silver from solution during the reduction of silver peroxide to silver was responsible for the formation of larger crystallites with low surface area.

MECHANICAL

One of the most common mechanical problems in silver-zinc cells is electrolyte or gas leakage around terminals. Particularly in sealed applications, leakage at any point can cause failures. In the case of electrolyte leakage, it is possible to have current leakage paths from cell to cell, resulting in slow capacity loss or catastrophic failure, depending upon the conductivity.

Puncture of separator by electrode grid wires sometimes occurs. By careful vendor inspection, assembly procedures, and acceptance testing, such faults are normally found and eliminated from use in flight cells and batteries.

Poor cement joints at the cell cover to case seal often result in gas or electrolyte leakage. By careful assembly and inspection, most poor

cement joints are rejected at the vendor.   If the cement joint is marginal and is a stress concentration point, however, it is possible, when using a brittle cement, to have failed cement joints after exposure to service environments.

Separator deterioration, due to hydrolysis and oxidation by the silver electrode, perforation of the separator by zinc dendrites, and changes in the shape and surface of the zinc electrode because of solution of zinc oxide in the electrolyte, are all common wearout modes.   These have already been discussed.

Dry-Tape Discharge Characteristics

A unique concept for the development of achievement of high-energy density through storage of active materials and electrolyte in dry-tape form was applied to silver-zinc batteries (ref. 62).   The dry-tape concept is discussed in detail in chapter 10.   In this concept, fresh materials are constantly being added to the cell as it discharges, and the cell takes on the characteristics of a fuel cell.   Consequently, the electrical characteristics of this type of cell are not directly comparable with those of an ordinary cell.

INORGANIC SEPARATOR CELLS

The Astropower Laboratory, Douglas Aircraft Co., has developed experimental cells using a proprietary ceramic separator material stable in KOH solutions at relatively high temperatures.   Separator materials, in the form of a ceramic powder, are milled with a binder, pressed in a die, and sintered in a furnace to form a permeable disk or sheet.   Details of preparation of the proprietary separator, such as composition, compaction pressure, sintering conditions, etc., are not given.

The ceramic separator has proven to be resistant to deterioration in high-temperature KOH electrolyte solutions, and open experimental Ag-Zn cells containing a single pair of electrodes separated by the inorganic separator have survived for more than 1500 cycles of operation at 100° C.

Multiplate cells have been made, in which the separators are cemented into grooves in a plastic retainer.   Control over electrode thickness was maintained to 0.001 inch to maintain tight packing of the electrodes between the separator sheets.   Cells of this type have survived vibration to 5 g, shock (level unreported), acceleration (level unreported), and acoustic noise (148 decibels) without major failure, although leakage of the bunsen-valve closure and cracking of the epoxy seals was observed. The effect of environmental exposure upon electrical performance was not evaluated due to manufacturing defects in both test cells and controls which resulted in excessive gas evolution from the zinc electrodes.

Sterilization of the cells at 145° C was attempted, in the discharged condition, but the electrodes dried out at these temperatures.

The primary obstacle to good performance at 100° C appears to be the loss of oxygen from the silver electrode.   In vented cells, this leads

to loss of capacity. In sealed cells, it would lead to high-pressure performance and ultimate cell failure due to case rupture. In one case, pressure rose above 30 psi in 9 hours of cycling.

Arrance et al. (ref. 63) reported discharge and charge characteristics of silver-zinc cells with ceramic inorganic separator material. Operating characteristics at 25° and 100° C show a deterioration in voltage as a function of cycling. However, valid performance comparisons between inorganic separator cells and conventional separator cells cannot be made because of a lack of sufficient data for preparation of voltage-current density plots.

ELECTROLYTE RESERVOIRS

The silver-zinc cell requires a maximum amount of electrolyte in contact with the electrodes during charge and discharge operation and a minimum amount of electrolyte during overcharge. During overcharge, excess electrolyte can reduce gas recombination. Work is currently in progress (refs. 64 to 66) by Chreitzberg and Cushing to develop a bellows device for control of cell electrolyte level. During discharge and charge, the bellows would be inflated, forcing electrolyte into the cell from a reservoir; during overcharge the bellows would be collapsed to return any excess electrolyte to the reservoir. Test results are not yet available for evaluation.

A bellows arrangement would probably require a gravity environment to operate successfully, limiting the general applicability of the technique. In addition, some external source of gas pressure would be required for operation.

ENVIRONMENTAL FACTORS

RADIATION

Nicholson, Recht, Argue, and Kelchner (refs. 67 to 70) are investigating the effects of radiation on silver-zinc cells. The radiation levels simulate those encountered in space applications due to cosmic rays and the Van Allen radiation field. Cells irradiated to 7.2×10^7 and 9.8×10^7 rad were dissected and analyzed.

Early results showed considerable scatter of cell performance data. Improvements in capacity and gas collection measurement equipment reduced the data scatter. Irradiation increased the amount of silver flaking off the electrode by a factor of approximately 2. Pressure buildup in irradiated cells was significantly higher than in controlled cells. The pressure was due to hydrogen evolution and a mechanism was proposed. Capacity changes in irradiated cells did not follow any pattern. Any changes were attributed to electrochemical variation rather than irradiation.

Additional work is planned to study radiation effects at differing depths of discharge and higher radiation levels. Improvement in analysis techniques is expected to result in meaningful relationships between radiation and zinc-electrode performance and gas evolution.

HIGH IMPACT

The Voyager interplanetary probe has created a need for a battery capable of withstanding hard landings without affecting electrical performance. J. L. Adams (ref. 71) tested silver-zinc and silver-cadmium cells at impact levels from 1800- to 11 600-g peak shock. Results indicate that cells can withstand shocks of up to 5000 g at velocities of about 160 ft/sec. At higher shock and velocity conditions, cases cracked, plates shifted or crumpled, and internal shorting occurred. Several standard production models (sample size appears to be limited to one cell of any particular manufacturer at a given condition) survived shocks at 10 000-g peak and velocities of 170 ft/sec.

ESB is developing a heat-sterilizable sealed cell capable of withstanding a shock level of 5000-g peak from a velocity of 110 ft/sec and an additional requirement of 10 000-g peak from a velocity of 180 ft/sec. Three designs were tested in each of three orthogonal directions. Deterioration of voltage underload was the primary criterion for internal damage. Some of the more common failure modes encountered were:

    (1) Cell case wall cracks at corners.
    (2) Epoxy bond between cell cover and jar sheared.
    (3) Positive and negative support struts broke in tension.
    (4) Separator was creased and cut slightly at bottom of U-folds.
    (5) Silver sheet electrode tabs failed in compression.

Electrode damage varied with thickness. Thin plates wrinkled, while heavier plates lost considerable active material by flaking.

An improved design cell is presently under construction and will be tested. Modifications such as electrode support frame, support struts, plate lead wires, separator, and cell-jar design have been incorporated.

REFERENCES

1. FRANCIS, H. T.: Space Batteries. Technology Handbook, Armour Research Foundation, 1964. (Available as NASA SP-5004, N64-18052.)
2. SHAW, M.: Fundamentals of Electrochemistry as Applied to Battery Technology. Rept. no. 3106, Whittaker Corp., Dec. 1964.
3. BUTLER, E. A.: Studies of Reaction Geometry in Oxidation and Reduction of the Alkaline Silver Electrode. Final Report on Jet Propulsion Laboratory Contract no. JPL 951157, Reorder no. 66-259, Chem. Dept., Brigham Young Univ. (Provo, Utah), Apr. 1966.
4. BLACKMAN, A. U.; AND BUTLER, E. A.: Reaction Geometry in Oxidation and Reduction of the Alkaline Silver Electrode. Third Quarterly Report on Jet Propulsion Laboratory Contract no. 951554, Chem. Dept., Brigham Young Univ. (Provo, Utah), Jan. 10, 1967. (Available as NASA N65-17972.)
5. McCLELLAND, D. H.; AND SHAW, M.: Study of the Silver Oxide Electrode by Potentiostatic Sweep. Abstract No. 12, presented at the fall meeting of the Electrochem. Soc. (Buffalo, N.Y.), Oct. 10-14, 1965.
6. LEIBECKI, H. F.: Argentic Oxysalt Electrodes. Rept. no. TN D 3208, Lewis Research Center, Jan. 1966.
7. ARCAND, G. M.: The Reactions Pertaining to Zinc-Silver and Cadmium-Silver Batteries. First Quarterly Report on Jet Propulsion Laboratory Contract

no. 951458, Idaho State Univ., Chem. Dept., May 17, 1966. (Available as NASA CR-76047, N66-29755.)

8. RHYNE, J. W.: Development of Sealed Secondary Silver-Oxide Zinc Battery. Final Report on Jet Propulsion Laboratory Contract no. 950811, Rept. no. 64-674, Whittaker Corp., Power Sources Division (Denver, Colo.), Dec. 31, 1964.

9. BODAMER, G. W.: Heat Sterilizable, Impact Resistant Cell Development. First Annual Report on Jet Propulsion Laboratory Contract no. 951296, Sept. 24, 1965, to Dec. 31, 1966, Rept. no. 67-218, Electric Storage Battery Co., Carl F. Norberg Research Center (Yardley, Pa.), Apr. 21, 1967.

10. DALIN, G. A.; STACHURSKI, Z.; AND SULKES, M.: Sealed Silver-Zinc Batteries. Paper presented at the 18th Annual Power Sources Conference (Fort Monmouth, N.J.), May 19-21, 1964, p. 54.

11. CARSON, W. N., JR.; CONSIGLIO, J. A.; AND MARR, J. W.: Study of the Use of Auxiliary Electrodes in Silver Cells. Final Report of Goddard Space Flight Center Contract no. NAS 5-3669, General Electric Co., Advanced Technology Laboratories (Schenectady, N.Y.), Mar. 1966. (Available as NASA CR-405, N66-18430.)

12. LANDER, J. J.; AND SNYDER, R. N.: Rate of Hydrogen Evolution of Zinc Electrodes in Alkaline Solutions. Electrochem. Tech., vol. 3, no. 5-6, 1965, p. 161.

13. BOGNER, R. S.: Heat Sterilizable Silver-Zinc Battery Investigation. Final Report on Jet Propulsion Laboratory Contract no. 950364, General Motors Corp., Delco-Remy Division (Anderson, Ind.), Mar. 15, 1965. (Available as NASA CR-63597, N65-27367.)

14. HAWKINS, B. R.: Investigations Leading to the Development of a Primary Zinc-Silver Oxide Battery of Improved Performance Characteristics. Final Report no. 1 on Marshall Space Flight Center Contract no. NAS 8-5493, July 1, 1963, to June 29, 1964, Rept. no. CPB 13-1600-63, Eagle-Picher Co. (Joplin, Mo.), July 31, 1964. (Available as NASA CR-59627, N65-12500.)

15. HAWKINS, B. R.: Investigation Leading to the Development of a Primary Zinc-Silver Oxide Battery of Improved Performance Characteristics. First Summary Report on Marshall Space Flight Center Contract no. NAS 8-5493, July 1 to Dec. 31, 1963, Eagle-Picher Co. (Joplin, Mo.). No date. (Available as NASA CR-56363, N64-24032.)

16. HAWKINS, B. R.: Investigations Leading to the Development of a Primary Zinc-Silver Oxide Battery of Improved Performance Characteristics. Second Summary Report on Marshall Space Flight Center Contract no. NAS 8-5493, Jan. 1 to Mar. 31, 1964, Eagle-Picher Co. (Joplin, Mo.), Apr. 30, 1964. (Available as NASA CR-56077, N64-20645.)

17. HAWKINS, B. R.: Investigations Leading to the Development of a Primary Zinc-Silver Oxide Battery of Improved Performance Characteristics. Third Summary Report on Marshall Space Flight Center Contract no. NAS 8-5493, July 1 to Sept. 30, 1964, Eagle-Picher Co. (Joplin, Mo.), Oct. 31, 1964. (Available as NASA CR-59623, N65-12499.)

18. ANON.: Investigations Leading to the Development of a Primary Zinc-Silver Oxide Battery of Improved Performance Characteristics. Sixth Quarterly Report on Marshall Space Flight Center Contract no. NAS 8-5493, Oct. 1 to Dec. 31, 1964, Eagle-Picher Co. (Joplin, Mo.). No date. (Available as NASA CR-64592, N65-33127.)

19. ANON.: Investigations Leading to the Development of a Primary Zinc-Silver Oxide Battery of Improved Performance Characteristics. Seventh Quarterly Report on Marshall Space Flight Center Contract no. NAS 8-5493, Jan. 1 to Mar. 31, 1965, Eagle-Picher Co. (Joplin, Mo.), 1965. (Available as NASA CR-64223, N65-30542.)

20. DALIN, G. A.; AND SULKES, M.: Sealed Zinc-Silver Oxide Batteries, Part I. Paper presented at the 19th Annual Power Sources Conference (Fort Monmouth, N.J.), May 18-20, 1965, p. 69.

21. BODAMER, G. W.: Heat Sterilizable, Impact Resistant Cell Development. Second Quarterly Report on Jet Propulsion Laboratory Contract no. 951296, Apr. 1 to June 30, 1967, Electric Storage Battery Co., Carl F. Norberg Research Center (Yardley, Pa.), Aug. 1, 1967.

22. LANDER, J. J.: Sealed Silver-Zinc Batteries. AIAA No. 64-749. Presented at the Third Biennial Aerospace Power Systems Conference (Philadelphia, Pa.), Sept. 1-4, 1964.

23. STACHURSKI, Z. O. J.: Investigation and Improvement of Zinc Electrodes for Electrochemical Cells. Third Quarterly Report on Goddard Space Flight Center Contract no. NAS 5-3873, Jan. 1 to Mar. 31, 1965, Rept. no. 556-65, Yardney Electric Co. (New York), July 1, 1965.

24. DALIN, G. A.; AND STACHURSKI, Z.: Abstract No. 246, On the Mechanism of Penetration of Separators by Zinc Growth. Presented at spring meeting, Electrochem. Soc. (San Francisco, Calif.), May 9-13, 1965.

25. STACHURSKI, Z.: Investigation and Improvement of Zinc Electrodes for Electrochemical Cells. Final Report on Goddard Space Flight Center Contract no. NAS 5-3873, Rept. no. 617-65, Yardney Electric Co. (New York), Dec. 1965.

26. STACHURSKI, Z. O. J.: Study To Investigate and Improve the Zinc Electrode for Spacecraft Electrochemical Cells. First Quarterly Report on Goddard Space Flight Center Contract no. NAS 5-10231, Aug. 1 to Oct. 31, 1966, Yardney Electric Co. (New York), June 1967.

27. McBREEN, J.: Study To Investigate and Improve the Zinc Electrode for Spacecraft Electrochemical Cells. Second Quarterly Report on Goddard Space Flight Center Contract no. NAS 5-10231, Nov. 1, 1966, to Jan. 31, 1967, Yardney Electric Co. (New York), June 1967.

28. McBREEN, J.: Study To Investigate and Improve the Zinc Electrode for Spacecraft Electrochemical Cells. Third Quarterly Report on Goddard Space Flight Center Contract no. NAS 5-10231, Feb. 1 to Apr. 30, 1967, Yardney Electric Co. (New York). No date.

29. AROUET, S.; AND BLURTON, K. F.: The Improvement of Zinc Electrodes for Electrochemical Cells. Final Report on Goddard Space Flight Center Contract no. NAS 5-9591, June 3, 1965, to Oct. 31, 1966, Leesona Moos Laboratories (Great Neck, N.Y.). No date.

30. OXLEY, J. E.: The Improvement of Zinc Electrodes for Electrochemical Cells. Final Report on Goddard Space Flight Center Contract no. NAS 5-3908, June 12, 1964, to Mar. 24, 1965, Leesona Moos Laboratories (Great Neck, N.Y.), July 1965.

31. OXLEY, J. E.: The Improvement of Zinc Electrodes for Electrochemical Cells. Miscellaneous Report on Goddard Space Flight Center Contract no. NAS 5-3908, Leesona Moos Laboratories (Great Neck, N.Y.), Feb. 1966. (Available as NASA CR-377, N66-15794.)

32. HOYT, H. E.; AND PFLUGER, H. L.: Improved Separators for Silver Oxide-Zinc and Silver Oxide-Cadmium Cells for Spacecraft. First Quarterly Report (Mod 6) on Goddard Space Flight Center Contract no. NAS 5-9107, The Borden Chemical Co., Central Research Laboratory (Philadelphia, Pa.). No date.

33. HIMY, A.: Development of One Ampere-Hour Heat Sterilizable Silver-Zinc Cell. Final Report on Ames Research Center Contract no. NAS 2-3819,

Period Ending June 1967, Rept. no. SM-49109-F, Douglas Aircraft Co., Inc., Astropower Laboratory (Newport Beach, Calif.), July 1967. (Available as NASA CR-73110.)

34. WILBURN, N. T.: Dry Process Electrodes for Zinc-Silver Oxide Batteries. Paper presented at the 19th Annual Power Sources Conference (Fort Monmouth, N.J.), May 18-20, 1965.

35. CHARKEY, A.; AND GOODKIN, J.: High Rate Charge and Low Rate Discharge of the Silver Electrodes. Abstract no. 11, presented at fall meeting, Electrochem. Soc. (Buffalo, N.Y.), Oct. 10-14, 1965.

36. CARSON, W. N., JR.; CONSIGLIO, J. A.; AND MARR, J. W.: Study of the Use of Auxiliary Electrodes in Silver Cells. Final Report on Goddard Space Flight Center Contract no. NAS 5-3669, General Electric Co., Advanced Technology Laboratories (Schenectady, N.Y.), July 1965.

37. ANON.: Study-Papers on the Auxiliary Electrode. Report on Interagency Advanced Power Group Contract no. NASr-191, Rept. no. PIC-BAT 209/9, Power Information Center (Philadelphia, Pa.), Oct. 1965. (Available as NASA CR-67987, N66-11765.)

38. COOPER, J.; AND FLEISCHER, A.: Screening Methods. Air Force Aero Propulsion Laboratory (Wright-Patterson Air Force Base, Ohio). No date.

39. HENNIGAN, T. J.: Separator Materials for Silver Oxide Zinc and Silver Oxide Cadmium Electrochemical Cells. Interim Rept. no. TM X-55325, Goddard Space Flight Center, Aug. 1965. (Available as NASA N66-11220.)

40. WEISS, E.: Alkaline Battery Separator Study. Eighth Quarterly and Final Report on Goddard Space Flight Center Contract no. NAS 5-2860, Mar. 29 to June 28, 1964. Rept. no. ESB 7054.8, Electric Storage Battery Co., Carl F. Norberg Research Center (Yardley, Pa.), July 31, 1964. (Available as NASA CR-59591, N65-11631.)

41. COLBECK, D. B.: Sealed Silver-Zinc Rechargeable Batteries. Final Report on Goddard Space Flight Center Contract no. NAS 5-1607. Rept. no. E-6-63, Electric Storage Battery Co., Missile Battery Division (Raleigh, N.C.), Mar. 21, 1963. (Available as NASA CR-55770, N64-16015.)

42. JPL Spec. XSO-30275-TST-A.

43. BODAMER, G. W.: Heat Sterilizable, Impact Resistant Cell Development. First Quarterly Report on Jet Propulsion Laboratory Contract no. 951296, Jan. 1 to Mar. 31, 1967. Rept. no. 67-284, Electric Storage Battery Co., Carl F. Norberg Research Center (Yardley, Pa.), May 9, 1967.

44. SCARDAVILLE, P. A.; AND WETHERELL, T. J.: Fabrication and Test of Battery Separator Materials Resistant to Thermal Sterilization. Final Report on Jet Propulsion Laboratory Contract no. 951015, Radiation Applications, Inc. (Long Island, N.Y.), Dec. 1965. (Available as NASA CR-69884, N66-16190.)

45. ADAMS, L. M.; LAWRASON, G. C.; AND HARLOWE, W. W., JR.: Fabrication and Testing of Battery Separator Material from Modified Polyethylene. Final Report on Jet Propulsion Laboratory Contract no. CA 384805, Southwest Research Institute (San Antonio, Tex.), June 7, 1966. (Available as NASA CR-75951, N66-29543.)

46. ANON.: Fabrication and Testing of Battery Separator Material. Report on Jet Propulsion Laboratory Contract no. CA 384807, Rept. no. ER 8487, Lockheed Aircraft Corp., Lockheed-Georgia Division, Apr. 1966. (Available as NASA CR-75980, N66-29710.)

47. TRISCHLER, F. D.: Separator Development for Heat Sterilizable Battery. Final Report on Jet Propulsion Laboratory Contract no. 951091, Whittaker Corp., Narmco Research & Development Division (San Diego, Calif.), Oct. 1966. (Available as NASA CR-81161, N67-15399.)

48. LANGELAN, H. C.; AND SHEPHERD, C. M.: High Rate Battery Electrodes. J. Electrochem. Soc., vol. 114, no. 1, 1967, p. 8.

49. DIRKSE, T. P.: Cycling Characteristics of the Silver Electrode in Alkaline Solutions. Electrochem. Tech., vol. 4, no. 3-4, 1966, p. 163.

50. BUTLER, E. A.: Discharge Behavior of the AgO-Ag Electrode. Technical Rept. no. 32-535, Jet Propulsion Laboratories, Dec. 22, 1963.

51. HAWKINS, B. R.: Investigations Leading to the Development of a Primary Zinc-Silver Oxide Battery of Improved Performance Characteristics. Final Rept. no. 2 on Marshall Space Flight Center Contract no. NAS 8-5493, July 1, 1964, to June 30, 1965, Eagle-Picher Co. (Joplin, Mo.). No date. (Available as NASA CR-68563, N66-13637.)

52. WYLIE, G. M.: Zinc-Silver Oxide Non-Reserve Battery. Paper presented at the 16th Annual Power Sources Conference (Fort Monmouth, N.J.), May 22-24, 1962.

53. GRUN, C.: Design of Sealed Secondary Silver-Zinc Battery. Final Report on Jet Propulsion Laboratory Contract no. 950959, Rept. no. 570-65, Yardney Electric Co. (New York), Aug. 1965.

54. ANON.: Design of Sealed Secondary Silver-Zinc Battery. Addendum to Final Report on Jet Propulsion Laboratory Contract no. 950959, Rept. no. 637-66, Yardney Electric Co. (New York), Jan. 1966.

55. ANON.: Development of a Mariner "A" Energy Source. Weekly Rept. no. 1-13 on Jet Propulsion Laboratory Contract no. 950107, Rept. no. 61-652, Electric Storage Battery Co., Missile Battery Division (Raleigh, N.C.), Aug. 7, 1961.

56. ANON.: Development of a Mariner "A" Energy Source. Weekly Rept. no. 14-26 on Jet Propulsion Laboratory Contract no. 950107, Rept. no. 62-839, Electric Storage Battery Co., Missile Battery Division (Raleigh, N.C.), Jan. 9, 1962.

57. ANON.: Mariner MK VI Battery Development. Biweekly Reports 1-5 on Jet Propulsion Laboratory Contract no. 950495, May 7 to July 15, 1963, Rept. no. 63-683, Electric Storage Battery Co., Missile Battery Division (Raleigh, N.C.), May 21, 1963.

58. FRANK, H.; AND STRIER, M. P.: Small Fuel Cell To Eliminate Pressure Caused by Gassing in High Energy Density Batteries. Final Report on Goddard Space Flight Center Contract no. NAS 5-9594, Rept. no. SM-48457-F, Douglas Aircraft Co., Inc., Astropower Laboratory (Newport Beach, Calif.). No date.

59. HOYT, H. E.; AND PFLUGER, H. L.: Improved Separators for Silver Oxide-Zinc and Silver Oxide-Cadmium Cells for Spacecraft. Final Rept. no. 1 on Goddard Space Flight Center Contract no. NAS 5-9107, Nov. 10, 1964, to Nov. 10, 1965, The Borden Chemical Co., Central Research Laboratory (Philadelphia, Pa.). No date. (Available as NASA CR-80108, N67-12244.)

60. BROOKE, C. W., JR.: Development of an Electrochemical Energy Source for the Mariner II Spacecraft. Technical Rept. no. 32-854, Jet Propulsion Laboratory, Mar. 15, 1966.

61. LANDER, J. J.: Battery Workshop. NASA Headquarters (Washington, D.C.), Oct. 6-7, 1966.

62. BORSANYI, A. S.; GRUBER, B. A.; KAFESJIAN, R.; KLUNDER, K. W.; AND SMITH, J. O.: Development and Feasibility Proof of the Dry Tape Battery Concept. Final Report on Lewis Research Center Contract no. NAS 3-2777, June 14, 1963, to Jan. 23, 1964, Rept. no. MRB 5001F, Monsanto Research Corp., Boston Laboratories (Everett, Mass.), Mar. 31, 1964. (Available as NASA CR-56132, N64-20703.)

63. ARRANCE, F. C.; BERGER, C.; AND TAYLOR, A. D.: Inorganic Separator for High Temperature Silver-Zinc Battery. Final Report on Lewis Research Center Contract no. NAS 3-6007, Rept. no. SM-46220-F, Douglas Aircraft Co., Inc., Missile and Space Systems Division, Astropower Lab. (Newport Beach, Calif.), Sept. 30, 1965. (Available as NASA CR-54749, N66-10655.)

64. CHREITZBERG, A. M.; AND CUSHING, F. S.: Research and Development of Cells With Bellows Controlled Electrolyte Levels. Second Quarterly Report on Goddard Space Flight Center Contract no. NAS 5-3813, Sept. 10 to Dec. 10, 1964, Rept. no. E-3-65, Electric Storage Battery Co. (Raleigh, N.C.). (Available as NASA CR-60932, N65-17885.)

65. CHREITZBERG, A. M.; AND CUSHING, F. S.: Research and Development of Cells With Bellows Controlled Electrolyte Levels. Third Quarterly Report on Goddard Space Flight Center Contract no. NAS 5-3813, Dec. 10, 1964, to May 10, 1965, Rept. no. E-4165, Electric Storage Battery Co. (Raleigh, N.C.). No date. (Available as NASA CR-63903, N65-29135.)

66. CHREITZBERG, A. M.; AND CUSHING, F. S.: Research and Development of Cells With Bellows Controlled Electrolyte Levels. First Quarterly Report on Goddard Space Flight Center Contract no. NAS 5-3813, June 10 to Sept. 10, 1964, Electric Storage Battery Co. (Raleigh, N.C.). No date. (Available as NASA CR-59373, N64-33918.)

67. McCOLLUM, W. A.; NICHOLSON, M. M.; RECHT, H. L.; AND SCHLESINGER, G.: Radiation Effects on Silver and Zinc Battery Electrodes. Third Quarterly Report on Jet Propulsion Laboratory Contract no. 951109, Oct. 1965 to Jan. 1966. Rept. no. 66-33, North American Aviation, Inc., Atomics International Division (Canoga Park, Calif.), Mar. 21, 1966. (Available as NASA CR-74905, N66-26234, or NASA CR-74240.)

68. KELCHNER, R. E.; McCOLLUM, W. A.; NICHOLSON, M. M.; AND RECHT, H. L.: Radiation Effects on Silver and Zinc Battery Electrodes. Fourth Quarterly Report on Jet Propulsion Laboratory Contract no. 951109, Jan. to Apr. 1966, Rept. no. AI 66-83, North American Aviation, Inc., Atomics International Division (Canoga Park, Calif.), May 27, 1966. (Available as NASA CR-75394, N66-27530.)

69. ARGUE, G. R.; McCOLLUM, W. A.; AND RECHT, H. L.: Radiation Effects on Silver and Zinc Battery Electrodes. Second Quarterly Report on Jet Propulsion Laboratory Contract no. 951109, July to Oct. 1965, Rept. no. AI 65-264, North American Aviation, Inc., Atomics International Division (Canoga Park, Calif.). No date. (Available as NASA CR-71256, N66-19706.)

70. ARGUE, G. R.; McCOLLUM, W. A.; AND RECHT, H. L.: Radiation Effects on Silver and Zinc Battery Electrodes. First Quarterly Report on Jet Propulsion Laboratory Contract no. 951109, Apr. to July 1965, Rept. no. AI 65-158, North American Aviation, Inc., Atomics International Division (Canoga Park, Calif.), Aug. 16, 1965. (Available as NASA CR-64970, N65-34010.)

71. ADAMS, J. L.: The JPL High-Impact Program—1965. Technical Rept. no. 32-844, Jet Propulsion Laboratory, Feb. 1, 1966.

CHAPTER 7

Lead-Acid Batteries

Lead-acid storage batteries are the most common storage batteries used today. The first practical battery, built by Planté in 1859, remained a laboratory curiosity until the 1880's when the pasted plate was developed. This development enabled the economic production of lead-acid batteries and furthered their use in vehicle propulsion and lighting.

The net chemical reaction which takes place in the lead-acid battery is

$$PbO_2+Pb+2H_2SO_4=2PbSO_4+2H_2O$$

Vinal (ref. 1) gives a complete dissertation on the lead-acid battery, including history, materials and methods of construction, chemistry, electrical characteristics, applications, and testing procedures.

An examination of the chemical reaction in the lead-acid battery shows that the electrolyte, an aqueous solution of sulfuric acid, participates in the reaction. Sulfuric acid is consumed during discharge and regenerated during charge. To allow operation, a predetermined quantity of sulfuric acid must be supplied to the battery—the cells cannot operate in a starved or semidry condition. This makes the lead-acid battery less attractive for applications in which the absence of gravity causes an uncertain distribution of the electrolyte in the cell.

NASA-sponsored work on lead-acid batteries was limited to the Howard and Willihnganz program for the development of a sealed prismatic cell for space application (ref. 2). The developed cell was nonmagnetic, capable of high-rate discharges and comparable to the nickel-cadmium system in capacity at the 30-minute rate. Capacities of 6.9 W-h/lb at 77° F and 6.2 W-h/lb at 32° F were found for 0.90-inch-thick electrode cells. Calculated capacities for thin-electrode cells were 10 W-h/lb at the 30-minute rate. A major disadvantage of the lead-acid battery was its inability to accept charge at a sufficiently high rate to permit recharge during the 60-minute sunlight period of a 90-minute orbit.

Excess negative-electrode material exposed in the gas space above the electrodes was used to control the pressure by recombining any oxygen which evolved on discharge. The rate of hydrogen evolution on charge was minimized by clamping the potential applied to the cell to values below 2.3 volts.

Five-cell batteries were made using a monoblock construction and operated using a battery-level modified constant-potential charging system. Pressure failures resulted from cell divergence. No solution is

189

suggested to improve performance at zero gravity in a cell having large amounts of free electrolyte.

NAD Crane (ref. 3) tested 5-A-h cells made under the above program by operating them at a 25-percent discharge depth at 25°, 0°, and 40° C (environmental temperature) for a total of 210 cycles. Ampere-hour and watt-hour efficiencies are reported, but some of the measurements showed efficiencies considerably greater than 100 percent and are, therefore, erroneous.

End-of-discharge voltages fell rapidly at 0° C (probably caused by failure to recharge), but slowly during the first 100 cycles at 25° C and during the last 100 cycles at 40° C. All cells operated at an average of 2.10 volts per cell after 210 cycles, after which the test was terminated.

Considering the relatively successful results obtained from this limited development effort, it appears that the lead-acid sealed battery might compete with the nickel-cadmium battery system for some aerospace applications, if the problem of electrolyte distribution can be solved. The lead-acid battery is nonmagnetic, has higher operating efficiencies (both ampere-hour and watt-hour), lower self-discharge rates, fewer cells required for a given voltage, and better predictability of bus voltage characteristics than the nickel-cadmium battery. However, operation would be restricted to somewhat higher temperatures or to longer orbit periods, and thermal-control problems would be greater due to absorption of heat by lead-acid system on discharge instead of on charge as in the nickel-cadmium cells. Its energy density is unlikely to exceed that of the nickel-cadmium cell.

REFERENCES

1. VINAL, GEORGE W.: Storage Batteries: A General Treatise on the Physics and Chemistry of Secondary Batteries and Their Engineering Applications. John Wiley & Sons, Inc. (New York, N.Y.), 1966.

2. HOWARD, A. M.; AND WILLIHNGANZ, E. A.: Development of a Sealed Lead-Acid Battery for Use in Space. Final Report on Goddard Space Flight Center Contract no. NAS 5-2872, Eltra Corp., C and D Battery Division (Conshohocken, Pa.), Feb. 26, 1966. (Available as NASA CR-71293, N66-23780.)

3. ANON.: Evaluation Program for Secondary Spacecraft Cells, Acceptance Test on C and D 5.0 AH Sealed Lead-Calcium Cells. Test Report on Goddard Space Flight Center Contract no. W11, 252B, Rept. no. QE/C 66-399, U.S. Naval Ammunition Depot, Quality Evaluation Laboratory (Crane, Ind.), June 6, 1966. (Available as NASA CR-76517, N66-31896.)

CHAPTER **8**

Batteries for Low-Temperature Operation

All types of aqueous electrolyte batteries are limited in performance at low operating temperatures due to both increased activation polarization and decreased conductivity of electrolytes. These limitations have stimulated the development of batteries specifically designed to operate at low environmental temperatures. For the most part, in the United States, this work has been sponsored by the U.S. Army and the U.S. Air Force, since Army equipment must occasionally operate under arctic conditions and Air Force equipment must contend with the low temperatures encountered in high-altitude flight. Only the NASA-sponsored work, representing a small proportion of the total, is reported here.

AMMONIA ELECTROLYTE BATTERIES

Armstrong and Meyers (ref. 1) conducted investigations directed toward the development of an ammonia electrolyte battery operable at temperatures of $-73°$ C, with an ultimate goal of operation at $-90°$ C. The chemical system employed a magnesium-alloy anode, potassium thiocyanate (KSCN) as an electrolyte, in solution in liquid ammonia, and several compositions of cathode, including mercuric sulfate ($HgSO_4$), lead sulfate ($PbSO_4$), and meta-dinitrobenzene.

Bobbin cathodes operated successfully with sheet-magnesium alloy electrodes at temperatures between $-63°$ and $-73°$ C, using both mercuric-sulfate and lead-sulfate cathodes. The less-active lead-sulfate cathode, however, limited cell voltage at high drain rates. Later experiments using lead-sulfate pasted-plate cathodes succeeded in increasing load voltage. The wet-stand time of the mercuric-sulfate cathode was short because of oxidation of the thiocyanate ion by the mercuric sulfate, which resulted in reduction of the cathode-active material to metallic mercury. This self-discharge reaction was inhibited by the addition of sulfur to the cathode-active material in the ratio of 2 sulfur to 1 mercuric sulfate. Even so, capacity was totally lost after 4 days of activated stand at $-63°$ C. Lead sulfate was found to be stable in solutions of potassium thiocyanate in ammonia.

Several attempts were made at minimizing corrosion of the magnesium anode in the electrolyte. Chromate dipping passivated the magnesium anode, but lost its protective effect because pinholes developed. Lead deposition on magnesium was effective only for short periods of time

191

(about 5 seconds). Zinc coatings were formed by immersion plating (i.e., by substitution) from a pyrophosphate bath, followed by further zinc plating from a cyanide-electroplating bath. This coating protected the magnesium from corrosion, but the cell could not be activated even on very heavy loads because of uneven zinc stripping from the electrode surface. The activated stand of the lead-sulfate cathode cells was erratic in behavior, with variations being attributed to the behavior of the separator. The greater stability of some cells indicates that greater activated stand periods are achievable with lead sulfate as a cathode. No practical flight batteries were built.

HEATED BATTERIES

Sparks (ref. 2) studied the application of heated batteries in several types of space probe and interplanetary flight missions. He concluded, after a comprehensive survey of heating methods, that three types of battery heating were promising. Where small amounts of excess electrical power are available from the primary power source, electrical heating, combined with lightweight, high-efficiency insulation, is the lightest and most readily controllable type of heating. Chemical heating, in the form of cartridges fired sequentially by a combination of logic and thermal sensors in the battery, is attractive for short-term applications of 100 hours or less. Radioisotope heating is most attractive where electric power is at a premium (such as solar-array-powered probes going away from the Sun). Radioisotope heating introduces a thermal control problem, however, because the heat source cannot be turned off. Several methods for controls of the heat acceptance or rejection rate of batteries were analyzed.

Sparks also reviewed the properties of the main types of batteries used for space applications, with particular emphasis on the thermal effects occurring within the cells and the effects of temperature upon the cells. Four specific applications were analyzed with the following conclusion: Spinning solar probes, with or without a rotating despun shield, are not promising applications of radioisotope-heated batteries, primarily because the margin of tolerable solar heating of the solar array approximates that of battery operation without heating. Both systems failed at identical times and distances from the Sun.

Analysis of a Mars landing capsule demonstrates the ability of a radioisotope heat source to maintain battery temperatures at reasonable levels throughout the Martian night.

A Mercury darkside landing capsule is a promising application of the radioisotope-heated battery, if a sunshade is used to minimize the variation in spacecraft temperatures during transit between Earth and Mercury. The landing capsule is visualized as a single insulated compartment containing electronic equipment and a battery. Additional heat is provided by adding a radioisotope source, determinable in size by the total surface area of the capsule, and the expected internal heat sources.

An asteroid belt probe study showed that serious thermal problems would be encountered at a distance of 2 astronomical units from the Sun. By suitable modifications and the addition of a radioisotope heat source to the battery, this distance could be increased to 3 astronomical units. Conceptual designs for heated batteries were shown.

REFERENCES

1. ARMSTRONG, G. M.; MEYERS, W. F.; AND CORSON, W. H.: Development of a Low-Temperature Battery for Space Probe Applications. Final Report on Lewis Research Center Contract no. NAS 3-6009, June 24, 1964, to June 23, 1965, Livingston Electronics Corp. (Montgomeryville, Pa.). No date. (Available as NASA CR-54733, N66-12347.)
2. SPARKS, R. H.: A Study To Develop a Low-Temperature Battery Suitable for Space Probe Applications. Final Report on Lewis Research Center Contract no. NAS 3-6018, TRW Systems (Redondo Beach, Calif.). No date. (Available as NASA CR-54737, N65-35406.)

CHAPTER 9

High-Temperature Batteries

The varying environments in space and in the planetary bodies of the solar system have generated some interest in the development of galvanic cells and batteries capable of operating at temperatures higher than the ordinary aerospace cell. NASA sponsored the study of two approaches. The first considered the development of an inorganic separator for use in silver-zinc cells at temperatures around 100° C, and was discussed in chapter 5. The second used molten-salt electrolytes at temperatures from 600° to 800° F as discussed below.

Subcasky et al. (ref. 1) investigated single electrodes, separators, molten-salt electrolytes, and cells made from combinations of these for use at temperatures of 800° F. Several combinations of cells were tried, using various types of anode, cathode, and separator materials. Among the anode materials, lithium and sodium corroded separator materials at an excessive rate. Lithium failed the compatibility tests, and sodium, which was tried in a complete cell, caused separator failure after a short time. Further work was done with magnesium and lithium-magnesium alloy.

Cathode materials (salts and metal oxides) were present as solids or in solution in the catholyte (i.e., the electrolyte associated with the cathode and separated from the remainder of the electrolyte by the separator). Various inert metals were used as cathode contacts (silver, gold, tungsten). A molten lithium-chloride–potassium-chloride eutectic was used as an electrolyte. Of the cathode materials tested, chromium (IV) compounds either reacted with the electrolyte or formed insoluble high-resistance films. V_2O_5 reacted with the electrolyte and had a low energy density. Ferric chloride shifted the reaction mechanism, delivering low-voltage outputs at higher current densities. Silver chloride had good electrochemical performance, but low energy density. Cupric chloride was a very strong oxidant and reacted with electrode and container materials, and bismuth trichloride formed soluble or liquid reaction products, and permitted corrosion of the cathode current collector. The most promising cathode material tested was cuprous chloride.

Various separator materials were tried, including fritted glass, porcelain, and zeolites (sodium aluminosilicates). Zeolite structures permit considerable mobility of ions within the solid body at elevated temperatures. Successful experimental cells, capable of 72 hours of discharge at 6.7 mA/cm² of separator area, were built with a Li-Mg alloy anode, cuprous chloride cathode and zeolite separator; and lithium-magnesium

anode, copper oxide cathode, and porous glass separator. All cells constructed were of the laboratory test-tube type. No prototypes of operational cells were constructed.

One of the most severe problems encountered in the program was the sealing of the separator to the ceramic tube containing the anolyte or catholyte. In addition, volume changes occurred in the anode and cathode compartments during operation of the cell which must be compensated for by a mechanical motion of structural components of the cell in order to eliminate free gas spaces.

REFERENCES

1. ANDERSON, W. G.; PARKER-JONES, H. A.; PLACE, T. M.; SALISBURY, R. G.; SEGOVIA, G.; STAMIRES, D. N.; AND SUBCASKY, W. J.: Development of a High-Temperature Battery. Final Report on Lewis Research Center Contract no. NAS 3-6002, Philco Corp., Aeroneutronics Division, Newport Beach, Calif., Oct. 15, 1965. Rept. no. 1-3313, WO 2261. (Also available from NASA CR-54731, N65-36781.)

CHAPTER 10

High-Energy-Density Systems

Recent demands for improved power sources have led to efforts to develop higher energy-density batteries. Two approaches are: (1) the use of higher potential electrodes which increase energy density by increasing cell voltage; and (2) the use of materials of low equivalent weights. In the latter systems, the number of electrons (and, consequently, the number of ampere-hours) attainable per unit weight of reactant material is increased.

The high-energy-density system consists of an active, high-potential anode material which gives up electrons, a low-density cathode material which accepts large numbers of electrons per unit weight, and an electrolyte system which must be compatible with both. Because the active anode materials, such as lithium, tend to liberate hydrogen from water spontaneously (unless they are passivated by an adherent layer of oxide), an aprotic electrolyte system must be used (one which has a low availability of hydrogen ions in solution).

Even though the potentialities of the nonaqueous battery systems are well known, the materials and research are comparatively expensive and, in the past, no large-scale market was promising. However, when the use of portable electronic equipment became more common through the advent of semiconductor electronics, the need for energy storage in a minimum size and weight became obvious.

Work on these systems had to start at a very basic level, since no empirical technological background existed, such as for inorganic electrochemical energy-storage systems. Extensive studies of organic-solvent electrolyte systems were undertaken to determine such properties as conductivity, viscosity, solubilities of electrolyte salts, and compatibility with anode, cathode, and structural materials. It was found that trace impurities have a greater effect on electrode performance than they do in aqueous systems.

The choice of solvent systems for investigation has been somewhat limited because there are only a few solvents which have the proper combination of properties. To function in a battery system, organic solvents must be made conductive by the dissolution of ionic solutes. Therefore, solvents having a high ion-solvation energy must be used. A high dielectric constant is also desirable to reduce the electrostatic forces between the dissolved ions, which will reduce the extent of ion-pair formation.

The most serious limitation of the organic solvent electrolyte batteries is that they are restricted to low current-density applications because of the relatively low conductivity of the organic electrolytes. The investigation of cathode systems is still incomplete. Thermodynamically, the most attractive cathode materials are the halogen gases and oxygen. However, because of their gaseous state, these are more suited to fuel cells. Most of the cathode research has been directed toward metal halides such as NiF_2, CuF_2, and $CuCl_2$, which function as "halogen carriers," or to organic compounds with electrochemically reducible functional groups such as nitro groups.

Batteries composed of a lithium anode, a metal halide cathode, and an organic electrolyte containing dissolved salts presently promise to be the most effective high-energy-density system. Those using organic cathode materials have the greatest long-term promise because of the greater coulombic capacity of the organic oxidants.

ANODES

Work on materials for use as anodes in high-energy-density batteries has been directed toward metals with a high electrode potential and a low equivalent weight, such as Li, Na, Mg, Al, Ca, and Be. The results of these studies indicate that, of the above, only Li shows significant promise as an anode material. The open-circuit and discharge potentials of the others are less reproducible than those of Li, and oscillations and transients in voltage are common during discharge. A further complication is the formation of passivating films.

Lithium anodes are fabricated in several ways. Lithium may be electrochemically deposited on a current collector, or the metal may be formed into a sheet by pressing or rolling it onto a substrate metal screen in argon, or other inert atmosphere (refs. 1 through 8). A powder or paste of the active material, with or without additives or binder, may be pressed onto a current-collecting screen or substrate (refs. 7 though 9). Lithium anodes have been fabricated by dipping a metal screen into the molten metal (refs. 2 and 10), although this was found to give poor adhesion between the lithium and substrate. The best results have been obtained by pressing lithium onto an expanded metal screen substrate (ref. 11).

Although Al is easy to fabricate and use, it is less active than Li in the same solvent system. Whereas Al can be deposited and discharged with high efficiencies in some organic solvents, in solvents that are suitable for high-energy-density batteries, open-circuit potentials are erratic and nonreproducible (ref. 12).

The behavior of Mg is similar to that of Al in that high efficiencies can be obtained for deposition and discharge at low current densities in certain solvents, but the results in those solvents suitable to high-energy-density cells are unsatisfactory. Furthermore, because Mg passivates in aqueous solutions, its performance in nonaqueous solutions would be very sensitive to the presence of traces of water (ref. 40).

Calcium has had little use in organic electrolyte battery systems, but has been applied in fused-salt thermal batteries.

The lithium electrode behaves reversibly in several solvents, and the polarization level during discharge is small (refs. 5, 6, 8, and 13 through 17). The deposition of Li during charging takes place with high ampere-hour efficiency (95 to 100 percent), but the discharge and cycling efficiencies are somewhat lower. In the past, the cycling efficiencies of lithium electrodes have been only about 85 percent. The loss in cycling efficiency is usually ascribed to several phenomena. Side reactions result in efficiency decreases with increases in the number of cycles, indicating a buildup of deleterious impurities (ref. 13). Mechanical losses also occur. As more Li is deposited, it becomes less adherent (refs. 6 and 14). Loss of electrical contact during discharge can occur by preferential attack at the base of lithium dendrites (ref. 13). Certain substrates, such as silver and platinum, may form lithium alloys, which may prevent complete discharge of the Li. While minor amounts of water (50 to 200 ppm) have little influence on the discharge of Li, the presence of H_2O during deposition causes a significant decrease in the charging efficiency (refs. 13 and 19). Recent results (reported by R. C. Shair, A. E. Lyall, and H. N. Seiger of Gulton Industries at the Advances in Battery Technology Symposium, Los Angeles, Calif., Dec. 1, 1967) indicate that the cycling problem can be overcome.

Some nonmetallic compounds such as hydrazine derivatives, thiourea and its derivatives, and sodium borohydride have been tested as anode materials, but with limited success. In general, the nonmetallic compounds are not particularly attractive because of their low electrode potentials.

CATHODES

Typical cathode materials tested in high-energy-density batteries include NiF_2, CuF_2, $CuCl_2$, $CuCl$, $AgCl$, other metal halides, metal oxides, air or oxygen, and various organic materials. Inorganic-cathode materials have received more attention than organic cathodes because inorganic compounds have less complicated overall reactions and more favorable solubility characteristics. However, organic cathodes have potentially higher energy densities than known inorganic cathodes, and their electrochemical reduction products are more compatible with organic solvent electrolyte systems.

The development of organic-cathode–organic-electrolyte batteries is a more complex problem than that of aqueous electrolyte batteries because of the large variety of possible electroactive organic-cathode compounds, the absence of an adequate theoretical treatment of electro-organic reactions, and the paucity of data on the electrochemical behavior of most of these compounds in organic solvents.

INORGANIC CATHODE MATERIALS

CuF_2 has a low equivalent weight and a high electrode potential. At present, its use is limited to primary batteries because recharging the

electrode has not proven feasible. The discharge characteristics of CuF_2 depend on current density, solvent, and on type and concentration of solute. At low current densities, CuF_2 discharges with high-coulombic efficiency and low polarization, but both the coulombic efficiency and the electrode potential decrease as the current density increases (refs. 16 and 20). Efficiency can be improved by increasing the temperature; however, this also increases the tendency of the electrode to discharge in two steps rather than in one, which lowers the available energy density (ref. 8). Optimum coulombic efficiency at room temperature is 70 to 80 percent (ref. 11).

The $CuCl_2$-$CuCl$ electrode has also been investigated because it is applicable to secondary batteries. However, the energy density of $CuCl_2$ is lower than that of CuF_2, and it is more soluble in the electrolyte, which makes it susceptible to self-discharge in a working cell. Therefore, pending the development of migration-inhibiting separators, the copper-chloride electrode is limited in use to reserve batteries. Further disadvantages are the stepwise discharge of $CuCl_2$ to $CuCl$ and then Cu, and the fact that the coulombic efficiencies are only moderate (varying between 50 and 75 percent) (ref. 11).

The $AgCl$ electrode is both reversible and efficient, but its theoretical energy density is lower than that of many other cathode materials. Coulombic efficiencies up to 100 percent have been obtained with $AgCl$ at low current densities decreasing rapidly with increasing current density (ref. 6). Cycling efficiencies of 93 to 100 percent have been achieved by adding $LiCl$ to the cathode mix to provide a source of chloride ions during charging (ref. 14).

AgF and AgF_2 have also been studied, but only preliminary results are available at present.

Various transition metal fluorides and chlorides have been tested as cathode materials for use in aprotic solvents. The results obtained with compounds such as CoF_3, CrF_3, and $NiCl_2$ have been unsatisfactory because of low efficiencies and high polarization. The fluorides of Mn, Sb, and Cd are being investigated, but only preliminary results are available at present.

With the exception of silver peroxide, all metal oxides tested are unsatisfactory for use in organic-solvent electrolyte solutions. In the case of AgO, coulombic efficiencies of up to 40 percent have been obtained (ref. 3). The nature of the discharge product of AgO is uncertain in aprotic solvents, but because of the high polarizations observed, it is believed that the electrolyte solution participates in the discharge reaction. Addition of water to the electrolyte solution reduces polarization.

It is doubtful that metal oxides can be developed into satisfactory cathode materials for use in organic-solvent electrolyte solutions. Air and oxygen have also been studied (ref. 21), but as in the case of the metal oxides, the reduction products do not appear to be compatible with organic solutions, and the results have been unsatisfactory.

ORGANIC OXIDANTS

A number of organic compounds with electrochemically reducible functional groups have been studied as possible cathode materials. The potentially large numbers of electrons available per molecule result in a low equivalent weight and a high-energy density. The reduction products of organic-cathode materials are more compatible with organic solvents than those of inorganic-cathode materials.

The chief disadvantages of organic oxidants are the lack of basic data on their behavior in organic-solvent electrolytes; stepwise multi-electron reduction processes, resulting in a decreasing voltage during discharge; and irreversibility in the latter steps of multielectron processes. While the initial reduction steps of organic compounds in organic-solvent electrolyte solutions are frequently reversible, the complete reduction commonly involves irreversible reactions and, therefore, the maximum energy density may be obtainable only in primary batteries. Solubility of the cathode material in the electrolyte frequently results in self-discharge; adequate migration-inhibiting separators have not been developed.

Some of the types of compounds that have been investigated are the chloroisocyanuric acids, chloromelamines, other chlorinated compounds, nitroalkanes, nitroaromatic and nitrosoaromatic compounds. Comparison of the performance of these compounds is difficult because of differences in test techniques, and because in many cases there is a lack of certainty about both the reaction mechanisms and products. Frequently, for lack of better information, the reaction paths are hypothesized to follow similar paths to those in aqueous solution. This uncertainty of the reaction mechanisms makes estimation of the coulombic efficiency and cathode performance uncertain.

Tri- and dichloroisocyanuric acids and their salts have been studied as cathodes by reduction to a 2-volt cutoff potential versus a lithium anode (ref. 22). These reductions gave low efficiencies (≤ 50 percent), and indicated that only one chlorine functional group was reducible at potentials greater than 2 volts versus lithium.

Solutions of hexa- and trichloromelamine have been studied by steady-state-controlled potential methods (ref. 2). The results indicate that hexachloromelamine has a higher electrochemical activity than tri-chloromelamine or trichloroisocyanuric acid. However, the opposite conclusion was reached during cathode development for the dry-tape system.

Solutions of N-chlorosuccinimide were studied voltammetrically, and a high potential (versus Li) and good peak currents were obtained (ref. 20). Dichlorobenzoquinonediimine was tested and provided satisfactory capacity, but the voltage was poor compared to trichloroisocyanuric acid. Investigations were made of 4-nitrosophenol and p-quinonedioxime, but they were not reduced in a favorable potential range (ref. 20). Studies on nitroaliphatic compounds indicated that they have little promise as cathode materials (ref. 23).

A number of nitroaromatic compounds have been investigated, including nitrobenzenes, the dinitrozenes, substituted dinitrobenzenes, and picric acid. The higher capacity dinitrobenzenes give better performance than nitrobenzene. The reduction processes of solutions of *m*-dinitrobenzene derivatives are influenced by the substituents on the ring, by the addition of water or lithium ions to the electrolyte solution, and by the choice of solvent (ref. 23). An enhancement of the effective capacity of *m*-dinitrobenzene was observed when lithium ions were present in the electrolyte solution, indicating that reduction beyond the *m*-dinitrobenzenedianion occurs more readily (ref. 23).

Discharge of *m*-dinitrobenzene and picric acid cathodes gave high coulombic efficiencies; the *m*-dinitrobenzene discharged in two steps, giving two voltage plateaus, while picric acid discharged with a gradual decrease in voltage.

Despite the many problems that must be solved before organic oxidant-organic electrolyte solution batteries can become functional, the potential rewards are high enough to make this a worthwhile area of research for the development of primary batteries. Achieving the desired goals requires patience, sustained effort, and a logical, systematic approach, as well as the application of sophisticated experimental techniques.

Some commonly used cathode fabrication methods are:

(1) Pasting a mixture of electroactive material, conductive additive, binder, and solvent onto a metal screen or graphite plate (refs. 3, 6, 7, 8, 16, 24, 25, and 26).

(2) Preparing a filter cake of cathode material, conductive additive, and fibrous material on a metal screen (refs. 2, 3, 7, and 27).

(3) Pressing a mixture of electroactive material, conductive additive, with or without binder of fibrous material, onto a metal screen or graphite plate (refs. 2, 3, 8, 16, 18, and 20).

(4) Hot pressing a mixture of cathode material, conductive additive, and binder on a metal screen (refs. 8 and 16).

(5) Sintering of electroactive material and conductive additive onto a metal sheet or screen (refs. 2 and 16).

(6) Pressing a cathode mix around a carbon rod in the conventional bobbin configuration.

Because of the number of variables involved in electrode fabrication such as particle size, quantity and type of additives and binders, compacting temperature and pressure, and electrode thickness, plus the fact that many of these factors are frequently interrelated, it is difficult to make valid comparisons between electrodes prepared with different methods of fabrication. The major difficulty in fabrication of cathodes appears to be that sufficient compacting to produce an electrode with satisfactory mechanical strength frequently results in slow and incomplete wetting of the electrode by the electrolyte solution because of insufficient porosity. The incomplete wetting then results in an incomplete reaction and a loss of coulombic efficiency.

The test methods used to evaluate high-energy cathodes include those discussed in the previous section. Additional tests that are frequently used with cathodes are:

(1) Solubility of the cathode material in the electrolyte solution.

(2) Amount of electrolyte absorption into the cathode.

(3) Cyclic and linear voltammetry on cathode materials dissolved in the electrolyte solution to evaluate the number of steps, number of electrons, and reversibility of the electrochemical reactions of the cathode material.

(4) Cyclic voltammetry with a metal electrode such as Cu or Ni in an electrolyte solution to determine if suitable cathode materials can be formed by anodization of the metal in the electrolyte solution.

ELECTROLYTE SOLUTIONS

To take advantage of the high-energy densities provided by active metal anodes such as Li, it is necessary to replace aqueous electrolytes with aprotic media. While this requirement can be satisfied with fused salts, aprotic organic-solvent electrolyte solutions offer the advantages of ambient temperature operation and solid anodes.

The typical organic-solvent electrolyte consists of a solution of an inorganic salt or acid in an organic liquid. Those organic solvents which dissolve the greatest quantities of ionizing salts are generally most attractive.

The three major requirements for a battery electrolyte solution are stability, high conductivity, and low viscosity. The electrolyte solution must not react with the electrode materials or decompose under normal operating conditions. In the case of secondary batteries, the electrolyte solution must be sufficiently stable to withstand the potentials used during the charging step. High conductivity is necessary to minimize IR losses. Low viscosity is desirable to permit rapid diffusion of solution species involved in the electrochemical reactions, thereby minimizing concentration polarization.

For a potential solvent to yield a satisfactory electrolyte solution, it must have certain desirable properties: high dielectric constant, large ion solvation energy, and low viscosity. Low solubility of the active materials in the solvent and a wide liquid temperature range are also desirable.

Table 10–I (ref. 11) lists the properties of a number of solvents which have been considered for use in high-energy batteries. Those in the upper half of the list are the most common. Organic sulfur derivatives have also been considered. However, the conductivities of their electrolyte solutions have been generally unsatisfactory (ref. 28).

Purification and characterization of organic solvents are important to the development of suitable electrolyte systems. Trace impurities, especially water, can have a significant effect on cell performance. For example, it has been calculated (ref. 29) that 1 ppm of water in 1 milliliter of otherwise pure solvent could produce an oxide film 1000 angstroms thick

TABLE 10–I.—*Solvent Properties*

Solvent	Dielectric constant	Viscosity (centipoise)	Melting point, °C	Boiling point, °C
Propylene carbonate (PC)	64.4	2.2	−49	242
γ-Butyrolactone (BL)	39	1.67	−4	206
Dimethylsulfoxide (DMSO)	48	1.93	6	189
Nitromethane (NM)	39.4	.619	−29	101
Acetonitrile (AN)	38.8	.36	−42	82
N,N-Dimethyl formamide (DMF)	36.7	.633	−61	153
Methylformate (MF)	8.5	.330	−99	+31
N-Nitrosodimethylamine (MDA)	53.0	.865		153
Ethylene carbonate (EC)	89	1.9	36	248
Dimethyl carbonate (DMC)	15	.60	1	90
Formamide (FM)	111.5	3.76	3	211
2-Pentanone	22	.47	−78	102
Cyclohexanone	18	2.8	−16	156
Methyl acetate	7.2	.41	−98	57

on 1 cm² of smooth, clean lithium. Furthermore, the solubility of certain cathode materials such as CuF_2 depends on the H_2O concentration in the solvent (ref. 30).

At present, the solvents are purified by fractional distillation (refs. 31 through 36), and characterized by gas chromatography. Continued work on both purification and characterization methods is desirable in the development of electrolytes, especially for secondary batteries.

The important properties of solutes in organic-solvent electrolytes are high solubility in organic solvents, formation of stable solutions, and a high degree of dissociation in organic solvents to give good conductivity. The types of solutes most frequently used are simple salts such as $LiClO_4$; Lewis acids such as $AlCl_3$, either alone or in combination with an alkali metal halide; complex fluorides such as KPF_6; and complex salts such as tetraalkylammonium perchlorates. Organic beryllium compounds have been tested, but have so far shown no promise as solutes in battery electrolyte solutions.

The following general conclusions concerning organic-solvent electrolyte solutions can be made (ref. 11):

(1) The specific conductivities of organic-solvent electrolyte are about an order of magnitude lower than those for corresponding aqueous solutions.

(2) The properties of the solvent have a pronounced effect on the conductivity of the solution. Generally, increasing the dielectric constant of the solution increases the conductivity, whereas increasing the viscosity of the solution has the opposite effect.

(3) The specific conductivity of electrolytes increases as the size of the solute ions increases.

(4) The specific conductivity is a maximum for most electrolytes when the concentration of the solute is about one normal. The decrease in conductivity above this concentration has been attributed to increased viscosity (ref. 37) and increased ion-pair formation.

One approach to the determination of the stabilities of solvent-solute systems has been the measurement of decomposition potentials (refs. 3, 4, 8, 35, 38, and 39), but because solvent decomposition is an irreversible process and is dependent upon the experimental conditions used for the measurement, this method is of questionable significance (ref. 11).

Acetonitrile, nitromethane, and dimethylsulfoxide form high-conductivity solutions with many solutes. Lithium causes polymerization of acetonitrile. Nitromethane may be susceptible to reduction during the charging of secondary batteries (ref. 40). Dimethylsulfoxide appears to be compatible with lithium.

There is no immediate degradation of N,N-dimethyl formamide electrolyte solutions, but there is some indication from extended compatibility tests that a long-term, wet-stand operation might result in some difficulties (ref. 9). However, these effects may be caused by residual impurities in the solution, especially water. n-Butyl formate is stable in the presence of Li, but gives low-conductivity electrolyte solutions. Methyl formate gives much better conductivities, but slow gassing has been observed in the presence of Li (ref. 3).

Propylene carbonate has been extensively studied and is compatible with Li and most cathode materials. Major disadvantages are the comparatively low conductivities and high viscosities of propylene carbonate electrolyte solutions which limit their use to very low-rate applications. It has been reported that binary mixtures of propylene carbonate with other solvents such as ethylene carbonate performed better than either solvent alone (refs. 3, 6, and 41).

The nature and concentrations of solutes in various solvents have a significant effect on the solubilities of certain cathode materials such as CuF_2 and $CuCl_2$ (refs. 12, 14, and 27). However, attempts to reduce the solubility of $CuCl_2$ by the use of mixed solvents or by the common ion effect have been unsuccessful (ref. 11).

Attempts at increasing electrolyte solution conductivities by dissolving polar gases such as SO_2 or CO_2 in the organic solvents have been unsuccessful. It was hoped that the polar gas molecules would interact with the solute ions, increasing the degree of dissociation, and thereby increasing the conductivity (refs. 3 and 4). However, no significant improvement was observed.

SEPARATORS

The desirable properties of separator materials are compatibility with organic solvent electrolyte solutions; high ionic (and hence ohmic) conductivities to reduce IR losses and concentration polarization; low permeability to dissolved cathode materials to reduce self-discharge losses and give long wet-stand life; and sufficient mechanical strength to prevent short circuiting of the cell.

The materials with the best overall performance include (ref. 11) nonwoven porous materials like asbestos filter paper, glass-fiber filter paper, polyolefin mats, and microporous rubber. No separator has yet been developed which will prevent the diffusion of dissolved cathode materials to the anode and subsequent self-discharge of the cell.

The tests that are usually performed on separator materials are:

(1) *Compatibility.* (Usually a qualitative test, based on visual examination of the material after contact with electrolyte solutions for extended periods of time.)

(2) *Separator resistance.* (Measured in the usual manner with an ac impedance bridge.)

(3) *Electrolyte absorption and retention.* (Measured by weighing the separator material before and after equilibration with the electrolyte solution and again after drainage or centrifugation to remove the excess electrolyte (refs. 7 and 8).)

(4) *Separator swelling.* (Measured by comparing the thickness of the material before and after equilibration with the electrolyte solution (ref. 8).)

Cell-discharge tests measure the performance of a given anode–cathode combination using various separator materials after wet stand and in a charged condition (refs. 1, 3, and 8). After standing in a charged condition, the cell may be disassembled without discharge, and the amount of cathode material which has reacted with the anode may be measured (ref. 42).

Known separators that are compatible with organic solvents are all unsatisfactory because of high electrolyte-solution absorptivity (which increases the total cell weight), and because they do not prevent self-discharge during activated storage. Investigations should be continued to find more suitable separator materials.

Because the development of organic-solvent battery systems is still in its initial stages, structural materials have not been extensively investigated. However, no significant difficulties are anticipated. Prototype cells have been made using a variety of cell casings. Polyethylene and polypropylene are the most frequently used materials, and they appear to be compatible with commonly used organic-solvent electrolyte solutions and with electrode materials. Certain solutes such as KPF_6 can cause corrosion of some metals, but in the absence of water, this problem is minor. For example, in a KPF_6-PC electrolyte solution containing less than 50 ppm water, aluminum and stainless steel were negligibly attacked after 60 days at 165° F (ref. 43). The satisfactory use of standard metal casings used in other types of commercial batteries has been reported (ref. 44).

WHOLE-CELL STUDIES

While half-cell studies are useful in studying the behavior of the individual electrodes, interference by other reactions, or physical effects, full-cell studies make necessary the evaluation of electrodes in an environment more nearly that in which they are to be used. Whole-cell studies

also provide information on the compatibility of materials and reaction products, and on operating characteristics with limited quantities of electrolyte solution. They may also expose the existence of other difficulties, such as the formation of impervious films on the electrodes, the formation of insoluble precipitates in the electrolyte solution or separators, or the formation of high-volume reaction products which might physically damage the cell.

A large number of combinations of whole cells have been investigated. However, comparisons between the results reported by different investigators are difficult because of a lack of consistency in the testing methods and in reported results. Also, in most cases, the configurations of the test cells have not been optimized, and the electrode development is still incomplete. A standard method of reporting whole-cell test results would allow valid comparison of the data.

Lithium has been used almost exclusively as the anode material. In most cases, the cell configurations have been based on laboratory convenience rather than optimization of energy density. Because cell development is still in a state of rapid flux, only a few examples of the more common combinations are given here.

$Li-CuF_2$

In the $Li-CuF_2$ combinations a flat-plate-configuration cell with two lithium anodes and a cathode composed of CuF_2, graphite, and paper pulp in a propylene carbonate-$LiClO_4$ electrolyte solution yielded 223 W-h/lb at a 265-hour discharge rate with an average voltage of 3.06 volts. However, when stored at 35° C, the cells self-discharged in a few days. Dissolution of the CuF_2 was the cause of the self-discharge (refs. 1, 3, and 27).

$Li-CuCl_2$

The $Li-CuCl_2$ combination cells with pressed lithium anodes and cathodes of a pressed mixture of $CuCl_2$, silver powder, and carbon black in a propylene carbonate-nitromethane-$AlCl_3$-LiCl electrolyte solution gave good rate capability, but poor energy density. Self-discharge caused by $CuCl_2$ solubility was a significant problem (refs. 42 and 45).

Li-Dichloroisocyanuric Acid

Static discharge tests with a lithium anode, a cathode consisting of a mixture of dichloroisocyanuric acid, Shawinigan black, and carbon fiber and a methyl formate-$LiClO_4$ electrolyte solution delivered 144 W-h/lb. Only the weight of active material, electrolyte solution, and separator were considered (ref. 22).

SECONDARY BATTERIES

Li-AgCl

Flat-plate cells with pressed lithium anodes, cathodes pressed from a mixture of AgCl, Ag_2O, and graphite, and a propylene carbonate-$LiAlCl_4$ electrolyte solution gave 28 W-h/lb and cycle lives of 30 to 50 cycles at moderate depths of discharge (refs. 5 and 6).

Li-NiF$_2$

The secondary system with the most immediate promise is Li-NiF$_2$ in a propylene carbonate-LiPF$_6$ electrolyte solution. Prototype cells have demonstrated 100 W-h/lb at a 10-hour discharge rate; because the solubility of NiF$_2$ is small, the shelf life of the system is quite good. The system appears to be stable upon cycling (refs. 9, 10) (R. C. Shair, A. E. Lyall, and H. N. Seiger, Gulton Industries, Advances in Battery Technology Symposium, Los Angeles, Calif., Dec. 1, 1967).

THE DRY-TAPE DEVICE

A novel approach to the improvement of energy density in batteries is the dry-tape-battery concept, conceived and developed by Monsanto Research Corp. A dry-tape system consists of (1) a thin separator tape, (2) dry coatings of the active anode and cathode components of a battery system on either side of the separator tape, and (3) an electrolyte supply. The tape is continuously or intermittently fed between a set of current collectors after the electrolyte is released and allowed to wet the tape. The electrolyte is introduced to the tape by (1) mixing with the coatings in microencapsulated form, (2) attachment of electrolyte-filled pods to the separator tape or to a special tape, and (3) feeding liquid from a reservoir. Thus, a dry-tape battery can utilize high-energy-density reserve components, not yet feasible in conventional battery configurations, with the additional advantage of a stop-start capability.

The dry-tape concept minimizes some of the common limitations of batteries and fuel cells, and is itself a fuel cell employing solid fuels. The system is time invariant in performance, since not only the fuel and oxidant but also the separator, electrodes, catalyst, and electrolytes are continuously fed. Thus, constant performance and power output can be maintained. A summary of the dry-tape concept and its features is given in figure 10-1.

ANODE DEVELOPMENT AND TESTING

In the initial development work, a zinc block was used as a combined anode and current collector (ref. 46) in opposition to a silver-oxide tape cathode. However, high-energy anode materials, such as Mg, Al, Li (ref. 47), Be (ref. 48), and lithium-beryllium alloy (ref. 48), were tested. None of these materials are used in conventional batteries because of corrosion and self-discharge. Three magnesium-anode configurations were studied in aqueous electrolytes: (1) solid or foil, (2) pressed powder, and (3) flame-sprayed films on tape backing (nylon, Dynel, polypropylene) (refs. 46 and 48). Testing was conducted in a sandwich-type cell with fixed interelectrode distance (ref. 47). The counterelectrode was platinum foil. Polarization data were obtained with the use of both acid and neutral electrolytes.

Continuous foil, pressed powder, and flame-sprayed anodes all showed IR losses due to gas evolution (hydrogen blockage). A significant improvement occurred when expanded or perforated anode foil was used,

FIGURE 10-1.—Features of the dry-tape battery.
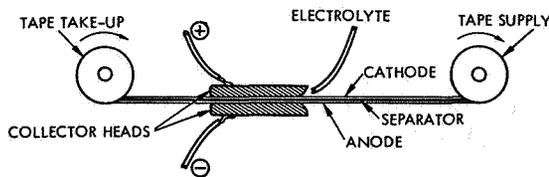
Design Attribute	Beneficial Effect	Resultant Advantage
Use of thin electrode structures —	Minimized (electrolyte) concentration polarization	Higher voltage
Elimination of metallic grid support	Decreased weight	Higher energy density
Continuous feed of anode and cathode	Continuous refreshment with unused active materials	Constant potential maintained
	Continuous removal of discharged products	Low internal impedance maintained
Continuous separator feed	Separator renewal	Separator shorting, if occurring, is only a temporary problem
Continuous electrolyte wetout only as required	Unused electrode sections remain dry	Reserve capability maintained even under stop-start conditions
	Use of incompatible couples	Higher energy density
Adjustable motor-drive speed	Control over feed rate of reactants	Programed power or self-adjustment through voltage monitor and feedback
Separation of active material from auxiliary components	Renewable tape reels for each unit	Logistic storage and transport advantage
Unipotential current collectors	Improved electrochemical efficiency	Higher energy density

and the gases were vented. In the neutral electrolyte ($MgBr_2$), the perforated magnesium functions better than a solid anode. Even though Mg evolves gases in acidic electrolyte, it is superior to Al because of its higher single-cell voltage and potentially higher power output. The other materials tested were not usable as anodes because of power performance (refs. 47 and 48). Corrosion of magnesium occurred in acidic electrolyte (2 M $AlCl_3$). In actual tape configuration cells, the chemical corrosion and gas evolution were less significant than anticipated. Silver peroxide was used to allow comparison with the performance of a known battery system (ref. 46). Other systems using magnesium for the anodes and organic-nitro compounds, positive-

chlorine compounds, or potassium periodate as cathodes were considered (ref. 47).

Cathode materials were evaluated in a sandwich cell with an expanded or perforated magnesium anode (ref. 47) and a platinum foil or graphite sheet as the cathode-current collector. Electrolyte was supplied by a prewetted separator or by immersing the entire cell in the electrolyte.

Efficiencies of 80 percent at 50 mA/in.^{2} were obtained with potassium periodate and picric-acid cathodes when discharged with magnesium anodes in an acid electrolyte. The magnesium-potassium periodate cell operated at 1.9 to 2.1 volts; the picric acid-magnesium cell operated at 1.0 to 1.2 volts. Large amounts of acid were required for satisfactory discharge of periodate and organic-nitro-compound cathodes.

The active chlorine compound, trichlorotriazinetrione, discharged in acid electrolyte with a magnesium anode, gave high current densities (80 mA/cm^2), whereas in neutral electrolytes the current density was 15 mA/cm^2. Bromine, tested as a liquid cathode, gave 50 W-h/lb at the 20-minute rate in $Mg/MgBr_2/Br_2$ tests (ref. 48).

ELECTROLYTE DEVELOPMENT AND TESTING

The major electrolyte screening was conducted during magnesium-anode development (ref. 47). Magnesium, in a tape configuration, was efficiently discharged with no gassing in acid aqueous electrolytes of $AlCl_3$ or mixed $AlCl_3$-HCl. The best neutral electrolyte was 1.5 M $MgBr_2$ and surfactants did not appreciably affect cell performance in the 1.5 M electrolyte. However, the performance of cells using 2 M $MgBr_2$ equaled that of 1.5 M solution when surfactant was added to 2 M electrolytes (ref. 48). The neutral electrolyte, $MgBr_2$, was superior to acidic electrolytes ($AlCl_3$, HCl), giving higher energy densities, lower gas evolution, and less depolarizer decomposition. Acidic electrolytes drastically reduced the active chlorine content of trichlorotriazinetrione.

The nonaqueous solvent system, $Li/LiClO_4$, methyl formate/dichloroisocyanuric acid, delivered 213 W-h/lb at 3.2 volts (based on weights of anode, cathode, separator, and electrolyte). Under constant load the same couple gave 190 W-h/lb at the 5-hour rate. The maximum short-circuit current density was 200 mA/cm^2.

Electrolyte screening revealed that methyl formate-(2 M)-$LiClO_4$ solution would support the highest current densities. Dichloroisocyanuric acid and CuF_2 depolarizers were superior to other depolarizers tested; Li/CuF_2 tape cells had energy densities about 75 percent of that of Li/dichloroisocyanuric acid cells. Pure lithium anodes were superior to lithium-magnesium-alloy anodes (ref. 48).

MANUFACTURING METHODS

In the earlier phase of dry-tape work, the tape was prepared by pressing the cathode mix into the separator tape. The final cathode tapes were machine made.

The best methods of cathode preparation by pressing were:
(1) Aqueous cathode:
    Composition:
        Trichlorotriazinetrione (78 percent)
        Shawinigan acetylene black (18 percent)
        Paper pulp (4 percent)

The cathode mix was dry blended, 3.5 milliliters of trichloromethylene were added for each gram of cathode mix, and the mixture was stirred for 1.5 minutes. Cathodes were pressed between blotting paper at 100 psi and dried; 1.2 ml of $MgBr_2$ electrolyte (1.5 and 2.0 M) were used per gram of cathode mix.

(2) Nonaqueous cathode:
    Composition:
        Dichloroisocyanuric acid (93 percent)
        Shawinigan acetylene black (16 percent)
        Carbon fibers (1 percent)

The acetylene black and carbon fibers were blended for 1 minute and after addition of dichloroisocyanuric acid, the entire mix was blended for 30 seconds. Each 3-in.^{2} cathode was pressed at 300 lb/in.^{2}; 0.78 milliliter of electrolyte ($LiClO_4$ in methyl formate (2 M) was required per gram of cathode mix (ref. 48)).

Machine-made cathodes were prepared by spreading the cathode mix on a 2-mil Dynel separator surface and bonding a 4-mil magnesium ribbon to the opposite side of the separator with small amounts of neoprene cement. The complete tapes were wound on reels for storage.

Macroencapsulation of electrolytes in Kel-F 81 tubing was achieved with payloads (grams electrolyte/gram of tubing) greater than 80 percent. Loss rate of the electrolyte was about 1 percent per year, measured at ambient conditions. The microencapsulation of aqueous solutions in 1000-micron-diameter capsules showed high water loss rates (0.3 to 4 percent/day), and initial payloads ranged from 40 to 75 percent (ref. 47).

ANODE-CATHODE COUPLE TESTING

The anode-cathode couples were tested both statically and dynamically. Used in the static tests was a sandwich-type cell in which a tape cell was held together between two polypropylene plates by means of spring clamps. In the case of the aqueous static test cell, holes were drilled in one of the plates to permit gas venting. The nonaqueous static cell was essentially the same as the aqueous cell except for its vaportight construction. Platinum foil was used as the cathode-current collector in both cells. A buret or hypodermic needle was used to feed 0.5 to 1 ml of electrolyte into the cell. Static polarization measurements were used for screening and optimizing materials and parameters of tape cells.

The dynamic tests were conducted on a tester capable of continuously testing a tape cell at speeds of 0.002 to 1.0 in./min. An automatic voltage-current recording system was used for 24-hour operation. The electrolyte was fed to the tape by means of a pump. Dynamic tests of the machine-made Mg/trichlorotriazinetrione tape cell were conducted

for 4 hours at 2.0 volts and 15 mA/cm². These tape cells could be bent 180° around an 0.5-inch rod with no change in either physical or electrochemical properties.

Mechanical Device Development

The first prototype model of the dry-tape battery was driven by a 16-millimeter motion-picture camera motor with clock escapement mechanism (ref. 46). The anode, which also served as the current collector, was a zinc block, while the cathode current collector was a thin silver plate. The electrolyte was supplied by a second tape prewetted with electrolyte and stored separately ("dual-tape system"). The tape cell was a porous polypropylene tape coated with AgO. The two tapes were activated by bringing them together just before their entry between the current collectors.

The "dual-tape system" was replaced by a single-tape unit driven by a permanent magnet 4-Vdc gear motor. Four tapes were connected in series to provide 8 volts at a current of 1.5 to 2 amperes using the magnesium/potassium periodate system. Tape-speed adjustment was from 0.1 to 0.25 in./min with capacity for approximately 75 feet of tape and total device weight of 2.4 pounds. The parasitic power requirement for tape drive was approximately 0.3 watt, or 2 to 3 percent of the power output (ref. 47).

Overall Capabilities and Promise

The aqueous $Mg/MgBr_2$/trichloroisocyanuric acid system delivered 115 to 120 W-h/lb at a constant 2.0 volts. The nonaqueous $Li/LiClO_4$-methyl formate/dichloroisocyanuric acid cell was developed as a system which delivered 213 W-h/lb at a constant 3.2 volts based on the weights of the anode, cathode, separator, and electrolyte. Preliminary tests of a $Zn/KOH/O_2$ cell gave in excess of 100 W-h/lb (ref. 48).

The feasibility of the dry-tape concept has been demonstrated. The device is essentially a fuel cell using a combination of liquid electrolyte and solid fuels, all of which are individually storable. Because of the relatively short time of contact between anode, cathode, and electrolyte, unstable combinations of materials may be used which offer higher energy density than more stable battery combinations. For the same reason, no consideration need be given to the wet-stand capabilities of the materials.

A number of problems must be solved before the dry-tape system can be used as a working device. A mechanical tape drive of sufficiently high reliability must be designed. This is obviously not beyond the state of the art, but considerable engineering must be done before it becomes a reality. A demand-controlled, variable-speed drive must be designed and built to take advantage of the energy densities offered by the system.

The advisability of continuing the development to the flight-hardware stage depends on mission requirements. The dry-tape device itself, assuming a final design weight of 50 lb/kW (similar to that of a fuel cell) and a final fuel-electrolyte energy density of 200 W-h/lb, is clearly not competitive with the 1000 W-h/lb of the H_2-O_2 fuel cell over relatively

short missions. On longer continuous-duty missions, the total mass of fuel required (assuming that the H_2-O_2 fuel cell cannot be used because of fuel-storage problems) would be too great to be competitive with solar-energy-conversion systems. The dry-tape device can be effective in a mission, such as an interplanetary probe, in which power consumption rises drastically at the end of the mission, and the total energy requirement is large enough to offset the weight disadvantage imposed by the tape drive and control system.

REFERENCES

1. ABENS, S. G.; CORBETT, R.; MERZ, W. C.; AND G. AND W. H. CORSON, INC.: Development of High-Energy Density Primary Batteries. Third Quarterly Report on Lewis Research Center Contract no. NAS 3-7632, Dec. 22, 1965, to Mar. 21, 1966, Livingston Electronic Corp. (Montgomeryville, Pa.). No date. (Available as NASA CR-54992, N66-31225.)

2. ELLIOTT, W. E.; HUFF, J. R.; JAMROZY, J. L.; McDONALD, G. D.; SIMMONS, G. L.; AND TOWLE, W. L.: A Program To Develop a High-Energy Density Primary Battery With a Minimum of 200 Watt-Hours per Pound of Total Battery Weight. Sixth Quarterly Report on Lewis Research Center Contract no. NAS 3-6015, Globe-Union, Inc., Globe Battery Div. (Milwaukee, Wis.), Jan. 15, 1966. (Available as NASA CR-54873, N66-16139.)

3. ABENS, S. G.; MAHY, T. X.; MERZ, W.; MEYERS, W. F.; AND G. AND W. H. CORSON, INC.: Development of High-Energy Density Primary Batteries, 200 Watt-Hours per Pound Total Battery Weight Minimum. Final Report on Lewis Research Center Contract no. NAS 3-6004, June 10, 1964, to June 9, 1965, Livingston Electronic Corp. (Montgomeryville, Pa.). No date. (Available as NASA CR-54803, N66-29446.)

4. MEYERS, W. F.; AND G. AND W. H. CORSON, INC.: High-Energy Density Primary Batteries. Final Report on Lewis Research Center Contract no. NAS 3-2775, Livingston Electronic Corp. (Montgomeryville, Pa.), 1964. (Available as NASA CR-54083, N64-31454.)

5. BAUMAN, H. F.; CHILTON, G. E.; CONNER, W. J.; AND COOK, G. M.: New Cathode-Anode Couples Using Nonaqueous Electrolytes. AF33(616)-7957, RTD-TDR-63-4083, Lockheed Missiles & Space Co. (Sunnyvale, Calif.), Oct. 1963.

6. CHILTON, J. E.; CONNER, W. J.; COOK, G. M.; AND HOLSINGER, R. W.: Lithium-Silver-Chloride Secondary Battery Investigation. Final Report, AF33(615)-1195, AFAPL-TR-64-147, Lockheed Missiles & Space Co. (Sunnyvale, Calif.), Feb. 1965.

7. BAUMAN, H. F.; ET AL.: Lithium Anode Limited Cycle Battery Investigation. Annual Report, AF33(615)-2455, AFAPL-TR-66-35, Lockheed Missiles & Space Co. (Sunnyvale, Calif.). No date.

8. BODEN, D. P.; BUHNER, H. R.; AND SPERA, V. J.: High-Energy System (Organic Electrolyte). Final Report, DA 28-043 AMC-01394(E), Electric Storage Battery Co. (Raleigh, N.C.), Sept. 1966.

9. LYALL, A. E.; AND SEIGER, H. N.: Lithium-Nickel Halide Secondary Battery Investigation. Final Report, AF33(615)-1266, AFAPL-TR-65-11, Gulton Industries, Inc. (Metuchen, N.J.), Jan. 1965.

10. LYALL, A. E.; AND SEIGER, H. N.: Lithium-Nickel Halide Secondary Battery Investigation. Final Report, AF33(615)-2166, AFAPL-TR-65-128, Gulton Industries, Inc. (Metuchen, N.J.), Mar. 1966.

11. BRAEUER, K. H. M.; AND HARVEY, J. A.: Status Report on Organic Electrolyte High-Energy Density Batteries. Technical Report ECOM-2844, U. S. Army Electronics Command, May 1967.

12. FARRAR, J.; KELLER, R.; AND MAZAC, C. J.: Investigation of High-Energy Density Electrochemical Systems, Part 4. High-Energy Battery System Study. Paper presented at the 18th Annual Power Sources Conference (Fort Monmouth, N.J.), May 19–21, 1964, p. 92.

13. SELIM, R. G.: Investigations of High-Energy Density Electrochemical Systems, Part 2. Electrode Behavior in Organic Solvent. Paper presented at the 18th Annual Power Sources Conference (Fort Monmouth, N.J.), May 19–21, 1964, p. 86.

14. HILL, K. R.; RAO, M. L. B.; AND SELIM, R. G.: Research and Development of a High Capacity, Nonaqueous Secondary Battery. Final Report on Lewis Research Center Contract no. NAS 3-6017, Oct. 1964 to Dec. 1965, P. R. Mallory & Co., Inc. (Burlington, Mass.), Feb. 14, 1965 [sic 1966]. (Available as NASA CR-54969, N66-35218.)

15. ATHEARN, L. F.; BYRNE, J. J.; MACDONALD, J. C.; AND WILLIAMS, D. L.: Research and Development of the Dry Tape Battery Concept. First Quarterly Report on Lewis Research Center Contract no. NAS 3-7624, June 9 to Sept. 8, 1965, Rept. no. MRB 5010Q1, Monsanto Research Corp., Boston Laboratory (Everett, Mass.), Oct. 8, 1965. (Available as NASA CR-54782, N66-12169.)

16. BAUMAN, H. F.: Limited Cycle Secondary Battery Investigation. Final Report, AF33(657)-11709, APL-TDR-64-59, Lockheed Missiles & Space Co. (Sunnyvale, Calif.), May 1964.

17. HILL, K. R.; AND SELIM, R. G.: Research and Development of a High Capacity Nonaqueous Secondary Battery. Final Report on Lewis Research Center Contract no. NAS 3-2780, July 1963 to Sept. 1964, P. R. Mallory &.Co., Inc., Laboratory for Physical Science (Burlington, Mass.), Aug. 15, 1965. (Available as NASA CR-54880, N66-22942.)

18. CHILTON, J. E.; DUFFEK, E. F.; AND REED, A. E.: Development of High Energy Batteries. Final Report on NASA Headquarters Contract no. NASw-111, Project no. SU-3045, Stanford Research Institute (Menlo Park, Calif.), Apr. 28, 1961. (Available as NASA CR-74410, N66-23660.)

19. BAUMAN, H. F.; CHILTON, J. E.; CONNER, W. J.; AND COOK, G. M.: New Cathode-Anode Couples Using Nonaqueous Electrolytes. AF33(616)-7957, ASD-TDR-62-1, Lockheed Missiles & Space Co. (Sunnyvale, Calif.), Apr. 1962.

20 ADLER, R. W.; ELLIOTT, W. E.; HUFF, J. R.; JAMROZY, J. L.; AND TOWLE, W. L.: A Program to Develop a High-Energy Density Primary Battery With a Minimum of 200 Watt-Hours per Pound of Total Battery Weight. Fifth Quarterly Report on Lewis Research Center Contract no. NAS 3-6015, July 1 to Sept. 30, 1965, Globe-Union, Inc., Globe Battery Division (Milwaukee, Wis.), Oct. 15, 1965. (Available as NASA CR-54744, N66-11247.)

21. ELLIOTT, W. E.; MCDONALD, G. D.; AND TONI, J. E. A.: Lithium-Moist Air Battery. First Semiannual Report, DA-44-009-AMC-1552(T), Globe-Union, Inc. (Milwaukee, Wis.), Oct. 1966.

22. DRISCOLL, J. S.; AND WILLIAMS, D. L.: Research and Development of the Dry Tape Battery Concept. Fourth Quarterly Report on Lewis Research

Center Contract no. NAS 3-7624, Mar. 9 to June 9, 1966, Rept. no. MRB 5010Q4, Monsanto Research Corp., Boston Laboratory (Everett, Mass.), Aug. 2, 1966. (Available as NASA CR-54771, N66-37408.)

23. PAEZ, O.; SEO, E. T.; AND SILVERMAN, H. P.: Voltammetric Studies of Nonaqueous Systems. First Semiannual Report, DA-28-043-AMC-02464(E), TRW Systems (Redondo Beach, Calif.), Apr. 1967.

24. ABENS, S. G.; MAHY, T. X.; MERZ, W. C.; AND G. AND W. H. CORSON, INC.: Development of High-Energy Density Primary Batteries. Second Quarterly Report on Lewis Research Center Contract no. NAS 3-7632, Sept. 22 to Dec. 21, 1965, Livingston Electronic Corp. (Montgomeryville, Pa.). No date. (Available as NASA CR-54920, N66-23463.)

25. BODEN, D. P.; BUHNER, H. R.; AND SPERA, V. J.: High Energy System (Organic Electrolyte). First Quarterly Report, DA 28-043 AMC-02304(E), Electric Storage Battery Co. (Raleigh, N.C.), Dec. 1966.

26. BRUINS, P. F.: Calorimetric Study of the Thermodynamic Properties of the Nickel-Cadmium Cell. Semiannual Report on Goddard Space Flight Center Grant no. NGR 33-006-015, Oct. 1, 1964, to Apr. 1, 1965, Polytechnic Institute of Brooklyn, Dept. of Chem. Engineering (New York, N.Y.). No date. (Available as NASA CR-63338, N65-85671.)

27. ABENS, S. G.; MAHY, T. X.; MERZ, W. C.; AND G. AND W. H. CORSON, INC.: Development of High Energy Density Primary Batteries. First Quarterly Report on Lewis Research Center Contract no. NAS 3-7632, June 22 to Oct. 21, 1965, Livingston Electronic Corp. (Montgomeryville, Pa.), Dec. 28, 1965. (Available as NASA CR-54859, N66-15342.)

28. JOHNSON, R. E.: Electrolyte Solvent Properties of Organic Sulfur Derivatives. Rept. no. E-3494. No date. Lewis Research Center.

29. JASINSKI, R. J.; AND KIRKLAND, S.: Anal. Chem., vol. 39, 1967, p. 1663.

30. ABENS, S.; ET AL.: Third Quarterly Report, NAS 3-7632, Apr. 1967.

31. FOSTER, J. N.; HON, J. F.; KELLER, R.; AND SULLIVAN, J. M.: Properties of Nonaqueous Electrolytes. Third Quarterly Report on Lewis Research Center Contract no. NAS 3-8521, Dec. 20, 1966, to Mar. 19, 1967, Rept. no. R-6754-3, North American Aviation, Inc., Rocketdyne Division (Canoga Park, Calif.), Apr. 19, 1967. (Available as NASA CR-72065.)

32. FOSTER, J. N.; HON, J. F.; KALMAN, O. F.; KELLER, R.; AND SULLIVAN, J. M.: Properties of Nonaqueous Electrolytes. Fourth Quarterly Report on Lewis Research Center Contract no. NAS 3-8521, Mar. 20 to June 19, 1967, Rept. no. R-6754-4, North American Aviation, Inc., Rocketdyne Division (Canoga Park, Calif.), July 19, 1967. (Available as NASA CR-72277.)

33. FOSTER, J. N.; KELLER, R.; AND SULLIVAN, J. M.: Properties of Nonaqueous Electrolytes. First Quarterly Report on Lewis Research Center Contract no. NAS 3-8521, June 20 to Sept. 19, 1966, Rept. No. R-6754-1, North American Aviation, Inc., Rocketdyne Division (Canoga Park, Calif.), Oct. 19, 1966. (Available as NASA CR-72106.)

34. FOSTER, J. N.; KELLER, R.; RAY, J. D.; AND SULLIVAN, J. M.: Properties of Nonaqueous Electrolytes. Second Quarterly Report on Lewis Research Center Contract no. NAS 3-8521, Sept. 20 to Dec. 19, 1966, Rept. no. R-6754-2, North American Aviation, Inc., Rocketdyne Division (Canoga Park, Calif.), Jan. 19, 1967. (Available as NASA CR-72168.)

35. FOLEY, R. T.; HELGEN, L. E.; AND SCHUBERT, L.: Investigation of Electrochemistry of High Energy Compounds in Organic Electrolytes. Third Semiannual Report on Lewis Research Center Grant no. NGR-09-003-005,

Nov. 1, 1965, to Apr. 30, 1966, The American Univ., Chem. Dept. (Washington, D.C.). No date.

36. BOGAR, F. D.; AND FOLEY, R. T.: Investigation of Electrolytes of High Energy Compounds in Organic Electrolytes. Fifth Semiannual Report on Lewis Research Center Grant no. NGR–09–003–005, Nov. 1 to Apr. 30, 1967, The American Univ., Chem. Dept. (Washington, D.C.). No date.

37. ELLIOTT, W. E.; HSU, S.; AND TOWLE, W. L.: The Development of High Energy Density Primary Batteries, 200 Watt-Hours per Pound of Total Battery Weight Minimum. Final Report on Lewis Research Center Contract no. NAS 3–2790, Aug. 1, 1963, to July 31, 1964, Globe-Union, Inc. (Milwaukee, Wis.), Jan. 1965. (Available as NASA CR–54153, N65–17991.)

38. FOLEY, R. T.; SWINEHART, J. S.; AND SCHUBERT, L.: Investigation of Electrochemistry of High Energy Compounds in Organic Electrolytes. First Semiannual Report on Lewis Research Center Grant no. NGR–09–003–005, Nov. 1, 1964, to Apr. 1965, The American Univ., Chem. Dept. (Washington, D.C.). No date. (Available as NASA CR–63741, N65–27831.)

39. FOLEY, R. T.; HELGEN, L. E.; AND SCHUBERT, L.: Investigation of Electrochemistry of High Energy Compounds in Organic Electrolytes. Second Semiannual Report on Lewis Research Center Grant no. NGR–09–003–005, May 1 to Oct. 31, 1965, The American Univ., Chem. Dept. (Washington, D.C.). No date. (Available as NASA CR–62023, N66–14600.)

40. JASINSKI, R. J.: An Analysis of All Potentially Useful High-Energy Battery Systems. Final Report, NOw 64–0653–f, Tyco Laboratories, Inc., July 1965.

41. ELLIOTT, W. E.; ET AL.: A Program To Develop a High-Energy Density Primary Battery With a Minimum of 200 Watt-Hours per Pound of Total Battery Weight. First Quarterly Report, NAS 3–6015, July–Sept. 1964, Globe-Union, Inc. (Milwaukee, Wis.). No date.

42. EISENBERG, M.: Research on a High Energy Nonaqueous Battery System. Second Quarterly Report, NOw 66–0342–c, Mar.–May 1966, Electrochimica Corp. (Menlo Park, Calif.). No date.

43. EISENBERG, M.: Paper presented at the fall meeting of the Electrochem. Soc. (Washington, D.C.), Oct. 1964.

44. EISENBERG, M.: Paper presented at the fall meeting of the Electrochem. Soc. (Philadelphia, Pa.), Oct. 1966.

45. EISENBERG, M.: Research on a High Energy Nonaqueous Battery System. First Quarterly Report, NOw 66–0342–c, Dec. 1965 to Mar. 1966, Electrochimica Corp. (Menlo Park, Calif.). No date.

46. BORSANYI, A. S.; GRUBER, B. A.; KAFESJIAN, R.; KLUNDER, K. W.; AND SMITH, J. O.: Development and Feasibility Proof of the Dry Tape Battery Concept. Final Report on Lewis Research Center Contract no. NAS 3–2777, June 14, 1963, to Jan. 23, 1964, Rept. no. MRB 5001F, Monsanto Research Corp., Boston Laboratories (Everett, Mass.), Mar. 31, 1964. (Available as NASA CR–56132, N64–20703.)

47. BYRNE, J. J.; GRUBER, B. A.; KAFESJIAN, R.; KLUNDER, K. W.; McELHILL, E. A.; POWER, W. H.; WOLANSKI, T. J.; AND ZIRIN, L. I.: Development of the Dry Tape Battery Concept. Final Report on Lewis Research Center Contract no. NAS 3–4168, Monsanto Research Corp., Boston Laboratories (Everett, Mass.), Dec. 1965. (Available as NASA CR–347, N66–12128.)

48. BORSANYI, A. S.; BYRNE, J. J.; DRISCOLL, J. S.; AND WILLIAMS, L.: Research and Development of the Dry Tape Battery Concept. Final Report on Lewis Research Center Contract no. NAS 3–7624, June 9, 1965, to Mar. 1, 1967, Monsanto Research Corp., Boston Laboratory (Everett, Mass.), Apr. 26, 1967.

CHAPTER 11

Fundamental Studies

In addition to supporting battery design, development, and testing, NASA has given a small amount of support to fundamental electrochemical studies. The studies which are directly related to the field of batteries are summarized here. A program concerned with the behavior of porous electrodes resulted in a series of reports and masters' theses based on work conducted at the University of California at Berkeley and summarized in reference 1. In these studies, Grens (ref. 2) developed a one-dimensional mathematical model of a porous electrode in the form of a complex set of nonlinear differential equations. The porous-electrode behavior model provides both steady-state and transient predictions of the reaction distribution in a porous electrode and the relationship between current density and overpotential. Because the final equation was too complex for analytical solution, an iterative numerical procedure for converging on a solution was devised and implemented in a computer program.

To provide experimental verification for the electrode behavior model, three independent investigations were conducted based upon reactions at the solid-liquid interface of a flooded porous electrode. Bomben (ref. 3) simulated a porous electrode structure by forming a multilayer electrode with alternate layers of fine nickel mesh and nylon mesh. Each layer of mesh was insulated from the others to allow the flow of current through each layer to be measured independently. The convection effects at the surface of the electrode were minimized by establishing conditions of turbulent fluid flow.

The ferroferricyanide oxidation-reduction reaction was investigated using this multilayer electrode. When the results of this experiment were compared with the theoretical one-dimensional model, the agreement was poor. This disagreement was attributed to several factors, including the large pore size (about 100 μ), which permitted convective electrolyte flow within the pores; inadequate turbulence of flow across the electrode face; and the need for introduction of current-measuring shunts in each of the circuits, which, although compensated for in the solution of the mathematical model, largely destroyed the model's utility. Other factors were also cited, such as trace impurities, and nonhomogeneity of electrode porosity due to buckling of the screens.

Better control of pore dimensions was achieved in a second experiment in which 5- and 10-layer segmented electrodes were assembled,

machined flat, and a single pore created by mating the surfaces of 2 segmented electrode halves. Pores of from 50- to 500-μ diameter were formed and the behavior of the electrode studied using the ferroferricyanide reaction. To avoid convection within the fissure or pore, a porous glass filter disk was used to stabilize the fluid. When the measured data disagreed with the theoretical model, the differences were attributed to dimensional instability of the fissure over a period of time, natural convection in the fissure, and the larger thickness of the electrode layers which made the measurements too coarse grained. Alkire (ref. 4) approached the problem of experimental verification of the model by electrolytically dissolving in sulfuric acid a porous copper electrode made of spherical particles of uniform diameter, and by determining the average rate of solution by microscopic examination and mapping of the electrode after it had been filled with a potting compound, sectioned, and polished.

The accuracy of copper-loss estimation as a function of the depth in the electrode was reduced by variations in the uniformity of the starting porous electrode. Only qualitative agreement was found between theory and experiment. Other experimental difficulties included exfoliation of copper particles from the electrode surface due to weakening of the sintered bonds by removal of copper, occlusion of reaction products within the pores of the metal, and poor correspondence between the calculated electrolytic metal removal and the actual weight changes of the electrodes.

Nanis and Javet (ref. 5) studied the transient behavior of theoretical electrodes during faradaic capacitance charging. An equation was derived which enabled the calculation of the electrode overpotential as a function of time during the charging period. Specimen calculations are shown for cases in which the capacitance increases, decreases, and remains constant as the overpotential changes. The calculation results suggest that caution be used in interpreting the initial slope of the overpotential transient voltage wave as being proportional in all cases to the faradaic capacitance.

Nanis and Adubifa (refs. 6 and 7) investigated a method of determining the thickness of boundary layers by measuring overpotential. There was good agreement with theory in most cases.

A series of reports by DeWane and Hamer give values of various electrochemical properties, including equivalent conductance of aqueous HCl solutions (refs. 8 and 9) and equivalent conductance of aqueous HI solutions (ref. 10).

Mean activity coefficients of dilute solutions of electrolytes were calculated by several approximate equations and printed in tabular form as a function of ionic strength and temperature (ref. 11).

REFERENCES

1. ALKIRE, R. C.; GRENS, E. A., II; MULLER, R. H.; AND TOBIAS, C. W.: Research on the Dynamic Behavior of Porous Electrode Systems. Final Report on NASA Headquarters Contract no. NSG 150-61, Series no. 6, Issue no. 22, Univ. of Calif., Space Sciences Laboratory (Berkeley, Calif.), June 24, 1965. (Available as NASA CR-64108, N65-30473.)

2. GRENS, E. A., II: Dynamic Analysis of a One-Dimensional Porous Electrode Model. Ph.D. thesis written under NASA Headquarters (Washington) Contract no. NSG 150-61, Series no. 4, Issue no. 55, Univ. of Calif., Space Sciences Laboratory (Berkeley, Calif.), Sept. 1963.

3. BOMBEN, J. L.: Current Distribution in a Porous Electrode. Master's thesis written under NASA Headquarters (Washington) Contract no. NSG 150-61, Series no. 4, Issue no. 56, Univ. of Calif., Space Sciences Laboratory (Berkeley, Calif.), Sept. 1963. (Available as NASA CR-52415, X64-10180.)

4. ALKIRE, R. C.: Reaction Distribution in a Porous Anode. Master's thesis written under NASA Headquarters (Washington) Contract no. NSG 150-61, Univ. of Calif., Space Sciences Laboratory (Berkeley, Calif.), 1963.

5. ANON.: Conversion of Various Forms of Energy by Unconventional Techniques. Eleventh Progress Report on NASA Headquarters (Washington) Contract no. NSG 316, Rept. no. INDEC-SR-11, Univ. of Pa., Institute for Direct Energy Conversion (Philadelphia, Pa.), Mar. 1967.

6. ANON.: Conversion of Various Forms of Energy by Unconventional Techniques. Ninth Progress Report on NASA Headquarters (Washington) Contract no. NSG 316, Rept. no. INDEC-SR-9, Univ. of Pa., Institute for Direct Energy Conversion (Philadelphia, Pa.), Oct. 31, 1966.

7. ANON.: Conversion of Various Forms of Energy by Unconventional Techniques. Sixth Progress Report on NASA Headquarters (Washington) Contract no. NSG 316, Rept. no. INDEC-SR-6, Univ. of Pa., Institute for Direct Energy Conversion (Philadelphia, Pa.), July 1, 1965.

8. DeWANE, H. J.; AND HAMER, W. J.: Compilation of Critically Evaluated Electrochemical Data, Part IV. Eighth Quarterly Report on NASA Headquarters Contract no. NAS R-09-022-029, July 1 to Sept. 30, 1966, NBS Rept. no. 9432, U.S. Dept. of Commerce, National Bureau of Standards (Washington, D.C.), Oct. 12, 1966.

9. DeWANE, H. J.; AND HAMER, W. J.: Compilation of Critically Evaluated Electrochemical Data, Part III. Seventh Quarterly Report on NASA Headquarters Contract no. NAS R-09-002-029, Apr. 1 to June 30, 1966, NBS Rept. no. 9394, U.S. Dept. of Commerce, National Bureau of Standards (Washington, D.C.), Aug. 15, 1966.

10. DeWANE, H. J.; AND HAMER, W. J.: Compilation of Critically Evaluated Electrochemical Data, Part V. Ninth Quarterly Report on NASA Headquarters Contract no. NAS R-09-022-029, Oct. 1 to Dec. 31, 1966, NBS Rept. no. 9472, U.S. Dept. of Commerce, National Bureau of Standards (Washington, D.C.), Jan. 16, 1967.

11. HAMER, W. J.: Compilation of Critically Evaluated Electrochemical Data, Part II. Sixth Quarterly Report on NASA Headquarters Contract no. NAS R-09-022-029, Jan. 1 to Mar. 31, 1966, Institute of Basic Standards no. 9047, U.S. Dept. of Commerce, National Bureau of Standards (Washington, D.C.). No date. (Available as NASA CR-74558, N66-24494.)

Principles of DC Electric-Power System Design

A primary requirement of an aerospace electric-power system is the delivery of closely regulated electric power to a variety of consuming load-equipment types at an almost equally large variety of voltages.   If the lifetime of the equipment is intended to be more than a few hours or days, the logistics of energy supply are such that a secondary battery system and solar-energy-gathering power source are lighter in weight than a primary battery or fuel-cell system.   Such secondary systems employ solar arrays for gathering energy from the Sun, converting approximately 10 percent of the incident energy to electrical energy, and storing a portion of the energy in secondary batteries for use when the power requirements exceed the solar-array output power.   Other primary power sources have been investigated, and radioisotope thermoelectric power sources have been flown in a few satellites in the Tiros program.   However, solar arrays remain the mainstay of the long-life satellite primary power source field at the present time.

In most cases, the solar array (or other primary power source) is the single most expensive item in the entire satellite.   The total radiant energy falling on a flat surface normal to the satellite Sun line is approximately 130 W/ft². The solar array can convert only 10 percent of this energy at the beginning of its life, and approximately 7 to 7.5 percent after a period in space.   The result is an electric-power availability of approximately 8 to 10 W/ft².

When solar arrays are mounted on spinning cylindrical or spherical vehicles, the efficiency of the solar array must be divided by π in the cylindrical case, and by 4 in the spherical case, leading to overall power outputs of 2 to 3.5 W/ft² of installed solar-array surface area.   Similar considerations apply to other power sources as well.   The result is a stringent requirement for the conservation of electric energy by the design of high-efficiency power systems.   In recognition of this, NASA has supported systems studies leading to the maximum utilization of power (ref. 1).

SYSTEM EFFICIENCY

The overall efficiency of an electric-power system is defined as

$$H = \frac{\epsilon_o}{\epsilon_i} \tag{12-1}$$

221

where

    ϵ_o output energy
    ϵ_i input energy

Note that it is not possible to describe efficiency as the ratio of output to input powers. If the system is running on stored energy, the input power is zero and the efficiency value is therefore infinity.

ENERGY BALANCE AND EFFICIENCY

Generally, satellite and space-vehicle power systems without a battery are power limited. When a battery is introduced into the system, the high current-delivery capability of the battery, and the relatively small energy-collection area of the solar array (or the limited primary source power if another power source is used), make the system essentially energy limited. Without a battery, the system must be optimized at the maximum load power, and the efficiency under all other circumstances is of little significance. With a battery in the system, the efficiency must be optimized over the entire cycle, so that the total energy transferred from source to the load, through the intermediacy of an energy storage system, is a maximum.

In a solar-array-powered satellite having a constant load power demand, P_L, in an orbit of eclipse duration, t_e, and illuminated period, t_d, the total energy required from the energy storage units, ϵ_s, is given by

$$\epsilon_s = \left(\frac{t_e}{\eta_d \eta_b}\right) P_L \tag{12-2}$$

where η_d is the efficiency of the battery discharge circuit, and η_b the watt-hour efficiency of the battery itself. The minimum power required to recharge the battery is

$$P_R = \frac{\epsilon_i}{t_d \eta_c} = P_L \left(\frac{t_e}{\eta_c \eta_d \eta_b t_d}\right) \tag{12-3}$$

where η_c is the efficiency of the charging circuit.

If the power is delivered from the source to the loads (which are considered to contain their own conditioning equipment) without further processing, the total source power required to operate the system is:

$$P_{sa} = P_L \left(1 + \frac{t_d}{\eta_b \eta_c \eta_d t_d}\right) = P_L \left(1 + \frac{t_d}{\eta_s t_d}\right) \tag{12-4}$$

where η_s is the storage system efficiency $= \eta_b \eta_c \eta_d$.

If power-consuming logic and controls are associated with the power subsystem and operate continuously, the losses in such equipment may be expressed as an efficiency, η_r, and the final solar-array power required for full system operation is

$$P_{sa} = \frac{P_L}{\eta_r} \left(1 + \frac{t_e}{\eta_s t_d}\right) \tag{12-5}$$

Obviously, in an entirely loss-free system $\eta_r = \eta_s = 1.0$ and the loss-free system power, P°_{sa}, is expressed as

$$P^\circ_{sa} = P_L(1 + t_e/t_d) \tag{12-6}$$

System efficiency,

$$H = \frac{P^\circ_{sa}}{P_{sa}} = \frac{1 + t_e/t_d}{(1/\eta_r)(1 + t_e/\eta_s t_d)} \tag{12-7}$$

The significance of this relationship in determining the effect of storage system efficiency upon solar-array requirements is that the required charge power, including losses, is multiplied by the fraction t_e/t_d, which varies from 0.667 in 100-minute circular orbits to 0.0526 in 24-hour circular orbits, and may become vanishingly small in some interplanetary probe applications. Thus, in the longer orbits the impact of efficiency of energy storage upon solar-array size is reduced.

INFLUENCE OF EFFICIENCY UPON BATTERY CAPACITY

The only efficiency factor influencing battery capacity is that of the discharge circuit, η_d; the required installed capacity (C_r) varies with the efficiency as follows:

$$C_r = \frac{P_L t_e}{\eta_d}$$

The above relationship assumes a constant battery-discharge voltage in eclipse, and shows that maximizing the efficiency of the discharge circuit is critical in minimizing battery weight.

BATTERY EFFICIENCY

The efficiency of the battery may be divided into two independent terms: an ampere-hour efficiency and an average discharge-charge voltage ratio. By doing this, the data in the foregoing chapters may be readily substituted into the system-efficiency equations. Efficiencies of various battery systems differ considerably from one another, and are, therefore, discussed in the chapters dealing with the particular battery systems.

EFFICIENCIES OF POWER-CONDITIONING EQUIPMENT

Efficiencies of various types of conversion and regulation equipment are dependent upon the design characteristics and circuit elements chosen. They also vary with the input voltage so that as the voltage of the unregulated bus changes with battery voltage, the efficiency of the entire system undergoes small changes which may, when added together, make significant changes in the overall system performance capability. Leisenring (ref. 1) discusses system efficiency considerations in great detail, and presents a method of designing for optimum system efficiency with considerable parametric data relating the size, weight, operating frequency, and efficiency of various types of electric-power-conversion equipment. However, the efficiencies of equipment shown are based upon the basic, nonredundant form of the device, and may be optimistic when compared with similar equipment employing high-reliability,

redundant circuitry. Similarly, the technique employed for system optimization is valid when considered from the standpoint of efficiency and weight alone. Reliability considerations, electromagnetic interference problems, and other detailed problems are not treated in the referenced work. Consequently, the conclusions reached must be considered in the light of the assumptions made and the omissions of important factors before they are accepted for a specific hardware application.

SOURCE—LOAD MATCHING

One of the major causes of power losses in spacecraft electric-power systems is a mismatch between the source and the main power subsystem bus. Figures 12-1 and 12-2 show the relationships between current and voltage and between power and voltage of two typical satellite primary power sources: the solar array and the radioisotope thermoelectric generator. Each of these has an optimum operating point at which the transfer of power from source to load is a maximum. Operation at
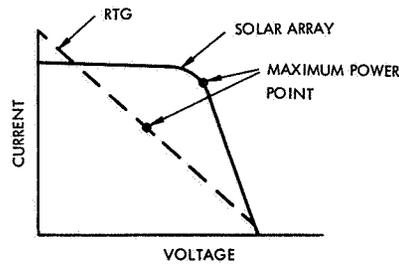
FIGURE 12-1.—Typical current-voltage characteristics of solar array and radioisotope thermoelectric generator (RTG).
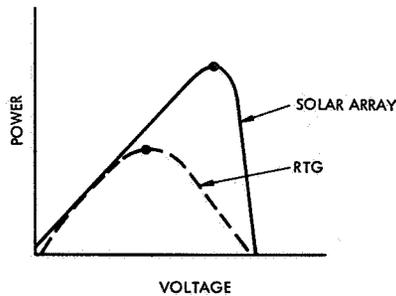
FIGURE 12-2.—Typical power characteristics of solar array and RTG.

the maximum power point permits the lightest weight and usually lowest cost design of the power source.

When the source delivers its power to an operating load, the operating point is determined by the intersection of the current-voltage characteristics of source and load. Figure 12-3 shows the operation of a solar array into a constant power load at the maximum power point. Should the load change, a mismatch in characteristic would shift the operating point away from the maximum power point, and the efficiency of power transfer would be reduced. An additional complication is introduced when a battery is added to the system. As an example of the difficulties created when three elements interact within a power system, consider a straight-through system as shown in figure 12-4. In this system, power is delivered directly from the solar array or other source to the loads without an intervening element which might introduce losses into the system. Theoretically, any energy which is not consumed by the loads
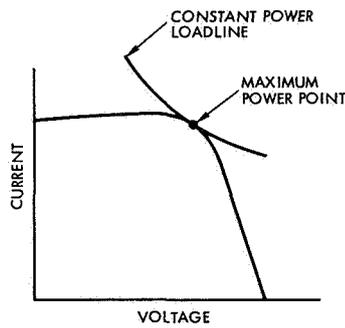
FIGURE 12-3.—Solar array/load interface diagram showing operation at the maximum power point.
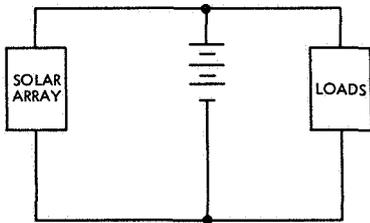
FIGURE 12-4.—Basic straight-through power subsystem block diagram.

will be dumped into the battery and stored there, since the battery appears to the source as another load in parallel with the operating loads. To achieve maximum power transfer during the battery-charging period in this type of system, the voltage of the solar array must be matched at the maximum power point to the charging voltage of the battery. Consequently, it is not possible to achieve a perfect match at the discharge voltage of the battery. If charge and discharge voltages are sufficiently disparate, the loads may operate at a far less favorable operating point than the original design point because of the mismatch in voltage characteristics (fig. 12-5). This condition can be severely aggravated by a large change in source-output characteristics such as may be encountered in solar-array-powered interplanetary vehicles.
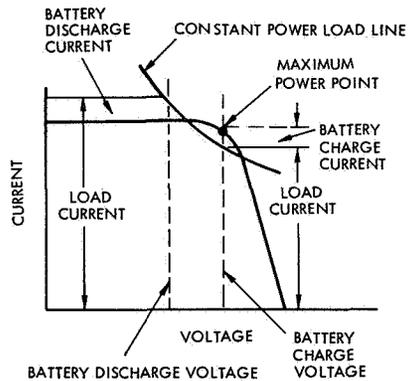
FIGURE 12-5.—Solar array/load battery interface diagram.

By introducing various kinds of control and conditioning elements into the power-system design, the relationship between the source, load, and battery can be altered. A comprehensive discussion of the interaction between solar arrays, batteries, and loads under changing source conditions may be found in reference 2, which is directed specifically toward interplanetary missions but whose underlying principles are valid in most situations.

SELECTION OF SYSTEM VOLTAGE

In many cases, the selection of system voltage is an arbitrary decision based upon factors which have little to do with power-system-design considerations. Frequently, the decision is made on the basis that existing equipment, already designed for operation at a specific voltage level, can be used somewhere in the spacecraft at a significant cost savings. Where decisions can be made on the basis of optimization of a power system, they are still made on a qualitative basis, rather than on any quantitative formula.

The useful range of system voltages is bounded by the following considerations:

(1) The main power-switching semiconductors in spacecraft electric-power conditioning and control devices are limited to approximately 100 volts by present technology. Although a few semiconductors having 400 volts and higher ratings exist, 100 volts appear to be a reasonable estimate of the maximum bus voltage practical at the present time.

(2) The minimum bus voltage practical at the present time is determined by the losses in the system, and the desire for high operating efficiency. Losses such as voltage drop in leads, diodes, and other semiconductors become increasingly significant as the system voltage falls. The effect is worsened by the increase in current required at a given power as system voltage decreases. Small systems of a few watts can be efficiently operated at voltages as low as 5 volts. Larger systems require higher voltages.

(3) The voltage of a system containing a battery is limited by reliability considerations. As voltage increases, the number of series-connected cells required increases proportionately, and the reliability falls.

Thus far, practical bus-voltage levels for spacecraft- and satellite-power systems have fallen in the 18- to 35-volt range. As power-system sizes increase in the near future, it is probable that bus voltages will tend to increase, perhaps as far as 100 volts. A study of device limitations upon electric-power systems is in progress at TRW Systems, but no published reports are available at this time.

FILTERING OF CONDUCTED NOISE AND RIPPLE

The use of a battery permanently connected to the main dc power bus provides a significant filtering action, reducing the bus-voltage excursions by supplying or absorbing the current swings fed back from dc-dc converters and other equipment. To date, no published work has been found which investigates this filtering action in detail, so that the relative effect of battery charging, discharging, etc., is not known. In addition, the charge-control requirements of the battery require that at some time during its operating cycle, the battery be isolated from the bus either completely, or by a resistance path whose values determine the overcharge current. This isolation requirement prevents use of the battery as a filter during the overcharge period.

TRANSIENT BEHAVIOR OF BATTERY SYSTEMS

Typically, batteries will absorb or deliver large current transients with moderate changes in voltage, provided that the duration of these transients is of the order of a few seconds. Nickel-cadmium batteries are rapid in their transient action; silver-zinc and silver-cadmium batteries sometimes require a few milliseconds of recovery time after the initiation of a step change in load before they reach a stable current

delivery level. This transient behavior is important in spacecraft applications because of the common requirement for large pulses of energy for purposes of ordnance ignition.

Data on the pulse-current delivery of most battery types as a function of the voltage change is conspicuously unavailable in the published literature.

DESIGNING FOR THE WORST CASE

It is common practice in spacecraft-system designs to design for the worst set of conditions likely to be encountered by the component in question. Frequently, the most obvious worst-case condition, the maximum eclipse case, is not necessarily the true worst case. Among the typical worst-case situations which have occurred in various systems designs are the following:

(1) The minimum-temperature, maximum-depth-of-discharge case, in which problems are encountered in recharging the battery at an acceptable rate due to its low temperature.

(2) The maximum-temperature, maximum-depth-of-discharge case, in which the lowered efficiency of the battery does not permit recharging.

(3) The mid-eclipse-season case, where the depth of discharge is at or near a maximum, but the memory effect has reduced the available capacity to an unacceptable level.

(4) The end-of-life case, in which the source has insufficient energy available to charge the battery at relatively low currents (typical of longer orbit periods, such as synchronous) because the efficiency of battery charge is reduced at the low current.

(5) Transient cases during launch, orbit adjustment, orbit acquisition, when the satellite may be operating under an entirely different set of conditions than the usual orbit-design conditions.

Other critical situations may occur because of large current demands for firing of ordnance, which can cause momentary loss of bus-voltage regulation, or when a fully charged battery has been decoupled from the bus to prevent overcharging or reconditioning and is unavailable in the event of a sudden demand.

REFERENCES

1. LEISENRING, J. G.: Study and Analysis of Satellite Power Systems Configurations for Maximum Utilization of Power. Phase I Technical Report on NASA Contract no. NAS 5–9178, Rept. no. 04898–6001–R000, TRW Systems (Redondo Beach, Calif.), Dec. 30, 1966.

2. BINCKLEY, W. G.: Power System Configuration Study and Reliability Analysis. Final Report on Jet Propulsion Laboratory Contract no. 951574, Rept. no. 07171–6001–R000, TRW Systems (Redondo Beach, Calif.), Sept. 18, 1967.

CHAPTER 13

Applications

TYPICAL APPLICATION NO. 1, COMMUNICATIONS SATELLITE

An analysis is made of one of the intermediate design stages of the Intelsat satellite, varying the design to illustrate specific points. Intelsat is a global commercial-satellite system designed to operate in a synchronous-equatorial orbit and provide continuous relay of telephone and television signals. Its 24-hour orbit spends a minimum of 22.8 hours in sunlight and a maximum of 1.2 hours in the Earth's shadow. The satellite is occulted by the Earth 48 successive days in each eclipse season. The period of each occultation increases from a few minutes for the initial occurrence to 1.2-hour maximum during the first half of the season and decreases during the second half. For almost 5 months after that the satellite is in constant sunlight. Two eclipse seasons occur each year.

Five years of continuous operation are desired prior to satellite replacement. Therefore, the nickel-cadmium system was selected because of its longevity. The power requirements of the Intelsat satellite are almost constant, except for single events such as firing of ordnance to ignite rocket motors, separation devices, etc., and for short-duration current pulses to operate relays. Both of these phenomena will be ignored in the following analysis because the energy consumed is negligible in comparison with the total energy balance of the satellite.

LOAD ANALYSIS

The initial step in the design and analysis of a spacecraft electric-power system is the analysis of load requirements. Load data are presented in the form of current-voltage curves which are then added to obtain an aggregate current-voltage characteristic curve for the entire satellite. The accuracy with which this is done determines the overall accuracy of the final result. However, to simplify this analysis, assume that the Intelsat power-consuming loads are concentrated in four elements.

The two traveling-wave-tube amplifiers are the final stage of the transmitter and provide the radiofrequency energy which is beamed back to Earth during relay operations. Their power consumption is constant and essentially independent of signal strength. They are fed several closely regulated voltages by individual regulated converters, which operate directly from the main power bus and perform both conversion

229

and regulation functions. The regulated converter has a "constant power" characteristic, and adjusts its current consumption as the input voltage varies so that the product of input voltage and current is approximately constant. Deviation from true-constant power is caused by varying efficiency with input voltage; the efficiency decreases slightly as the voltage increases.

The central equipment converter provides closely regulated voltages to all subsystems of the spacecraft except the power subsystem. It has a constant power characteristic like that of the traveling-wave-tube amplifier, and consumes approximately 21 watts at an input voltage of 29.4 volts.

The power-control unit contains power-system switching, logic, voltage-limiting controls, and battery-charge-control logic. It operates directly from the unregulated dc bus and is assumed to have a pure resistive characteristic. Throughout most, but not all, of its operating range, the power-control unit is essentially resistive in nature. Although the resistive characteristic is perturbed by the presence of active elements such as zener diodes, differential amplifiers, etc., the low power consumption reduces the impact of any error introduced by the assumption of a pure resistive characteristic. The power-control unit has a power consumption of 3 watts at 29.4 volts. Battery-reversal-protection electronics are also assumed to operate from the unregulated bus, and consume a maximum of 300 milliwatts at 29.4 volts.
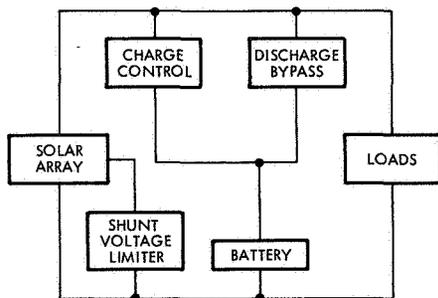
FIGURE 13-1.—Electric-power-system block diagram.

A block diagram of the power system and its loads is shown in figure 13-1. Figure 13-2 shows the characteristic curves of each of the loads, and the aggregate load characteristic of the entire satellite. Because of the narrow voltage range, the curvature of some of the constant power lines is slight.

SELECTION OF SYSTEM VOLTAGE AND VOLTAGE RANGE

On the basis of both convenience and common practice for a satellite power system of this size, approximately 28 volts is arbitrarily selected as the system voltage. The system-voltage range is determined in a system
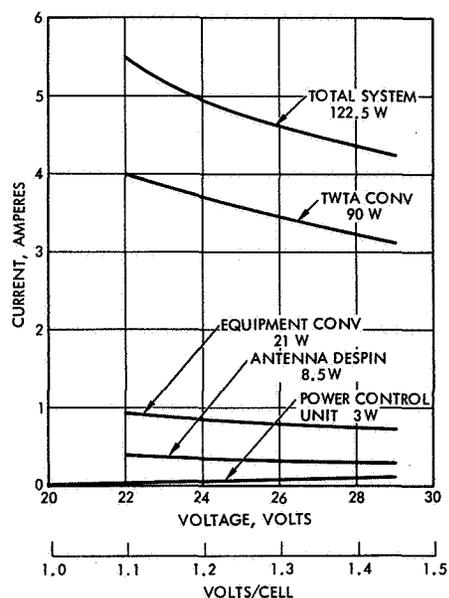
FIGURE 13-2.—Estimated   Intelsat   load
characteristic.

of this kind (parallel delivery of power from the solar array and battery to the loads) by the ratio of the maximum charge voltage to the minimum discharge voltage of the battery.   Early analysis of some of the individual loads resulted in a requirement for a minimum of 22 volts to be delivered to the equipment converter and the traveling-wave-tube converter. A convenient end-of-discharge voltage for a nickel-cadmium cell is 1.1 volts, resulting in a 20-cell battery.   The end-of-charge voltage is limited by the battery tolerance to 1.45 to 1.47 volts per cell, depending upon the method of charge control used.   This sets the maximum voltage which may be applied to the battery bus at 29.0 to 29.4 volts.   If the system design is such that the battery is decoupled from the main bus at the end of charge, system voltage may be allowed to go higher at that time, if advantageous.

ESTIMATION OF REQUIRED BATTERY SIZE

Because of stringent weight limitations on the satellites (designed to be launched in clusters, separated in space, and individually deployed to their operating stations), power subsystem and battery weights are critical.   The battery should operate at a high depth of discharge to minimize excess capacity, and should be reconditioned during the continuous sunlit periods after each eclipse cycle.   A conservative assumption, therefore, is that the battery will experience 48 deep-discharge cycles, and the electrical characteristics will then be representative of those at end of life.   Figure 13-3 shows the estimated electrical charac-

teristics of a nickel-cadmium cell at the end of a 48-cycle, 80-percent depth-of-discharge operation. Current is normalized to read amperes/ ampere-hour of cell capacity. A preliminary assumption of 59° F operation is made, and a maximum allowable depth-of-discharge constraint is placed upon the cell.

The minimum acceptable voltage line intersects the 20-percent capacity line at a current/capacity ratio of 0.3. This is equivalent to a discharge period of $(0.8)(3.33) = 2.66$ hours. However, the discharge period is only 1.2 hours in the worst eclipse. A more rapid discharge rate is required, up to the maximum possible rate of $1.2/0.8 = 1.5$ hours. This leads to a current/capacity ratio of $1/1.5 = 0.667$. A new current-voltage load line intersecting the minimum acceptable voltage line at or near 0.667 is overlaid on the I–V characteristic of the cell, and a preliminary estimate is made of the state of charge. In this case, the state of charge at which an interpolated current-voltage-cell characteristic line intersects the minimum allowable cell-voltage line at 0.667 is approximately 30 percent (dotted line). The capacity of the cell is estimated as

$$\text{Required capacity} = (P)(t)/(E_d)(n)(DOD) \qquad (13\text{--}1)$$

where

P	is system power $= 120$
E_d	is the average discharge voltage $= 1.2$ volts
t	is the maximum discharge time $= 1.2$ hours
n	is the number of series-connected cells $= 20$
DOD	is $1 -$ state of charge $= 0.7$

$$C = (120)(1.2)/(1.2)(20)(0.7) = 8.7 \text{ A-h}$$

of which

$$(120)(1.2)/(1.2)(20) = 6.0 \text{ A-h}$$

are actually used.

The nearest available size of a prismatic nickel-cadmium cell is the 9-A-h cell. Based upon the above calculation, a 9-A-h battery is assumed for further detailed analyses.

ESTIMATION OF THE ACTUAL DEPTH OF DISCHARGE

The preliminary estimate shown above leaves little or no margin for error, and one is tempted to size the battery at the next larger size to provide a degree of safety. However, a more detailed analysis may disclose the existence of a margin not yet apparent.

The current-voltage characteristic of the total spacecraft load is adjusted to match the scale of the cell characteristic curves by dividing the current axis by the battery capacity (9 A-h), and the voltage axis by the number of series-connected cells in the battery (20). This characteristic curve is then superimposed upon the cell's characteristic curves and the intersection points are read. The time between intersection points is calculated by using equation (3–1), and the voltage and current are plotted as functions of time. The area under the current-time curve is then integrated between $t = 0$ and $t = 1.2$ hour to determine the actual depth of discharge, and the voltage at the 1.2-hour mark is read to
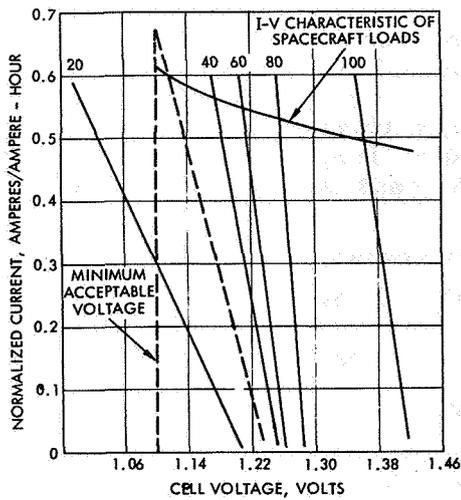
FIGURE 13-3.—59° F end-of-life current-voltage characteristic (estimated).
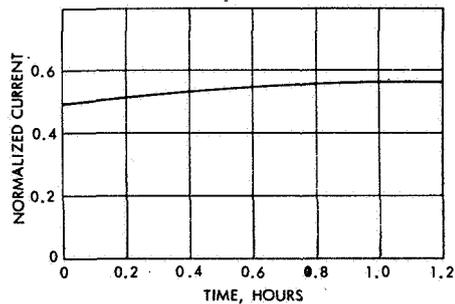
FIGURE 13-4.—Load current as a function of time at constant power.

determine the minimum voltage. Figure 13-4 shows the plotted current curve as a function of time. After integration, this curve indicates that the actual capacity withdrawn from the battery is only 5.82 A-h, instead of the originally estimated 6.0 A-h, in spite of an increase in load from 120 watts in the initial crude calculation to 123 watts in the detailed analysis. This gives a depth of discharge of 64 percent, adding slightly to the design margin.

ESTIMATION OF THE STATE OF CHARGE ON RECHARGING

Clearly, the above calculations can be valid only if the cell or battery begins its discharge from a state of charge of 100 percent. Some assessment must therefore be made of the state of charge of the battery at the end of charge, under the actual operating conditions, and, if necessary,

the discharge analysis must be repeated using a new and different state of charge as a starting point. In principle, the method of calculation is the same as that of the discharge analysis, the primary difference being the need to analyze the simultaneous interaction of the charging power source (in this case the solar array), the loads, and the battery. It is, of course, necessary to take into account the charge-control logic and its effect upon the state of charge.

PRELIMINARY ESTIMATION OF PRIMARY SOURCE POWER REQUIREMENTS

Since all of the losses in the electric-power system except battery losses have been included in the power requirement estimates, equation (12–4) for the loss-free source power may be used. Neglecting battery losses

$$P_{sa} = P_{load}(1 + t_e/t_d) = (122.5)(1 + 1.2/22.8) = 128.0 \text{ W}$$

This power must be deliverable at the maximum charging voltage of the battery, 29.0 to 29.4 volts. The solar array is, therefore, sized to deliver a minimum of this amount of power at the end of its service life, when its power output has degraded to a minimum. The maximum power point is set at approximately 29.4 volts, although this value may change as a result of later analyses. Figure 13–5 shows an expanded portion of the current-voltage characteristic of such a solar array at the end of life. Superimposed upon this curve are the characteristics of the voltage limiter (a vertical line at 29.4 volts) and of the system loads as previously computed.

The current available for charging the battery varies as a function of the solar-array voltage. A plot of the available current as a function of system bus voltage, shown in figure 13–6, was derived by subtraction of the load current curve from the solar-array current curve in figure 13–5.
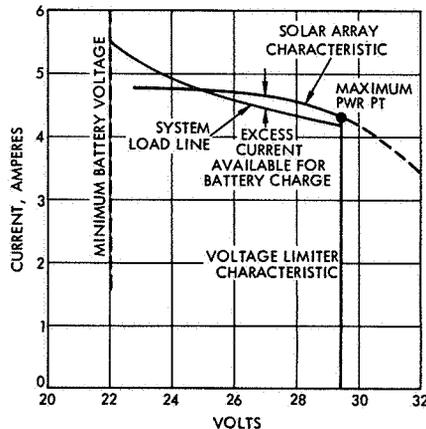
FIGURE 13–5.—Solar array/load interface diagram.
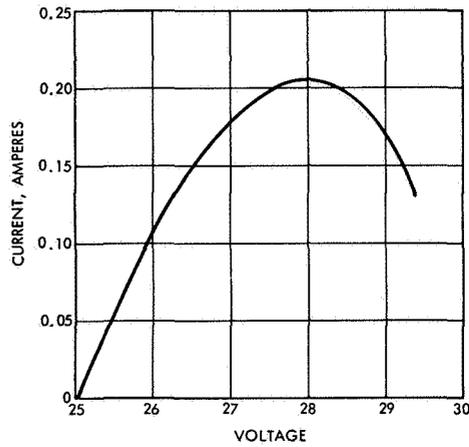
FIGURE 13-6.—Available charging current
calculated from figure 13-5.

For this exercise, it will be arbitrarily assumed that the maximum
temperature of the battery during the charging period is 90° F. There-
fore, the battery has a relatively low charging efficiency at low currents.
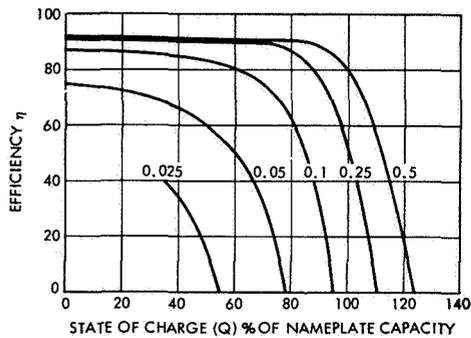
FIGURE 13-7.—Nickel-cadmium ampere-hour
efficiency at 90° F as a function of state of
charge and temperature. Normalized cur-
rent (I/C) as the third variable.

It can be seen from a cursory examination of the efficiency curves for
90° F operation (fig. 13-7) that at a charging current of 0.20 ampere
(C/45), the maximum state of charge which can be reached is 50 percent
or less before the conversion efficiency of the battery equals zero. At 90°
F, the available charge current must be increased to a value above C/10
before the 100-percent state of charge is achievable. Alternatively, if it
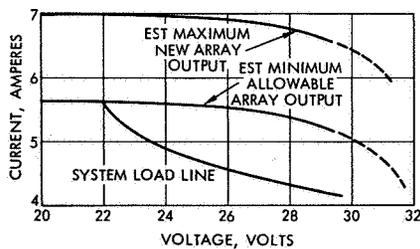
FIGURE 13-8.—Maximum and minimum
revised solar-array output and system
load characteristics.

is possible to manipulate the properties of the thermal control system so
as to decrease the temperature of the battery during charge, its efficiency
will be increased and a smaller available charge current will be required.

In this case, the option is to increase solar-array current by adding
additional strings of solar cells in parallel until the solar-array current
available for charging is increased to approximately 1 ampere, or C/9 at
the end of life of the solar array (fig. 13-8). The new curve for the
availability of charging current as a function of voltage is superimposed
upon the current-voltage characteristics of the cell (normalizing to I/C)
(fig. 13-9). This kind of relationship is valid because the impedance of
the battery is very much lower than that of the load or the solar array.
Therefore, the battery alone determines the system bus voltage as long as
it and the load are connected in parallel across the solar-array generator.
From the intersection of the available current curve with the battery
current-voltage curves at various states of charge, it is possible to compute
the state of charge and battery voltage as a function of time by means of
the equation:

$$Q = Q_0 + \sum_{t=0}^{t} (I)(\eta_{A-h})\Delta t$$

η_{A-h} = efficiency (A-h)

(13-2)

The product of the current and the efficiency are integrated over the
available charging period to determine state of charge. The variables
are manipulated until this integrated value indicates a return to the fully
charged state. Figure 13-10 shows the result of the charging process at
90° F. (Again, an alternative exists—that of failing to recharge the
battery beyond a specific point, and derating the battery performance
accordingly.)

CONTROL OF MAXIMUM BATTERY VOLTAGES

Having established that the battery will be returned to an acceptable
state of charge at the end of the charging period, it is necessary to prevent
overcharge at excessive rates in order to avoid overpressure damage.
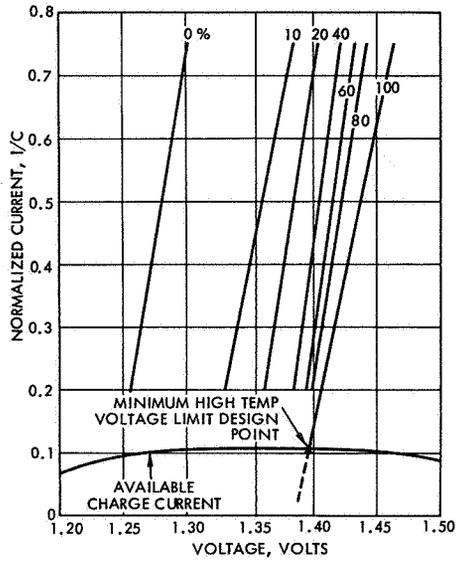
FIGURE 13-9.—High-temperature battery/
solar array/load interface (90° F). State-
of-charge, percent rated capacity:

$$Q = Q_0 + \int_{t=0}^{t} I \eta_{\text{A-h}} \, dt$$
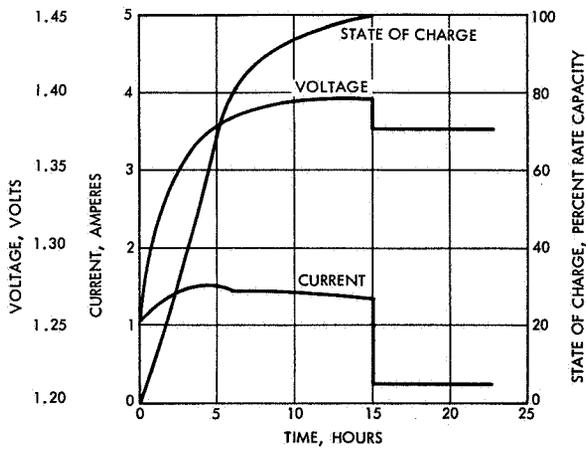
FIGURE 13-10.—System charging characteristics at 90° F
as a function of time.

Usually, the worst-case situation is a combination of maximum solar-array current and minimum battery temperature (if the two can occur together). Assuming (for purposes of illustration) a minimum battery temperature of 40° F, and a maximum possible solar-array characteristic as in figure 13-8, and superimposing the charge current curve upon the current-voltage characteristics of the battery at 40° F (fig. 13-11), it is
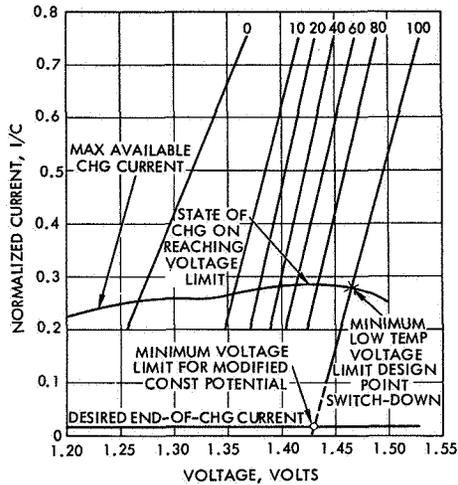
FIGURE 13-11.—Low-temperature battery/solar array/load interface diagram (40° F). State-of-charge, percent rated capacity:

$$Q = Q_0 + \int_{t=0}^{t} I \eta_{A\text{-}h} \, dt$$

possible that the battery will reach dangerously high voltages at some time in its charging cycle. Some method of control must be used which will prevent the battery from reaching dangerous voltages and yet permit it to return to a fully charged state within the available charging period. This defines the requirements of the charging period and the requirements of the charge-control system for this mode of operation.

SELECTION OF THE CHARGE-CONTROL METHOD

In general, if a charge control can be devised which will function properly at the extremes (maximum charge current with minimum battery temperature, and minimum charge current with maximum battery temperature), it will perform its function at all intermediate points.

Examination of the various alternatives for battery charge control

shows that it is possible to eliminate several after only cursory considera- tion. Slow charging is eliminated because of low efficiency. Stabistors are rejected because of low efficiency and marginal effectiveness in preventing overpressure failures. Amp-Gate diodes depend upon a sensitive thermal interface which must be designed independently of the equally sensitive battery-thermal interface. This causes almost insuper- able design complications. Coulometers (or A-h integrators) can be used only if the battery temperature can be held quite low. Since temperature has not yet been established, this method is held in reserve.

Two methods remain for consideration: modified constant-potential charging, and constant or full-array current charging. Either of these may be combined with switchdown to trickle charge from some external stimulus related to battery state of charge. This may be temperature, pressure (via pressure switch or auxiliary electrode) coulometer or A-h integrator, or time. The modified constant potential may be compen- sated for temperature variation.

Constant or Full-Array Current Charging With Switchdown to Trickle Charge.—The only stimulus which can be used safely for return to trickle charge after a high current charge is cell or battery terminal voltage, since no other stimulus can give assurance that the cell voltage will never exceed the maximum permissible voltage. It is also clear from exami- nation of the worst-case current-voltage characteristic data that if acquisition of full charge is essential, a single voltage limit cannot be used over the temperature range of 40° to 90° F or over the full range of charging currents. If, however, the charging current is limited by the introduction of a series element, and if the voltage is compensated for temperature, the method becomes a viable control system. The tem- perature compensation factor may be determined from figures 13–9 and 13–11 by reading the voltage at which the cell reaches the full state of charge at the two extreme conditions (fig. 13–11). The limitation of this control system appears when the two temperatures are so far apart that the battery fails to reach full charge at the low temperature end in spite of temperature compensation, or when the battery requires excessive voltages for charge completion. Tolerance requirements in the voltage sensor aggravate this problem.

Modified Constant-Potential Charging With Switchdown to Trickle.— Modified constant-potential charging is somewhat easier to implement over a wide temperature range. The limiting potential is selected at the low temperature end by setting it at or above the intersection of the full charge current-voltage line with a line representing a modest charging current (say C/40). This assures that voltage limiting will permit full charge at all temperatures above 40° F if efficiency requirements are also satisfied. If this voltage is low enough (below 1.47 volts per cell), temperature compensation of the voltage limit level is not essential, since one may depend upon the switchdown to trickle charge to prevent overheating and thermal runaway. If the low temperature voltage is too high, then temperature compensation is required; the voltage limit at

high temperature is set at approximately the intersection of the minimum charge-current curve with the full-charge current-voltage characteristic curve (fig. 13–12). Auxiliary electrodes, coulometers, thermal switches, etc., can be used individually or in combination for switching to trickle charge. However, it is necessary to evaluate the "set point" of each switching function to make sure that premature switchdown cannot occur, preventing the battery from reaching full charge.
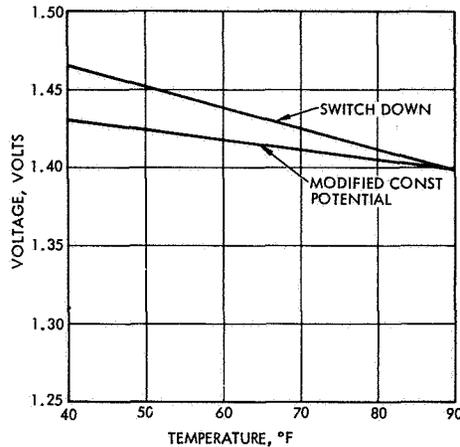
FIGURE 13–12.—Voltage-temperature c o m-
pensation curves for return to 100 percent of
nameplate capacity (curves for 110 percent
and 120 percent would be higher).

A variation of the above method is deliberate switchdown to trickle charge, depending upon the charge accumulated during the trickle period, prior to reaching the state of full charge. In all of the above methods it is essential to make sure, by integration of the product of current and efficiency, that the battery reaches an acceptable state of charge before it is called upon to deliver energy.

Estimation of Battery Heat Evolution.—Heat evolved as a result of battery operation cannot, at the present time, be accurately predicted. Estimates of the heat evolved as a function of time, however, can be made.

During discharge, the values of current and voltage can be used in equation (2–16) to determine heat evolved. Assume the value of E_{rev} varies linearly with state of charge from 1.290 at full charge to 1.277 at a 50-percent state of charge. (See ch. 4.) Figure 13–13 shows E_{rev} as a function of state of charge. Terminal voltage and charging current as a function of state of charge are known (fig. 13–3). ΔS is assumed to have an absolute value of -10 calories per equivalent. Substituting into equation (2–16) and calculating a heat evolution for each 20 percent state of charge gives heat evolution during discharge as a function of state of
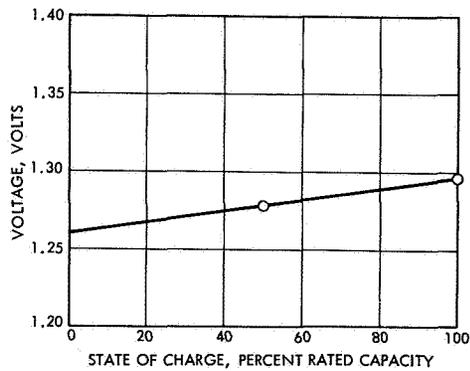
FIGURE 13-13.—Nickel-cadmium   reversible
potential versus state of charge.

charge. This may be changed to a heat evolution versus time relation-
ship by calculation of the state of charge as a function of time and
replotting.

During charge, equation (2–16) is valid only if the equivalent current is
known for each of the reactions. Efficiency data (ch. 4) may be used to
estimate the division of current between the charge and overcharge
reactions, and the expression for heat evolution then becomes:

$$q=[(E_{rev}-E)\ I+KIT]\eta-EI(1-\eta) \qquad (13-3)$$

This expression takes into account neither the heat evolved during
the beginning of discharge because of recombination of stored oxygen,
nor the energy stored in the cell in the form of oxygen during the transi-
tion period between charge and overcharge. In addition, the heat-
evolution rate calculated with this expression is on the surfaces of the
electrodes, so that an appreciable timelag may occur before these rates
are measured at the exterior of the cell. Figure 13–14 shows the heat-
evolution rate at the cell electrodes as a function of time for one cycle of
charge based upon the assumption of a full-array current charge to the
voltage switchdown point. Similar discharge calculations are practical.

Since the rates of heat evolution and the battery temperature are
interdependent, and since the battery temperature affects all of the design
decisions, the entire design process is necessarily iterative and must be
repeated until the battery temperature converges to a constant profile.
The calculation of battery temperature from heat evolution rates is
dependent upon the thermal characteristics of the vehicle upon which the
battery is mounted. Consequently, consideration of this aspect of the
design process is beyond the scope of this book.

AUTOMATION OF THE DESIGN PROCESS

The entire design process can be automated in a digital computer,
provided that applicable data can be found and that a temperature
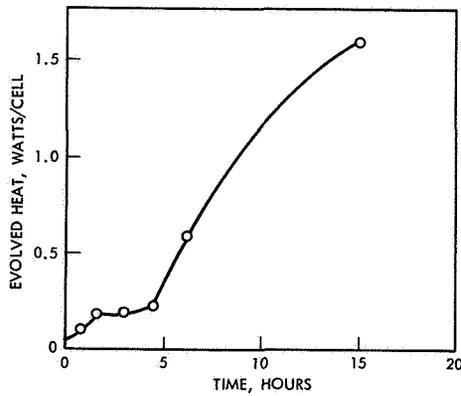
FIGURE 13-14.—Calculated battery heat evolution during active charging (constant temperature).

calculation subroutine can be conveniently added to the program. Although no published information is yet available, work in this subject is known to be in progress at TRW Systems and Grumman Aircraft Engineering Corp. Sufficient progress has been made along these lines to permit "flying" the system in the computer.

APPLICATION NO. 2, A PLANETARY ORBITER

As a second example of aerospace battery applications, we will briefly study a proposed configuration of the Voyager spacecraft. Voyager will be thrust into a trajectory in which it will encounter Mars. During the cruise made between Earth and Mars, it will orient itself with relation to three celestial bodies: Earth, Sun, and the star Canopus; make measurements of the properties of interplanetary space; and upon command perform any necessary corrections in trajectory required to assure accuracy of encounter with Mars. For the last, a self-contained propulsion system is provided.

Upon encounter with Mars, it releases a landing capsule and places itself in orbit about Mars, again using its propulsion system, where it remains for approximately 6 months making scientific measurements. It also receives data transmissions from the landing capsule and records them for relay to Earth when transmission conditions are favorable. The total mission duration is 15 months.

The power requirements are highly variable; the minimum being 79 watts, and the peak power 625 watts, a total variation of nearly an order of magnitude. A detailed study of the Voyager power system and loads is beyond our scope. However, by making certain simplifying assumptions, it is possible to utilize this example to demonstrate appropriate design methods.

The basic power-system concept is that of an oriented solar array which provides source power and battery storage to permit operation when demand exceeds this source power. Several system design concepts were considered; the configuration finally selected, on the basis of efficiency and reliability, is shown in figure 13-15.
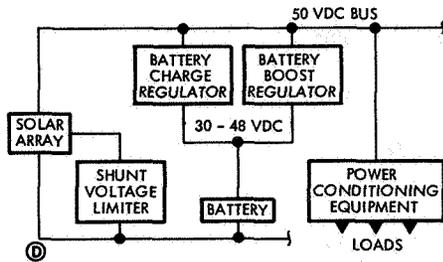
FIGURE 13-15.—Power-subsystem block diagram.

Unlike Earth-orbiting solar arrays which undergo only modest degradation of output with time, the Voyager solar array deteriorates to less than one-third its original capability during its 9-month cruise to Mars. In addition, the characteristics of the solar-array change. Its open-circuit voltage rises with a decrease in solar-array temperature, while its current delivery capability decreases with the decrease in illumination intensity as the spacecraft recedes from the Sun. This results in operating characteristics as shown in figure 13-16.
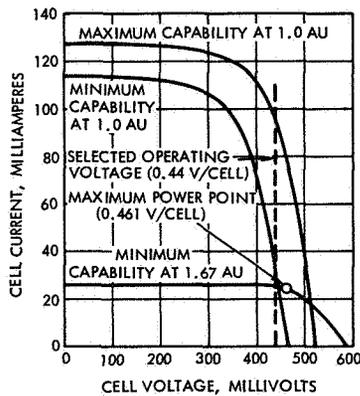
FIGURE 13-16.—Solar-array characteristics of an interplanetary space vehicle at Earth (1.0 AU) and at Mars (1.67 AU).

MISSION PHASES

The Voyager spacecraft goes through a number of mission phases, some of which may be critical in the battery-design calculations.

During launch and acquisition, the spacecraft injects into its trajectory, rotates until the solar array is fully illuminated by the Sun, acquires the Earth, and orients itself with the star Canopus. Only the initial period requires full battery power.

Having attained its final orientation, the spacecraft enters the cruise phase, where it remains for 9 months, except for occasional course-correction maneuvers. During cruise, the battery supplies none of the electrical energy for spacecraft operation.

When midcourse corrections are commanded, the spacecraft loses lock on the Sun, Earth, and Canopus; orients itself for thrust; delivers a timed thrust with its propulsion system; and then reacquires the Sun, Earth, and Canopus. Since the orientation may be such that the solar array is not illuminated during this period, the battery supplies all of the energy.

At orbit injection about Mars, the spacecraft again loses its three reference points, orients and thrusts, and then reacquires the Sun and Earth. It is now in an orbit about Mars, and may be expected to go through a series of occultations, during which solar radiation is occluded by the planet and all energy must be supplied by the battery.

The power and energy requirements during these critical phases are summarized in table 13-I. The duration of the eclipse period may vary from orbit to orbit, with a resulting variation in energy consumption. However, here it will be assumed that all eclipses are identical, and we will design for the worst case.

TABLE 13-I.—*Simplified Summary of Voyager Power and Energy Requirements*

Phase	Battery power, W	Battery energy, W-h	Approximate number of cycles
Launch_____	225	340	1
Midcourse maneuvers_____	402	804	4
Injection maneuver_____	393	786	1
Orbital eclipses_____	408	940	140

SELECTION OF THE BATTERY SYSTEM

A total of approximately 150 cycles is required of the battery, the majority of cycles to be applied after encounter and orbit injection. The use of the silver-zinc system seems inadvisable in view of the large number of cycles, which would require a shallow depth of discharge. In

the absence of adequate data on the variation of electrical characteristics as a function of the cycle life of the cells, an alternative method must be used to estimate the allowable depth of battery discharge. Figure 13–17 shows a tentative comparison of the cycle lives of silver-cadmium and nickel-cadmium batteries. At 150 cycles, the silver-cadmium batteries may be used at a depth of discharge of 50 percent, the nickel-cadmium at 87 percent. Applying the same arbitrary rule as was used in Application No. 1, the maximum allowable depth of discharge is set at 80 percent. Because the relationship between cycle life and depth of discharge has not been demonstrated to hold under all circumstances, the data must be considered questionable.
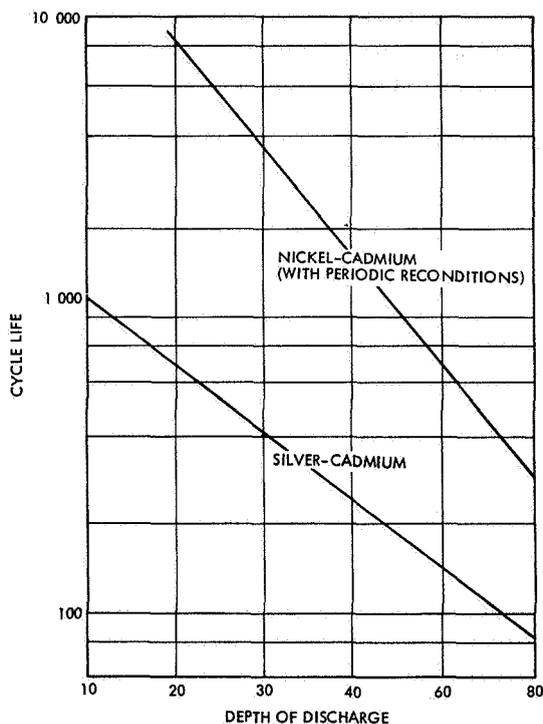
FIGURE 13–17.—Service life of space batteries at 75° F as a function of depth of discharge. NOTE.—Data of questionable validity.

The use of the arbitrary 80 percent depth-of-discharge rule results in the silver-cadmium system being the lighter weight of the two candidates. It is clear from a consideration of table 13–I that the design point for the batteries is the maximum eclipse orbital condition. Battery

recharge power is lowest at Mars, recharge time is shortest, and the total energy demand is greatest. A battery capable of satisfying the requirements of the maximum-eclipse orbit will have energy reserves after each of the other design conditions. The analysis therefore becomes similar to that of Application No. 1 and need not be repeated except where differences exist.

The discharge data used in design calculations are similar to those of figures 5-1 through 5-3. However, in view of the relative unpredictability of the duration of the upper discharge plateau and its possible disappearance after long periods in the float-charge condition, a more conservative design approach would be to assume that discharge occurred only on the lower plateau and then proceed accordingly.

Both upper and lower charge-plateau data are relatively predictable, and all design calculations may follow the general approach of Application No. 1. However, in calculation of heat-evolution rates, it may be assumed that the efficiency is unity in any safe battery-operating mode, and that equation (2-16) holds for both charge and discharge. The resulting heat-evolution calculations will result in overestimates of heat evolved during some parts of the cycle and underestimates during other parts. However, the estimate of total heat evolved will approximate actual heat evolution reasonably well. (See discussion of heat evolution in ch. 5.)

APPLICATION NO. 3, TYPICAL LAUNCH VEHICLE

The typical launch vehicle has an operating life of a few minutes, after which succeeding stages are detached and the vehicle discarded. Electric power is normally supplied by silver-zinc primary batteries, which are either automatically or manually activated, and designed to deliver their energy to the loads in 10 to 15 minutes. Wet storage life of the batteries is not usually a problem. Power requirements are generally quite high (of the order of several kilowatts) and highly variable with time.

A typical launch-vehicle power profile is shown in figure 13-18. This type of profile, however, does not fully describe the electric-power requirements since it gives no information about the variation of current demand with bus voltage or of bus voltage with time. System analysis based upon this type of information will lead to small errors in estimating depth of discharge and forces the system designer to abdicate the responsibility of maintaining voltage regulation to the battery manufacturer. If a more accurate estimate of depth of discharge is desired or if an accurate voltage-time profile is needed, an analysis should be conducted by the current-voltage characteristic method as presented in chapter 2 and as applied in Application No. 1 in this chapter.

To simplify calculations to a manageable level for illustration, a highly simplified system is assumed, which consists of a battery and three loads individually turned on and off in accordance with a predetermined time schedule. The three loads, A, B, and C, are assumed to be 1 kW
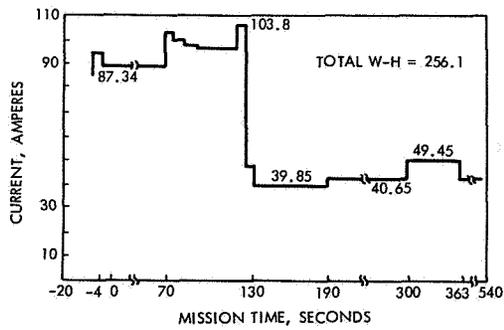
FIGURE 13-18.—Typical launch-vehicle power profile.

at 30 V each, and to be resistive, constant current, and constant power. The load schedule is assumed as follows:

Minutes	Load	kW	
0-2	A	1	Resistive
2-4	A+B	2	Resistive, plus constant current
4-6	A+C	2	Resistive, plus constant power
6-8	A+B+C	3	Resistive, constant current, constant power

The total energy requirements are roughly estimated at 14 kW-min, at 30 volts, and require a battery capacity of approximately 14 000/ (60)(30) A-h, or 7.8 A-h.

A rigorous treatment of the analysis would require that the cell characteristic data be presented at constant temperature. As heat is evolved in the cell, the temperature is calculated for each time increment before calculating the next small increment and the electrical characteristics modified accordingly. Such data are not available for silver-zinc batteries, nor are they likely to become available in the near future. The battery-characteristic data are therefore confounded in temperature, and are based upon the assumption that the discharge is so rapid that all heat deposited in the cell remains in the cell during the discharge period.

ESTIMATION OF BATTERY SIZE

The estimate of battery size is dependent upon the voltage regulation required. The initial load is 1 kilowatt resistive. The final load is 3 kilowatts complex and is the largest load. The battery must be able to support this load at its lowest state of charge.

If it is assumed that the allowable voltage range is 27 to 32 volts, then the minimum acceptable cell voltage varies with the number of cells as follows:

Cells:
19 ---- 1.42 volts
20 ---- 1.35 volts
21 ---- 1.28 volts
22 ---- 1.22 volts
23 ---- 1.17 volts

Figure 13-19 shows silver-zinc characteristic data upon which are super-imposed minimum voltage lines based upon varying numbers of series-connected cells. The crossing of lines representing different states of charge is due to the initial dip in discharge voltage. The cross-hatched area represents the range in which the state-of-charge lines are crowded too closely for convenient presentation.
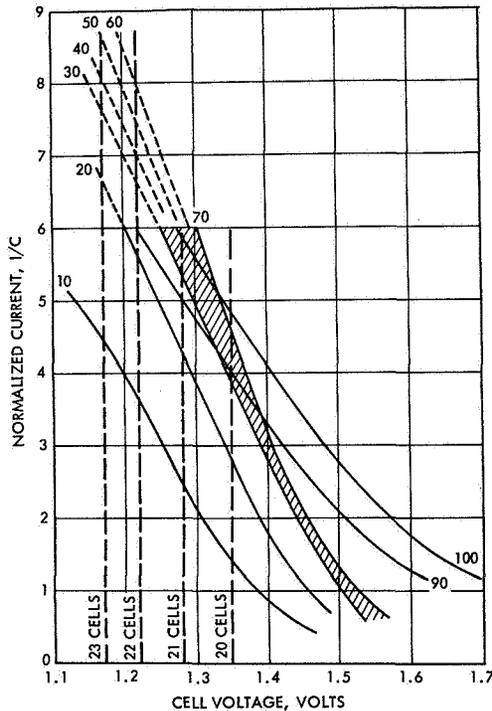
FIGURE 13-19.—Primary Ag-Zn cell characteristics and minimum system voltage characteristics as a function of the number of series cells. State of charge as the third variable.

From the intersection of the minimum voltage lines with the state-of-charge lines, it is possible to calculate the total installed capacity required as a function of depth of discharge and number of series cells.

$$\text{Capacity (W-h)} = \frac{(I)(E)(n)}{(I/C)\left(\dfrac{100-Q}{100}\right)} \qquad (13\text{-}4)$$

Since no specific design point has yet been established, equation (13-4) has several unknowns, and must be evaluated parametrically for several values of Q (state of charge), N (number of series-connected cells).

TABLE 13–II.—*Installed Capacity (W-h) as a Function of Number-of-Series Cells and Depth of Discharge*

	Percent			
	90	80	70	60
20_____	2130	1215	1000	_____
21_____	1260	784	736	_____
22_____	814	608	592	647
23_____	680	515	513	560

Table 13–II is derived by solving equation (13–4).for several assumed values of depths of discharge $(100-Q)$ and N, and shows the installed capacity required as a function of depth of discharge and number of series-connected cells.

From table 13–II it is clear that the minimum required capacity is given by the 23-cell, 70-percent depth-of-discharge case. Since this occurs at the lower edge of the table, further optimization is possible by increasing the number of cells. However, since it is obvious that initial voltages would be excessive, no further optimization will be attempted. Having selected this case as the tentative design point, the normalized current, I/C, is 7.6 at 30 percent state of charge (70 percent depth of discharge). Current for loads $A+B+C$ is 100.4 amperes at 27 volts; therefore, capacity required is given by:

$$C = \frac{(I)}{(I/C)} = 13.2 \text{ A-h} \qquad (13\text{–}5)$$

This does not imply a total energy-storage requirement of 13.2 A-h. Rather, it shows that in order to maintain a minimum voltage of 27 volts on discharge with a battery whose characteristics are described in figure 13–19, the minimum installed capacity is 13.2 A-h, or more than twice the required energy storage. If the cells were lower in impedance, or if the minimum voltage was decreased to 26 volts, the required capacity would be much lower.

The current-voltage load characteristics, shown in figure 13–20, are superimposed upon the same battery-cell characteristics, with the load current divided by the cell capacity of 13.2 A-h, and the voltage by 23. If a cell of some commercially available capacity is selected, the scales are adjusted to be compatible with the actual cell used. If maximum and minimum voltage lines are added to the diagram, then

$$E_{max} = 32 \text{ V}/23 \qquad E_{min} = 27 \text{ V}/23 \qquad (13\text{–}6)$$
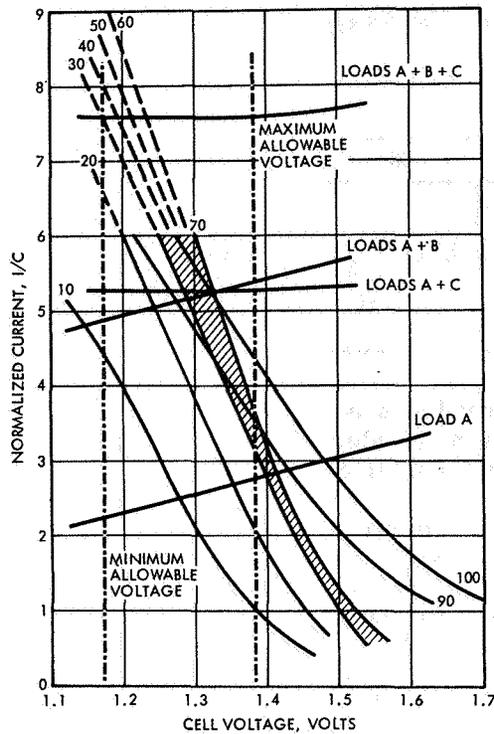
FIGURE 13–20.—Battery/load interface diagram. Ag-Zn cell and system load current-voltage characteristics.

Examination of the diagram shows that the voltage during the initial part of the discharge period (intersection of load line A with the maximum voltage line) exceeds the upper limit of 32 volts. Several alternatives are available; all of them depend upon the judgment of the systems engineer rather than upon any predetermined logic.

(1) The number of series-connected cells may be reduced and the capacity increased by selecting one of the other alternatives of table 13–II. This represents a weight penalty.

(2) The actual requirements for the regulation limits may be re-examined for possible widening.

(3) The load programing may be altered, if the mission permits, to turn the high-current portion on at the beginning of discharge, and the low-current portion on at the end. Reanalysis of this case would probably show a significant savings in installed capacity.

(4) Cells which have been specially treated for removal of the upper voltage plateau may be used if their other characteristics are suitable.

(5) A regulating device with wider tolerance for input-voltage variation may be used between the battery and the loads. The load characteristics must then be modified to represent the input current-voltage characteristic of the regulator under each of the load characteristics.

The above analysis assures that the battery will be able to carry the maximum load current without falling below minimum load voltage and has shown that with load A, only the system voltage will exceed the maximum of 32 volts. The system designer, having been warned, has resolved the overvoltage problem by increasing the dissipation capability of load A and of the heat rejection system associated with load A so that it will tolerate the overvoltage.

It appears from an examination of the required capacity (approximately 7.8 A-h) and the installed capacity (13.2 A-h) that the battery contains more than enough energy to support the load, and that the system is power limited rather than energy limited. This is not always the case, however. If the possibility exists that the system is energy limited, it is then necessary to perform the analysis for depth of discharge and voltage-time profile as previously demonstrated in Application No. 1. As the loads change at 2-minute intervals, a shift is made on the diagram from one load line to the other along a constant state-of-charge line parallel to the nearest cell current-voltage characteristic line.

Heat evolution rates may be calculated using equation (2–16), but will be inaccurate because of the uncertainty in the division of current between the two reactions of the silver electrode. An initial assumption of equal division of currents between the $AgO\text{-}Ag_2O$ and the $Ag_2O\text{-}Ag$ reactions seems reasonable over most of the operating range.

Bibliography

1. BECK, T. R.; AND KEMP, F. S.: Heat Generation in Lunar Orbiter Battery. Rept. no. D2-23612-1, The Boeing Co. (Seattle, Wash.), Contract no. NAS1-3800, Oct. 1964.
2. BETZ, F. E.: Design and Fabrication of 100 Ampere-Hour Nickel-Cadmium Battery Cells. Gulton Industries, Contract no. NAS1-4289, Final Report, Mar. 14, 1967.
3. LISKA, J.: Investigation of Sterilization of Secondary Batteries. Gulton Industries, Contract no. NAS1-5708, Final Report, June to Oct. 1966.
4. LISKA, J.: Investigation of Sterilization of Secondary Batteries. Gulton Industries, Contract no. NAS1-5708, Rept. no. NASA CR-66105, First Quarterly Report, Oct. 26, 1965, to Jan. 26, 1966.
5. LISKA, J.: Investigation of Sterilization of Secondary Batteries. Gulton Industries, Contract no. NAS1-5708, Second Quarterly Report, Jan. to Apr. 1966.
6. HIMY, A.: Development of One Ampere-Hour Heat Sterilizable Silver-Zinc Cell. Astropower Laboratory, Rept. no. SM-49109-F, NASA CR-73110, Contract no. NAS2-3819, Final Technical Evaluation, Period Ending June 1967.
7. HIMY, A.: Development of One Ampere-Hour Heat Sterilizable Silver-Zinc Cell. Astropower Laboratory, Rept. no. SM-49109-Q1, Contract no. NAS2-3819, Progress Report, July 1 to Sept. 30, 1966.
8. HIMY, A.: Development of One Ampere-Hour Heat Sterilizable Silver-Zinc Cell. Astropower Laboratory, Rept. no. SM-49109-Q2, Contract no. NAS2-3819, Progress Report, Oct. 1 to Dec. 31, 1966.
9. HIMY, A.: Development of One Ampere-Hour Heat Sterilizable Silver-Zinc Cell. Astropower Laboratory, Rept. no. SM-49109-Q3, Contract no. NAS2-3819, Progress Report, Jan. 1 to Mar. 31, 1967.
10. VOGT, J. W.: Materials for Electrochemical Cell Separators. TRW Equipment Laboratories (Cleveland, Ohio), Rept. no. NASA CR-72267, Contract no. NAS2-8522, Second Summary Report, July 3, 1967.
11. MEYERS, W. F.: Development of High Energy Density Primary Batteries 200 Watt-Hours per Pound Total Battery Weight Minimum. G. & W. H. Corson, Inc., Rept. no. NASA CR-54083, Contract no. NAS3-2775, Final Report, 1964.
12. ANON.: High Energy Density Primary Batteries. Livingston Electronic Corp., Rept. no. NASA CR-52550, Contract no. NAS3-2775, First Quarterly Report, Oct. 28, 1963.
13. ANON.: High Energy Density Primary Batteries. Livingston Electronic Corp., Rept. no. NASA CR-55743, Contract no. NAS3-2775, Second Quarterly Report, Nov. 1963.

14. MEYERS, W. F.: Development of High Energy Density Primary Batteries. Livingston Electronic Corp., Rept. no. NASA CR-54024, Contract no. NAS3-2775, Third Quarterly Report, Nov. 20, 1963, to Feb. 16, 1964.

15. BORSANYI, A.; ET AL.: Feasibility Proof of Dry Tape Battery Concept. Monsanto Research Corp., Rept. no. MRB 5001-F, Contract no. NAS3-2777, Final Report, June 14, 1963, to Jan. 23, 1964.

16. BORSANYI, A.; ET AL.: Development and Feasibility Proof of the Dry Tape Battery Concept. Monsanto Research Corp., Rept. no. MRB 5001-Q1, Contract no. NAS3-2777, First Quarterly Report, June 14 to Sept. 30, 1963.

17. HILL, K. R.; AND SELIM, R. G.: Research and Development of a High Capacity Nonaqueous Secondary Battery. P. R. Mallory & Co., Rept. no. NASA CR-54880, Contract no. NAS3-2780, Final Report, Aug. 15, 1965.

18. ANON.: Research and Development of a High Capacity Nonaqueous Secondary Battery. P. R. Mallory & Co., Rept. no. NASA CR-55015, Contract no. NAS3-2780, First Quarterly Report, July to Nov. 1963.

19. ANON.: Research and Development of a High Capacity Nonaqueous Secondary Battery. P. R. Mallory & Co., Rept. no. NASA CR-53087, Contract no. NAS3-2780, Second Quarterly Report, Nov. 1963 to Feb. 1964.

20. ANON.: Research and Development of a High Capacity Nonaqueous Secondary Battery. P. R. Mallory & Co., Rept. no. NASA CR-56463, Contract no. NAS3-2780, Third Quarterly Report, Feb. to May 1964.

21. ANON.: Research and Development of a High Capacity Nonaqueous Secondary Battery. P. R. Mallory & Co., Rept. no. NASA CR-54164, Contract no. NAS3-2780, Fourth Quarterly Report, May to Aug. 1964.

22. ELLIOTT, W. E.; HSU, S.; AND TOWLE, W. L.: The Development of High Energy Density Primary Batteries, 200 Watt-Hours per Pound of Total Battery Weight Minimum. Globe Union Inc., Applied Research Lab, Rept. no. NASA CR-54153, Contract no. NAS3-2790, Final Report, Jan. 1965.

23. BYRNE, J. J.; ET AL.: Development of the Dry Tape Battery Concept. Monsanto Research Corp., Rept. no. NASA CR-347, Contract no. NAS3-4168, Final Report, Dec. 1965.

24. BYRNE, J. J.; ET AL.: Development of the Dry Tape Battery Concept. Monsanto Research Corp., Rept. no. NASA CR-54076, Contract no. NAS3-4168, First Quarterly Report, Jan. 24 to Apr. 30, 1964.

25. BYRNE, J. J.; ET AL.: Development of the Dry Tape Battery Concept. Monsanto Research Corp., Rept. no. NASA CR-54165, Contract no. NAS3-4168, Second Quarterly Report, May 1 to Aug. 1, 1964.

26. BYRNE, J. J.; ET AL.: Development of the Dry Tape Battery Concept. Monsanto Research Corp., Rept. no. NASA CR-54231, Contract no. NAS3-4168, Third Quarterly Report, Aug. 1 to Oct. 31, 1964.

27. RITTERMAN, P.; AND SEIGER, H. N.: Investigation of Battery Active Nickel Oxides. Gulton Industries, Rept. no. NASA CR-54654, Contract no. NAS3-4178, Final Report, June 11, 1965.

28. RITTERMAN, P.: Investigation of Battery Active Nickel Oxides. Gulton Industries, Rept. no. NASA CR-54196, Contract no. NAS3-4178, First Quarterly Report, June to Sept. 1964.

29. RITTERMAN, P.: Investigation of Battery Active Nickel Oxides. Gulton Industries, Rept. no. NASA CR-54295, Contract no. NAS3-4178, Second Quarterly Report, Sept. 12 to Dec. 12, 1964.

30. RITTERMAN, P.: Investigation of Battery Active Nickel Oxides. Gulton Industries, Rept. no. NASA CR-54402, Contract no. NAS3-4178, Third Quarterly Report, Dec. 1964 to Mar. 1965.

31. ANDERSON, W. G.; ET AL.: Development of a High Temperature Battery. Aeroneutronics, Rept. no. NASA CR–54731, Contract no. NAS3–6002, Final Report, Oct. 15, 1965.

32. PARKER-JONES, A.; ET AL.: Development of a High Temperature Battery. Philco Corp., Applied Research Lab, Rept. no. NASA CR–54208, Contract no. NAS3–6002, First Quarterly Report, Oct. 20, 1964.

33. PARKER-JONES, A.; ET AL.: Development of a High Temperature Battery. Philco Corp., Aeroneutronics, Rept. no. NASA CR–54289, Contract no. NAS3–6002, Second Quarterly Report, Jan. 15, 1965.

34. PARKER-JONES, A.; ET AL.: Development of a High Temperature Battery. Philco Corp., Aeroneutronics, Rept. no. NASA CR–54404, Contract no. NAS3–6002, Third Quarterly Report, Apr. 20, 1965.

35. FAUST, C. L.; ET AL.: Development of Large-Internal-Surface-Area Nickel-Metal Plaques. Battelle Memorial Institute, Rept. no. CR–54831, Contract no. NAS3–6003, Final Report, Sept. 30, 1965.

36. FAUST, C. L.; ET AL.: Development of Large-Internal-Surface-Area Nickel-Metal Plaques. Battelle Memorial Institute, Rept. no. NASA CR–54114, Contract no. NAS3–6003, First Quarterly Report, June 18 to Sept. 18, 1964.

37. FAUST, C. L.; ET AL.: Development of Large-Internal-Surface-Area Nickel-Metal Plaques. Battelle Memorial Institute, Rept. no. NASA CR–54299, Contract no. NAS3–6003, Second Quarterly Report, Sept. to Dec. 1964.

38. FAUST, C. L.; ET AL.: Development of Large-Internal-Surface-Area Nickel-Metal Plaques. Battelle Memorial Institute, Rept. no. NASA CR–54385, Contract no. NAS3–6003, Third Quarterly Report, Apr. 8, 1965.

39. ABENS, S. G.; ET AL.: Development of High Energy Density Primary Batteries, 200 Watt-Hours per Pound Total Battery Weight Minimum. Livingston Electronic Corp., Rept. no. NASA CR–54803, Contract no. NAS3–6004, Final Report, June 1964 to June 1965.

40. BIDLER, J. L.; AND FISHER, J. I.: Preparation and Evaluation of Fiber Metal Nickel Battery Plaques. Huyck Metals Co., Rept. no. NASA CR–54777, Contract no. NAS3–6006. Final Report, Aug. 1964 to July 1965.

41. ARRANCE, F. C.; BERGER, C.; AND TAYLOR, A. D.: Inorganic Separator for High Temperature Silver-Zinc Battery. Douglas Aircraft, Rept. no. CR–54749, Contract no. NAS3–6007, Final Report, Sept. 1965.

42. ARMSTRONG, G. M.; AND MEYERS, W. F.: Development of a Low Temperature Battery for Space Probe Applications. Livingston Electronic Corp., Rept. no. CR–54733, Contract no. NAS3–6009, Final Report, June 24, 1964, to June 23, 1965.

43. MEYERS, W. F.: Development of a Low Temperature Battery for Space Probe Applications. Livingston Electronic Corp., Rept. no. NASA CR–54205, Contract no. NAS3–6009, First Quarterly Report, Nov. 15, 1964.

44. MEYERS, W. F.: Development of a Low Temperature Battery for Space Probe Applications. Livingston Electronic Corp., Rept. no. NASA CR–54292, Contract no. NAS3–6009, Second Quarterly Report, Sept. to Dec. 1964.

45. MEYERS, W. F.: Development of a Low Temperature Battery for Space Probe Applications. Livingston Electronic Corp., Rept. no. CR–54378, Contract no. NAS3–6009, Third Quarterly Report, Dec. 24, 1964, to Mar. 23, 1965.

46. ELLIOTT, W. E.; HSU, S.; AND TOWLE, W. L.: A Program To Develop a High Energy Density Primary Battery With a Minimum of 200 Watt-Hours per Pound of Total Battery Weight. Globe-Union, Inc., Rept. no. NASA CR–54298, Contract no. NAS3–6015, Second Quarterly Report, Oct. to Dec. 1966.

47. ADLER, R. W.; ELLIOTT, W. E.; HUFF, J. R.; AND TOWLE, W. L.: A Program To Develop a High Energy Density Primary Battery With a Minimum of 200 Watt-Hours per Pound of Total Battery Weight. Globe-Union, Inc., Rept. no. NASA CR-54375, Contract no. NAS3-6015, Third Quarterly Report, Apr. 19, 1965.

48. ADLER, R. W.; ELLIOTT, W. E.; HUFF, J. R.; AND TOWLE, W. L.: A Program To Develop a High Energy Density Primary Battery With a Minimum of 200 Watt-Hours per Pound of Total Battery Weight. Globe-Union, Inc., Rept. no. NASA CR-54450, Contract no. NAS3-6015, Fourth Quarterly Report, Aug. 9, 1965.

49. ADLER, R. W.; ET AL.: A Program To Develop a High Energy Density Primary Battery With a Minimum of 200 Watt-Hours per Pound of Total Battery Weight. Globe-Union, Inc., Rept. no. NASA CR-54744, Contract no. NAS3-6015, Fifth Quarterly Report, Oct. 15, 1965.

50. ELLIOTT, W. E.; ET AL.: A Program To Develop a High Energy Density Primary Battery With a Minimum of 200 Watt-Hours per Pound of Total Battery Weight. Globe-Union, Inc., Rept. no. NASA CR-54873, Contract no. NAS3-6015, Sixth Quarterly Report, Jan. 1966.

51. ELLIOTT, W. E.; ET AL.: A Program To Develop a High Energy Density Primary Battery With a Minimum of 200 Watt-Hours per Pound of Total Battery Weight. Globe-Union, Inc., Rept. no. NASA CR-54928, Contract no. NAS3-6015, Seventh Quarterly Report, Apr. 15, 1966.

52. ELLIOTT, W. E.; ET AL.: A Program To Develop a High Energy Density Primary Battery With a Minimum of 200 Watt-Hours per Pound of Total Battery Weight. Globe-Union, Inc., Rept. no. NASA CR-72040, Contract no. NAS3-6015, Eighth Quarterly Report, July 15, 1966.

53. ELLIOTT, W. E.; ET AL.: A Program To Develop a High Energy Density Primary Battery With a Minimum of 200 Watt-Hours per Pound of Total Battery Weight. Globe-Union, Inc., Rept. no. NASA CR-72158, Contract no. NAS3-6015, Ninth Quarterly Report, Oct. 15, 1966.

54. ELLIOTT, W. E.; ET AL.: A Program To Develop a High Energy Density Primary Battery With a Minimum of 200 Watt-Hours per Pound of Total Battery Weight. Globe-Union, Inc., Rept. no. NASA CR-72189, Contract no. NAS3-6015, 10th Quarterly Report, Oct. 1 to Dec. 31, 1966.

55. HILL, K. R.; RAO, M. L. B.; AND SELIM, R. G.: Research and Development of a High Capacity Nonaqueous Secondary Battery. P. R. Mallory & Co., Rept. no. NASA CR-54969, Contract no. NAS3-6017, Final Report, Oct. 1964 to Dec. 1965.

56. ANON.: Research and Development of a High Capacity Nonaqueous Secondary Battery. P. R. Mallory & Co., Rept. no. CR-54407, Contract no. NAS3-6017, Second Quarterly Report, Jan. to Mar. 1965.

57. ANON.: Abstracts on High Capacity Nonaqueous Secondary Batteries. P. R. Mallory & Co., Contract no. NAS3-6017, Final Report.

58. SPARKS, R. H.: A Study To Develop a Low Temperature Battery Suitable for Space Probe Applications. TRW Systems, Rept. no. NASA CR-54737, Contract no. NAS3-6018, Final Report.

59. SPARKS, R. H.; ET AL.: A Study To Develop a Low Temperature Battery Suitable for Space Probe Applications. TRW Systems, Rept. no. 4189-6002-TU000, Contract no. NAS3-6018, Phase I Report, Nov. 1964.

60. ANON.: Low Temperature Battery for Deep Space Probes. TRW Systems, Contract no. NAS3-6018, Technical Briefing.

61. Lerner, S.; Ritterman, P.; and Seiger, H. N.: Investigation of Battery Active Nickel Oxides. Gulton Industries, Rept. no. NASA CR–72128, Contract no. NAS3–7620, Final Report, Sept. 12, 1966.

62. Ritterman, P.; and Seiger, H. N.: Investigation of Battery Active Nickel Oxides. Gulton Industries, Rept. no. NASA CR–54832, Contract no. NAS3–7620, First Quarterly Report, Sept. 12, 1965.

63. Ritterman, P.; and Seiger, H. N.: Investigation of Battery Active Nickel Oxides. Gulton Industries, Rept. no. NASA CR–54903, Contract no. NAS3–7620, Second Quarterly Report, Dec. 12, 1965.

64. Lerner, S.; Ritterman, P.; and Seiger, H. N.: Investigation of Battery Active Nickel Oxides. Gulton Industries, Rept. no. NASA CR–54957, Contract no. NAS3–7620, Third Quarterly Report, Mar. 12, 1966.

65. Lerner, S.; Ritterman, P.; and Seiger, H. N.: Investigation of Battery Active Nickel Oxides. Gulton Industries, Rept. no. NASA CR–72018, Contract no. NAS3–7620, Fourth Quarterly Report, June 12, 1966.

66. Borsanyi, A. S.; et al.: Research and Development of the Dry Tape Battery Concept. Monsanto Research Corp., Contract no. NAS3–7624, Final Report, Apr. 26, 1967.

67. Athearn, L. F.; Byrne, J. J.; MacDonald, J. C.; and Williams, D. L.: Research and Development of the Dry Tape Battery Concept. Monsanto Research Corp., Rept. No. NASA CR–54782, Contract no. NAS3–7624, First Quarterly Report, Oct. 8, 1965.

68. Byrne, J. J.; et al.: Development of the Dry Tape Battery Concept. Monsanto Research Corp., Rept. no. NASA CR–54902, Contract no. NAS3–7624, Second Quarterly Report, Jan. 18, 1965.

69. Byrne, J. J.; et al.: Development of the Dry Tape Battery Concept. Monsanto Research Corp., Rept. no. NASA CR–54981, Contract no. NAS3–7624, Third Quarterly Report, Apr. 28, 1966.

70. Driscoll, J. W.; and Williams, D. L.: Development of the Dry Tape Battery Concept. Monsanto Research Corp., Rept. no. NASA CR–54771, Contract no. NAS3–7624, Fourth Quarterly Report, Aug. 1966.

71. Borsanyi, A. S.; Driscoll, J. S.; and Williams, D. L.: Development of the Dry Tape Battery Concept. Monsanto Research Corp., Rept. no. NASA CR–72170, Contract no. NAS3–7624, Fifth Quarterly Report, Dec. 31, 1966.

72. Abens, S. G.; Mahy, T. X.; and Merz, W. C.: Development of High Energy Density Primary Batteries. Livingston Electronic Corp., Rept. no. NASA CR–54859, Contract no. NAS3–7632, First Quarterly Report, Dec. 28, 1965.

73. Abens, S. G.; Mahy, T. X.; and Merz, W. C.: Development of High Energy Density Primary Batteries. Livingston Electronic Corp., Rept. no. NASA CR–54920, Contract no. NAS3–7632, Second Quarterly Report, Sept. 22 to Dec. 21, 1965.

74. Abens, S. G.; Corbett, R.; and Merz, W. C.: Development of High Energy Density Primary Batteries. Livingston Electronic Corp., Rept. no. NASA CR–54992, Contract no. NAS3–7632, Third Quarterly Report, Dec. 22, 1965, to Mar. 21, 1966.

75. Abens, S. G.; Corbett, R.; and Merz, W. C.: Development of High Energy Density Primary Batteries. Livingston Electronic Corp., Rept. no. NASA CR–72071, Contract no. NAS3–7632, Fourth Quarterly Report, Mar. 22 to June 21, 1966.

76. Korger, H. H.: Development of Improved Cadmium Electrodes for Sealed Secondary Batteries. General Electric Co., Rept. no. NASA CR–72084, Contract no. NAS3–7636, Final Report, Aug. 1966.

77. KORGER, H. H.: Development of Improved Cadmium Electrodes for Sealed Secondary Batteries. General Electric Co., Rept. no. NASA CR–54937, Contract no. NAS3–7636, Interim Rept. no. 1, Mar. 30, 1966.

78. ARRANCE, F. C.; BERGER, C.; HIMY, A.; AND TAYLOR, A. D.: Program To Develop an Inorganic Separator for a High Temperature Silver-Zinc Battery. Douglas Aircraft Co., Rept. no. SM–48461–Q1, Contract no. NAS3–7639, First Quarterly Report, Jan. 1966.

79. ARRANCE, F. C.; ET AL.: Program To Develop an Inorganic Separator for a High Temperature Silver-Zinc Battery. Douglas Aircraft Co., Rept. no. NASA CR–54919, Contract no. NAS3–7639, Second Quarterly Report, Mar. 1966.

80. ARRANCE, F. C.; ET AL.: Program To Develop an Inorganic Separator for a High Temperature Silver-Zinc Battery. Douglas Aircraft Co., Rept. no. NASA CR–54987, Contract no. NAS3–7639, Third Quarterly Report, May 1966.

81. ARRANCE, F. C.; ET AL.: Program To Develop an Inorganic Separator for a High Temperature Silver-Zinc Battery. Douglas Aircraft Co., Rept. no. NASA CR–72062, Contract no. NAS3–7639, Fourth Quarterly Report, July 29, 1966.

82. ANON.: Program To Develop an Inorganic Separator for a High Temperature Silver-Zinc Battery. Douglas Aircraft Co., Rept. no. NASA CR–70978, Contract no. NAS3–7639, Interim Progress Report, July 1966 to Oct. 1966.

83. ARMSTRONG, G. M.: Low Temperature Battery. Livingston Electronic Corp., Rept. no. CR–54970, Contract no. NAS3–8503, First Quarterly Report, Dec. 14, 1965, to Mar. 13, 1966.

84. ARMSTRONG, G. M.: Low Temperature Battery. Livingston Electronic Corp., Rept. no. NASA CR–72173, Contract no. NAS3–8503, Second and Third Quarterly Reports, Mar. 14 to Sept. 13, 1966.

85. REMANICK, A. H.; AND SHAW, M.: Electrochemical Characterization of Systems for Secondary Battery Application. Whittaker Corp., Rept. no. NASA CR–72069, Contract no. NAS3–8509, First Quarterly Report, Aug. 17, 1966.

86. REMANICK, A. H.; ET AL.: Electrochemical Characterization of Systems for Secondary Battery Application. Whittaker Corp., Rept. no. NASA CR–72138, Contract no. NAS3–8509, Second Quarterly Report, Nov. 18, 1966.

87. REMANICK, A. H.; ET AL.: Electrochemical Characterization of Systems for Secondary Battery Application. Whittaker Corp., Rept. no. NASA CR–72181, Contract no. NAS3–8509, Third Quarterly Report, Nov. 1966 to Jan. 1967.

88. REMANICK, A.; ET AL.: Electrochemical Characterization of Non-Aqueous Systems for Secondary Battery Application. Whittaker Corp., Rept. no. NASA CR–72256, Contract no. NAS3–8509, Fourth Quarterly Report, Feb. to Apr. 1967.

89. HIMY, A.: Improved Zinc Electrode. Astropower Lab, Rept. no. NASA CR–72265, Contract no. NAS3–8513, Final Report, July 1967.

90. FOSTER, J. N.; KELLER, R.; AND SULLIVAN, J. M.: Properties of Nonaqueous Electrolytes. Rocketdyne, Rept. no. NASA CR–72106, Contract no. NAS3–8521, First Quarterly Report, Oct. 19, 1966.

91. FOSTER, J. N.; ET AL.: Properties of Nonaqueous Electrolytes. Rocketdyne, Rept. no. NASA CR–72168, Contract no. NAS3–8521, Second Quarterly Report, Sept. 20 to Dec. 19, 1966.

92. FOSTER, J. N.; ET AL.: Properties of Nonaqueous Electrolytes. Rocketdyne, Rept. no. NASA CR-72065, Contract no. NAS3-8521, Third Quarterly Report, Apr. 19, 1967.

93. ANON.: Abstracts on Properties of Nonaqueous Electrolytes. Rocketdyne, Contract no. NAS3-8521.

94. FOSTER, J. N.; ET AL.: Properties of Nonaqueous Electrolytes. Rocketdyne, Rept. no. NASA CR-72277, Contract no. NAS3-8521, Fourth Quarterly Report, July 19, 1967.

95. COHEN, H.; ET AL.: Design, Development and Manufacture of Storage Batteries for Future Satellites. Gulton Industries, Rept. no. NASA CR-60819, Contract no. NAS5-809, Final Report, July 1, 1963.

96. ANON.: OGO Design Modification and Evaluation Study. TRW Systems, Rept. no. 2310-0001-TU000, Contract no. NAS5-899, Final Report, vol. I, Mar. 1961.

97. ANON.: OGO Design Modification and Evaluation Study. TRW Systems, Rept. no. 2310-0001-TU000, Contract no. NAS5-899, Final Report, vol. II, Appendices, Mar. 1961.

98. BAUER, P.; AND SPARKS, R. H.: Nickel-Cadmium Batteries for the Orbiting Geophysical Observatory. TRW Systems, Rept. no. 2315-6005-TU000, Contract no. NAS5-899, vol. I, Apr. 1, 1963.

99. BAUER, P.; AND SPARKS, R. H.; Nickel-Cadmium Batteries for the Orbiting Geophysical Observatory. TRW Systems, Rept. no. 2315-6008-RU000, Contract no. NAS5-899, Final Report, vol. II, Apr. 1, 1963.

100. ANON.: OGO Miscellaneous Test Reports. TRW Systems, Contract no. NAS5-899.

101. RALSTEN, M. W.: OGO Nickel-Cadmium Battery Serial No. 14 Acceptance Test. TRW Systems, Rept. no. 9363.4-514, Contract no. NAS5-899, Test Report, Dec. 12, 1965.

102. MILLER, R. S.; ROBINSON, R. L.; AND WRIGHT, W. H.: System Design Considerations for the Power Supply of the Orbiting Geophysical Observatory. TRW Systems, Contract no. NAS5-899, IEEE Meeting, Mar. 31, 1964.

103. BAUER, P.: Pressure Characteristics of Sealed Nickel-Cadmium Cells. TRW Systems, Contract no. NAS5-899, Electrochemical Technical Paper, Feb. 1965.

104. BAUER, P.: Electrical Charging Characteristics of Nickel-Cadmium Cells. TRW Systems, Contract no. NAS5-899, Prepublication Draft.

105. BAUER, P.: Characteristics of Three-Electrode, Sealed, Nickel-Cadmium Cells. TRW Systems, Contract no. NAS5-899.

106. STAFFORD, W. T.: Silver-Cadmium Cell Evaluation Study. TRW Systems, Rept. no. 2315-6002-KU000, Contract no. NAS5-899, Interim Report, May 16, 1962.

107. BIESS, J. J.; STAFFORD, W. T.; AND WRIGHT, W. H.: OGO Silver-Cadmium Battery Study. TRW Systems, Rept. no. 2314-6001-RU000, Contract no. NAS5-899, Final Report, May 1963.

108. ANON.: Investigation of OGO II Malfunctions. TRW Systems, Rept. no. 2360-6005-RU000, Contract no. NAS5-899, Final Report, vol. II, AgCd Battery, May 17, 1966.

109. FULBRIGHT, D. E.: OGO Silver-Cadmium Cell Acceptance Tests. TRW Systems, Rept. no. 9363.4-311, Contract no. NAS5-899, Test Report, Mar. 11, 1965.

110. FULBRIGHT, D. E.: Test Report on OGO Silver-Cadmium Battery Pressure Evaluation Test (3-Cell Test). TRW Systems, Rept. no. 9363.4-331, Contract no. NAS5-899, Test Report, Apr. 6, 1965.

111. IMAMURA, M. S.: Characteristics of Sealed Silver-Cadmium Battery. TRW Systems, Rept. no. 9361.11-71, Contract no. NAS5-899, Engineering Report, Dec. 3, 1965.

112. IMAMURA, M. S.: Evaluation of New Silver-Cadmium Cells for Use in OGO Batteries for Polar Orbit Missions. TRW Systems, Rept. no. 7062.7-2, Contract no. NAS5-899, Engineering Report, May 1966.

113. SCOTT, W. R.: Evaluation of YS-12(S)-2 Silver-Cadmium Cells for FOOGO. TRW Systems, Rept. no. 7062.3-39, Contract no. NAS5-899, Evaluation Report, May 13, 1966.

114. VOYENTZIE, P. R.: Improving Performance and Reliability of Sealed Secondary Type Nickel-Cadmium Storage Batteries for Satellite and Space Application. Sonotone Corp., Rept. no. NASA CR-53258, Contract no. NAS5-977, Final Report, Jan. 10, 1961, to Jan. 11, 1963.

115. JAKOBI, W.: Research and Development Program on Sealed Nickel-Cadmium Cells for Space Use. Gould-National Batteries, Rept. no. NASA CR-55845, Contract no. NAS5-1045, Final Report, Apr. 30, 1963.

116. ANON.: The Muter Co., Contract no. NAS5-1047, Final Report, Nov. 30, 1962.

117. ANON.: Testing and Evaluation of Nickel-Cadmium Spacecraft-Type Cells. Cook Electric Co., Contract no. NAS5-1048, Final Technical Report.

118. ANON.: Testing and Evaluation of Nickel-Cadmium Spacecraft-Type Cells. Cook Electric Co., Contract no. NAS5-1048, Final Report.

119. BUCCI, N. W., JR.; AND DOUGHMAN, C. L.: Space Electric Power Systems Study. Westinghouse Electric, Rept. no. NASA CR-50861, Contract no. NAS5-1234, Final Report, vol. 4, Nov. 1961 to Dec. 1962.

120. BAKER, A. R.; ET AL.: Space Electric Power Systems Study. Westinghouse Electric, Rept. no. NASA CR-55800, Contract no. NAS5-1234, Final Report, vol. 5, May 1963 to Dec. 1963.

121. DOUGHMAN, C. L.; AND STUMP, F. C.: The Effect of System Parameters on Space Electric Power System Weights. Westinghouse Electric, Rept. no. AIAA 63-243, Contract no. NAS5-1234, June 1963.

122. ANON.: Design and Development of Silver-Cadmium Storage Batteries. Eagle-Picher, Rept. no. NASA CR-78069, Contract no. NAS5-1318, Final Report, July 1, 1961, to June 30, 1962.

123. RICE, J. M.: Silver-Cadmium Battery Development Program. Telecomputing Corp., Rept. no. NASA CR-85, Contract no. NAS5-1431, Sept. 1964.

124. RHYNE, J. W.: Silver-Cadmium Battery Development Program. Telecomputing Corp., Rept. no. NASA CR-55792, Contract no. NAS5-1431, Second Quarterly Report, Mar. 28, 1962.

125. COLBECK, D. B.: Design, Development and Test of Sealed, Secondary Silver-Oxide-Zinc Cells. Electric Storage Battery Co., Rept. no. E-6-63, Contract no. NAS5-1607, Final Report, Mar. 21, 1963.

126. COLBECK, D. B.: Sealed Silver-Zinc Rechargeable Batteries. Electric Storage Battery Co., Rept. no. NASA CR-55785, Contract no. NAS5-1607, Final Report Addendum, June 1963.

127. ANON.: Design and Development of a Hermetically Sealed 12 Ampere-Hour Silver-Cadmium Cell in a Non-Magnetic Metallic Case. Yardney Electric Corp., Rept. no. NASA CR-60026, Contract no. NAS5-2155, Final Report.

128. WHITNEY, C. B.: Evaluation of Silver-Cadmium Batteries for Satellite Applications. The Boeing Co., Rept. no. D2-90023, Contract no. NAS5-2155, Feb. 1962.

129. KEMP, F. S.; AND MacLEAN, J. T.: Evaluation of Silver-Cadmium Batteries. The Boeing Co., Rept. no. D2-20496-1, Contract no. NAS5-2155, June 1964.

130. ANON.: Research Study on the Use of Auxiliary Electrodes in Sealed Silver-Cadmium Cells. General Electric Co., Contract no. NAS5-2817, Final Project Report, July 1962 to June 1963.

131. MELTZER, T. H.: Alkaline Battery Separator Study. Electric Storage Battery Co., Rept. no. 7054.1, Contract no. NAS5-2860, First Quarterly Report, Oct. 11, 1962.

132. GARVIN, C.; AND WEISS, E.: Alkaline Battery Separator Study. Electric Storage Battery Co., Rept. no. 7054.2, Contract no. NAS5-2860, Second Quarterly Report, Jan. 7, 1963.

133. OBERHOLZER, C. G.; AND WEISS, E.: Alkaline Battery Separator Study. Electric Storage Battery Co., Rept. no. NASA CR-56084(N64-20630), Contract no. NAS5-2860, Third Quarterly Report, Apr. 11, 1963.

134. OBERHOLZER, C. G.; SALKIND, A. J.; AND WEISS, E.: Alkaline Battery Separator Study. Electric Storage Battery Co., Rept. no. NASA CR-52491, Contract no. NAS5-2860, Fourth Quarterly Report, July 11, 1963.

135. OBERHOLZER, C. G.; OCKERMAN, J. B.; AND WEISS, E.: Alkaline Battery Separator Study. Electric Storage Battery Co., Rept. no. NASA CR-52478, Contract no. NAS5-2860, Fifth Quarterly Report, Oct. 11, 1963.

136. OBERHOLZER, C. G.; OCKERMAN, J. B.; AND WEISS, E.: Alkaline Battery Separator Study. Electric Storage Battery Co., Rept. no. NASA CR-53713, Contract no. NAS5-2860, Seventh Quarterly Report, Dec. 1963 to Mar. 1964.

137. WEISS, E.: Alkaline Battery Separator Study. Electric Storage Battery Co., Rept. no. NASA CR-59591, Contract no. NAS5-2860, Eighth Quarterly and Final Report, July 31, 1964.

138. COOKE, L. M.; ET AL.: Characteristics of Separators for Alkaline Silver Oxide-Zinc Secondary Batteries. Electric Storage Battery Co., Contract no. NAS5-2860, Screening Methods.

139. HOWARD, A. M.; AND WILLIHNGANZ, E. A.: Development of a Sealed Lead-Acid Battery for Use in Space. C&D Batteries, Contract no. NAS5-2872, Final Report, Feb. 26, 1966.

140. ANON.: Acceptance Testing, Phase One of NASA Nickel-Cadmium Battery Test Project. Martin-Marietta Corp., Rept. no. NASA CR-59663, Contract no. NAS5-3027, Final Report, Oct. 1963.

141. ANON.: Acceptance Testing, Phase One of NASA Nickel-Cadmium Battery Test Project. Martin-Marietta Corp., Rept. no. NASA CR-59664, Contract no. NAS5-3027, Suppl. no. 1 to Final Report, Nov. 1963.

142. ANON.: Nickel-Cadmium Battery Test Project: Relationship Between Operation, Life, and Failure Mechanism. Martin-Marietta Corp., Rept. no. ER-14543, Contract no. NAS5-3027, vol. I, Experimental Design, Feb. 1, 1964, to July 31, 1966.

143. ANON.: Final Report on Study of Relationships Between Acceptance Test Data and Nickel-Cadmium Life. Martin-Marietta Corp., Rept. no. ER-14473, Contract no. NAS5-3027, Final Report, vol. III, Jan. 1967.

144. ANON.: Card to Tape Editing Programs for the IBM 7094. Martin-Marietta Corp., Rept. no. ER-13941, Contract no. NAS5-3027.

145. ANON.: Synchronous Meteorological Satellite (SMS) Study. Republic Aviation Corp., Rept. no. NASA CR-55931, Contract no. NAS5-3189, vol. 2, Configurations and Systems, June 17, 1963.

146. ANON.: Synchronous Meteorological Satellite (SMS) Study. Republic Aviation Corp., Rept. no. NASA CR-55928, Contract no. NAS5-3189, Communications, Power Supply and Thermal Control, vol. 5, Final Report, June 17, 1963.

147. CARSON, W. N.: Study of Additive To Improve Nickel Hydroxide Electrode Behavior. General Electric Co., Contract no. NAS5-3349, Final Report, Mar. 15, 1964.

148. SERENYI, J. R.: Development of a 12 Ampere-Hour Sealed Silver-Zinc Cell for Satellite Applications. Yardney Electric Corp., Rept. no. NASA CR-63880, Contract no. NAS5-3351, Final Report, Oct. 1964.

149. CHARKEY, A.; AND DALIN, G. A.: Research and Development Study of the Silver-Cadmium Couple for Space Applications. Yardney Electric Corp., Rept. no. NASA CR-62610, Contract no. NAS5-3452, Final Report, July to Sept. 1964.

150. DALIN, G. A.: Research and Development Study of the Silver-Cadmium Couple for Space Applications. Yardney Electric Corp., Rept. no. NASA CR-553831, Contract no. NAS5-3452, First Quarterly Report, July 1 to Sept. 30, 1963.

151. CHARKEY, A.; AND DALIN, G. A.: Research and Development Study of the Silver-Cadmium Couple for Space Applications. Yardney Electric Corp., Rept. no. NASA CR-53832, Contract no. NAS5-3452, Second Quarterly Report, Oct. to Dec. 1963.

152. CHARKEY, A.; AND DALIN, G. A.: Research and Development Study of the Silver-Cadmium Couple for Space Applications. Yardney Electric Corp., Rept. no. NASA CR-57008, Contract no. NAS5-3452, Third Quarterly Report, Jan. to Mar. 1964.

153. CHARKEY, A.; AND DALIN, G. A.: Research and Development Study of the Silver-Cadmium Couple for Space Applications. Yardney Electric Corp., Rept. no. NASA CR-57014, Contract no. NAS5-3452, Fourth Quarterly Report, Apr. to June 1964.

154. HOYT, H. E.; AND PFLUGER, H. L.: Improved Separators for Silver-Oxide-Zinc and Silver Oxide-Cadmium Cells for Spacecraft Applications. Borden Chemical Co., Rept. no. NASA CR-64607, Contract no. NAS5-3467, Final Report, June 1963 to Nov. 1964.

155. CARSON, W. N., JR.; CONSIGLIO, J. A.; AND NILSON, R. R.: Characterization of Nickel-Cadmium Electrodes. General Electric Co., Rept. no. NASA CR-63916, Contract no. NAS5-3477, Final Report, July 1, 1963, to Dec. 31, 1964.

156. ANON.: Characterization of Nickel-Cadmium Electrodes. General Electric Co., Rept. no. NASA CR-55772, Contract no. NAS5-3477, First Quarterly Report, July 1 to Oct. 1, 1963.

157. ANON.: Characterization of Nickel-Cadmium Electrodes. General Electric Co., Rept. no. NASA CR-53731, Contract no. NAS5-3477, Second Quarterly Report, Oct. 1963 to Jan. 1964.

158. ANON.: Characterization of Nickel-Cadmium Electrodes. General Electric Co., Contract no. NAS5-3477, Third Quarterly Report, Jan. 1 to Apr. 1, 1964.

159. ANON.: Characterization of Nickel-Cadmium Electrodes. General Electric Co., Rept. no. NASA CR-59576, Contract no. NAS5-3477, Fourth Quarterly Report, Apr. 1 to July 1, 1964.

160. ANON.: Characterization of Nickel-Cadmium Electrodes. General Electric Co., Rept. no. NASA CR-60418, Contract no. NAS5-3477, Fifth Quarterly Report, July 1 to Oct. 1, 1964.

161. RITTERMAN, P.; AND SEIGER, H. N.: Hermetically Sealed Cells Capable of Overdischarge as Well as Overcharge. Gulton Industries, Contract no. NAS5-3667, Final Report, May 1964.

162. CARSON, W. N.; CONSIGLIO, J. A.; AND MARR, J. W.: Study of the Use of Auxiliary Electrodes in Silver Cells. General Electric Co., Contract no. NAS5-3669, Final Report, July 1965.

163. CARSON, W. N.; CONSIGLIO, J. A.; AND MARR, J. W.: Study of the Use of Auxiliary Electrodes in Silver Cells. General Electric Co., Rept. no. NASA CR-405, Contract no. NAS5-3669, Final Report, Mar. 1966.

164. CATOTTI, A. J.; AND READ, M. D.: Development of a Nickel-Cadmium Storage Cell Immune to Damage From Overdischarge and Overcharge. General Electric Co., Rept. no. NASA CR-62019, Contract no. NAS5-3707, Final Report, June 21, 1965.

165. CHREITZBERG, A. M.; AND CUSHING, F. S.: Research and Development on Cells With Bellows Controlled Electrolyte Levels. Electric Storage Battery Co., Rept. no. E-13-66, Contract no. NAS5-3813, Fourth and Final Report, May 11, 1965, to Apr. 1, 1966.

166. CHREITZBERG, A. M.; AND CUSHING, F. S.: Research and Development on Cells with Bellows Controlled Electrolyte Levels. Electric Storage Battery Co., Rept. no. NASA CR-59373, Contract no. NAS5-3813, First Quarterly Report, June 10 to Sept. 10, 1964.

167. CHREITZBERG, A. M.; AND CUSHING, F. S.: Research and Development on Cells With Bellows Controlled Electrolyte Levels. Electric Storage Battery Co., Rept. no. NASA CR-60932, Contract no. NAS5-3813, Second Quarterly Report, Sept. 10 to Dec. 10, 1964.

168. CHREITZBERG, A. M.; AND CUSHING, F. S.: Research and Development on Cells With Bellows Controlled Electrolyte Levels. Electric Storage Battery Co., Rept. no. NASA CR-63903, Contract no. NAS5-3813, Third Progress Report, Dec. 10, 1964, to May 10, 1965.

169. APGAR, G. M.; AND CALLAHAN, J.: Prototype Nickel-Cadmium Cells for a Future Meteorological Spacecraft. Gulton Industries, Contract no. NAS5-3839, Final Report, May 1, 1966.

170. STACHURSKI, Z. O. J.: Investigation and Improvement of Zinc Electrodes for Electrochemical Cells. Yardney Electric Co., Rept. no. 617-65, Contract no. NAS5-3873, Final Report, Dec. 1965.

171. DALIN, G. A.; AND STACHURSKI, Z. O. J.: Investigation and Improvement of Zinc Electrodes for Electrochemical Cells. Yardney Electric Co., Rept. no. NASA CR-59945, Contract no. NAS5-3873, First Quarterly Report, July to Sept. 1964.

172. DALIN, G. A.; AND STACHURSKI, Z. O. J.: Investigation and Improvement of Zinc Electrodes for Electrochemical Cells. Yardney Electric Co., Rept. no. NASA CR-62446, Contract no. NAS5-3873, Second Quarterly Report, Oct. to Dec. 1964.

173. STACHURSKI, Z. O. J.: Investigation and Improvement of Zinc Electrodes for Electrochemical Cells. Yardney Electric Corp., Rept. no. 556-65, Contract no. NAS5-3873, Third Quarterly Report, Jan. 1 to Mar. 31, 1965.

174. OXLEY, J. E.: The Improvement of Zinc Electrodes for Electrochemical Cells. Leesona Moos Laboratories, Contract no. NAS5-3908, Final Report, June 12, 1964, to Mar. 24, 1965.

175. ANON.: The Improvement of Zinc Electrodes for Electrochemical Cells. Leesona Moos Laboratories, Rept. no. NASA CR-59362, Contract no. NAS5-3908, First Quarterly Report, June 12 to Sept. 12, 1964.

176. OXLEY, J. E.: The Improvement of Zinc Electrodes for Electrochemical Cells. Leesona Moos Laboratories, Rept. no. CR-377, Contract no. NAS5-3908, Feb. 1966.

177. ANON.: Testing and Evaluation of Nickel-Cadmium Spacecraft-Type Cells. Cook Electric Co., Rept. no. 9PD-4667-2, Contract no. NAS5-9073, Final Technical Report, Jan. 1 to Nov. 1, 1965.

178. LUKE, I. F.; AND ROEGER, E. A., JR.: Testing and Evaluation of Nickel-Cadmium Spacecraft-Type Cells. Cook Electric Co., Rept. no. NASA CR-67580, Contract no. NAS5-9073, Semiannual Report, Jan. 1 to July 1, 1965.

179. CHARKEY, A.: Research and Development Study of the Silver-Cadmium Couple for Space Application. Yardney Electric Corp., Contract no. NAS5-9106, Final Report.

180. CHARKEY, A.: Research and Development of the Silver Oxide-Cadmium Electrochemical System. Yardney Electric Corp., Rept. no. NASA CR-68796, Contract no. NAS5-9106, Third Quarterly Report, May 10 to Aug. 9, 1965.

181. HOYT, H. E.; AND PFLUGER, H. L.: Improved Separators for Silver-Oxide-Zinc and Silver Oxide-Cadmium Cells for Spacecraft Applications. Borden Chemical Co., Rept. no. NASA CR-80108, Contract no. NAS5-9107, Final Report, Nov. 1964 to Nov. 1965.

182. HOYT, H. E.; AND PFLUGER, H. L.: Improved Separators for Silver Oxide-Zinc and Silver Oxide-Cadmium Cells for Spacecraft Applications. Borden Chemical Co., Rept. no. NASA CR-68227, Contract no. NAS5-9107, First Quarterly Report, Nov. 10, 1964, to Feb. 9, 1965.

183. HOYT, H. E.; AND PFLUGER, H. L.: Improved Separators for Silver Oxide-Zinc and Silver Oxide-Cadmium Cells for Spacecraft Applications. Borden Chemical Co., Rept. no. NASA CR-68847, Contract no. NAS5-9107, Second Quarterly Report, Feb. 10 to May 9, 1965.

184. HOYT, H. E.; AND PFLUGER, H. L.: Improved Separators for Silver Oxide-Zinc and Silver Oxide-Cadmium Cells for Spacecraft Applications. Borden Chemical Co., Rept. no. NASA CR-74407, Contract no. NAS5-9107, Third Quarterly Report, May 10 to Aug. 9, 1965.

185. HOYT, H. E.; AND PFLUGER, H. L.: Improved Separators for Silver Oxide-Zinc and Silver Oxide-Cadmium Cells for Spacecraft Applications. Borden Chemical Co., Contract no. NAS5-9107, Mod. 6, First Quarterly Report. No date.

186. HOYT, H. E.; AND PFLUGER, H. L.: Improved Separators for Silver Oxide-Zinc and Silver Oxide-Cadmium Cells for Spacecraft Applications. Borden Chemical Co., Contract no. NAS5-9107, Second Quarterly Report, June 1967.

187. HOYT, H. E.; AND PFLUGER, H. L.: Improved Separators for Silver Oxide-Zinc and Silver Oxide-Cadmium Cells for Spacecraft Applications. Borden Chemical Co., Contract no. NAS5-9107, Mod. 6, Third Quarterly Report, July 1967.

188. CARSON, W. N.; AND CONSIGLIO, J. A.: Electrodeposited Inorganic Separators. General Electric Co., Rept. no. S-66-1019, Contract no. NAS5-9168, Final Report, Aug. 1966.

189. HENNIGAN, T. J.: Results of Tests on Silver-Cadmium Cells Containing Inorganic Electrodeposited Separators on the Positive Electrodes. NASA/GSFC, Report after Final Contract Report, Rough Draft, Contract no. NAS5-9168, Jan. 25, 1967.

190. ANON.: Research and Development on Electrodeposited Inorganic Separators. General Electric Co., Rept. no. NASA CR-70374, Contract no. NAS5-9168, Second Quarterly Report, July 15 to Oct. 15, 1965.

191. ANON.: Research and Development on Electrodeposited Inorganic Separators. General Electric Co., Rept. no. NASA CR–74147, Contract no. NAS5–9168, Third Quarterly Report, Oct. 15, 1965, to Jan. 15, 1966.

192. LEISENRING, J. G.: Study and Analysis of Satellite Power Systems Configurations for Maximum Utilization of Power. TRW Systems, Rept. no. 4898–6001–R000, Contract no. NAS5–9178, Phase I Technical Report, Final Report, May 18, 1965, to July 18, 1966.

193. BINCKLEY, W. G.: Study and Analysis of Satellite Power Systems Configurations for Maximum Utilization of Power. TRW Systems, Contract no. NAS5–9178, First Quarterly Report, May 18 to Aug. 18, 1965.

194. BINCKLEY, W. G.: Study and Analysis of Satellite Power Systems Configurations for Maximum Utilization of Power. TRW Systems, Contract no. NAS5–9178, Second Quarterly Report, Aug. 19 to Nov. 18, 1965.

195. BINCKLEY, W. G.: Study and Analysis of Satellite Power Systems Configurations for Maximum Utilization of Power. TRW Systems, Rept. no. E–7061.2–225, Contract no. NAS5–9178, Third Quarterly Report, Nov. 19, 1965, to Feb. 18, 1966.

196. LEISENRING, J. G.: Study and Analysis of Satellite Power Systems Configurations for Maximum Utilization of Power. TRW Systems, Rept. no. E–7061.2–242, Contract no. NAS5–9178, Fourth Quarterly Report, Feb. 19 to May 18, 1966.

197. LEISENRING, J. G.: Study and Analysis of Satellite Power Systems Configurations for Maximum Utilization of Power. TRW Systems, Rept. no. E–7061.2–252, Contract no. NAS5–9178, Fifth Quarterly Report, May 18 to July 18, 1966.

198. CARSON, W. N.: A Study of Nickel-Cadmium Spacecraft Battery Charge Control Methods. General Electric Co., Rept. no. NASA CR–62029, Contract no. NAS5–9193, Final Report, Apr. 1966.

199. BAUMSTARK, G. A.: Procurement and Development Program for Nickel-Cadmium Cells to Specification S–615–P–2. Sonotone Corp., Rept. no. N66–90003, Contract no. NAS5–9226, First Semimonthly Report, Aug. 23 to 26, 1965.

200. ANON.: Procurement and Development Program for Nickel-Cadmium Cells to Specification S–615–P–2. Sonotone Corp., Rept. no. X66–90262, Contract no. NAS5–9226, Second Semimonthly Report, Aug. to Sept. 1965.

201. BAUMSTARK, G. A.: Procurement and Development Program for Nickel-Cadmium Cells to Specification S–615–P–2. Sonotone Corp., Rept. no. N66–90087, Contract no. NAS5–9226, Third Semimonthly Report, Sept. 11 to Sept. 28, 1965.

202. BAUMSTARK, G. A.: Procurement and Development Program for Nickel-Cadmium Cells to Specification S–615–P–2. Sonotone Corp., Rept. no. N66–90082, Contract no. NAS5–9226, Fifth Semimonthly Report, Oct. 14 to 27, 1965.

203. BAUMSTARK, G. A.: Procurement and Development Program for Nickel-Cadmium Cells to Specification S–615–P–2. Sonotone Corp., Rept. no. N66–90083, Contract no. NAS5–9226, Sixth Semimonthly Report, Oct. 28 to Nov. 11, 1965.

204. BAUMSTARK, G. A.: Procurement and Development Program for Nickel-Cadmium Cells to Specification S–615–P–2. Sonotone Corp., Rept. no. N66–90121, Contract no. NAS5–9226, Seventh Semimonthly Report, Nov. 12 to 29, 1965.

205. BAUMSTARK, G. A.: Procurement and Development Program for Nickel-Cadmium Cells to Specification S-615-P-2. Sonotone Corp., Rept. no. NASA CR-78517, Contract no. NAS5-9226, Technical Status Rept. no. 12, May to Aug. 1966.

206. ANON.: Study of Nickel-Cadmium Cells. General Electric Co., Rept. no. NASA CR-68995, Contract no. NAS5-9586, First Quarterly Report, May to Aug. 1965.

207. ANON.: Study of Nickel-Cadmium Cells. General Electric Co., Rept. no. NASA CR-74024, Contract no. NAS5-9586, Second Quarterly Report, Aug. to Nov. 1965.

208. ANON.: Study of Nickel-Cadmium Cells. General Electric Co., Rept. no. NASA CR-75192, Contract no. NAS5-9586, Third Quarterly Report, Nov. 1965 to Feb. 1966.

209. AROUETE, S.; AND BLURTON, K. F.: The Improvement of Zinc Electrodes for Electrochemical Cells. Leesona Moos Labs, Contract no. NAS5-9591, Final Report, June 3, 1965, to Oct. 31, 1966.

210. FLEISCHMANN, C. W.; AND OXLEY, J. E.: The Improvement of Zinc Electrodes for Electrochemical Cells. Leesona Moos Labs, Rept. no. NASA CR-68646, Contract no. NAS5-9591, First Quarterly Report, June to Sept. 1965.

211. FLEISCHMANN, C. W.; AND OXLEY, J. E.: The Improvement of Zinc Electrodes for Electrochemical Cells. Leesona Moos Labs, Rept. no. NASA CR-70724, Contract no. NAS5-9591, Second Quarterly Report, Sept. 4 to Dec. 4, 1965.

212. FLEISCHMANN, C. W.; AND OXLEY, J. E.: The Improvement of Zinc Electrodes for Electrochemical Cells. Leesona Moos Labs, Rept. no. NASA CR-75237, Contract no. NAS5-9591, Third Quarterly Report, Dec. 5, 1965, to Mar. 4, 1966.

213. FRANK, H.; AND STRIER, M. P.: Small Fuel Cell To Eliminate Pressure Caused by Gassing in High Energy Density Batteries. Douglas Aircraft Co., Rept. no. SM 48457-F, Contract no. NAS5-9494, Final Report, June 1965 to June 1966.

214. FRANK, H.; AND STRIER, M. P.: Small Fuel Cell To Eliminate Pressure Caused by Gassing in High Energy Density Batteries. Douglas Aircraft Co., Rept. no. SM 48457-Q2, Contract no. NAS5-9594, Second Quarterly Progress Report, Sept. 30 to Dec. 30, 1965.

215. FRANK, H.; AND STRIER, M. P.: Small Fuel Cell To Eliminate Pressure Caused by Gassing in High Energy Density Batteries. Douglas Aircraft Co., Rept. no. SM 48457-Q3, Contract no. NAS5-9594, Third Quarterly Progress Report, Dec. 30, 1965, to Mar. 31, 1966.

216. FOLEY, R. T.; AND WEBSTER, W. H.: Research Into Fundamental Phenomena Associated With Spacecraft Electrochemical Devices—Calorimetry of Nickel-Cadmium Cells. The American Univ., Contract no. NAS5-10105, Third Report, Jan. 1 to Mar. 31, 1967.

217. FOLEY, R. T.; AND WEBSTER, W. H.: Research Into Fundamental Phenomena Associated With Spacecraft Electrochemical Devices—Calorimetry of Nickel-Cadmium Cells. The American Univ., Contract no. NAS5-10105, First Quarterly Report, Jan. 1 to Sept. 30, 1966.

218. FOLEY, R. T.; AND WEBSTER, W. H.: Research Into Fundamental Phenomena Associated With Spacecraft Electrochemical Devices—Calorimetry of Nickel-Cadmium Cells. The American Univ., Contract no. NAS5-10105, Second Quarterly Report, Oct. 1 to Dec. 31, 1966.

219. CHARLIP, S.; AND LYALL, A.: Development of Pile Type, High Discharge Rate Nickel-Cadmium Squib Batteries. Gulton Industries, Contract no. NAS5-10160, First Quarterly Report, Mar. 4 to June 4, 1966.

220. CHARLIP, S.: Development of Pile Type, High Discharge Rate Nickel-Cadmium Squib Batteries. Gulton Industries, Contract no. NAS5–10160, Second Quarterly Report, June 5 to Sept. 4, 1966.

221. CHARLIP, S.; AND STAUB, T.: Development of Pile Type, High Discharge Rate Nickel-Cadmium Squib Batteries. Gulton Industries, Contract no. NAS5–10160, Third Quarterly Report, Sept. 5 to Dec. 4, 1966.

222. MAUCHLY, J. W.; AND WAITE, J. H.: Computer Methods for the Reduction, Correlation and Analysis of Space Battery Test Data. Mauchly Systems, Inc., Contract no. NAS5–10203, Final Report, May 1 to Dec. 31, 1966.

223. EPSTEIN, S. D.; AND WAITE, J. H.: Nickel-Cadmium Space Battery Test Data Analysis Project, Phase 2. Mauchly Systems, Inc., Contract no. NAS5–10203, First Quarterly Report, Jan. 1 to Apr. 30, 1967.

224. INGLING, W.: Satellite Battery Test and Evaluation. Dayrad Labs, Contract no. NAS5–10213, Jan. 1961.

225. STACHURSKI, Z. O. J.: Study To Investigate and Improve the Zinc Electrode for Spacecraft Electrochemical Cells. Yardney Electric Corp., Contract no. NAS5–10231, First Quarterly Report, June 1967.

226. McBREEN, J.: Study To Investigate and Improve the Zinc Electrode for Spacecraft Electrochemical Cells. Yardney Electric Corp., Contract no. NAS5–10231, Second Quarterly Report, June 1967.

227. McBREEN, J.: Study To Investigate and Improve the Zinc Electrode for Spacecraft Electrochemical Cells. Yardney Electric Corp., Contract no. NAS5–10231, Third Quarterly Report, Feb. 1 to Apr. 30, 1967.

228. LERNER, S.: Characterization of Recombination and Control Electrodes for Spacecraft Nickel-Cadmium Cells. Gulton Industries, Contract no. NAS5–10241, First Quarterly Report, June 9 to Sept. 9, 1966.

229. LERNER, S.: Characterization of Recombination and Control Electrodes for Spacecraft Nickel-Cadmium Cells. Gulton Industries, Contract no. NAS5–10241, Third Quarterly Report, Dec. 9, 1966, to Mar. 9, 1967.

230. POWERS, R. A.: Secondary Zinc-Oxygen Cell for Spacecraft Applications. Union Carbide Corp., Contract no. NAS5–10247, First Quarterly Report, June 23 to Sept. 23, 1966.

231. POWERS, R. A.: Secondary Zinc-Oxygen Cell for Spacecraft Applications. Union Carbide Corp., Contract no. NAS5–10247, Second Quarterly Report, Sept. 23 to Dec. 23, 1966.

232. CARSON, W. N., JR.; RAMPEL, G.; AND WEINSTOCK, I. B.: Characterization of Recombination and Control Electrodes for Spacecraft Nickel-Cadmium Cells. General Electric Co., Contract no. NAS5–10261, First Quarterly Report, Oct. 1966.

233. CARSON, W. N., JR.; RAMPEL, G.; AND WEINSTOCK, I. B.: Characterization of Recombination and Control Electrodes for Spacecraft Nickel-Cadmium Cells. General Electric Co., Contract no. NAS5–10261, Second Quarterly Report, Jan. 1967.

234. CARSON, W. N., JR.; RAMPEL, G.; AND WEINSTOCK, I. B.: Characterization of Recombination and Control Electrodes for Spacecraft Nickel-Cadmium Cells. General Electric Co., Contract no. NAS5–10261, Second Quarterly Report, May 1967.

235. ANON.: Research Summary no. 36–12, vol. I. Jet Propulsion Laboratory, Contract no. NAS7–100, Jan. 2, 1962.

236. GOLDING, H. O.; HILMAN, J.; AND PUBLISI, A. G.: Design Evaluation/Qualification Test of the Engine Primary Battery, Douglas Specification Control no. 1A65819-1, Eagle-Picher P/N MAP-4168, Model no. Saturn S-IV. Douglas Aircraft Co., Rept. no. SM-44202, Contract no. NAS7-100, Qualification Test Report, Oct. 25, 1963.

237. ANDREWS, P. J.: Master List of Reports, Saturn S–IVB Program. Douglas Aircraft Co., Rept. no. SM–46534, Contract no. NAS7–101, Jan. 1, 1964.

238. ANON.: Qualification and Reliability Test Report of Battery, Primary, Silver-Zinc, 28 Volt, Part no. ME461–0004–0003, and ME461–0004–0004. North American Aviation, Rept. no. TR–14–66, Contract no. NAS7–200, Oct. 19, 1966.

239. ANON.: Documentation List for Saturn Stage S–II. North American Aviation, Rept. no. SID 62–430, Contract no. NAS7–200, Feb. 12, 1963.

240. COLICHMAN, E. L.; NAIDITCH, S.; AND ROWLETTE, J. J.: Gaseous Electrolytes for Batteries and Fuel Cells. Unified Science Associates, Rept. no. NASA CR–60430, Contract no. NAS7–326, First Quarterly Report, Aug. 21 to Nov. 20, 1964.

241. NAIDITCH, S.: Gaseous Electrolytes for Batteries and Fuel Cells. Unified Science Associates, Rept. no. NASA CR–62348, Contract no. NAS7–326, Second Quarterly Report, Nov. 21, 1964, to Feb. 20, 1965.

242. NAIDITCH, S.: Gaseous Electrolytes for Batteries and Fuel Cells. Unified Science Associates, Rept. no. NASA CR–64347, Contract no. NAS7–326, Third Quarterly Report, Feb. to May 1965.

243. NAIDITCH, S.: Gaseous Electrolytes for Batteries and Fuel Cells. Unified Science Associates, Rept. no. NASA CR–69248, Contract no. NAS7–326, Fourth Quarterly Report, May to Aug. 1965.

244. NAIDITCH, S.: Gaseous Electrolytes for Batteries and Fuel Cells. Unified Science Associates, Rept. no. NASA CR–70581, or NASA CR–70841, Contract no. NAS7–326, Fifth Quarterly Progress Report, Aug. 21 to Nov. 20, 1965.

245. NAIDITCH, S.: Gaseous Electrolytes for Batteries and Fuel Cells. Unified Science Associates, Rept. no. NASA CR–74671, Contract no. NAS7–326, Sixth Quarterly Report, Nov. 21, 1965, to Feb. 20, 1966.

246. NAIDITCH, S.: Gaseous Electrolytes for Batteries and Fuel Cells. Unified Science Associates, Rept. no. NASA CR–76976, Contract no. NAS7–326, Seventh Quarterly Report, Feb. to May 1966.

247. NAIDITCH, S.: Gaseous Electrolytes for Batteries and Fuel Cells. Unified Science Associates, Rept. no. NASA CR–79087, Contract no. NAS7–326, Eighth Quarterly Report, Period Ending July 31, 1966.

248. NAIDITCH, S.: Gaseous Electrolytes for Batteries and Fuel Cells. Unified Science Associates, Contract no. NAS7–437, First Quarterly Report, Aug. 1 to Oct. 30, 1966.

249. NAIDITCH, S.: Gaseous Electrolytes for Batteries and Fuel Cells. Unified Science Associates, Contract no. NAS7–437, Second Quarterly Report, Nov. 1966 to Jan. 1967.

250. NAIDITCH, S.: Gaseous Electrolytes for Batteries and Fuel Cells. Unified Science Associates, Contract no. NAS7–437, Third Quarterly Report, Feb. 1 to Apr. 30, 1967.

251. HAWKINS, B. R.: Investigation Leading to the Development of a Primary Zinc-Silver Oxide Battery of Improved Performance Characteristics. Eagle-Picher Co., Rept. no. NASA CR–59627, Contract no. NAS8–5493, Final Report, July 1963 to June 1964.

252. HAWKINS, B. R.: Investigations Leading to the Development of a Primary Zinc-Silver Oxide Battery of Improved Performance Characteristics. Eagle-Picher Co., Rept. no. NASA CR–68563, Contract no. NAS8–5493, Final Report, July 1964 to June 1965.

253. HAWKINS, B. R.: Investigations Leading to the Development of a Primary Zinc-Silver Oxide Battery of Improved Performance Characteristics. Eagle-Picher Co., Rept. no. NASA CR–56363, Contract no. NAS8–5493, Summary Rept. no. 1, July to Dec. 1963.

254. HAWKINS, B. R.: Investigations Leading to the Development of a Primary Zinc-Silver Oxide Battery of Improved Performance Characteristics. Eagle-Picher Co., Rept. no. NASA CR–56077, Contract no. NAS8–5493, Summary Report no. 2, Jan. 1 to Mar. 31, 1964.

255. HAWKINS, B. R.: Investigations Leading to the Development of a Primary Zinc-Silver Oxide Battery of Improved Performance Characteristics. Eagle-Picher Co., Rept. no. NASA CR–59623, Contract no. NAS8–5493, Summary Report no. 3, July to Sept. 1964.

256. ANON.: Investigations Leading to the Development of a Primary Zinc-Silver Oxide Battery of Improved Performance Characteristics. Eagle-Picher Co., Rept. no. NASA CR–64592, Contract no. NAS8–5493, Sixth Quarterly Report, Oct. to Dec. 1964.

257. ANON.: Investigations Leading to the Development of a Primary Zinc-Silver Oxide Battery of Improved Performance Characteristics. Eagle-Picher Co., Rept. no. NASA CR–64223, Seventh Quarterly Report, Jan. to Mar. 1965.

258. HAWKINS, B. R.: Investigations Leading to the Development of a Primary Zinc-Silver Oxide Battery of Improved Performance Characteristics. Eagle-Picher Co., Contract no. NAS8–5493, First Progress Report, July 1 to 31, 1963.

259. HAWKINS, B. R.: Investigations Leading to the Development of a Primary Zinc-Silver Oxide Battery of Improved Performance Characteristics. Eagle-Picher Co., Contract no. NAS8–5493, Second Progress Report, Aug. 1 to 31, 1963.

260. HAWKINS, B. R.: Investigations Leading to the Development of a Primary Zinc-Silver Oxide Battery of Improved Performance Characteristics. Eagle-Picher Co., Contract no. NAS8–5493, Third Progress Report, Sept. 1 to 30, 1963.

261. HAWKINS, B. R.: Investigations Leading to the Development of a Primary Zinc-Silver Oxide Battery of Improved Performance Characteristics. Eagle-Picher Co., Contract no. NAS8–5493, Fourth Progress Report, Oct. 1 to 31, 1963.

262. HAWKINS, B. R.: Investigations Leading to the Development of a Primary Zinc-Silver Oxide Battery of Improved Performance Characteristics. Eagle-Picher Co., Contract no. NAS8–5493, Fifth Progress Report, Nov. 1 to 30, 1963.

263. HAWKINS, B. R.: Investigations Leading to the Development of a Primary Zinc-Silver Oxide Battery of Improved Performance Characteristics. Eagle-Picher Co., Contract no. NAS8–5493, Sixth Progress Report, Dec. 1 to 31, 1963.

264. HAWKINS, B. R.: Investigations Leading to the Development of a Primary Zinc-Silver Oxide Battery of Improved Performance Characteristics. Eagle-Picher Co., Contract no. NAS8–5493, Seventh Progress Report, Jan. 1 to 31, 1964.

265. HAWKINS, B. R.: Investigations Leading to the Development of a Primary Zinc-Silver Oxide Battery of Improved Performance Characteristics. Eagle-Picher Co., Contract no. NAS8–5493, Eighth Progress Report, Feb. 1 to 29, 1964.

266. HAWKINS, B. R.: Investigations Leading to the Development of a Primary Zinc-Silver Oxide Battery of Improved Performance Characteristics. Eagle-Picher Co., Contract no. NAS8–5493, Ninth Progress Report, Mar. 1 to 31, 1964.

267. HAWKINS, B. R.: Investigations Leading to the Development of a Primary Zinc-Silver Oxide Battery of Improved Performance Characteristics.

Eagle-Picher Co., Contract no. NAS8–5493, 10th Progress Report, Apr. 1 to 30, 1964.

268. HAWKINS, B. R.: Investigations Leading to the Development of a Primary Zinc-Silver Oxide Battery of Improved Performance Characteristics. Eagle-Picher Co., Contract no. NAS8–5493, 11th Progress Report, May 1 to 31, 1964.

269. ANON.: Investigations Leading to the Development of a Primary Zinc-Silver Oxide Battery of Improved Performance Characteristics. Eagle-Picher Co., Contract no. NAS8–5493, 17th Progress Report, Nov. 1964.

270. ANON.: Investigations Leading to the Development of a Primary Zinc-Silver Oxide Battery of Improved Performance Characteristics. Eagle-Picher Co., Contract no. NAS8–5493, 19th Progress Report. No date.

271. ANON.: Investigations Leading to the Development of a Primary Zinc-Silver Oxide Battery of Improved Performance Characteristics. Eagle-Picher Co., Contract no. NAS8–5493, 20th Progress Report. No date.

272. ANON.: Investigations Leading to the Development of a Primary Zinc-Silver Oxide Battery of Improved Performance Characteristics. Eagle-Picher Co., Contract no. NAS8–5493, 21st Progress Report. No date.

273. ANON.: Investigations Leading to the Development of a Primary Zinc-Silver Oxide Battery of Improved Performance Characteristics. Eagle-Picher Co., Contract no. NAS8–5493, 22d Progress Report, Apr. 30, 1965.

274. ANON.: Investigations Leading to the Development of a Primary Zinc-Silver Oxide Battery of Improved Performance Characteristics. Eagle-Picher Co., Contract no. NAS8–5493, 23d Progress Report, May 1 to 31, 1965.

275. ANON.: Investigations Leading to the Development of a Primary Zinc-Silver Oxide Battery of Improved Performance Characteristics. Eagle-Picher Co., Contract no. NAS8–5493, 24th Progress Report, June 1 to 30, 1965.

276. SEABOURN, C. M.; SMITH, L. D.; AND STAGER, D. N.: Program for the Analysis of Electrical Systems Operations. TRW Systems, Rept. no. 2124–H004–R0-000, Contract no. NAS9–4810, Project Technical Report, Task ASPO–15, July 30, 1966.

277. GROSS, S.: Development and Fabrication of Advanced Battery Energy Storage System. The Boeing Co., Contract no. NAS9–6470, Midterm Report, Apr. 10, 1967.

278. ANON.: Manufacturing and Testing Problems, Volume I. Power Information Center, Rept. no. PIC–BAT 209/6, Transcript of Conference on Secondary Space Batteries, June 1963.

279. ANON.: User's Problems, Conclusions, and Recommendations, Volume II. Power Information Center, Rept. no. PIC–BAT 209/6.1, Transcript of Conference on Secondary Space Batteries, Sept. 1963.

280. ANON.: Study Papers on the Auxiliary Electrode. Power Information Center, Rept. no. NASA CR–67987, Contract no. NASr–191, Oct. 1965.

281. ANON.: Background Material for Study of National Space Power Program. Volume I: Electrochemical Papers. Power Information Center, Rept. no. PIC 120/1 (AD 452617), Contract no. NASr–191, Nov. 1964.

282. ANON.: Organic Electrolyte Batteries. Power Information Center, Rept. no. PIC–BAT 209/10, Contract no. NASr–191, Jan. 19, 1967.

283. HAMER, W. J.: Electrochemical Data, Part I. National Bureau of Standards, Rept. no. NASA CR–62024, Contract no. NAS R–09–022–029, Quarterly Report, Oct. 1 to Dec. 31, 1965.

284. HAMER, W. J.: Electrochemical Data, Part II. National Bureau of Standards, Rept. no. NBS 9047, Contract no. R–09–022–029, Quarterly Report, Jan. to Mar. 1966.

285. DeWane, H. J.; and Hamer, W. J.: Electrochemical Data, Part III. National Bureau of Standards, Rept. no. NBS 9394, Contract no. R–09–022–029, Quarterly Report, Apr. 1 to June 30, 1966.

286. DeWane, H. J.; and Hamer, W. J.: Electrochemical Data, Part IV. National Bureau of Standards, Rept. no. NBS 9432, Contract no. R–09–022–029, Quarterly Report, July 1 to Sept. 30, 1966.

287. DeWane, H. J.; and Hamer, W. J.: Electrochemical Data, Part V. National Bureau of Standards, Rept. no. NBS 9472, Contract no. R–09–022–029, Quarterly Report, Oct. 1 to Dec. 31, 1966.

288. Metzger, W. H.; and Sherfey, J. M.: Electrochemical Calorimetry: Thermal Effects of Nickel-Cadmium Batteries. National Bureau of Standards, Rept. no. 1–650–62–15, Contract no. NASr–09–022–029.

289. Chilton, J. E.; Duffek, E. F.; and Reed, A. E.: Development of High Energy Batteries. Stanford Research Institute, Rept. no. NASA CR–74410, Contract no. NASw–111, Final Report, Apr. 28, 1961.

290. Francis, H. T.: Space Battery Handbook. Armour Research Foundation, Rept. no. NASA CR–56514, Contract no. NASw–401, Apr. 15, 1963.

291. Shulman, I. M.: Correlation of Data From Tests on Nickel-Cadmium Batteries. Radio Corp. of America, Contract no. NASw–1001, Final Report, Nov. 1965.

292. Shulman, I. M.: Correlation of Data From Tests on Nickel-Cadmium Batteries. Radio Corp. of America, Rept. no. NASA CR–480, Contract no. NASw–1001, Final Report, May 1966.

293. Giner, J.; Jasinski, R. J.; and Makrides, A. C.: Development of Cathodic Electrocatalysts for Use in Low Temperature H_2/O_2 Fuel Cells With an Alkaline Electrolyte. Tyco Labs, Rept. no. NASA CR–68891, Contract no. NASw–1233, First Quarterly Report, July to Sept. 1965.

294. Giner, J.; Jasinski, R. J.; and Makrides, A. C.: Development of Cathodic Electrocatalysts for Use in Low Temperature H_2/O_2 Fuel Cells With an Alkaline Electrolyte. Tyco Labs, Rept. no. NASA CR–79030, Contract no. NASw–1233, Second Quarterly Report, Oct. to Dec. 1965.

295. Giner, J.; Jasinski, R. J.; and Makrides, A. C.: Development of Cathodic Electrocatalysts for Use in Low Temperature H_2/O_2 Fuel Cells With an Alkaline Electrolyte. Tyco Labs, Rept. no. NASA CR–75199, Contract no. NASw–1233, Third Quarterly Report, Jan./Mar. 31, 1966.

296. Giner, J.; Jasinski, R.; and Makrides, A. C.: Development of Cathodic Electrocatalysts for Use in Low Temperature H_2/O_2 Fuel Cells With an Alkaline Electrolyte. Tyco Labs, Rept. no. Q–4, Contract no. NASw–1233, Fourth Quarterly Report, July 1, 1965, to June 30, 1966.

297. Giner, J.; et al.: Development of Cathodic Electrocatalysts for Use in Low Temperature H_2/O_2 Fuel Cells With an Alkaline Electrolyte. Tyco Labs, Rept. no. Q–5, Contract no. NASw–1233, Fifth Quarterly Report, July 1 to Sept. 30, 1966.

298. Giner, J.; et al.: Development of Cathodic Electrocatalysts for Use in Low Temperature H_2/O_2 Fuel Cells With an Alkaline Electrolyte. Tyco Labs, Rept. no. Q–6, Contract Subscript no. NASw–1233, Sixth Quarterly Report, Oct. 1 to Dec. 31, 1966.

299. Anon.: Nickel-Cadmium Spacecraft Batteries. National Aeronautics and Space Administration Internal Report, July 1961.

300. Anon.: Sealed Silver-Cadmium Systems. National Aeronautics and Space Administration Internal Report, Jan. 1961.

301. Grens, E. A., II; and Tobias, C. W.: Analysis of the Dynamic Behavior of Flooded Porous Electrodes. Univ. of California (Berkeley), Contract no. NSG 150–61, Dec. 1963.

302. TOBIAS, C. W.: Dynamic Behavior of Porous Electrode Systems. Univ. of California (Berkeley), Rept. no. NASA CR–50013, Contract no. NSG 150–61, First Semiannual Report, Feb. 1962.

303. NEWMAN, J. S.; AND TOBIAS, C. W.: Theoretical Analysis of Current Distribution in Porous Electrodes. Univ. of California (Berkeley), Contract no. NSG 150–61, Nov. 1962.

304. ALKIRE, R. C.: Reaction Distribution in a Porous Anode. Univ. of California (Berkeley), Contract no. NSG–150–61, M.S. thesis, 1963.

305. BOMBEN, J. L.: Current Distribution in a Porous Electrode. Univ. of California (Berkeley), Contract no. NSG 150–61, Technical Report, Sept. 1963.

306. GRENS, E. A., II: Dynamic Analysis of a One Dimensional Porous Electrode Model. Univ. of California (Berkeley), Contract no. NSG 150–61, Technical Report, Ph.D. thesis, Sept. 1963.

307. GRENS, E. A., II; AND TOBIAS, C. W.: The Influence of Electrode Reaction Kinetics on the Polarization of Flooded Porous Electrodes. Univ. of California (Berkeley), Rept. no. NASA CR–59573, Contract no. NSG 150–61, 1964.

308. TOBIAS, C. W.: Dynamic Behavior of Porous Electrode Systems. Univ. of California (Berkeley), Rept. no. NASA CR–53688, Contract no. NSG 150–61, Semiannual Status Report, Apr. 1964.

309. ALKIRE, R. C.; GRENS, E. A.; MULLER, R. H.; AND TOBIAS, C. W.: Dynamic Behavior of Porous Electrode Systems. Univ. of California (Berkeley), Rept. no. NASA CR–64108, Contract no. NSG 150–61, Final Report, June 24, 1965.

310. ANON.: Conversion of Various Forms of Energy by Unconventional Techniques. Univ. of Pennsylvania, Institute for Direct Energy Conversion, Contract no. NSG–316, Progress Report, Nov. 15, 1962.

311. ANON.: Conversion of Various Forms of Energy by Unconventional Techniques. Univ. of Pennsylvania, Institute for Direct Energy Conversion, Contract no. NSG–316, Progress Report, Oct. 21, 1963.

312. ANON.: Conversion of Various Forms of Energy by Unconventional Techniques. Univ. of Pennsylvania, Institute for Direct Energy Conversion, Contract no. NSG–316, Progress Report, Feb. 28, 1964.

313. ANON.: Conversion of Various Forms of Energy by Unconventional Techniques. Univ. of Pennsylvania, Institute for Direct Energy Conversion, Contract no. NSG–316, Progress Report, Aug. 10, 1964.

314. ANON.: Conversion of Various Forms of Energy by Unconventional Techniques. Univ. of Pennsylvania, Institute for Direct Energy Conversion, Rept. no. INDEC SR–6, Contract no. NSG–316, Sixth Progress Report, July 1, 1965.

315. ANON.: Conversion of Various Forms of Energy by Unconventional Methods. Univ. of Pennsylvania, Institute for Direct Energy Conversion, Rept. no. NASA CR–75115, Contract no. NSG–316, Seventh Progress Report, Apr. 1, 1966.

316. ANON.: Conversion of Various Forms of Energy by Unconventional Techniques. Univ. of Pennsylvania, Institute for Direct Energy Conversion, Rept. no. INDEC SR–8, Contract no. NSG–316, Eighth Progress Report, July 1, 1966.

317. ANON.: Conversion of Various Forms of Energy by Unconventional Techniques. Univ. of Pennsylvania, Institute for Direct Energy Conversion, Rept. no. INDEC SR–9, Contract no. NSG–316, Ninth Progress Report, Oct. 31, 1966.

318. ANON.: Conversion of Various Forms of Energy by Unconventional Techniques. Univ. of Pennsylvania, Institute for Direct Energy Conversion, Rept. no. INDEC SR-11, Contract no. NSG-316, 11th Progress Report, Mar. 1967.

319. FOLEY, R. T.; SCHUBERT, L.; AND SWINEHART, J. S.: Investigation of Electrochemistry of High Energy Compounds in Organic Electrolytes. The American Univ., Rept. no. NASA CR-63741, Contract no. NGR-09-003-005, First Semiannual Report, Nov. 1, 1964, to Apr. 30, 1965.

320. FOLEY, R. T.; HELGEN, L. E.; AND SCHUBERT, L.: Investigation of Electrochemistry of High Energy Compounds in Organic Electrolytes. The American Univ., Rept. no. NASA CR-62023, Contract no. NGR-09-003-005, Second Semiannual Report, May 1 to Oct. 31, 1965.

321. FOLEY, R. T.; HELGEN, L. E.; AND SCHUBERT, L.: Investigation of Electrochemistry of High Energy Compounds in Organic Electrolytes. The American Univ., Contract no. NGR-09-003-005, Third Progress Report, Nov. 1, 1965, to Apr. 30, 1966.

322. FOLEY, R. T.; AND MARCINISZYN, J. P., JR.: Investigation of Electrochemistry of High Energy Compounds in Organic Electrolytes. The American Univ., Rept. no. NASA CR-78235, Contract no. NGR-09-003-005, Third Progress Report Supplement, Sept. 12, 1966.

323. FOLEY, R. T.: High Energy Compounds in Organic Electrolytes. The American Univ., Contract no. NGR-09-003-005, Fourth Semiannual Report, May to Oct. 1966.

324. BOGAR, F. D.; AND FOLEY, R. T.: Investigation of Electrochemistry of High Energy Compounds in Organic Electrolytes. The American Univ., Contract no. NGR-09-003-005, Fifth Semiannual Report, Nov. 1, 1966, to Apr. 1967.

325. BRENNER, A.; AND SLIGH, J.: Electron Beam Electrolysis. National Bureau of Standards, Rept. no. NBS 9062, Contract no. R-09-022-052, First Quarterly Report, Mar. 1, 1966.

326. BRENNER, A.; AND SLIGH, J.: Electron Beam Electrolysis. National Bureau of Standards, Rept. no. NBS 9331, Contract no. R-09-022-052, Second Quarterly Report, June 1, 1966.

327. BRENNER, A.; AND SLIGH, J.: Electron Beam Electrolysis. National Bureau of Standards, Rept. no. NBS 9430, Contract no. R-09-022-052, Third Quarterly Report, Sept. 30, 1966.

328. BRENNER, A.; AND SLIGH, J.: Electron Beam Electrolysis. National Bureau of Standards, Contract no. R-09-022-052, Fourth Quarterly Report, Dec. 15, 1966.

329. BRENNER, A.; AND SLIGH, J. L.: Electron Beam Electrolysis. National Bureau of Standards, Contract no. R-09-022-052, Sixth Quarterly Report, Feb. 20, 1967.

330. BRENNER, A.; AND SLIGH, J. L.: Electron Beam Electrolysis. National Bureau of Standards, Contract no. R-09-022-052, Seventh Quarterly Report, Mar. 20, 1967.

331. BRUINS, P. F.; CAULDER, S. M.; AND SALKIND, A. J.: Calorimetric Study of the Thermodynamic Properties of the Nickel-Cadmium Cell. Brooklyn Polytechnic Institute, Rept. no. NASA CR-71408, Contract no. NGR-33-006-015, Final Report, Oct. 1964 to Dec. 1965.

332. BRUINS, P. F.: Calorimetric Study of the Thermodynamic Properties of the Nickel-Cadmium Cell. Polytechnic Institute of Brooklyn, Rept. no. NASA CR-63338, Contract no. NGR-33-006-015, Semiannual Report, Oct. 1964 to Apr. 1965.

333. PORTNER, D. M.: The Effect of Nickel-Cadmium Batteries Upon Bacterial Spores. Army Biological Labs, Rept. no. NASA CR–50246, Contract no. PO R35, Test No. 20–63, Apr. 11, 1963.

334. GREENLER, P. H.: Study of Sonotone Corporation Nickel-Cadmium Size F Battery Cells. TRW Systems, Rept. no. 2303–0003–RU000, Contract no. PO S236–5G, Final Report, Apr. 1961.

335. LIWSKI, P. P. M.: Charge-Current Control Circuit for Nickel-Cadmium Cells with Control Electrodes. U.S. Navy Marine Engineering Laboratory, Rept. no. NASA CR–62959, Contract no. PO S12730G, Apr. 1965.

336. FORD, F. E.: Automatic Battery Formation Cycler and Controller. U.S. Navy Marine Engineering Laboratory, Rept. no. NASA CR–68529, Contract no. S12730G, July 1965.

337. FORD, F. E.; AND LIWSKI, P. P. M.: Shunt Voltage Regulator Circuit for Nickel-Cadmium Cells With Auxiliary Electrodes. U.S. Navy Marine Engineering Laboratory, Rept. no. NASA CR–74787, Contract no. SO 12730G, Apr. 1966.

338. FORD, F. E.: Nickel-Cadmium Battery Reconditioner. U.S. Navy Marine Engineering Laboratory, Rept. no. NASA CR–78363, Contract no. PO S12730G, Aug. 1966.

339. LIWSKI, P. P. M.: Solid-State Circuit Development. U.S. Navy Marine Engineering Laboratory, Rept. no. MEL 283/64, Contract no. PO S12730G, Apr. 1965.

340. SCHULTZ, H.: Test and Evaluation Programs for Electrochemical Cells Developed on NASA/GSFC Contracts. Contract no. S23404G, June 1962.

341. ANON.: Electrochemical Corporation, 4 Ampere-Hour Silver-Cadmium Cells Program. U.S. Naval Ammunition Depot, Test and Evaluation Program for Electrochemical Cells Developed on NASA/GSFC Contracts. U.S. Naval Ammunition Depot, Quality Evaluation Laboratory, Rept. no. QE/C 65–123, NASA CR–57109, Contract no. S23404–0, Feb. 18, 1965.

342. ANON.: A Study of Electrochemical Processes in Silver-Cadmium Secondary Cells. National Bureau of Standards, Rept. no. NASA CR–62027, Contract no. S70008G, July 14, 1965.

343. OTTO, E. M.: Yardney Sealed Silver-Cadmium Cells Modified by General Electric. National Bureau of Standards, Contract no. PO S70008G, Test Report, Mar. 31, 1966.

344. ANON.: A Study of the Electrochemical Properties of Huyck Porous Metals in Silver-Cadmium Secondary Cells. National Bureau of Standards, Contract no. S70008G, Status Report, June 27, 1966.

345. BRUESS, E. C.: Evaluation Program for Nickel-Cadmium Sealed Cells: General Performance Test of Gould-National Batteries 20.0 Ampere-Hour Cells. U.S. Naval Ammunition Depot, Quality Evaluation Laboratory, Rept. no. QE/C 64–4, NASA CR–53639, Test Report, Feb. 28, 1964.

346. BRUESS, E. C.: Evaluation Program for Nickel-Cadmium Sealed Cells, General Performance Test of Gulton Industries, 20.0 Ampere-Hour Sealed Cells. U.S. Naval Ammunition Depot, Quality Evaluation Laboratory, Rept. no. QE/C 64–5, NASA CR–58202, Contract no. W11, 252B, Test Report, Apr. 1964.

347. BRUESS, E. C.: Evaluation Program for Secondary Spacecraft Cells. U.S. Naval Ammunition Depot, Quality Evaluation Laboratory, Rept. no. QE/C 65–356, NASA CR–63424, Contract no. W11, 252B, First Annual Report on Cycle Life Tests, May 1965.

348. BRUESS, E. C.: Evaluation Program for Secondary Spacecraft Cells. U.S. Naval Ammunition Depot, Quality Evaluation Laboratory, Rept. no.

QE/C 66-304, NASA CR-76034, Contract no. W11, 252B, Second Annual Report on Cycle Life Tests, May 13, 1966.

349. BRUESS, E. C.: Evaluation Program for Nickel-Cadmium Sealed Cells, Acceptance Test of Gulton Industries 20.0 Ampere-Hour Cells. U.S. Naval Ammunition Depot, Quality Evaluation Laboratory, Rept. no. QE/C 63-317, NASA CR-55627, Contract no. W11, 252B, Test Report, June 14, 1963.

350. BRUESS, E. C.: Evaluation Program for Nickel-Cadmium Sealed Cells. U.S. Naval Ammunition Depot, Quality Evaluation Laboratory, Rept. no. QE/C 64-274, NASA CR-58179, Contract no. NASA W11, 252B, First Quarterly Report, Life Cycling Test, June 15, 1964.

351. BRUESS, E. C.: Evaluation Program for Secondary Spacecraft Cells, Acceptance Test of General Electric 5.0 Ampere-Hour Nimbus Cells. U.S. Naval Ammunition Depot, Quality Evaluation Laboratory, Rept. no. QE/C 65-459, NASA CR-64687, Contract no. W11, 252B, Test Report, June 23, 1965.

352. BRUESS, E. C.: Evaluation Program for Secondary Spacecraft Cells, Acceptance Test of Gulton Industries, 5.0 Ampere-Hour Nickel-Cadmium Cells. U.S. Naval Ammunition Depot, Quality Evaluation Laboratory, Rept. no. QE/C 65-460, NASA CR-63912, Contract no. W11, 252B, Test Report, June 1965.

353. BRUESS, E. C.: Evaluation Program for Secondary Spacecraft Cells, Acceptance Test of Sonotone Corporation 3.0 Ampere-Hour Triple Seal Nickel-Cadmium Cells. U.S. Naval Ammunition Depot, Quality Evaluation Laboratory, Rept. no. QE/C 65-512, NASA CR-64353, Contract no. W11, 252B, Test Report, July 23, 1965.

354. BRUESS, E. C.: Evaluation Program for Nickel-Cadmium Sealed Cells; General Performance Test of Gould-National Batteries, Inc., 3.5 Ampere-Hour "D" Cells. U.S. Naval Ammunition Depot, Quality Evaluation Laboratory, Rept. no. QE/C 64-7, NASA CR-55631, Contract no. W11, 252B, Test Report, Jan. 2, 1964.

355. BRUESS, E. C.: Evaluation Program for Nickel-Cadmium Sealed Cells; General Performance Test of General Electric 3.0 Ampere-Hour Cells. U.S. Naval Ammunition Depot, Quality Evaluation Laboratory, Rept. no. QE/C 64-1, NASA CR-55630, Contract no. W11, 252B, Test Report, Jan. 6, 1964.

356. BRUESS, E. C.: Evaluation Program for Nickel-Cadmium Sealed Cells; General Performance Test of Sonotone Corporation 5 Ampere-Hour "F" Cells. U.S. Naval Ammunition Depot, Quality Evaluation Laboratory, Rept. no. QE/C 64-2, Contract no. W11, 252B, Test Report, Feb. 4, 1964.

357. BRUESS, E. C.: Evaluation Program for Nickel-Cadmium Sealed Cells; General Performance Test of Gulton Industries 6.0 Ampere-Hour Cells. U.S. Naval Ammunition Depot, Quality Evaluation Laboratory, Rept. no. QE/C 64-3, Contract no. W11, 252B, Test Report, Mar. 2, 1964.

358. BRUESS, E. C.: Evaluation Program for Secondary Spacecraft Cells; Acceptance Test of Gulton Industries, 6.0 Ampere-Hour Adhydrode Cells. U.S. Naval Ammunition Depot, Quality Evaluation Laboratory, Rept. no. QE/C 65-536, NASA CR-64617, Contract no. W11, 252B, Test Report, July 28, 1965.

359. BRUESS, E. C.: Evaluation Program for Secondary Spacecraft Cells; Acceptance Test of Sonotone Corporation 5.0 Ampere-Hour Nickel-Cadmium Cells. U.S. Naval Ammunition Depot, Quality Evaluation Laboratory, Rept. no. QE/C 65-583, NASA CR-67713, Contract no. W11, 252B, Test Report, Sept. 2, 1965.

360. BRUESS, E. C.: Evaluation Program for Secondary Spacecraft Cells; Evaluation of C and D Batteries Division, Eltra Corporation, 5.0 Ampere-Hour Lead-Calcium Cells. U.S. Naval Ammunition Depot, Quality Evaluation Laboratory, Rept. no. QE/C 65-838, NASA CR-68733, Contract no. W11, 252B, Test Report, Nov. 22, 1965.

361. BRUESS, E. C.: Evaluation Program for Secondary Spacecraft Cells; Acceptance Test of Gulton Industries 3.6 and 5.6 Ampere-Hour Nickel-Cadmium Cells With Vulcanized Neoprene Terminal Seals. U.S. Naval Ammunition Depot, Quality Evaluation Laboratory, Rept. no. QE/C 66-69, NASA CR-70852, Contract no. W11, 252B, Test Report, Jan. 28, 1966.

362. BRUESS, E. C.: Evaluation Program for Secondary Spacecraft Cells; Acceptance Test of Gulton Industries 1.25 Ampere-Hour Nickel-Cadmium Cells With High Overcharge Capability. U.S. Naval Ammunition Depot, Quality Evaluation Laboratory, Rept. no. QE/C 66-120, NASA CR-71296, Contract no. W11, 252B, Test Report, Feb. 28, 1966.

363. BRUESS, E. C.: Evaluation Program for Secondary Spacecraft Cells; Acceptance Test of Sonotone Corporation 3.5 Ampere-Hour Sealed Nickel-Cadmium Cells. U.S. Naval Ammunition Depot, Quality Evaluation Laboratory, Rept. no. QE/C 66-340, NASA CR-76520, Contract no. W11, 252B, Test Report, June 6, 1966.

364. BRUESS, E. C.: Evaluation Program for Secondary Spacecraft Cells; Acceptance Test of C&D Batteries 5.0 Ampere-Hour Sealed Lead-Calcium Cells. U.S. Naval Ammunition Depot, Quality Evaluation Laboratory, Rept. no. QE/C 66-399, NASA CR-76517, Contract no. W11, 252B, Test Report, June 6, 1966.

365. BRUESS, E. C.: Evaluation Program for Secondary Spacecraft Cells; Acceptance Test of Gulton Industries 3.5 Ampere-Hour Nickel-Cadmium Cells With Plitt Terminal Seal. U.S. Naval Ammunition Depot, Quality Evaluation Laboratory, Rept. no. QE/C 66-709, Contract no. W11, 259B, Test Report, Nov. 1966.

366. BRUESS, E. C.: Evaluation Program for Secondary Spacecraft Cells; Acceptance Test of General Electric 12.0 Ampere-Hour Auxiliary Electrode Cells. Naval Ammunition Depot, Quality Evaluation Laboratory, Rept. no. QE/C 66-803, Contract no. W11, 252B, Test Report, Dec. 1966.

367. BRUESS, E. C.: Evaluation Program for Secondary Spacecraft Cells; General Electric 12.0 Ampere-Hour Sealed Nickel-Cadmium Cells. U.S. Naval Ammunition Depot, Quality Evaluation Laboratory, Rept. no. QE/C 64-6, NASA CR-53923, Contract no. W11, 252B, Test Report, Apr. 1964.

368. BRUESS, E. C.: Evaluation Program for Secondary Spacecraft Cells; Acceptance Test of General Electric 12.0 Ampere-Hour Auxiliary Electrode Cells. U.S. Naval Ammunition Depot, Quality Evaluation Laboratory, Rept. no. QE/C 65-535, NASA CR-67056, Contract no. W11, 252B, Test Report, July 26, 1965.

369. BRUESS, E. C.: Evaluation Program for Secondary Spacecraft Cells; Acceptance Test of Gulton Industries, 12 and 20 Ampere-Hour Adhydrode Cells. U.S. Naval Ammunition Depot, Quality Evaluation Laboratory, Rept. no. QE/C 67-1, Contract no. W11, 252B, Test Report, Jan. 21, 1967.

370. BRUESS, E. C.: Evaluation Program for Secondary Spacecraft Cells; Acceptance Test of Gulton Industries, 12 Ampere-Hour Cells. U.S. Naval Ammunition Depot, Quality Evaluation Laboratory, Rept. no. QE/C 65-124, NASA CR-57470, Contract no. W11, 252B, Test Report, Feb. 16, 1965.

371. BRUESS, E. C.: Evaluation Program for Secondary Spacecraft Cells; Acceptance Test of General Electric 6.0 Ampere-Hour Sealed Nickel-Cadmium

Cells. U.S. Naval Ammunition Depot, Quality Evaluation Laboratory, Rept. no. QE/C 67–387, Contract no. W11, 252B, Test Report, June 28, 1967.

372. PROCHASKA, H.: Surveyor Power System. Hughes Aircraft Co., Contract no. JPL 950056, 1961.

373. ANON.: Development of a Mariner "A" Energy Source. Electric Storage Battery Co., Contract no. JPL 950107, Weekly Reports, July 28 to Dec. 31, 1961.

374. CHREITZBERG, A. M.: Development of a Mariner "A" Energy Source. Electric Storage Battery Co., Rept. no. ESB 62–839, Contract no. JPL 950107, Weekly Reports, Jan. 2 to May 31, 1962.

375. BOGNER, R. S.: Evaluation of Delco-Remy Design Sealed, Secondary, Silver-Zinc Electrolytic Cells for Heat Sterilization. Delco-Remy, Rept. no. 62–772, Contract no. JPL 950177, Final Report, Oct. 15, 1962.

376. FRANK, H.: Fuel Cell Assemblies. Electro-Optical Systems, Rept. no. 3070–Q1, Contract no. JPL 950258, First Quarterly Report, Apr. 10 to July 10, 1962.

377. BOGNER, R. S.: Heat Sterilizable Silver-Zinc Battery Investigation. Delco-Remy, Rept. no. NASA CR–63597, Contract no. 950364, Final Report, Mar. 15, 1965.

378. CHREITZBERG, A. M.: Mariner MK VI Battery Development. Electric Storage Battery Co., ESB Rept. no. 63–683, Contract no. JPL 950495, Biweekly Reports, May 7 to July 15, 1963.

379. CHREITZBERG, A. M.: Mariner MK VI Battery Development. Electric Storage Battery Co., Rept. no. ESB E–25–63, Contract no. JPL 950495, First Biweekly Report, May 7 to 20, 1963.

380. CHREITZBERG, A. M.: Mariner MK VI Battery Development. Electric Storage Battery Co., Rept. no. ESB E–35–63, Contract no. JPL 950495, Third Biweekly Report, June 3 to June 17, 1963.

381. ARGUE, G. R.; ET AL.: The Effects of Radiation on Nickel-Cadmium Battery Electrodes, I. Atomics International, Rept. no. AI–64–11, NASA CR–55760, Contract no. JPL 950514, Semiannual Report, June 1 to Dec. 31, 1963.

382. ARGUE, G. R.; ET AL.: The Effects of Radiation on Nickel-Cadmium Battery Electrodes. Atomics International, Rept. no. AI–65–66, NASA CR–62796, Contract no. JPL 950514, Apr. 1965.

383. ARGUE, G. R.; ET AL.: The Effects of Radiation on Nickel-Cadmium Battery Electrodes, II. Atomics International, Rept. no. AI–64–161, NASA CR–58570, Contract no. JPL 950514, Fourth Quarterly Report, Mar. 13 to June 13, 1964.

384. ARGUE, G. R.; McCOLLUM, W. A.; AND RECHT, H. L.: Radiation Effects on Electrode Behavior. Atomics International, Rept. no. AI–8971, NASA CR–55217, Contract no. JPL 950514, First Quarterly Report, June to Aug. 1963.

385. ARGUE, G. R.; ET AL.: The Effects of Radiation on Nickel-Cadmium Battery Electrodes, III. Atomics International, Rept. no. AI 64–240, NASA CR–60902, Contract no. JPL 950514, Second Interim Report, June to Sept. 1964.

386. RHYNE, J. W.: Development of Sealed Secondary Silver Oxide-Zinc Battery. Whittaker Corp., Rept. no. 64–674, Contract no. JPL 950811, Final Report, Dec. 31, 1964.

387. GRUN, C.: Design of Sealed Secondary Silver-Zinc Battery. Yardney Electric Corp., Rept. no. 570–65, Contract no. JPL 950959, Final Report, Aug. 1965.

388. ANON.: Design of Sealed Secondary Silver-Zinc Battery. Yardney Electric Corp., Rept. no. 637–66, Contract no. 950959, Final Report Addendum, Jan. 1966.

389. SCARDAVILLE, P. A.; AND WETHERELL, T. J.: Fabrication and Test of Battery Separator Materials Resistant to Thermal Sterilization. Radiation Applications, Inc., Rept. no. NASA CR–69884, Contract no. JPL 951015, Final Report, Dec. 1965.

390. TRISCHLER, F. D.: Separator Development Phase of Heat-Sterilizable Battery Development Program. Whittaker Corp., Rept. no. NASA CR–81161, Contract no. JPL 951091, Final Report, Oct. 1966.

391. RICHARDS, R. N.: Nickel-Cadmium Cell Heat Sterilization Test Program, Phase I. TRW Systems, Rept. no. 06030–6001–R000, Contract no. JPL 951092, Final Report, Oct. 1966.

392. RICHARDS, R. N.: Nickel-Cadmium Cell Heat Sterilization Test Program, Phase I. TRW Systems, Rept. no. 06030–6001–R01, Contract no. JPL 951092, Final Report, App. A, Oct. 1966.

393. ARGUE, G. R.; McCOLLUM, W. A.; AND RECHT, H. L.: Radiation Effects on Silver and Zinc Battery Electrodes, I. Atomics International, Rept. no. AI 65–158, NASA CR–64970, Contract no. JPL 951109, Interim Report, Apr. to July 1965.

394. ARGUE, G. R.; RECHT, H. L.; AND McCOLLUM, W. A.: Radiation Effects on Silver and Zinc Battery Electrodes, II. Atomics International, Rept. no. AI 65–264, NASA CR–71256, Contract no. 951109, Interim Report, July to Oct. 1965.

395. McCOLLUM, W. A.; ET AL.: Radiation Effects on Silver and Zinc Battery Electrodes, III. Atomics International, Rept. no. AI 66–33, NASA CR–74905 or NASA CR–74240, Contract no. JPL 951109, Interim Report, Oct. 1965 to Jan. 1966.

396. McCOLLUM, W. A.; ET AL.: Radiation Effects on Silver and Zinc Battery Electrodes, IV. Atomics International, Rept. no. AI 66–83, NASA CR–75394, Contract no. JPL 951109, Interim Report, Jan. to Apr. 1966.

397. KELCHNER, R. E.; NICHOLSON, M. M.; AND RECHT, H. L.: Radiation Effects on Silver and Zinc Battery Electrodes, V. Atomics International, Rept. no. AI 66–186, NASA CR–79489, Contract no. JPL 951109, Interim Report, Apr. to July 1966.

398. BUTLER, E. A.: Studies of Reaction Geometry in Oxidation and Reduction of the Alkaline Silver Electrode. Brigham Young Univ., Rept. no. 66–259, Contract no. JPL 951157, Final Report, Apr. 1966.

399. BUTLER, E. A.: Reaction Geometry in Oxidation and Reduction of the Alkaline Silver Electrode. Brigham Young Univ., Contract no. JPL 951911, Feb. 1964.

400. BODAMER, G. W.: Heat Sterilizable, Impact Resistant Cell Development. Electric Storage Battery Co., Rept. no. 67–218, Contract no. JPL 951296, First Annual Report, Sept. 24, 1965, to Dec. 31, 1966.

401. BODAMER, G. W.: Heat Sterilizable, Impact Resistant Cell Development. Electric Storage Battery Co., Rept. no. 67–284, Contract no. JPL 951296, First Quarterly Report, Jan. 1 to Mar. 31, 1967.

402. BODAMER, G. W.: Heat Sterilizable, Impact Resistant Cell Development. Electric Storage Battery Co., Contract no. JPL 951296, Second Quarterly Report, Aug. 1, 1967.

403. ARCAND, G. M.: The Reactions Pertaining to Zinc-Silver and Cadmium-Silver Batteries. Idaho State Univ., Rept. no. 67–148, Contract no. JPL 951458, Final Report, Apr. 1, 1967.

404. ARCAND, G. M.: The Reactions Pertaining to Zinc-Silver and Cadmium-Silver Batteries. Idaho State Univ., Rept. no. NASA CR–76047, Contract no. JPL 951458, First Quarterly Report, May 17, 1966.

405. ARCAND, G. M.: The Reactions Pertaining to Zinc-Silver and Cadmium-Silver Batteries. Idaho State Univ., Rept. no. NASA CR-80139, Contract no. JPL 951458, Second Quarterly Report, Aug. 15, 1966.

406. ARCAND, G. M.: The Reactions Pertaining to Zinc-Silver and Cadmium-Silver Batteries. Idaho State Univ., Rept. no. 66–941, Contract no. JPL 951458, Third Quarterly Report, Nov. 11, 1966.

407. LEHMAN, M.; McELHILL, E. A.; O'CONNELL, J. J.; AND STEEVES, R. C.: Separator Development for a Heat Sterilizable Battery. Monsanto Research Corp., Rept. no. MRB 6234F, Contract no. JPL 951524, Final Summary Report, May 1, 1966, to Mar. 15, 1967.

408. McELHILL, E. A.; AND O'CONNELL, J. J.: Separator Development for a Heat Sterilizable Battery. Monsanto Research Corp., Rept. no. MRB 623401, NASA CR-80530, Contract no. JPL 951524, First Quarterly Report, May 1 to Aug. 31, 1966.

409. McELHILL, E. A.; AND O'CONNELL, J. J.: Separator Development for a Heat Sterilizable Battery. Monsanto Research Corp., Rept. no. MRB 623402, NASA CR-81610, Contract no. JPL 951524, Second Quarterly Report, Sept. 1 to Nov. 30, 1966.

410. CHARLES, R. G.; LANGER, A.; AND RUFFING, C. R.: Separator Development for a Heat Sterilizable Battery. Westinghouse Electric Corp., Rept. no. 66–1B6–BSEPA–R1, Contract no. 951525, First Quarterly Report, Sept. 30, 1966.

411. SCALA, L. C.: Separator Development for a Heat Sterilizable Battery. Westinghouse Electric Corp., Contract no. 951525, Fourth Quarterly Report, June 30, 1967.

412. CHARLES, R. G.; LANGER, A.; AND RUFFING, C. R.: Separator Development for a Heat Sterilizable Battery. Westinghouse Electric Corp., Rept. no. 67–9B6–BSEPA–R1, Contract no. JPL 951525, Third Quarterly Report, Mar. 31, 1967.

413. BLACKHAM, A. U.; AND BUTLER, E. A.: Studies of Reaction Geometry in Oxidation and Reduction of the Alkaline Silver Electrode. Brigham Young Univ., Rept. no. NASA CR-80126, Contract no. JPL 951554, First Quarterly Report, July 9, 1966.

414. BLACKHAM, A. U.; AND BUTLER, E. A.: Studies of Reaction Geometry in Oxidation and Reduction of the Alkaline Silver Electrode. Brigham Young Univ., Rept. no. NASA CR-80528, Contract no. JPL 951554, Second Quarterly Report, Oct. 10, 1966.

415. BLACKHAM, A.; AND BUTLER, A.: Studies of Reaction Geometry in Oxidation and Reduction of the Alkaline Silver Electrode. Brigham Young Univ., Rept. no. N67–17972, Contract no. JPL 951554, Third Quarterly Report, Jan. 1967.

416. BINCKLEY, W. G.: Power System Configuration Study and Reliability Analysis. TRW Systems, Rept. no. 07171–6001–R000, Contract no. JPL 951574, Final Report, Sept. 18, 1967.

417. KELCHNER, R. E.; NICHOLSON, M. M.; AND RECHT, H. L.: Effects of High-Energy Protons on Selected Cells. Atomics International, Rept. no. AI–66–149, Contract no. JPL 951648, Final Report, June 1966 to Aug. 1966.

418. BUTLER, E. A.: Studies of Reaction Geometry in Oxidation and Reduction of the Alkaline Silver Electrode. Brigham Young Univ., Rept. no. NASA CR-57644, Contract no. AE 4–310901, Feb. 1965.

419. BANKS, H. O.; ET AL.: Spacecraft Electric Power System Sizing and Analysis Computations. TRW Systems, Rept. no. 8584–6001–RU–000, Contract no. JPL PO BK/3–211739, Final Report, Mar. 15, 1964.

420. ADAMS, L. M.; HARLOWE, W. W., JR.; AND LAWRASON, G. C.: Fabrication and Testing of Battery Separator Material from Modified Polyethylene. Southwest Research Institute, Rept. no. NASA CR-75951, Project no. 01-1842, Contract no. JPL PO CA 384805, Final Report, June 7, 1966.

421. ANON.: Fabrication and Testing of Battery Separator Material for the Jet Propulsion Laboratory. Lockheed Aircraft Corp., Rept. no. ER 8487, NASA CR-75980, Contract no. JPL PO CA 384807, Apr. 1966.

422. FULBRIGHT, D. E.: Silver-Zinc Battery Cell Test Program. TRW Systems, Rept. no. 7062.4-105, Contract no. JPL CA 388006, Final Report, Oct. 31 to Dec. 31, 1966.

423. ANON.: A Bibliography of the Saturn System. NASA/Marshall Space Flight Center, Rept. no. TMX-50409 (N64-14274), M-SAT-62-4, Dec. 12, 1962.

424. SOLTIS, D. G.: Alternate Approaches to Sterilizable Power Sources. NASA/Lewis Research Center, Rept. no. TMX-52137 (N66-14763), Technical Memorandum, Nov. 1965.

425. SCHWARTZ, H. J.; AND SHURE, L. I.: Survey of Electric Power Plants for Space Applications. NASA/Lewis Research Center, Rept. no. TMX 52158 (N66-14775), Dec. 1965.

426. GRAFF, G.: The Electrical Power System for the Pegasus Satellite. NASA/Marshall Space Flight Center, Rept. no. TMX 53419 (N66-32609). No date.

427. FUNGAN, E. E.: Electric Power Systems Studies at MSFC. NASA/Marshall Space Flight Center, Rept. no. TMX 53419 (N66-32612). No date.

428. GRAFF, C.: The Development of an Improved Zinc-Silver Oxide Battery. NASA/Marshall Space Flight Center, Rept. no. TMX 53419 (N66-32608). No date.

429. APELT, A. O.; AND STROUP, E. R.: NASA's Spacecraft Battery Evaluation Program. NASA/Goddard Space Flight Center, Rept. no. TMX 56176 (N66-18341), 1965.

430. SIZEMORE, K. O.; AND STROUP, E. R.: Nickel-Cadmium Spacecraft Battery Charge Control With Auxiliary Electrodes. NASA/Goddard Space Flight Center, Rept. no. TMX 56519 (TMX 56518), (N66-27211).

431. DONNELLY, P. C.; AND PALANDATI, C. F.: Silver-Zinc Batteries Power Supply for the Atmospheric Structure Satellite Explorer XVII. NASA/Goddard Space Flight Center, Rept. no. TMX-51150, X-636-63-206 (N64-10905), Oct. 1963.

432. PAULKOVICH, J.; AND RODRIGUEZ, G. E.: The Battery Charger for the Atmosphere Explorer B Spacecraft. NASA/Goddard Space Flight Center, Rept. no. TMX 55312, X-636-65-271, July 1965.

433. HENNIGAN, T. J.: Separator Materials for Silver Oxide-Zinc and Silver Oxide-Cadmium Electrochemical Cells. NASA/Goddard Space Flight Center, Rept. no. TMX 55325, X-716-65-331, Aug. 1965.

434. DONNELLY, P. C.; AND PALANDATI, C. F.: Silver Zinc Batteries Power Supply for the Atmosphere Explorer B Spacecraft (AE/B). NASA/Goddard Space Flight Center, Rept. no. TMX 55383, X-716-65-405, Oct. 1965.

435. SIZEMORE, K. O.: Use of the Adsorption Hydrogen Electrode and the Oxygen Fuel Cell Electrode in Nickel-Cadmium Cells. NASA/Goddard Space Flight Center, Rept. no. TMX 55469, X-716-66-83, Apr. 1966.

436. HENNIGAN, T. J.; AND SIZEMORE, K. O.: Auxiliary Electrode Instrumentation for Nickel-Cadmium Cells. NASA/Goddard Space Flight Center, Rept. no. TMX 55471, X-716-66-200, May 1966.

437. STROUP, E. R.: Analysis of Cadmium-Cadmium Coulometers Used for Charge Control in Nickel-Cadmium Space Batteries. NASA/Goddard Space Flight Center, Rept. no. TMX 59021, X-716-66-462, Sept. 1966.

438. HALPERT, G.: Some Factors To Consider in Determining the Capacity of a Nickel-Cadmium Cell. NASA/Goddard Space Flight Center, Rept. no. TMX 55610, X–735–66–275, Aug. 1966.

439. JOHANNSEN, K.; AND SHERFEY, J. M.: Reliability and Redundancy Considerations in Selecting Spacecraft Batteries. NASA/Goddard Space Flight Center, Rept. no. TN D–1452 (N62–16470), Oct. 1962.

440. APELT, A. O.; AND HENNIGAN, T. J.: Use of a Sealed Silver-Cadmium Battery on Explorer XII. NASA/Goddard Space Flight Center, Rept. no. TN D–1543 (N63–11741), Jan. 1963.

441. FINKE, R. C.; HOLMES, A. D.; AND KELLER, T. A.: Space Environment Facility for Electric Propulsion Systems Research. NASA/Lewis Research Center, Rept. no. TN D–2774, May 1965.

442. THALLER, L. H.: A Long-Life Thermal Cell. NASA/Lewis Research Center, Rept. no. TN D–2015 (N65–27818), July 1965.

443. LEIBECKI, H. F.: Argentic Oxysalt Electrodes. NASA/Lewis Research Center, Rept. no. TN D–3208, Jan. 1966.

444. BARRETT, D. A.; ET AL.: Power for Spacecraft. NASA/Washington, Rept. no. SP–21 (N63–11511), Dec. 1962.

445. BOMBERGER, D. C.; ET AL.: The Spacecraft Power Supply System, Telstar I, vol. 1. NASA/Goddard Space Flight Center, Rept. no. SP–32 (N64–10876), June 1963.

446. BOMBERGER, D. C.; AND MOOSE, L. F.: Nickel-Cadmium Cells for the Spacecraft Battery, Telstar I, vol. 3. NASA/Goddard Space Flight Center, Rept. no. SP–32 (N64–11082), June 1963.

447. ANON.: The Spacecraft Power Supply System, Relay I. NASA/Goddard Space Flight Center, Rept. no. SP–76 (N66–10234), Final Report, 1965.

448. COHEN, R.; DEMING, J.; AND MIGLICCO, P.: Gemini Midprogram Conference Including Experiment Results. NASA/Manned Spacecraft Center, Rept. no. SP–121 (N66–29631), Feb. 1966.

449. LUBARSKY, B.; ET AL.: Space Power Systems Advanced Technology Conference. NASA/Lewis Research Center, Rept. no. SP–131, Aug. 23–24, 1966.

450. FRANCIS, H. T.: Space Batteries. Armour Research Foundation, Technology Handbook, Rept. no. SP–5004, 1964.

451. MORRIS, J. F.; ET AL.: Electric Power Generation, Conference on New Technology. NASA/Lewis Research Center, Rept. no. SP–5015, June 1964.

452. HENLEY, E. J.; STAFFIN, H. K.; AND TUWINER, S. B.: Commercial Potentials of Semipermeable Membranes. NASA/Washington, Rept. no. SP–5061, 1967.

453. FICHTNER, H. J.: Electrical Systems in Missiles and Space Vehicles. NASA/ Marshall Space Flight Center, Rept. no. (N63–16005). No date.

454. ANON.: Qualification Tests for the Saturn Battery, Gulton Industries, 24–HVO–12. NASA/Marshall Space Flight Center, Rept. no. IN–R–ASTR–64–18, July 17, 1964.

455. ANON.: Qualification Tests for the Saturn Battery, Gulton Industries, 24–HVO–18. NASA/Marshall Space Flight Center, Rept. no. R–ASTR–IN–63–31, Nov. 29, 1963.

456. ANON.: Qualification Tests for the Saturn Battery E–P MAP–4070. NASA/ Marshall Space Flight Center, Rept. no. M–ASTR–IN–62–19, Aug. 13, 1962.

457. ANON.: Qualification Tests for the Saturn Battery. NASA/Marshall Space Flight Center, Rept. no. M–ASTR–EC, Feb. 15, 1962.

458. ANON.: Qualification Test Report for the Saturn Battery, Eagle-Picher MAP 4182. NASA/Marshall Space Flight Center, Rept. no. IN–R–ASTR–64–22, Oct. 29, 1964.

459. CHERDAK, A. S.; GREENBLATT, R. C.; AND MACKENZIE, C. M.: Nimbus Power Systems (1960–1969). NASA/Goddard Space Flight Center, Rept. no. X–450–66–333, June 1966.

460. MORRISON, R.; AND POTTER, N.: Two-Level Voltage Limiter. NASA/Goddard Space Flight Center, Rept. no. X–716–66–7, Jan. 1966.

461. SALAY, J.: Laboratory Test Evaluation of A–IMP Electric Power System. NASA/Goddard Space Flight Center, Rept. no. X–716–67–12, Jan. 1967.

462. MOSES, E. G.: Design Techniques for an ATS–4 Power System. NASA/Goddard Space Flight Center, Rept. no. X–716–67–59, Feb. 1967.

463. MACKENZIE, C. M.: Solar Power Systems for Satellites in Near-Earth Orbits. NASA/Goddard Space Flight Center, Rept. no. X–716–67–77, Mar. 1967.

464. ANON.: AIMP (IMP–D) Technical Summary Description. NASA/Goddard Space Flight Center, Rept. no. X–724–67–87, Mar. 1967.

465. HALPERT, G.: Computer Program for Analyzing Battery Performance Data. NASA/Goddard Space Flight Center, Rept. no. X–735–66–385. No date.

466. JOHNSON, R. E.: Electrolyte Solvent Properties of Organic Sulfur Derivatives. NASA/Lewis Research Center, Rept. no. E–3494, Technical Memorandum. No date.

467. COSTOGUE, E. N.: Mariner Venus Power Supply System. Jet Propulsion Laboratory, Rept. no. 32–424, Contract no. NAS7–100, Technical Report, Mar. 30, 1963.

468. BUTLER, E. A.: Discharge Behavior of the Silver Oxide-Silver Electrode. Jet Propulsion Laboratory, Rept. no. 32–535, NASA CR–53002, Contract no. NAS7–100, Technical Report, Dec. 22, 1963.

469. CLEVEN, G. C.; DAWSON, K. M.; AND FREDRICKSON, C. D.: Reliability Considerations in the Design, Assembly, and Testing of the Mariner IV Power System. Jet Propulsion Laboratory, Rept. no. 32–729, Contract no. NAS7–100, Technical Report, July 1, 1965.

470. ADAMS, J. L.: The JPL High-Impact Program—1965. Jet Propulsion Laboratory, Rept. no. 32–844, Feb. 1, 1966.

471. BROOKE, C. W., JR.: Development of an Electrochemical Energy Source for the Mariner II Spacecraft. Jet Propulsion Laboratory, Rept. no. 32–854, NASA CR–71772, Contract no. NAS7–100, Technical Report, Mar. 15, 1966.

472. PEDERSEN, E. S.: Heat Sterilizable Power Source Study for Advanced Mariner Missions. Jet Propulsion Laboratory, Rept. no. 33–180, Contract no. NAS7–100, Technical Memorandum, July 1, 1964.

473. SHAIR, R. C.: Sealed Secondary Cells for Space Power Systems. Gulton Industries, AIAA Paper no. 64–455, July 1964.

474. ROHNER, P.; AND WILLIHNGANZ, E.: Battery Impedance: Farads, Milliohms, Microhenrys. C&D Batteries, Inc., AIEE Paper no. 59–823, Sept. 1959.

475. SHAIR, R. C.: Hermetically Sealed Nickel-Cadmium Batteries for Aerospace Applications. Gulton Industries, AIEE Paper no. 61–426, Feb. 1961.

476. KANTNER, E.; SEIGER, H. N.; AND SHAIR, R. C.: Separators for Alkaline Batteries. Gulton Industries, presented at AIEE–NEMA Battery Separator Symposium, Electrical Insulation Conference, Feb. 21, 1962.

477. STROUP, E. R.: The Battery for the International Ionosphere Satellite Ariel I. NASA/Goddard Space Flight Center, ARS Paper no. 2510–62, Sept. 25, 1962.

478. METZGER, S.; OSGOOD, C.; AND SCHREINER, W.: Project Relay, RCA. ARS Paper no. 2620–62, Nov. 13, 1962.

479. YAGERHOFER, F. C.: The Design of the United Kingdom Scientific Satellite Solar Power System. NASA/Goddard Space Flight Center, ARS Paper no. 2498–62, Sept. 1962.

480. APELT, A. O.; AND HENNIGAN, T. J.: Use of a Sealed Silver-Cadmium Battery on Explorer XII. NASA/Goddard Space Flight Center, ARS Paper no. 2509-62, Sept. 1962.

481. ANON.: Proceedings of the 10th Annual Battery Research and Development Conference. U.S. Army Signal R&D Laboratory, May 23, 1956.

482. ANON.: Proceedings of the 12th Annual Power Sources Conference. U.S. Army Signal R&D Laboratory, May 1958.

483. ANON.: Proceedings of the 13th Annual Power Sources Conference. U.S. Army Signal R&D Laboratory, Apr. 1959.

484. ANON.: Proceedings of the 14th Annual Power Sources Conference. U.S. Army Signal R&D Laboratory, May 1960.

485. ANON.: Proceedings of the 15th Annual Power Sources Conference. U.S. Army Signal R&D Laboratory, May 1961.

486. ANON.: Proceedings of the 16th Annual Power Sources Conference. U.S. Army Signal R&D Laboratory, May 1962.

487. ANON.: Proceedings of the 17th Annual Power Sources Conference. U.S. Army Signal R&D Laboratory, May 1963.

488. ANON.: Proceedings of the 18th Annual Power Sources Conference. U.S. Army Signal R&D Laboratory, May 1964.

489. ANON.: Proceedings of the 19th Annual Power Sources Conference. U.S. Army Signal R&D Laboratory, May 1965.

490. LISKA, J.; RAMPEL, G.; AND SHAIR, R. C.: Silver-Cadmium Batteries. Gulton Industries, 18th Annual Power Sources Conference, Fort Monmouth, N.J., May 1964.

491. KORGER, H. H.: Characterization of Sealed Nickel-Cadmium Cells. General Electric Co., 18th Annual Power Sources Conference, Fort Monmouth, N.J., May 1964.

492. RAMPEL, G.; AND SHAIR, R. C.: The Silver-Cadmium Couple in Sealed Cells for Space. Gulton Industries, Electrochemical Society Meeting, Boston, Mass., Sept. 1962.

493. STRAUSS, H. J.: Fundamental Rate Theory—Reactions Involving Separators and Electrolyte. Electrochemical Society Meeting, San Francisco, Calif., May 9-13, 1965, Abstract no. 236.

494. SCARDAVILLE, P.; AND WETHERELL, T.: Battery Separators of the Radiation Induced Graft Copolymer Type. Electrochemical Society Meeting, San Francisco, Calif., May 9-13, 1965, Abstract no. 237.

495. SHAFFER, L. H.: The Use of Ion Exchange Materials as Separators in Batteries. Electrochemical Society Meeting, San Francisco, Calif., May 9-13, 1965, Abstract no. 238.

496. DIRKSE, T. P.: Measurement of Zincate Diffusion Through Membranes. Electrochemical Society Meeting, San Francisco, Calif., May 9-13, 1965, Abstract no. 240.

497. DIRKSE, T. P.: Use of Radioactive Silver for Determining Silver Diffusion Through a Membrane. Electrochemical Society Meeting, San Francisco, Calif., May 9-13, 1965, Abstract no. 241.

498. LANDER, J. J.; AND PROCTER, H. G.: Diffusion Through Experimental Separator Membranes for Secondary Silver-Zinc Batteries. Electrochemical Society Meeting, San Francisco, Calif., May 9-13, 1965, Abstract no. 242.

499. DALIN, G. A.; AND STACHURSKI, Z.: On the Mechanism of Penetration of Separators by Zinc Growth. Electrochemical Society Meeting, San Francisco, Calif., May 9-13, 1965, Abstract no. 246.

500. OSWIN, H. G.; OXLEY, J. E.; AND SOHNSON, G. D.: The Growth of Dendrites From Alkaline Zincate Solutions. Electrochemical Society Meeting, Buffalo, N.Y., Oct. 10-14, 1965, Abstract no. 2.

501. OKINAKA, Y.; AND TURNER, D. R.: Effects of Carbonate on the Charge Capacity of Sintered Positive Plate Used in the Sealed Nickel-Cadmium Battery. Electrochemical Society Meeting, Buffalo, N.Y., Oct. 10–14, 1965, Abstract no. 4.

502. WALES, C. P.: Charging the Silver Oxide Electrode With Periodically Varying Current. 1. Repeated Open-Circuit Periods. Electrochemical Society Meeting, Buffalo, N.Y., Oct. 10–14, 1965, Abstract no. 7.

503. ATKINSON, G.; AND COHEN, G. L.: The Formation of a Soluble Silver(III) Species in Aqueous Potassium Hydroxide Solution. Electrochemical Society Meeting, Buffalo, N.Y., Oct. 10–14, 1965, Abstract no. 10.

504. FEDER, D. O.; AND TURNER, D. R.: The Effect of Cell Assembly Compression on Sealed Nickel-Cadmium Battery Performance. Electrochemical Society Meeting, Buffalo, N.Y., Oct. 10–14, 1965, Abstract no. 26.

505. GOTTLIEB, M. H.; AND WILLIS, T. H.: Low Temperature Behavior of Sealed Nickel-Cadmium Batteries. Electrochemical Society Meeting, Buffalo, N.Y., Oct. 10–14, 1965, Abstract no. 27.

506. OKINAKA, Y.; AND TURNER, D. R.: Effects of Carbonate on the Rate of Oxygen Recombination in Sealed Nickel-Cadmium Batteries. Electrochemical Society Meeting, Buffalo, N.Y., Oct. 10–14, 1965, Abstract no. 28.

507. HENNIGAN, T. J.: Improvement of Charge and Overcharge Characteristics of Silver-Cadmium Cells. Electrochemical Society Meeting, Buffalo, N.Y., Oct. 10–14, 1965, Abstract no. 33.

508. SEIGER, H. N.: On Overdischargeable Sealed Cells. Electrochemical Society Meeting, Buffalo, N.Y., October 1965, Abstract no. 35.

509. SIZEMORE, K. O.; AND STROUP, E. R.: Nickel-Cadmium Spacecraft Battery Charge Control With Auxiliary Electrodes. Electrochemical Society Meeting, Buffalo, N.Y., October 1965, Abstract no. 36.

510. JASINSKI, R.: Electrochemical Power Systems in Non-Aqueous Solvents. Electrochemical Society Meeting, Dallas, Tex., May 1967, Abstract no. 129.

511. SCHAAP, W. R.: Precise Polarography in Ethyldiamine and Acetic Acid. Electrochemical Society Meeting, Dallas, Tex., May 1967, Abstract no. 130.

512. BODEN, D.: Electrochemistry in Propylene Carbonate. Electrochemical Society Meeting, Dallas, Tex., May 1967, Abstract no. 136.

513. LITTMAN, F. E.; AND STRIER, M. P.: Inorganic Separators for Non-Aqueous Electrolyte Batteries. Electrochemical Society Meeting, Dallas, Tex., May 1967, Abstract no. 139.

514. CATOTTI, A. J.; AND HADLEY, R. L.: The Use of Auxiliary Electrodes for Charge Control. General Electric Co., IEEE Region 3 Annual Meeting, Clearwater, Fla., May 4–6, 1964.

515. CARSON, W. N.; AND HADLEY, R. L.: Auxiliary Electrode Space Cells. General Electric Co., AIAA Paper no. 64–752, Sept. 1964.

516. LANDER, J. J.: Sealed Silver-Zinc Batteries. General Motors Corp., AIAA Paper no. 64–749, Sept. 1964.

517. MURPHY, J. J.: New Primary Battery Systems. U.S. Army Electronic Labs, AIAA Paper no. 64–750, Sept. 1964.

518. JAFFE, S. S.: Sealed Storage Cell Using Liquid Electrolyte. U.S. Patent no. 3,005,943, Apr. 10, 1957 (file date), Oct. 24, 1961.

519. BRODD, R. F.: Electrical Properties and Kinetics of Electrode Reactions. Journal of Research of the National Bureau of Standards, vol. 65A, no. 4, July–Aug. 1961.

520. BOURGAULT, P. L.; AND CONWAY, B. E.: The Electrochemical Behavior of the Nickel-Nickel Oxide Electrode, Part I. Kinetics of Self-Discharge. Canadian Journal of Chemistry, vol. 37, 1959.

521. BOURGAULT, P. L.; AND CONWAY, B. E.: The Electrochemical Behavior of the Nickel-Nickel Oxide Electrode, Part II. Quasi-Equilibrium Behavior. Canadian Journal of Chemistry, vol. 38, 1960.

522. ANON.: Batteries, Storage, Aircraft, Nickel-Cadmium, General Specification. Military Specification, MIL-B-26220C, Mar. 30, 1964.

523. ANON.: Batteries, Storage, Vented Nickel-Cadmium. Military Specification, MIL-B-55118 (SigC), Apr. 1, 1964.

524. ANON.: Batteries, Storage, Sealed, Nickel-Cadmium. Military Specification, MIL-B-55130 (SigC), May 19, 1961.

525. ANON.: Environmental Testing, Aeronautical and Associated Equipment, General Specification for. Military Specification, MIL-E-5272C, Jan. 20, 1960.

526. ANON.: Environmental Test Methods for Aerospace and Ground Equipment. Military Standard, MIL-STD-810A, June 23, 1964.

527. FAUST, C. L.; AND McCALLUM, J.: Failure Mechanisms in Sealed Batteries. Battelle Memorial Institute, Rept. no. BATT-7770, AFAPL-TR-67-48 (AD 813731), Contract no. AF 33(615)-3701, First Semiannual Report, May 1967.

528. BODEN, D. P.: Abstracts on High Energy System (Organic Electrolyte). Electric Storage Battery Co., Abstract no. N67-17250, AD 639-709, Final Report. No date.

529. GLADSTONE, B.; KANTNER, E.; LENNON, H.; AND WOUK, V.: Investigation of Maintenance-Free High-Rate, Nickel-Cadmium Batteries for Aircraft Application. Gulton Industries (AD-814002), Contract no. AF 33(615)-5357, Third Quarterly Report, Mar. 1967.

530. TROUT, J. B.: Evaluation and Test Results, Gemini Adapter Battery (Eagle-Picher Co., MAP 4138-3). Lockheed Electronics, Rept. no. IESD 12-113R, Test Report, Oct. 18, 1965.

531. TROUT, J. B.: Pulse Testing of the Entry and Post-Landing Battery (Eagle-Picher SAR-4265-0). Lockheed Electronics, Rept. no MSC/IESD 021-8, June 15, 1966.

532. TROUT, J. B.: Charge-Discharge Testing of the Entry and Post-Landing Battery and Spacecraft Battery Charger. Lockheed Electronics, Rept. no. MSC/IESD 21-15, Final Report, Apr. 30, 1967.

533. TROUT, J. B.: Pressure and Venting Test of the Pyrotechnic Battery (Electric Storage Battery Co., Model 264, NAA Specification ME-461-0007). Lockheed Electronics, Rept. no. MSC/IESD 21-23, June 5, 1967.

534. TROUT, J. B.: Pressure Testing of the Entry and Post-Landing Battery. Lockheed Electronics, Rept. no. MSC/IESD 21-33, Final Report, Aug. 7, 1967.

535. TROUT, J. B.: Discharge Test of the Hasselblad Camera Battery. Lockheed Electronics, Rept. no. MSC/IESD 21-34, Aug. 7, 1967.

536. TROUT, J. B.: Silver-Zinc Battery Data Sheet. Lockheed Electronics.

537. AMSTERDAM, R. E.: Cell Equalization Techniques. P. R. Mallory & Co., Contract no. AF 33(615)-2491, Third Quarterly Report, Nov. 1965.

538. SHEPHERD, C. M.: Theoretical Design of Primary and Secondary Cells. Naval Research Lab, NRL Problem C05-14, NRL Rept. no. 5211, pt. III, Dec. 27, 1962.

539. THIERFELDER, H.: Lunar Orbiter Nickel-Cadmium 12 Ampere-Hour Cell. Radio Corp. of America, Special Test Program, July 23 to Aug. 13, 1964.

540. THIERFELDER, H.: Failure Analysis of Lunar Orbiter Nickel-Cadmium 12 Ampere-Hour Cell, Gulton Serial No. 1215. Radio Corp. of America, Sept. 18, 1964.

541. EISEN, J.; AND THIERFELDER, H.:   Failure Mode Investigation for 12 Ampere-Hour Gulton Nickel-Cadmium Cells.   Radio Corp. of America, Mar. 4 to May 10, 1965.

542. BAHCER, J.:   T.O.S. Battery Cycling Test.   Radio Corp. of America, Final Report, Oct. 1965.

543. ANON.:   Application of Holography to Electrochemistry.   TRW Systems.

544. KNOX, C.; SAYANO, R. R.; SEO, E. T.; AND SILVERMAN, H. P.:   Holographic Interferometry in Electrochemical Studies.   TRW Systems, Journal of Physical Chemistry, Aug. 1967.

545. ANON.:   Holographic Analysis of Electrochemical Processes.   TRW Systems, Proposal no. 8079.000, Technical Discussion Section and Program Plan Section, Mar. 1967.

546. BRAEUER, K. H. M.; AND HARVEY, J. A.:   Abstracts on Organic Electrolyte High Energy Density Batteries.   U.S. Army Electronics Command, May 1967.

547. RADFORD, W. E.:   A Comparison of Silver-Cadmium and Nickel-Cadmium Batteries for Use on Satellites.   Johns Hopkins Univ., Applied Physics Lab. Rept. no. CF-2970A (AD 631700, N62-10142), Jan. 30, 1962.

548. ANON.:   Investigations Leading to the Development of a Primary Zinc-Silver Oxide Battery of Improved Performance Characteristics.   Eagle-Picher Co., Joplin, Mo.

549. CARSON, W. N., JR.:   Use of Auxiliary Electrodes in Sealed Nickel-Cadmium Cells.   General Electric Co., Rept. no. 63GL 113, July 1963.

550. CARSON, W. N.; AND ROBERTS, E. L.:   Hydrogen Combination Cell Study. General Electric Co., Rept. no. 65GL 91, May 21, 1965.

551. SEIGER, H. N.:   Cycling Behavior of Sealed Nickel-Cadmium Cells.   Gulton Industries.

552. PREUSSE, K. E.:   Micrometeorite Capsule, Flight Battery no. 5.   Gulton Industries, Metuchen, N.J., Nov. 11, 1963.

553. SHAIR, R. C.:   Primary and Secondary Electrochemical Cells for Space Vehicles Power Supplies.   Gulton Industries, Oct. 1963.

554. CARSON, W. N.:   Technical Background: Use of Auxiliary Electrode in Sealed Nickel-Cadmium Cells.   General Electric Co., Feb. 1963.

555. ANON.:   Dry Tape Battery Presentation for NASA/Washington, D.C.   Monsanto Research Corp., Rept. no. NASA CR-64219 (N65-30486), Jan. 15, 1964.

556. SPARKS, R. H.; AND WRIGHT, W. H.:   Integral Electronic Charge Controls for High Performance Secondary Batteries.   TRW Systems, 1966 Aerospace and Electronic Systems Conference, Oct. 1966.

557. HAZEN, R.:   Nickel-Cadmium Battery Life Test.   TRW Systems, Rept. no. 7062.8-080B, Nov. 14, 1966.

558. RALSTEN, M. W.:   Repetitive Cycle Behavior of General Electric 6 Ampere-Hour Nickel-Cadmium Cells.   TRW Systems, Rept. no. 7062.8-010B, Feb. 14, 1966.

559. RALSTEN, M. W.:   Vela Satellite General Electric 6 Ampere-Hour Nickel-Cadmium Characterization Test.   TRW Systems, Rept. no. 9363.4-403, July 2, 1965.

560. SCHULT, R. W.; AND STAFFORD, W. T.:   The State of Development of Silver Oxide-Zinc and Nickel-Cadmium Batteries.   TRW Systems, Rept. no. STL/TR-60-0000-09034, Contract no. AF 04(647)-309.

561. FRYSINGER, G. R.:   Electrochemical Energy Storage Systems for Vehicle Propulsion.   U.S. Army Engineer Research and Development Labs, Feb. 1965.   Status Summary.

562. SHAW, M.: Fundamentals of Electrochemistry as Applied to Battery Technology. Whittaker Corp., Rept. no. 3106, Dec. 1964.

563. ANON.: Barium-Oxygen and Barium-Chlorine High Energy Density Fuel Cell Systems. M. W. Kellogg Co., New Market, N.J.

564. SNYDER, N. W.: Research and Development on Power Sources and Energy Conversion in the Department of Defense, AEC, and NASA. Institute for Defense Analysis, Advanced Research Projects Division, Rept. no. 64-4/U. Abridged Version, May 16, 1960.

565. MacKENZIE, C.; AND WEINREB, M. B.: Nimbus Solar Power Supply. NASA/ Goddard Space Flight Center, Rept. no. 13, N63-18614.

566. ANON.: Battery Workshop. NASA/Headquarters, Oct. 1966.

567. ANON.: Battery Program Review. NASA/Headquarters, Apr. 1966.

568. RUSSELL, C. R.; AND SELIS, S. M.: An Analytic Representation of the Discharge Characteristics of Commercial Secondary Batteries. General Motors Corp., Electrochemical Technology, vol. 1, no. 3-4, p. 77, Mar.-Apr. 1963.

569. METZGER, W. H., JR.; AND SHERFEY, J. M.: Electrochemical Calorimetry, III. Thermal Effects of Nickel-Cadmium Batteries. Electrochemical Technology, vol. 2, no. 9-10, Sept.-Oct. 1964.

570. BRODD, R. J.; AND DeWANE, H. J.: Impedance of Sealed Nickel-Cadmium Dry Cells. Electrochemical Technology, vol. 3, no. 1-2, Jan.-Feb. 1965.

571. TRACEY, V. A.; AND WILLIAMS, N. J.: The Production and Properties of Porous Nickel for Alkaline Battery and Fuel Cell Electrodes. Electrochemical Technology, vol. 3, no. 1-2, Jan.-Feb. 1965.

572. LANDER, J. J.; AND SNYDER, R. N.: Rate of Hydrogen Evolution of Zinc Electrodes in Alkaline Solutions. Electrochemical Technology, vol. 3, no. 5-6, May-June 1965.

573. DIRKSE, T. P.: Cycling Characteristics of the Silver Electrode in Alkaline Solutions. Electrochemical Technology, vol. 4, no. 3-4, Mar.-Apr. 1966.

574. OCKERMAN, J. B.; AND RUETSCHI, P.: Sealed Cells With Auxiliary Electrodes. Electrochemical Technology, vol. 4, no. 7-8, July-Aug. 1966.

575. KOBER, F. P.: An Electrolytic Impregnation Method: Nickel Hydroxide Electrode. Electrochemical Technology, vol. 4, no. 7-8, July-Aug. 1966.

576. ATKINSON, G. S.: A Short History of the Jungner-Nife Nickel-Cadmium Battery. Electrochemical Technology, vol. 4, no. 7-8, July-Aug. 1966.

577. OKINAKA, Y.; AND TURNER, D. R.: Anodic Corrosion of Nickel Sinter in Positive Electrodes of Nickel-Cadmium Batteries Containing Carbonate. Electrochemical Technology, vol. 5, no. 3-4, Mar.-Apr. 1967.

578. HALPERT, G.; AND SHERFEY, J. M.: A New Technique for Measuring the Internal Pressure of Sealed Electrochemical Cells. NASA/Goddard Space Flight Center, rough draft for publication in future Electrochemical Technology issue, Mar. 1967.

579. BRENNER, A.; AND SHERFEY, J. M.: Electrochemical Calorimetry. Journal of the Electrochemical Society, vol. 105, no. 11, 1958.

580. LIEBHAFSKY, H. A.: The Fuel Cell and the Carnot Cycle. Journal of the Electrochemical Society, vol. 106, no. 12, Dec. 1959.

581. FALK, S. U.: Investigations on the Reaction Mechanism of the Nickel-Cadmium Cell. Journal of the Electrochemical Society, vol. 107, no. 8, 1960.

582. DUDDY, J. C.; AND SALKIND, A. J.: The Thermal Runaway Condition in Nickel-Cadmium Cells and Performance Characteristics of Sealed Light Weight Cells. Journal of the Electrochemical Society, vol. 109, no. 5, 1962.

583. SHERFEY, J. M.: Calorimetric Determination of Half-Cell Entropy Changes. Journal of the Electrochemical Society, vol. 110, no. 3, Mar. 1963.

584. SHEPHERD, C. M.: Design of Primary and Secondary Cells, I. Effect of Polarization and Resistance on Cell Characteristics. Journal of the Electrochemical Society, vol. 112, no. 3, Mar. 1965.

585. CASEY, E. J.; DUBOIS, A. R.; LAKE, P. E.; AND MOROZ, W. J.: Effects of Foreign Ions on Nickel Hydroxide and Cadmium Electrodes. Journal of the Electrochemical Society, vol. 112, no. 4, Apr. 1965.

586. SHEPHERD, C. M.: Design of Primary and Secondary Cells, II. An Equation Describing Battery Discharge. Journal of the Electrochemical Society, vol. 112, no. 7, July 1965.

587. KOBER, F. P.: Analysis of the Charge-Discharge Characteristics of Nickel-Oxide Electrodes by Infrared Spectroscopy. Journal of the Electrochemical Society, vol. 112, no. 11, Nov. 1965.

588. ROUSE, T. O.; AND WEININGER, J. L.: Electrochemical Studies of Single Crystals of Lithiated Nickel-Oxide, I. Distribution of Charge and Potential at Oxide Electrolyte Interface. Journal of the Electrochemical Society, vol. 113, no. 2, Feb. 1966.

589. KOBER, F. P.; AND LUBLIN, P.: Potassium Distribution in Nickel-Oxide Electrodes. Journal of the Electrochemical Society, vol. 113, no. 4, Apr. 1966.

590. DARBY, R.: Faradaic Impedance of Polarized Porous Electrodes. Journal of the Electrochemical Society, vol. 113, no. 4, Apr. 1966.

591. LANGELAN, H. C.; AND SHEPHERD, C. M.: High Rate Battery Electrodes. Journal of the Electrochemical Society, vol. 114, no. 1, Jan. 1967.

592. GUTMANN, F.; HERMANN, A. M.; AND REMBAUM, A.: Solid-State Electrochemical Cells Based on Charge Transfer Complexes. Journal of the Electrochemical Society, vol. 114, no. 4, Apr. 1967.

593. AIA, M. A.: Structure and Stoichiometry of Nickel Hydroxides in Sintered Nickel Positive Electrodes. Journal of the Electrochemical Society, vol. 114, no. 5, May 1967.

Glossary

TERMS

Activity—Corrected concentration values used to make observed electrochemical phenomena conform to theoretical predictions.

Activity coefficients—Correction factors used in converting concentration to activity. These are lumped factors expressing the net results of a number of complex physical phenomena.

Adhydrode—A proprietary electrode for detection of oxygen manufactured by Gulton Industries, Inc., in which hydrogen atoms are generated at the auxiliary electrode, and held adsorbed on its surface. Oxygen recombination occurs at the electrode surface. Hydrogen gas is not liberated from the Adhydrode under normal operating conditions.

Adiabatic calorimeter—A device for measuring total heat effects; no heat transfer is permitted into or out of the calorimeter chamber.

Amp-gate diode—A proprietary charge control device manufactured by the Mallory Battery Co., Inc., consisting of a stabistor mounted on a heat sink designed to increase the sensitivity of voltage of the silicon semiconductor junction to temperature changes.

Anion—A negatively charged ion.

Anode—An electrode at which an oxidation reaction (loss of electrons) occurs. In primary cells, the negative electrode of the cell. In secondary cells, either electrode may become cathode or anode, depending upon the direction of current flow.

Anolyte—In cells having separate electrolyte solutions around anode and cathode, the electrolyte solution surrounding the anode.

Aprotic electrolyte—An electrolyte solution having few available hydrogen ions.

Argand diagram—An impedance diagram in which the reactance is plotted on the ordinate and the resistance on the abscissa, as a function of the frequency of measurement.

Automatic crossover power supply—A regulated power supply having both voltage and current limiting, either of which may control the power supply output at any time, depending upon load conditions.

Battery—Two or more cells connected in series, parallel, or a combination of both.

Binder—A material, usually organic, used to promote adhesion between the particles of a powder.

Bipolar electrode—An electrode structure in which the anode of one cell and the cathode of the adjoining cell are combined to form a single member.

Capacitance—The ability of a system to store electrical energy in a pair of conductors separated by a dielectric, expressed as the ratio of charge stored to potential difference (coulombs/volt).

Capacity:

    Rated capacity—The nominal or nameplate capacity.

    Standard capacity—The capacity as measured under a standardized charge-discharge cycle.

    Measured capacity—The capacity as measured under other than standard conditions.

Catalyst—A material whose presence increases the rate of a chemical reaction, but which is itself unchanged by the net reaction.

Cathode—An electrode at which a reduction reaction (gain of electrons) occurs. In primary cells, the positive electrode of the cell. In secondary cells, either electrode may become cathode or anode, depending upon the direction of current flow.

Catholyte—In batteries having separate electrolyte solutions surrounding the anode and cathode, the electrolyte solution surrounding the cathode.

Cation—A positively charged ion.

Cell—An electrochemical device consisting of an anode and a cathode in a common electrolyte solution, or in separate electrolyte solutions connected by an ionic bridge. Each anode or cathode may consist of one or more parallel-connected electrodes.

Cell reversal—A reversing of the polarity of the terminals of a cell due to overdischarge.

Charge—The process of storing electrical energy in a secondary (rechargeable) battery by forcing current to flow through the battery in the reverse direction.

Common mode noise—Electrical noise coupled between circuits through the common return lines.

Concentration—The number of units of solute in solution in a solvent. Usually expressed as grams/liter, gram equivalents/liter, etc.

Constant current charging—Charging and overcharging a battery at a controlled constant current.

Constant potential charging—Charging a battery by applying a constant potential across the terminals, and allowing the current to seek its own level.

Converter (dc-to-dc)—A device for increasing or lowering the dc voltage by inverting the dc to ac, changing the voltage in a transformer, and rectifying the secondary power.

Crazing (of plastics)—The development of a network of surface cracks.

Crosslinking (of plastics)—The formation of chemical bonds from chain to chain of long-chain plastic molecules. Crosslinking usually results in greater strength and rigidity, but also in increased brittleness.

Crystallite—A small or submicroscopic crystal.

Coulombic capacity—The number of electrons or coulombs which can be usefully released or taken up by an electrode material.

Coulometer—An electrochemical ampere-hour meter.

Current collector—The electronically conductive part of a cell electrode.

Current density—Current/unit electrode area.

Cycle life—The number of cyclic operations (charge-discharge) which a cell or battery will tolerate prior to failure.

Cycling—Repetitive charge-discharge operation of a battery.

Dendrite—A needlelike or treelike branched crystalline growth.

Derivative—A compound formed or derived from a parent compound or element.

Discharge—The process of obtaining electric power from a battery by connecting a load across the battery terminals, allowing the voltage of the battery to force current through the load.

Discharge curve—A graph, measured during discharge, of voltage as a function of time.

Discharge plateau—The relatively flat portion of a discharge curve occurring at the middle of the discharge period.

Divalent—Able to exchange or share two electrons in chemical reaction.

Divergence—The tendency of cells to differ from one another in terminal voltage in spite of being operated at the same current. The phenomenon appears with increasing age.

Dry-tape device—A type of battery (or fuel cell) in which the electrodes take the form of continuous strips of tape coated with the cell active materials. These are fed to the reaction (with an electrolyte tape) at a rate determined by the power demand.

Edge effects—The phenomenon of unequal current distribution between edges and face of an electrode.

Efficiency—Ratio of output to input.

    Thermodynamic efficiency—Ratio of electrical work output to total heat content change.

    Electrical work efficiency—Ratio of electrical work output to total free energy change.

    Watt-hour efficiency—In secondary batteries, the ratio of electrical work output (on discharge) to electrical work input (on charge) watt-hour out/watt-hour in.

    Ampere-hour efficiency—In secondary batteries, the ratio of total charge output (on discharge) to total charge input (on charge) ampere-hour out/ampere-hour in.

    Utilization efficiency—That fraction of electrode active materials installed which are electrochemically available for discharge at useful voltages.

Electrode—A metallic or nonmetallic conducting body through which the current enters or leaves an electrochemical cell.

Electrolyte—1. An ionic salt dissolved in a solvent to form an ionically conductive solution. 2. The ionically conductive solution itself.

Energy density—A figure of merit in common use with batteries, expressing the stored energy as a function of the weight or volume (watt-hours/pound and watt-hours/cubic inch).

Enthalpy—The heat content of a system, usually expressed in terms of its changes, in a constant pressure process.

Entropy—A measure of the unavailable energy of a thermodynamic system, commonly expressed in terms of its changes on an arbitrary scale.

Exchange capacity (of ion exchange material or membranes)—The number or quantity of ions which can be taken up by an ion-exchange resin in exchange for an equal number of different ions released.

Faradaic capacitance—The apparent capacitance exhibited by the electrode-electrolyte interface of a cell electrode.

Flooding—Filling of the pores of a porous electrode with electrolyte solution, thereby preventing access of gases to the electrode surface.

Formation cycle—A series of charge and/or discharge operations performed on a newly manufactured cell electrode to condition it for service.

Free energy—That portion of the energy content of a system which is the maximum available for doing work.

Fuel cell—An electrochemical energy-producing device employing inert electrodes to which are fed liquid or gaseous reactants, and from which the reaction products are continuously removed.

Fugacity—Corrected values of pressure used to make observed chemical phenomena conform to theory. Analogous to **activity.**

Fused salt—A molten ionized compound (used as an electrolyte).

Galvanostatic measurements—Voltammetric measurements made during and immediately after an abrupt change in current flow.

Guarded input—An electrical signal input which has been protected against noise.

Half-cell reaction—The reaction occurring at one of the two cell electrodes.

Hermetic seal—A gastight seal, usually of the glass-to-metal or ceramic-to-metal type.

Impedance—The total resistance to the flow of current consisting of a resistance and a reactance.

$$Z = R + j \sin \theta$$

Indicator (chemical)—A chemical which can exist in two differently colored states at different values of pH.

Inorganic compound—All chemical compounds containing no carbon.

Interface—The junction or dividing line between two different media or systems.

Integrating voltmeter—A voltmeter designed to integrate the measured voltage over a small but finite period, thus minimizing the effects of high-frequency noise components.

Intermediate peak—*See* Transition voltage.

Ion—A charged radical, atom, or molecule. Positive ions are formed by the loss of electrons. Negative ions are formed by gaining electrons (from the neutral state).

Ion conductivity—The process of conducting electric charge by movement of ions.

Ion pair—Two ions of opposite charge closely joined in solution so as to be unavailable as individual ions.

Ion solution energy—The energy consumed or released in the solution of an ion.

Isothermal flow calorimeter—A device for measuring heat effects by measuring the temperature rise of a calibrated stream of fluid of known heat capacity and flow rate.

Junction—The interface between two dissimilar metals or two semi-conductors having a different type of majority current carrier.

Knee—The portion of maximum curvature of the discharge curve at the end of discharge.

Load cell—A device for measuring force by using electrical strain gages.

Magnetic amplifier—An amplification device in which the amplitude of an alternating current output signal is controlled by the magnitude of a small direct current signal in a control winding of a transformer.

Mass spectrometer—A device for qualitative and quantitative analysis which separates charged particles from one another according to their mass.

Memory effect—A phenomenon observed in the laboratory in which a nickel-cadmium battery, operated in successive cycles of constant depth of discharge, assumes the capacity demanded of it, losing all of its extra capacity.

Modified constant potential charging—Charging a battery at a moderate current until its potential reaches a predetermined level, then charging at constant potential thereafter.

Monovalent—Able to exchange or share one electron in an oxidation or reduction reaction.

Multiple current charging—*See* Voltage-actuated multistep charging.

Nitrogen shuttle—A proposed mechanism of self-discharge of the nickel-cadmium cell which involves nitrates and ammonia as inter-mediates.

Normalized current—Current/ampere-hour capacity.

Organic compounds—A large category of compounds of carbon.

Overcharge—Continued charge of the cell after it has been fully charged.

Overdischarge—Forcing current through the cell in the discharge direction after all of the active materials have been exhausted. This results in cell reversal.

Overpotential:

    Ohmic overpotential—The polarization resulting from the flow of current through the internal resistances of the battery.

    Activation overpotential—Polarization resulting from the rate-controlling step of the electrode reaction.

    Concentration overpotential—A shift in electrode potential caused by a change in the concentration of electrolyte at the surface of the electrode due to depletion or buildup of ions as a result of current flow.

Oxidation—The process of loss of electrons; one-half of a redox reaction.

Phase shift—A change in the angle by which alternating current leads or lags the voltage.

Plaque—A porous body of sintered metal used as a current collector and holder of electrode active materials.

Pocket-plate electrode—An electrode in which the active materials are held in pockets or cavities in the current collector structure.

Poisoning (of catalysts)—The process by which catalytic activity of a substance is reduced by contamination with foreign substances.

Polarization—A shift in the potential of the battery from the open-circuit voltage which results from the flow of current through the battery in either direction.

Polar solvent—A solvent whose molecules have centers of positive and negative charge separated from one another. Such solvents act as dielectrics.

Potential gradient—The rate of change of electrode potential (usually as a function of distance from the electrode surface).

Radiation grafting—The process of forming chemical compounds at the surface of a substrate by producing artificially induced reaction sites on the substrate under irradiation.

Reactance—That portion of the total impedance of a system due to capacitance or inductance. When impedance is expressed as a complex number, the reactance is the imaginary part.

Recombination (gas recombination)—In batteries, the chemical reaction of gases at the electrodes to form a nongaseous product.

Reconditioning—A process of restoration of the reserve capacity lost on cycling of a nickel-cadmium cell by deep discharge and recharge.

Redox reaction—A chemical reaction in which one of the reactants loses electrons to the other.

Reduction—The process of gaining electrons in a chemical reaction; one-half of a redox reaction.

Remote sensing—Sensing of the voltage at a remote location for the purpose of controlling the output voltage of a regulated power supply.

Reserve battery—A battery having very short wet-stand time but storable in the dry state. The battery is activated by addition of electrolyte and used immediately.

Residual magnetism—The magnetic field measured in a battery (or other device) containing magnetic materials which have become permanently magnetized as a result of current flow at some earlier time.

Reversible potential—The open-circuit, or zero-current, potential of a reversible electrode.

Reversible reaction—A chemical reaction which may be induced to go in either direction, depending upon the conditions.

Reynolds number—A dimensionless number used in calculation of flow patterns; i.e., determination when the fluid flow is laminar or turbulent.

Scavenger electrode—An auxiliary electrode designed for recombination of gases rather than detection or measurement of gas pressure.

Self-discharge—The spontaneous decomposition of battery materials from the charged to the discharged state.

Sensor—A detection device.

Separator—A porous or microporous, single- or multiple-layered electronically nonconductive material used between cell electrodes to

prevent their touching one another. It may also have other functions, such as electrolyte absorption and control of deterioration processes in the cell.

Shunt regulator—A regulator based upon the addition of a variable resistance load across the power supply terminals, in which voltage regulation is achieved by varying the shunt resistance.

Sintered plate electrode—An electrode formed by sintering metallic powders to form a porous structure which contains the electrode material in the pores of the current collector.

Spinel—A combined oxide having the formula AOB_2O_3, where A and B are metal atoms (usually alkali or alkaline earth metals).

Stabistor—A charge-control device consisting of two series-connected silicon semiconductor junctions.

Standard electrode potential—The potential of an electrode, relative to the normal hydrogen electrode, at standard conditions (25° C and unit activity).

Standard state—An arbitrarily defined set of standard conditions to which all thermodynamic properties are referenced. (A temperature of 25° C and unit activity of all reactants and reaction products.)

Stand time—*See* Wet-stand time.

Starved cell—A cell containing little or no free fluid solution; this enables gases to reach the electrode surfaces readily, and permits relatively high rates of gas recombination.

State of charge—That percentage of the total available active materials of the cell which are in the charged state. (If the cell is unbalanced, this refers to the active materials of the limiting electrode.)

Sterilization—The process of killing bacterial and other simple forms of life. Sterilization of planetary landers is performed to prevent contamination of the planets.

Strain gage—A device for the detection and measurement of small dimensional changes by measurement of the resistance of a small metallic film whose resistivity changes with strain.

Substrate—A base material upon which a coating or layer is placed.

Synchronous equatorial orbit—An orbit about the Earth in the equatorial plane having a period of 24 hours. The satellite in such an orbit remains stationary over a single spot.

Taper charge—A charging method which starts with a high charging current, which is reduced as the battery approaches the fully charged state. Usually similar or identical to modified constant potential charging.

Thermal runaway—In batteries, the process by which a cell or battery subjected to a constant applied voltage will undergo progressive temperature increase and overcharge current increase due to the negative temperature coefficient of voltage.

Thermocouple—A device for sensing and measuring temperature differences by the appearance of a potential difference between two dissimilar metal junctions or semiconductor junctions at different temperatures.

Thermopile—A device for sensing of small temperature differences, and consisting of multiple thermocouple junctions.

Threshold—The magnitude of a phenomenon at which it first becomes detectable.

Transducer—A device for changing one form of energy into another (i.e., mechanical to electrical).

Transition voltage—In silver-zinc and silver-cadmium cells, the peak voltage reached during the transition between upper and lower plateaus (on charge).

Triangular wave voltammetry—Voltammetric measurements made during a period of slow linear rise and fall of applied voltage.

Trickle charge—A low-level charging current used to maintain the battery at the fully charged level with a minimum of damage due to overcharging.

Voltage-actuated multistep charging—Charging a battery at several decreasing levels of controlled charging current, switching from one level to the next when the battery potential reaches a predetermined level.

Voltage limit—In a charge-controlled battery, the limit beyond which the battery potential is not permitted to rise during or after the charging process.

Wetproofing (of electrodes, etc.)—Treatment of a porous body with materials having a high interfacial tension relative to the electrolyte solution to prevent flooding of the pores with the liquid.

Wet-stand time—The survival time of a completed battery or cell, filled with electrolyte, and stored unused. Wet-stand time may be expressed as the time of storage prior to loss of a portion of the battery capacity.

SYMBOLS

η_r	Ohmic overpotential $= IR$
I	Current
R	Resistance
η_a	Activation overpotential
i	Current density
η_c	Concentration overpotential
E_{rev}	Reversible potential
E	Potential, volts
ΔG	Gibbs free-energy change
ΔG°	Gibbs free-energy change at standard conditions
F	Faraday's constant $\cong 96500$ coulombs/gram equivalent
T	Temperature, °C or °F
T°	298.6° K (standard conditions)
a	Activity
$w_{e\,max}$	Electrical work
w_e	Maximum available electrical work
Q	Total heat; calories, watt-hour
ΔH	Enthalpy change

ΔS	Entropy change
g	Heat rate dQ/dt; calories/second, watts, etc.
S	Entropy
η_T	Thermodynamic efficiency $= \int_{t_1}^{t_2} EI\ dt / 4.186\ N\Delta H$
N	Number of mols reacted
η_w	Electrical work efficiency $= \int_{t_1}^{t_2} EI\ dt / 4.186\ N\Delta G$
$\eta_{w\text{-}h}$	Watt-hour efficiency $= \int_{t_2}^{t_3} EI\ dt \Big/ \int_{t_1}^{t_2} EI\ dt$
$\eta_{A\text{-}h}$	Ampere-hour efficiency $= \int_{t_2}^{t_3} I\ dt \Big/ \int_{t_1}^{t_2} I\ dt$
Z	Impedance
t	Time
Q_n	nth value of state of charge
$\bar{\eta}$	Average efficiency
$\bar{I}$	Average current
C	Capacity
I/C	Normalized current
K	Proportionality constant $= \Delta S/F$
R	Universal gas constant $=$ (liter-atm/mol °K)
E_H	$\Delta H/zF$
V	Battery voltage
H	Overall power system efficiency
ϵ_o	Energy output
ϵ_i	Energy input
ϵ_s	Stored energy
t_e	Eclipse period
η_d	Discharge circuit efficiency
η_b	Battery efficiency $= \eta_{w\text{-}h}$
η_c	Charge circuit efficiency
t_d	Daylight period
η_r	Regulator efficiency
P_L	Load power
P_{SA}	Solar array power
P°_{SA}	Solar array power received in a loss-free system
DOD	Depth of discharge
E_d	Average discharge voltage
n	Number of series-connected cells
P	System power
z	Number of electrons exchanged/molecule

Subject Index

Author Index

Abens, S. G.; et al., 204

Abens, S. G.; Corbett, R.; Merz, W. C.; and G. and W. H. Corson, 198, 206, 207

Abens, S. G.; Mahy, T. X.; Meyers, W. F.; Merz, W.; and G. and W. H. Corson, 198, 200, 202, 205, 206, 207

Adams, J. L., 183

Adams, L. M., 166

Adler, R. W.; Elliott, W. E.; Huff, J. R.; Jamrozy, J. L.; and Towle, W. L., 200, 201, 202

Alke, P. E.; Casey, E. J.; Dubois, A. R.; and Moroz, W. H., 71

Alkire, R. C., 218

Alkire, R. C.; Grens, E. A., II; Mueller, R. H.; and Tobias, C. W., 217

Alliegro, F.; Belove, L.; Voyentzie, P., 111

Anderson, W. G.; Parker-Jones, H. A.; Place, T. M.; Salisbury, R. G.; Segovia, G.; Stamires, D. N.; and Subcasky, W. J., 195

Apelt, A. O.; and Hennigan, T. J., 132

Arcand, G. M., 149, 151

Argue, G. R.; MacKenzie, D. E.; McCollum, W. A.; and Recht, H. L., 120

Argue, G. R.; McCollum, W. A.; and Recht, H. L., 182

Armstrong, G. M.; Meyers, W. F.; and Corson, W. H., 191

Arouet, S.; and Blurton, K. F., 154, 155, 156

Arrance, F. C.; Berger, C.; and Taylor, A. D., 182

Athearn, L. F.; Byrne, J. J.; MacDonald, J. C.; and Williams, D. L., 199

Atkinson, G. S., 69

Banks, H. O., Jr.; Bauer, P.; Binckley, W. G.; Riess, H.; and Robinson, R. L., 132, 133, 138

Bauer, P., 39, 73, 108

Bauer, P.; and Sparks, R. H., 83, 85, 88, 89, 91, 98, 107, 112, 113, 114, 118, 123, 139

Bauman, H. F., 199, 200, 202

Bauman, H. F.; Chilton, G. E.; Conner, W. J.; and Cook, G. M., 198, 199, 202, 206, 207

Beck, T. R.; and Kemp, F. S., 39, 96

Biess, J. J.; Stafford, W. T.; and Wright, W. H., 131, 132, 136, 142

Binckley, W. G., 226

Blackman, A. U.; and Butler, E. A., 148

Bodamer, G. W., 139, 150, 152, 164, 166

Boden, D. P.; Buhner, H. R.; and Spera, V. J., 198, 199, 200, 202, 205, 206

Bogar, F. D.; and Foley, R. T., 204

Bogner, R. S., 152, 153, 156, 163, 164, 165, 167

Bomben, J. L., 217

Bomberger, D. C.; and Moose, L. F., 122

Borsanyi, A. S.; Byrne, J. J.; Driscoll, J. S.; and Williams, L., 208, 209, 210, 211, 212

Borsanyi, A. S.; Gruber, B. A.; Kafesjian, R.; Klunder, K. W.; and Smith, J. O., 181, 208, 209, 212

Bourgault, P. L.; and Conway, B. E., 118

Braener, K. H. M.; and Harvey, J. A., 198, 200, 203, 204, 205, 206

Brodd, R. J., 91

Brodd, R. J.; and DeWane, H. J., 41, 70, 71, 91

Brooke, C. W., Jr., 178, 179

Bruess, E. C., 47, 48, 80, 86, 88, 92, 98, 99, 101, 113, 114, 140, 141

Bruins, P. F., 202

Bruins, P. F.; Caulder, S. M.; and Salkind, A. J., 39, 71, 96, 118

Butler, E. A., 147, 172

Byrne, J. J.; Gruber, B. A.; Kafesjian, R.; Klunder, K. W.; McElhell, E. A.; Power, W. H.; Wolanski, T. J.; and Zirin, L. I., 208, 209, 210, 211, 212

Carson, W. N., Jr., 14, 15, 26, 29, 73, 74, 88, 98, 105, 143

Corporate References